HYDROLOGICAL MODELLING OF THE OPERATIONAL ON-FARM IRRIGATION EFFICIENCIES.

By

AFSHIN SEHAT-NIAKI

B.Sc., M.Sc.

A thesis submitted for the degree of

Doctor of Philosophy of the

University of Strathclyde.

Water & Environmental Management Group,
Department of Civil Engineering,
University of Strathclyde,
Glasgow, Scotland. February, 1989.

" Read not to contradict and confute,

nor to believe and take for granted,

nor to find talk and discourse,

but to weigh and consider."

Sir Francis Bacon (1561–1626)

CONTENTS

Contents		
List of Figures		i
List of Tables		ix
List of Plates		xiii
Synopsis		xiv
Acknowledgements		xvi
CHAPTER 1	Introduction:	1
CHAPTER 2	Defining Irrigation Efficiencies:	
2.1	Introduction	15
2.2	Evaluating Irrigation Efficiencies	21
CHAPTER 3	Irrigation Scheduling:	
3.1	Introduction	26
3.2	Review of Existing Models	26
3.3	When to irrigate ?	34
3.4	How much to apply ?	37
3.5	Estimating root zone water gains and losses	40
3.5.1	Rainfall, Runoff and Infiltration	40
3.5.2	Drainage	42
3.5.3	Transpiration	43
3.5.4	Potential Evapotranspiration.	52
3.5.4.1	The Pan Evaporation Method (Option 1)	56
3.5.4.2	The Penman Method (Option 2)	57
3.5.4.3	The Penman-Montieth Method (Option 3)	59

3.5.5 Soil Evaporation 61

3.5.5.1 Stages of Soil Evaporation Rate 61

3.5.5.2 Bare Soil Lysimeter Tests 64

3.5.5.3 Estimation of Model Parameters 72

3.6 Chapter Summary 74

CHAPTER 4 Root Zone Water Balance Model:

4.1 Introduction 75

4.2 Root Zone Water Balance Model 75

4.2.1 Water Balance of Uniform Soils with Nonuniform, Growing, Root Zones. 75

4.2.2 Water Balance of Nonuniform Soils with Nonuniform, Growing, Root Zones. 82

4.2.3 Crop Rooting Pattern. 94

4.3 Lysimeter Experiment 98

4.4 Testing the Model 112

4.4.1 Criterion for Calibration 112

4.4.2 Sensitivity to Parameters 120

4.5 Management Practices 127

4.6 Chapter Summary 133

CHAPTER 5 Determination of Soil-Water Properties

5.1 Soil Physical Properties 135

5.2 Soil-Water Potential 137

5.2.1 Field Capacity 138

5.2.2 Wilting Point 138

5.2.3 Wetting Front Pressure 138

5.2.4 Methods of Evaluating the Soil Moisture Characteristic Curve. 140

5.2.4.1 Experimental Methods 140

5.2.4.2 Empirical Models 143

5.3 Summary of Measured Soil Properties 158

CHAPTER 6 Infiltration into Nonuniform Soils

6.1 Introduction 159

6.2 Existing Infiltration Models 160

6.3 Infiltration into Nonuniform Soils 165

6.3.1 Bouwer's One Dimensional Model 165

6.3.2 Two Dimensional Model (2DVAR) 178

6.3.2.1 Development of the 2DVAR Model 178

6.3.2.2 Validation of the 2DVAR Model 184

6.4 Chapter Summary 204

CHAPTER 7 Modelling the Operational Efficiencies of Surface Irrigation Systems:

7.1 Introduction 205

7.2 Surface Irrigation Modelling 207

7.2.1 Surface Irrigation Model (SURFOPRN) 212

7.2.2 Surface Irrigation Efficiency Evaluation 237

7.2.3 Applications in Operational Management 246

7.2.4 Applications in System Design 257

7.2.4.1 Design of Borders 257

7.2.4.2 Design of Furrows 264

7.3 Discussion 276

CHAPTER 8 Dynamic Water Balance Under Sprinkler Irrigation

8.1 Introduction 280

8.2 Excess Rainfall and Runoff 284

8.2.1 Point Runoff from Continuous Rain 285

8.2.2 Point Runoff from Intermittent Rain 285

8.3 Point Excess Rainfall Model (PERM) 289

8.3.1 Validation of the PERM model 311

8.3.2 Model sensitivity 319

8.4 Discussion 321

CHAPTER 9 Modelling the Operational Performance of Sprinkler Irrigation Systems.

9.1 Introduction 323

9.2 Sprinkler Performance Evaluation Model 326

9.3 Applications in Design and Operation 351

9.4 Discussion 354

CHAPTER 10 Discussions and Conclusions 355

References 360

Appendix 385

LIST OF FIGURES

CHAPTER 1:

Fig. 1.1	Flow chart of the methodology for solving problems.	3
Fig. 1.2	Flow chart of integrated operational irrigation management model.	13

CHAPTER 2:

Fig. 2.1	Schematic diagram of surface irrigation infiltration depth profile.	17
Fig. 2.2	Idealized wetting profile under sprinkleR irrigation.	19
Fig. 2.3	Schematic diagram of the cumulative frequency distribution of infiltrated water depth in sprinkler irrigation.	20
Fig. 2.4	Schematic diagram of the relation between deficit/excess (Ede), application (Ea) and distribution (Ed) efficiencies.	24

CHAPTER 3:

Fig. 3.1	Hydrological processes in the Soil-Plant-Atmosphere-Water continuum represented by the SPAW model of Saxton etal (1974).	31
Fig. 3.2	Relational flow chart of the irrigation scheduling model (SCHEDULE).	39
Fig. 3.3	Proposed shapes of transpiration response to depleting soil moisture.	48
Fig. 3.4	Schematic diagram of incoming and outgoing radiations at the earth's surface.	58
Fig. 3.5	Schematic diagram of the three stages of evaporation from soils.	62
Fig. 3.6	Measured relative soil evaporation decay with time.	65
Fig. 3.7	Measured relation of relative soil evaporation to soil moisture content.	67
Fig. 3.8	Measured class means (squares) and standard deviations (vertical bars) of (Es/Eo) vs SMC for undrained soil evaporation tests.	68

Fig. 3.9 Measured cumulative fractional water losses of the drying soils. 69

Fig. 3.10 Measured soil profile moisture changes due to evaporation from the bare-soil lysimeter. 71

CHAPTER 4:

Fig. 4.1 Schematic representation of a dynamic uniform root zone. 77

Fig. 4.2 Schematic representation of a nonuniform, dynamic root zone. 81

Fig. 4.3 Schematic diagram of discrete soil and root layers and the composite-layer profile. 83

Fig. 4.4 Definition skech of overlapping soil and root layers. 87

Fig. 4.5 Flow chart of composite-layer generation algorithm. 88

Fig. 4.6 Measured mean daily free-water evaporation rate in the glasshouse. 101

Fig. 4.7 Measured mean daily relative humidity in the glasshouse. 102

Fig. 4.8 Measured mean daily temperature of the glasshouse. 102

Fig. 4.9 Profile moisture content changes during drying cycle 4. 105

Fig. 4.10 Profile moisture content changes during drying cycle 9. 105

Fig. 4.11 Measured cumulative actual evapotranspiration (AET) for drying cycles 4 & 9. 106

Fig. 4.12 Ratio of actual (AET) to potential (PET) evapotranspiration during drying cycles 4 & 9. 106

Fig. 4.13 Measured cumulative actual evapotranspiration (AET) from the lysimeter by the profile method. 108

Fig. 4.14 Comparison of cumulative potential with actual evapotranspiration as measured by the profile and drainage methods. 108

Fig. 4.15	Measured soyabean root depth development.	110
Fig. 4.16	Measured Leaf Area Index of the stand.	110
Fig. 4.17	Measured height development of the stand.	111
Fig. 4.18	Simulated and observed cumulative water loss under optimum model parameter values.	116
Fig. 4.19	Simulated and observed cumulative water loss under upper boundary model parameter values.	117
Fig. 4.20	Simulated and observed cumulative water loss under lower boundary model parameter values.	118
Fig. 4.21	Simulated daily water losses from the lysimeter.	122
Fig. 4.22	Simulated cumulative water losses from the lysimeter.	123
Fig. 4.23	Comparison of measured and simulated moisture contents in the root layers.	125
Fig. 4.24	Comparison of measured and simulated moisture contents in the root zone.	126
Fig. 4.25	The effect of MNGSMD on the yield ratio (AT/PT), MNGIRG = 100% .	130
Fig. 4.26	The effect of MNGSMD on the yield ratio (AT/PT), MNGIRG = 50% .	130
Fig. 4.27	The effect of MNGSMD on the total req'd irrigation (MNGIRG = 100%).	132
Fig. 4.28	The effect of MNGIRG on the total req'd irrigation (MNGSMD = 50%).	132

CHAPTER 5:

Fig. 5.1	Typical soil moisture characteristics curve.	139
Fig. 5.2	Moisture characteristic of the Auchincruive sand measured by the pressure plate test.	144
Fig. 5.3	Comparison of empirical models with measured moisture characteristic curve. (see text for details of models).	152

Fig. 5.4a Log-Log plot of discrete-form models of moisture characteristic. 153

Fig. 5.4b Log-Log plot of closed-form models of moisture characteristic. 154

CHAPTER 6:

Fig. 6.1 Schematic diagram of piston-type flow with sharp wetting front in the Green-Ampt model. 164

Fig. 6.2 Flow chart of the Bouwer infiltration model for nonuniform soils. 169

Fig. 6.3 Simulated cumulative infiltration curve by Bouwer's model. 171

Fig. 6.4 Model sensitivity to depth of water on surface (parameter H). 174

Fig. 6.5 Model sensitivity to soil layer thickness (parameter L). 174

Fig. 6.6 Model sensitivity to saturated hydraulic conductivity (parameter Ks). 175

Fig. 6.7 Model sensitivity to saturated moisture content (parameter Θs). 175

Fig. 6.8 Model sensitivity to wetting front pressure (parameter Pw). 176

Fig. 6.9 Model sensitivity to initial soil moisture content (parameter Θi). 176

Fig. 6.10 Schematic representation of wetting fronts in two dimensional infiltration. 180

Fig. 6.11 Simulated 2-D wetting pattern for soil A. 186

Fig. 6.12 Simulated 2-D wetting pattern for soil B. 187

Fig. 6.13 Measured and predicted 2-D infiltration in soil A. 189

Fig. 6.14 Measured and predicted 2-D infiltration in soil B. 189

Fig. 6.15 Simulated 2-D wetting pattern for soil C. 190

Fig. 6.16 Simulated 2-D wetting pattern for soil D. 191

Fig. 6.17 Measured and predicted 2-D infiltration in soil C. 193

Fig. 6.18 Measured and predicted 2-D infiltration in soil D. 193

Fig. 6.19 Simulated 2-D wetting pattern for soil A, under reducing vertical Ks. 195

Fig. 6.20 Simulated 2-D wetting pattern for soil A, under reducing horizontal Ks. 197

Fig. 6.21 Simulated 2-D wetting pattern for soil A, with horizontal Ks > vertical Ks. 198

Fig. 6.22 Simulated 2-D wetting pattern for soil A, with vertical Ks > horizontal Ks. 199

Fig. 6.23 Simulated 2-D wetting pattern for soil A, with nonuniform moisture contents. 201

Fig. 6.24 Simulated 2-D wetting pattern for soil A, with nonuniform & anisotropic profile. 202

CHAPTER 7:

Fig. 7.1 Phases of surface irrigation flow process. 211

Fig. 7.2 Schematic diagram of surface and subsurface flow profiles. 214

Fig. 7.3 Assumed water surface profile at cutoff and recession times. 220

Fig. 7.4 Comparison of observed and simulated advance and recession curves for the border case of Strelkoff. 224

Fig. 7.5 Comparison of observed and simulated advance and recession curves for the border case of Jaynes (1). 225

Fig. 7.6 Comparison of measured and simulated advance and recession curves for the border case of Jaynes (2). 226

Fig. 7.7 Comparison of measured and simulated advance and recession curves for the furrow case of Levien & de Souza. 228

Fig. 7.8 Sensitivity of surface irrigation model to inflow rate. 229

Fig. 7.9 Sensitivity of surface irrigation model to Manning's roughness. 230

Fig. 7.10 Sensitivity of surface irrigation model to field slope. 231

Fig. 7.11 Sensitivity of surface irrigation model to infiltration coefficient (k). 232

Fig. 7.12 Sensitivity of surface irrigation model to infiltration coefficient (d). 233

Fig. 7.13 Sensitivity of surface irrigation model to furrow shape factor (C). 234

Fig. 7.14 Sensitivity of surface irrigation model to furrow shape factor (M). 235

Fig. 7.15 Diagram of discretization of advance-recession curve for volume calculations. 238

Fig. 7.16 Flow chart of surface irrigation efficiency optimization model. 247

Fig. 7.17 Simulated response of application efficiency (Ea) to inflow rate under constant duration of 22 mins. 254

Fig. 7.18 Simulated response of application efficiency (Ea) to inflow rate under constant duration of 29 mins. 254

Fig. 7.19 Simulated response of application efficiency (Ea) to inflow rate under constant duration of 36 mins. 255

Fig. 7.20 Simulated response of application efficiency (Ea) to inflow rate under constant duration of 43 mins. 255

Fig. 7.21 Simulated response of application efficiency (Ea) to inflow rate under constant duration of 50 mins. 256

Fig. 7.22 Flow chart of the border design model (BORDERDZ). 260

Fig. 7.23 Flow chart of the furrow spacing design model (FURROWSP). 265

Fig. 7.24 Schematic definition of the deep percolation loss ratio (DPLR) and time of root zone wetting (Trz). 267

CHAPTER 8:

Fig. 8.1 Schematic representation of application rate nonuniformity under single nozzle sprinkler irrigation. 283

Fig. 8.2 Schematic representation of infiltration and runoff processes. 286

Fig. 8.3 Flow chart of the Point Exces Rainfall Model (PERM). 292

Fig. 8.4 Schematic diagram of the Rutter interception model. 295

Fig. 8.5 Cascading flow model for redistribution of infiltrated water in the soil layers. 303

Fig. 8.6 Three possible flow conditions at the lower boundary of the soil profile. 307

Fig. 8.7 Schematic diagram of infiltration under intermittent rainfall when rain gap is less than redistribution time. 310

Fig. 8.8 Simulated excess rainfall and infiltration rates (case 1 of Table 8.2). 316

Fig. 8.9 Simulated excess rainfall and infiltration rates (case 2 of Table 8.2). 317

Fig. 8.10 Simulated excess rainfall and infiltration rates (case 3 of Table 8.2). 318

CHAPTER 9:

Fig. 9.1 Schematic diagram of cumulative distribution function for different coefficients of variation (Cv). 328

Fig. 9.2 Determination of the fractional area Q(Y), under normalized rate Y. 332

Fig. 9.3 Flow chart of the sprinkler efficiency evaluation model (SPRNDEFF). 334

Fig. 9.4 The effect of application rate and coeff. of variation on sprinkling uniformity. 341

Fig. 9.5 The effect of coeff. of variation on the application efficiency (Ea). 342

Fig. 9.6 The effect of rate and duration on application efficiency (Ea) for a normal distribution. 343

Fig. 9.7	The effect of rate and duration on the uniformity coefficient (Uc).	344
Fig. 9.8	The effect of application rate & saturated hydraulic conductivity on application efficiency (Ea).	346
Fig. 9.9	The effect of application rate & saturated hydraulic conductivity on uniformity coefficient (Uc).	347
Fig. 9.10	The effect of initial soil moisture content on application efficiency (Ea).	348
Fig. 9.11	The effect of initial soil moisture content on the uniformity coefficient.	350
Fig. 9.12	The effect of rate and duration on application efficiency (Ea) for a uniform distribution.	352

LIST OF TABLES

CHAPTER 1:

Table 1.1	Average application efficiencies of various irrigation methods.	7
Table 1.2	Example of water losses at different levels of the conveyance system.	9

CHAPTER 3:

Table 3.1	Hydrological characteristics of some irrigation models.	33
Table 3.2	Soil moisture deficit threshold levels for maximum crop yield.	36
Table 3.3	Data requirements of some empirical potential evapotranspiration (PET) models.	55
Table 3.4	Experimental results of soil evaporation model parameters.	72
Table 3.5	Soil evaporation parameters for several soil types.	73

CHAPTER 4:

Table 4.1	Definition of symbols used in Fig. 4.3.	84
Table 4.2	Definition of symbols used in the layer sorting algorithm.	91
Table 4.3	Lysimeter experiment sampling dates and water balance.	104
Table 4.4	Scheduling model simulation results for optimum, upper, and lower boundary parameter values.	115
Table 4.5	Sensitivity analysis of the scheduling model to input parameters.	121
Table 4.6	Simulated irrigation schedules for diefferent management practices.	128
Table 4.7	Simulated effects of MNGSMD and MNGIRG on the yield ratio and total required irrigation depth.	129

CHAPTER 5:

Table 5.1	Representative values for the Brooks-Corey parameters (after McCuen etal 1981).	149
Table 5.2	Representative values for the Brooks-Corey parameters (after Clapp & Hornberger 1978).	150
Table 5.3	Retention curve parameters estimated by various methods for the Auchincruive sand.	155
Table 5.4	Estimated field capacity, wilting point, and wetting front pressure parameters for Auchincruive sand.	157
Table 5.5	Summary of the measured properties of the Auchincruive sandy soil.	158

CHAPTER 6:

Table 6.1	Example of input parameters required for the model of Bouwer.	170
Table 6.2	Sensitivity of the infiltration parameters 'c' and 'n' to the soil physical properties.	177
Table 6.3	Soil parameters and test dimensions for the two dimensional infiltration model.	185

CHAPTER 7:

Table 7.1	Border irrigation data used in the simulations (after Strelkoff 1977).	244
Table 7.2	Simulated efficiencies for the border irrigation data of Table 7.1.	245
Table 7.3	Example of optimum border inflow rate and duration for maximum application efficiency (data of Table 7.1).	251
Table 7.4	Example of design of borders.	262
Table 7.5	The effect of maximum allowable soil moisture deficit on the design length, width and irrigable area of the border system in Table 7.4.	263
Table 7.6	Example of input data and results for the design of furrow spacing, depth and width.	269
Table 7.7	Example of furrow length design.	275

Table 7.8 Example of an operations schedule for a border irrigation system. 277

Table 7.9 Example of an operations schedule for the same data base as Table 7.8 but with managment factors: days 1 to 160: MNGSMD = 25%, MNGIRG = 100%). 278

CHAPTER 8:

Table 8.1 Definition of terms used in the flow chart in Fig. 8.3. 293

Table 8.2 Input rainfall data for 3 rainfall cases. 313

Table 8.3 Assumed soil physical parameters for all 3 rainfall case studies. 313

Table 8.4 Results of PERM simulated infiltration and excess rainfall runoff and comparison with Chu's model and recorded values. 315

Table 8.5 Sensitivity analysis of PERM to the soil parameters for case 3. 320

CHAPTER 9:

Table 9.1 Soil profile data set used in the sprinkler performance simulation model. 338

Table 9.2 Example run of the sprinkler performance evaluation model. 339

APPENDIX:

Table A3.1 Albedo values of some soils. 389

Table A3.2 Albedo values of some vegetation surfaces. 390

Table A3.3 Empirical coefficients for the Penman wind function f(u)= a'+b' U2. 395

Table A3.4 Minimum bulk stomatal resistance of several well watered crops. 401

Table A3.5 Meteorological data base used in the testing of the POTEVPTN model. 404

Table A3.6	Sensitivity analysis of POTEVPTN model to input variables.	407
Table A3.7	Alfalfa-based crop coefficients of various crops.	409
Table A3.8	Root depth growth, in time and space, of several crops, up to the day of maximum rooting depth.	410
Table A3.9	Leaf area indices of several crops.	414
Table A8.1	Canopy storage capacity (Sc) of several crops.	417

LIST OF PLATES

Plate 4.1	The lysimeter used in the experiment.	99
Plate 5.1	Pressure Plate apparatus.	142

SYNOPSIS

The world-wide average irrigation efficiency is only 30 % . Faced with dwindling supplies of suitable land and water, increasing the efficiency of water use is the most feasible non-capital intensive means of maintaining and increasing crop productions in many non-industrialized countries.

A major source of inefficiency is the existance of technical gaps between small-scale farmers and regional water authorities regarding the efficient operational management of on-farm irrigation systems. The objective of this study is to establish computer-based mathematical methods for the evaluation of surface and sprinkler irrigation efficiencies under a variety of environmental and operational conditions.

Irrigations are scheduled by simulating the continuous water balance of nonuniform soils with growing root zones and nonuniform rooting patterns. The model is calibrated with lysimetric data and is responsive to soil and crop characteristics and soil-moisture-deficit management practices.

A surface irrigation simulation model evaluates irrigation efficiencies for border and furrow systems. An optimization routine establishes the most efficient operating policy (ie: inflow rate and duration). For a case study, comparisons between actual and optimum policies show that application

efficiency is improved by 20%, the required irrigation volume is reduced by 33%, the runoff volume by 63%, and irrigation duration by 24 minutes.

A physically-based excess-rainfall model seperates point-applied, unsteady, intermittent, precipitation into it's hydrological components, and combined with a statistical model of the spatial application-rate distribution pattern, simulates the water balance under a sprinkler unit and determines the operational irrigation efficiencies.

The continuous and event-based irrigation processes are integrated through the developement of a composite-layer sorting algorithm and one and two dimensional models of infiltration into nonuniform soils. The integrated systems approach allows for the real-time management of irrigation systems where the best operating policies are chosen in response to environmental and economical changes.

ACKNOWLEDGEMENTS

The author wishes to express his gratitude to professor George Fleming for his supervision of this thesis and for his guidance and encouragement during the course of this research.

Thanks are also due to my friends and coleagues in the university and in the Water and Environmental Management Group whose company made this joūrney bearable.

Finally my heartfelt thanks go to my parents and sisters for their unending moral and financial support throughout these many years of study.

CHAPTER 1 INTRODUCTION

The importance of water resources management was realized as far back as 3200 BC when man learnt to divert rivers for irrigation (Biswas 1970). The construction of earth and masonary dams, diversion and irrigation canals and qanat systems in Egypt, Mesopotamia, Persia, India and China bear witness to the civil engineering skills of these ancient civilizations. The qanat systems of Iran for instance, first reported in 720 BC, still provide for two thirds of rural agricultural and domestic water supplies (Wulff 1966, Kayhan 1988).

In 1760 BC King Hammurabi of Babylon condemned those who neglected or mismanaged their irrigation systems to slavery and certain death. Today a simillar fate awaits millions of lives all over the globe. The seemingly endless expansion of world population has meant that on average 2.7 hungry mouths are added to the masses every second (UN 1988). For the period between 1970 and 1985 the world witnessed a 31% population increase , while the percentage of people working on the land dropped by 12.4%, the area of arable land decreased by 3.9% (UN 1985) and the world's forests were reduced by 4.8% (FAO 1986).

Today the rapid developments in the information and communication technologies have brought the miseries of drought and famine into every living room with the effect that human society makes increasing demands on the scientific community to find solutions to such unacceptable facets of existance.

There is no single magical solution to famine because it's causes stem not only from nature but also from social, political and economical roots which allow the unbridled exploitation of limited land, water and vegetative resources. The consequences are that populations grow and spread, forests retreat, climates change adversely, arable lands are exhausted and marginal lands soon cease to produce. The destruction of forests by chain saws and acid rains, the loss of productive soils to salinity and erosion, and the destruction of the planet's ozone layer bring nearer the environmental catastrophe that awaits mankind . Only with proper management of global resources can the negative effects of man's influence on nature be mitigated.

The methodology for the solution of any problem can be described by the flowchart in Fig. 1.1 . In the context of this thesis the need has already been recognised as the avoidance of famine and provision of food for future generations. The problem can be defined by considering that the world has limited resources of land and water which are becoming less and less suitable and available for food production. The causes are many but the losses of soils to salinity and erosion, siltation of rivers and reservoirs and the

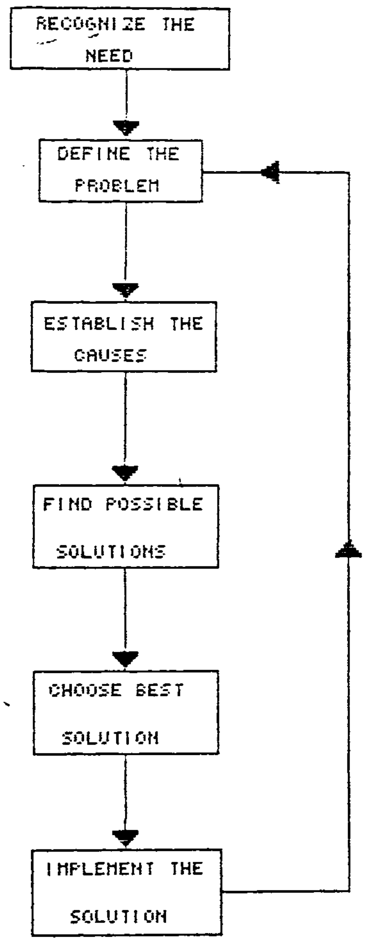

Fig. 1.1 Flow chart of the methodology for solving problems.

subsequent floods, pollution of surface and ground water resources, and increasing demands by municipal and industrial consumers have aggravated the situation.

The 1988 floods in Sudan and Bangladesh also testify to the catastrophic consequences of watershed de-vegetation . Removal of the vegetation canopy causes rapid runoff and increases soil erosion with the result that natural waterways and manmade reserviors silt up and flooding becomes inevitable (New Civil Engineer 1988) . The Bangladesh flood for instance inundated three quarters of the country's land area with devastating loss of cultivated land and safe drinking water (World Water 1988).

The depletion of the ozone layer, due in main to the buildup of man-made gaseous pollutants in the upper atmosphere, has given rise to the greenhouse effect in which the planet warms up and weather patterns undergo changes. The recent 1988 droughts in the American midwest and southeast, blamed partially on the greenhouse effect, lasted for three crucial months in which more than one fifth of the cereal crops were lost (New Scientist 1988).

As with any limited resource when demand is higher than supply then continued production can only be maintained by maximizing the efficiency of use of the basic materials. To maintain and increase crop production under limited land and water resources many solutions have been sought and implemented with good short term results though not necessarily with healthy long term prospects.

Intensive farming with increasing use of chemical fertilizers, pesticides and herbicides, along with new methods in plant micro-propagation and genetic manipulation have seen the efficiency of land use (in terms of yield per unit area) maximized to such an extent that in some parts of the world excess food production has become a problem in itself.

A case in point is that of Europe. The experiences of the second world war and the subsequent years of reconstruction and growth showed the inadequecies of food production. In 1958 the Common Agricultural Policy (CAP) of the European Economic Community (EEC) was brought into operation to guarantee a good price for whatever food the farmers produced. This level of economic security enabled both farmers and industrialists to invest heavily in land, machinary, chemicals and new high yielding crops. The success of the CAP has led to yield increases of between 1 and 2 percent annually ever since. This increase, paralleled in other industrial countries, together with the gradual successes of the 'green revolutions' in some developing countries, has given rise to surpluses in food production in Europe.

In 1986 the EEC produced 14 million tons of surplus grain (The Independent 1988). In 1987 the expenditure on the purchase of surplus agricultural produce , for storage and destruction, rose to 16 billion pounds. To reduce such losses, in 1988 a ceiling of 19.5 billion pounds was decided upon, along with a reduction in land area and production levels of 20 percent.

In Britain today, on average 150 kg/ha per year of inorganic nitrogen fertilizers are applied to the fields, ten times as much as in 1945, and at an annual cost to the farmer of 500 million pounds. It is estimated that of this amount of fertilizer about half is not used by the crops but is leached as dissolved nitrates to the water table. Nitrate pollution causes eutrophication in reservoirs, lakes and rivers leading to algal growth and loss of water quality and wild life.

While chemicals can help increase the efficiency of land use, proper management of irrigation systems can provide a means of increasing both land and water use efficiency without major environmental damage.

Some methods of irrigation have not changed since times of old. Perhaps the first irrigation method man witnessed was the inundation of fields by natural flooding of rivers. Soon he realised that the movement of water over the land could be controlled and he built basins, border checks and furrows. All ensuing developments in the field of water engineering were mainly concerned with the control, storage, diversion and conveyance of river and ground water resources while the basic method of irrigation remained the same for centuries.

Although surface irrigation methods are energy efficient (since conveyance and application are by gravity), the relatively large runoff and drainage losses result in low application efficiencies (Table 1.1). With the onset of the industrial revolution and the invention of pressure pumps the method of sprinkler irrigation was devised in early 1900 (Israelsen and Hansen 1962) to both increase application efficiency and to bring into use more marginal lands. Land grading is not necessary and runoff can be virtually eliminated if application rate is kept low.

Table 1.1 Average application efficiencies of various irrigation methods (UN 1985).

Irrigation method	Soil type	Application efficiency (%)
Basin	Clay, Heavy clay	40–50
Furrow	Light soil	60
Border	Light soil	60
Sprinkler	Sand, Loam	70
Trickle	–	90–100

In sprinkler irrigation water losses still occur by a combination of direct evaporation, wind transportation, interception, soil evaporation and drainage. In areas where such losses are significant localized methods of irrigation become necessary and so the trickle irrigation method was born in the 1930's (Balogh and Gergely 1985). As the name implies water is delivered through narrow emitters under each plant in small continuous trickles. Soil evaporation and drainage are drastically reduced resulting in very high application efficiencies (Table 1.1).

Other less commonly used methods include the sub-irrigation method where by carefull drainage and recharge control in low lying lands, the groundwater table can be kept at a desirable depth for root uptake. Micro-spray irrigation is similar to the sprinkler method with the difference that water is delivered below the canopy as a fine mist. Surge irrigation is a method of releasing water into furrows in surges rather than as a continuous stream in an effort to increase application uniformity. An idea which has not as yet met with great success is the 'Agronet' system in which the ground water is brought up to the root zone by an electrical field created between buried anodes and cathodes (New Scientist 1985). In some parts of the Middle East porous pots have been partially buried under plants and periodically filled with water and covered to allow slow seepage and wetting of the root zone. In the more arid regions worshipers are even obliged to perform their daily ablutions under saplings to save water.

From a world wide study of irrigation practices Bos and Nugteren (1974) concluded that the overall efficiency of irrigation is only about 30% . More than 70% of the water withdrawn at the source is lost in conveyance and application on the field with the result that potential crop yield is not realized. An example of the water losses in the conveyance system is shown in Table 1.2 .

Table 1.2 Example of water losses at different levels of the conveyance system (data for unlined canals in an Indian irrigation district, Datye and Patil 1987).

System Parts	Losses in percent	Efficiency in percent	Cumulative efficiency
Main Canal	23.8	76.2	
Branch II	18.5	81.5	62.1
Distributory	6.2	93.8	58.2
Minors	43.9	56.1	32.7
Field Channels	16.7	83.3	27.0

When new irrigation projects are being planned the total area of cultivation is often limited by the water available. If the efficiency of water use could be improved, the area of land irrigable would increase correspondingly to provide additional employment and crop production. While the lining of canals with impermeable material can reduce water losses in the conveyance system, the improvement of irrigation efficiencies at the individual farm level is a more complex proposition.

A recent report on the status of irrigation management in the non-industrialized countries (ODU Bulletin 1988) concluded that:

> " There can be no doubt that one of the principle factors contributing to inefficient water use in Third World irrigation is the lack of clear definition of management and farmer responsibilities. System managers cannot undertake to supply guaranteed amounts to individual farmers because, unlike irrigated lands in developed countries (where the land holdings are rarely less than 50 ha and may be as great as 1000 ha) the average plot size in Third World irrigation schemes is of the order of 0.5 to 1.0 ha . No irrigation authority can afford the resources to manage distribution at this level ."

Today, with the advent of inexpensive, high storage capacity micro-computers the efficient operational management of small-scale irrigation systems, as part of or independent from the larger-scale water resources management schemes, is technically feasible.

Organizations such as water-user groups and irrigation co-operatives have proved to be effective administrative links between the water supply authorities and the individual farmers. Important technical gaps however still exist on the operational level. Access to micro-computer based simulation systems will fill these gaps by allowing more flexible irrigation scheduling policies in response to real-time environmental changes.

Conventional irrigation scheduling models are often used to establish the frequency and the amounts of irrigation required at each farm. The responsibilty of the irrigation authority, however, is assumed to end at the farm turnout where the farmer is expected to apply the allocated volume of water as best he knows how. Idealy the farmer should not only be advised of the dates and the amounts of irrigation allocated to him, but also of the most efficient operating rule for the application of the water on the field (ie: the optimum flow rate and duration).

The aim of this thesis is to establish methods for the evaluation of irrigation efficiencies at the farm level, under a variety of soil, crop and management practices, so as to improve the operation of surface and sprinkler irrigation systems for optimal water use.

The method to be tested is the use of the mathematical model. The flow chart of the integrated systems approach is shown in Fig. 1.2 . Each hydrological process is modelled seperately and integrated into a continuous water balance model which also controls the parameters of the event-based operations models.

The various irrigation efficiency terms used in the performance evaluation of surface and sprinkler irrigation systems are defined in chapter 2. In chapter 3 the irrigation scheduling model is introduced and methods for the estimation of potential crop evapotranspiration, soil evaporation and transpiration are described.

The continuous water balance of a dynamic, nonuniform root zone is modelled in chapter 4 to estimate actual evapotranspiration losses and soil moisture content changes. The simulation results are compared with measured lysimeter data, and the effects of management practices on irrigation scheduling and water use are simulated.

Chapter 5 investigates the physical properties of soil-water interactions and compares a number of empirical methods of analysis with experimental data. The process of infiltration into nonuniform soils is analysed in chapter 6 and one-dimensional and two-dimensional models are developed.

The one-dimensional and two-dimensional infiltration models of chapter 6 are utilized in the

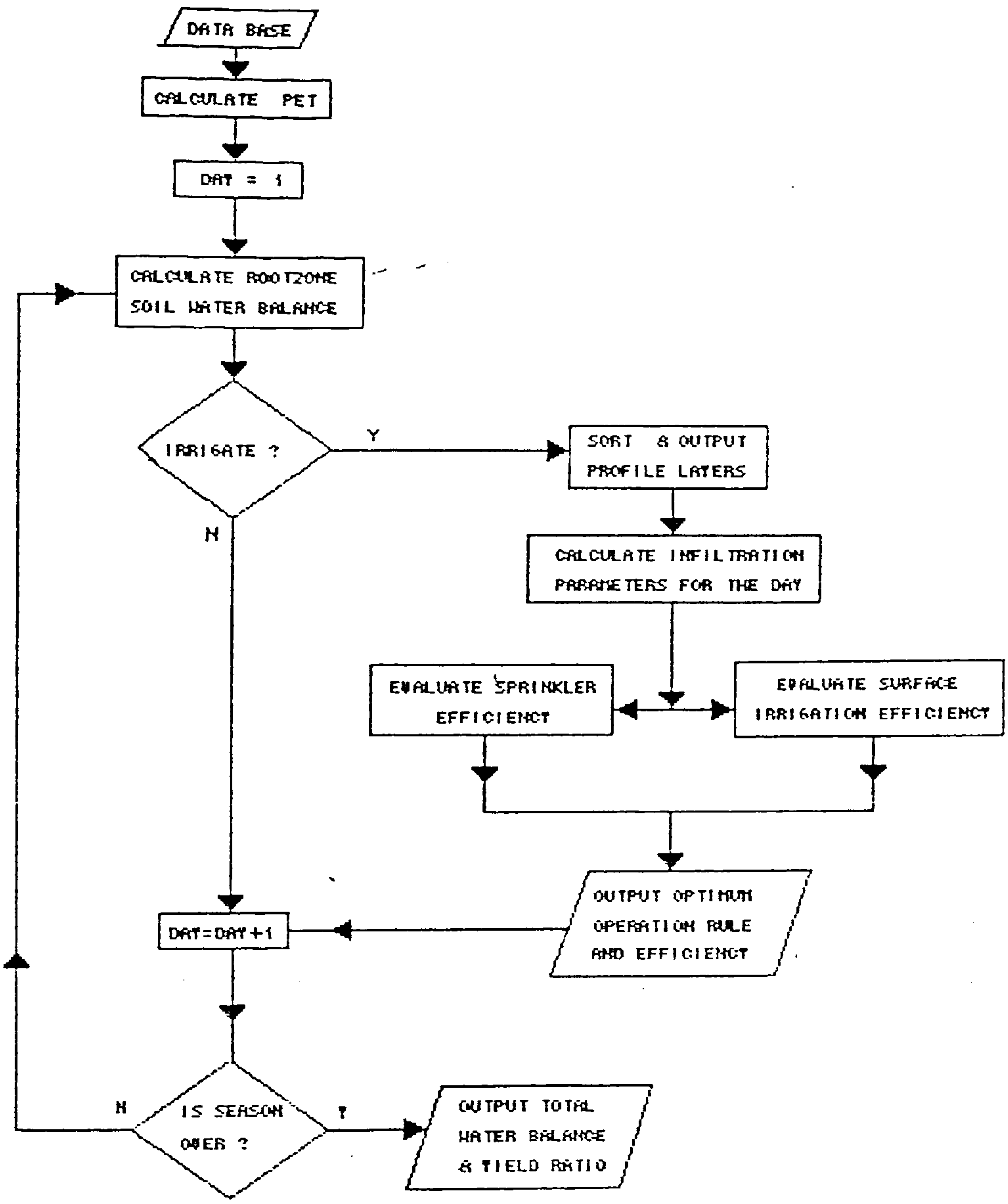

Fig. 1.2 Flow chart of the integrated operational irrigation management model.

surface irrigation model of chapter 7 for simulating the effects of operational practices on the efficiencies of border and furrow irrigation systems. Models for the design and optimum operational management of the systems are also presented.

The soil water balance under a sprinkler unit is simulated by a point excess-rainfall model which uses the one dimensional infiltration function of chapter 6 to estimate the water losses in the root zone from intermittent, unsteady precipitation.

Chapter 9 sees the introduction of a sprinkler irrigation performance evaluation model which combines a statistical application-rate distribution pattern and the point excess-rainfall model of chapter 8 to evaluate the irrigation efficiencies and application uniformity of a sprinkler unit .

Finally, chapter 10 consists of the discussions and conclusions. The references and appendix sections complete this thesis.

CHAPTER 2 DEFINING IRRIGATION EFFICIENCIES:

2.1 Introduction:

The term 'irrigation efficiency' is used to express the performance of a complete irrigation system or components of that system. Jensen etal (1967) defined irrigation efficiency as " the ratio, usually expressed as per cent, of the volume of the irrigation water transpired by the plant, plus that evaporated from the soil, plus that necessay to regulate the salt concentration in the soil solution, and that used by the plant in building plant tissue to the total volume of water delivered, stored or pumped for irrigation ".

Efficiency analysis is therefore a means for the quantitative evaluation of water losses at different stages of irrigation. Water losses by seepage and evaporation in the conveyance network, on-farm losses due to evaporation, deep percolation and runoff, all represent wastages of a precious resource. The factors which effect these water losses are many. The geometry and lining of canals, maintenance of canals, on farm irrigation methods and practices, quality of labour, soil and crop types, farm dimensions and irrigation scheduling practices, all influence losses of water from a system.

Each stage of the irrigation system, from conveyance to on-farm application, has therefore one or more associated efficiency terms which describe the relative water losses during that process. In the context of this study, only irrigation efficiencies at the farm level are considered for evaluation.

Two approaches are normally used to evaluate the water distribution profile on the field. The first is based on the actual distribution of water depths on the irrigated area and is a deterministic approach. The second is a statistical approach and is based on the cumulative frequency distribution of actual water depths and areas (Hart etal 1979).

In surface irrigation, the vertical and horizontal movement of water can be simulated by using deterministic mathematical models, based on the principles of hydrodynamics (see chapter 7). Using such models, the depth of infiltration, at any time and at any point on the filed, can be quantified. Figure 2.1 shows a typical post-irrigation infiltration-depth profile for surface irrigation. The volumetric distribution of water in the field can then be determined and the various irrigation efficiencies evaluated.

In sprinkler irrigation, the shape of the infiltration-depth profile is less predictable since the spatial distribution of the water emerging out of the sprinkler nozzle is subject to many unpredictable factors. The nozzle height, the orifice size, the water pressure, the wind speed and direction, the evaporation and interception rates, and the soil and crop types,

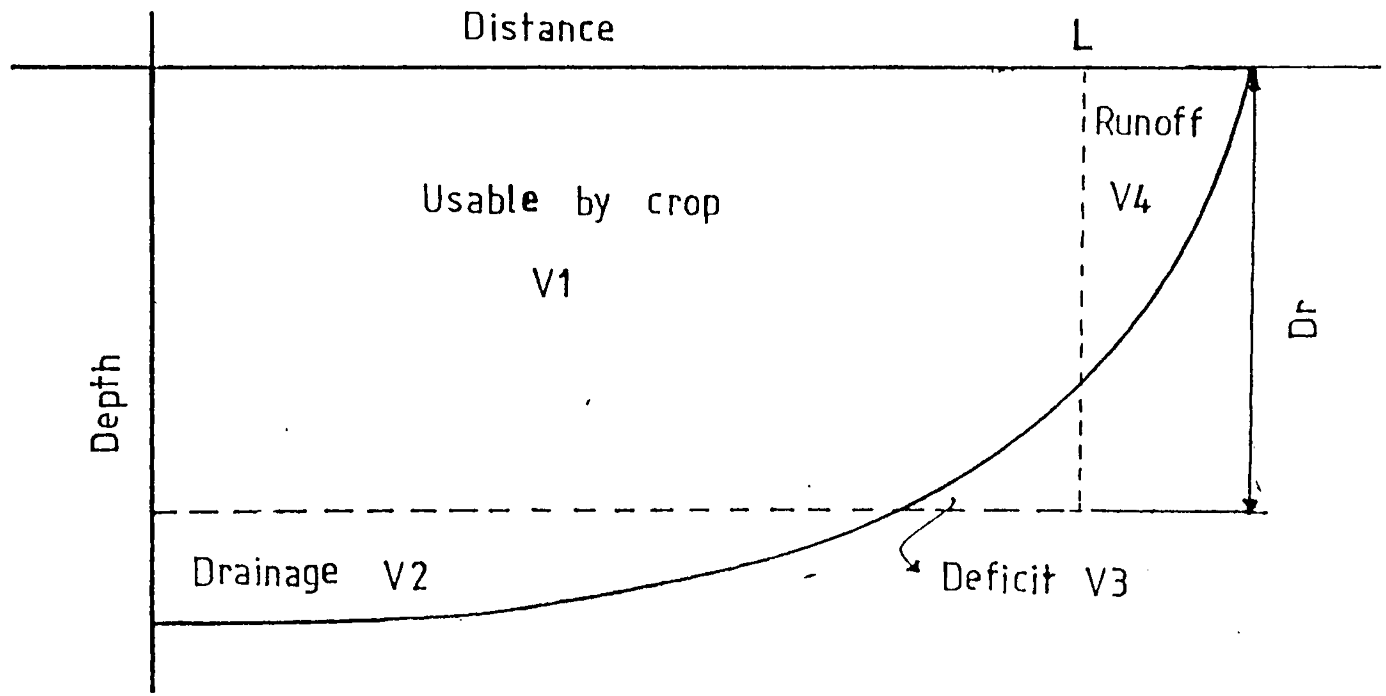

Fig. 2.1 Schematic diagram of surface irrigation infiltration depth profile (V1, V2, V3 & V4 are volumes of refill, drainage, deficit and runoff respectively (m3); and Dr is the required depth (mm) to fill the root zone).

all effect the horizontal and vertical distribution pattern of the applied water. Figure 2.2 shows an idealized wetting pattern under sprinkler irrigation. To compensate for the deficits near the outer edges, adjacent sprinklers are often spaced such that their radii of coverage overlap one another (Hillel 1987).

Under field conditions, where the spatial distribution of water cannot be accurately simulated by purely deterministic models, the statistical approach becomes necessary. The area of coverage of a sprinkler unit is divided into a number of segments and the depth of water received on the array of areas is measured. The cumulative frequency distribution of the infiltrated depths is then represented as the fraction (Ap) of the area that received a depth of water of (Yp) or greater (Fig. 2.3). The fraction of area receiving a depth ranging from between Yk and Yp is therefore found as (Ap-Ak).

The relationship between applied depth and receiving area can then be used to calculate the volumetric distribution of water on the field, and with knowledge of the required water depth to fill the root zone, the various irrigation efficienies can be evaluated. It should be noted that the statistical data are representative of the conditions for that site and sprinkler unit alone.

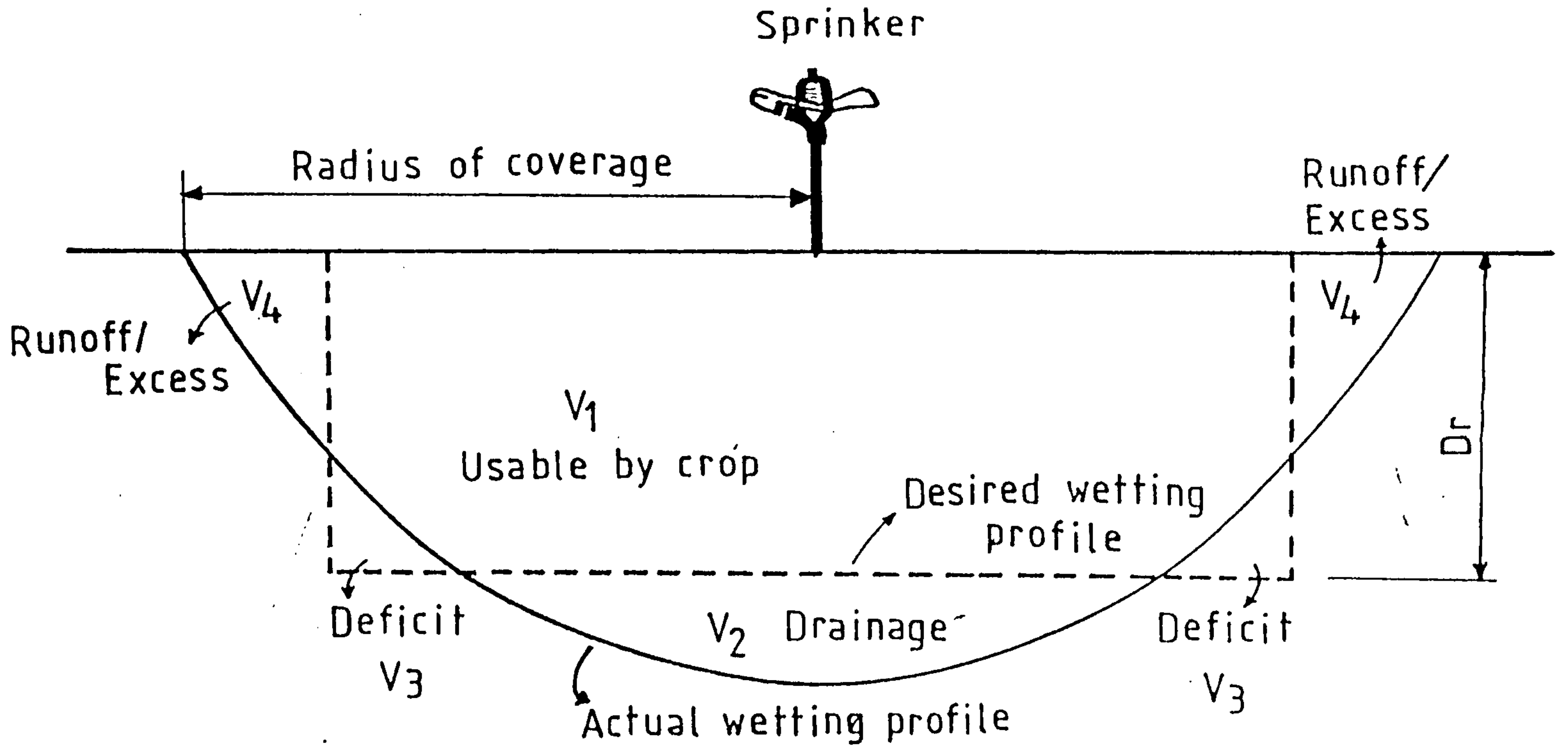

Fig. 2.2 Idealized wetting profile under sprinkler irrigation (V1, V2, V3 & V4 are volumes of refill, drainage, deficit and runoff/excess respectively (m3); and Dr is the required depth (mm) to fill the root zone).

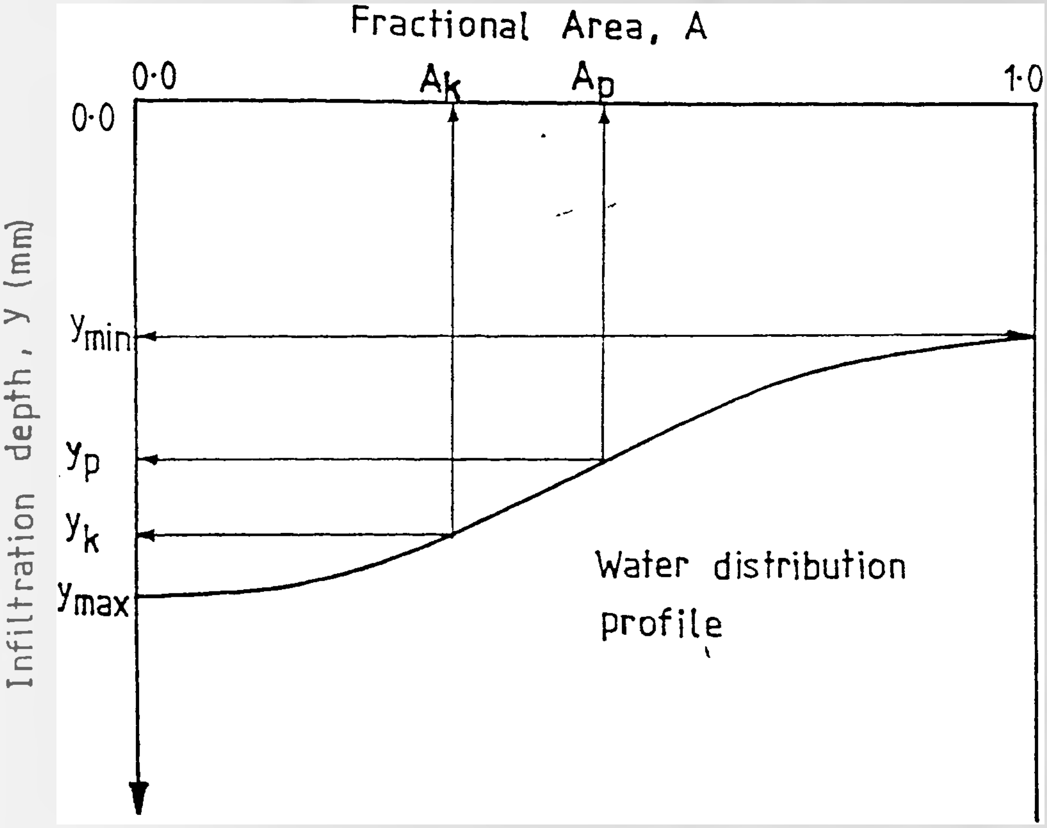

Fig. 2.3 Schematic diagram of the cumulative frequency distribution of infiltrated water depth in sprinkler irrigation.

2.2 Evaluating the Efficiencies:

Hart etal (1979) list some 18 different definitions of efficiencies used by researchers. Others have attempted to standardize various efficiency terms. These include the American Society of Civil Engineers (Kruse 1978), United Nations Food and Agricultural Organization (UN 1985), and the International Commission on Irrigation and Drainage (Bos 1985).

The efficiencies that are of interest in this study and which relate to the performance of farm irrigation methods and practices, are defined below for figures 2.1 and 2.2 .

1 - Application Efficiency (Ea) :

This is defined by Blair & Smerdon (1988) as the fraction of water applied to the field which remains in the root zone. The equation for Ea is :

$$Ea = 100 (V1 / (V1 + V2 + V4) \qquad (2.1)$$

where V1 = the volume which remains above the desired application depth (Dr); V2 = the volume which drains below Dr; and V4 = the volume of water which runs off the field.

The application efficiency is a measure of the volume of water remaining in the root zone, relative to the volume of water applied.

2 - Storage Efficiency (Es) :

This is defined by Hart etal (1979) as the fraction of the available root zone water storage that is filled by the irrigation :

$$Es = 100 \left[1- \left(V3/(V1+V3) \right) \right] \tag{2.2}$$

where V3 = the volume of deficit in the root zone.

Storage efficiency is a measure of the volume of water remaining in the root zone, relative to the volume required in the root zone.

3 - Distribution Efficiency (Ed) :

This is defined by Hansen etal (1979) as the extent to which water is uniformly distributed in the field. The equation of Ed is :

$$Ed = 100 \left(1- \left(Vd/Va \right) \right) \tag{2.3}$$

where Vd = average numerical deviation in volume of stored water from average volume stored during irrigation; and Va = average volume stored during irrigation.

The distribution efficiency is a measure of the volumetric sum of the drainage losses and deficiencies, relative to the applied water.

4 - Deficit/Excess Efficiency (Ede) :

The three efficiencies defined in equations 2.1, 2.2 and 2.3 independently describe one aspect of irrigation without indicating the response of the other terms to a chosen level of irrigation. Small applications of water produce a high application efficiency but low distribution and storage efficiencies. Conversely, large applications produce high distribution and storage efficiencies but a low application efficiency. Therefore none of the three definitions mentioned can be chosen singularly to establish the performance of an irrigation system.

Blair & Smerdon (1988) introduced a new concept of efficiency, which combines characteristics from the application, storage and distribution efficiencies. Ede is expressed mathematically by :

$$Ede = Ea.Es / (Ea + Es - (Ea.Es)) \qquad (2.4)$$

The relationship between Ede and Ea and Ed is shown schematically in Fig. 2.4 . At small applications Ede is simillar to Ed. This new concept in efficiency can be used as a criterion for performance when comparing different types and practices of surface irrigation.

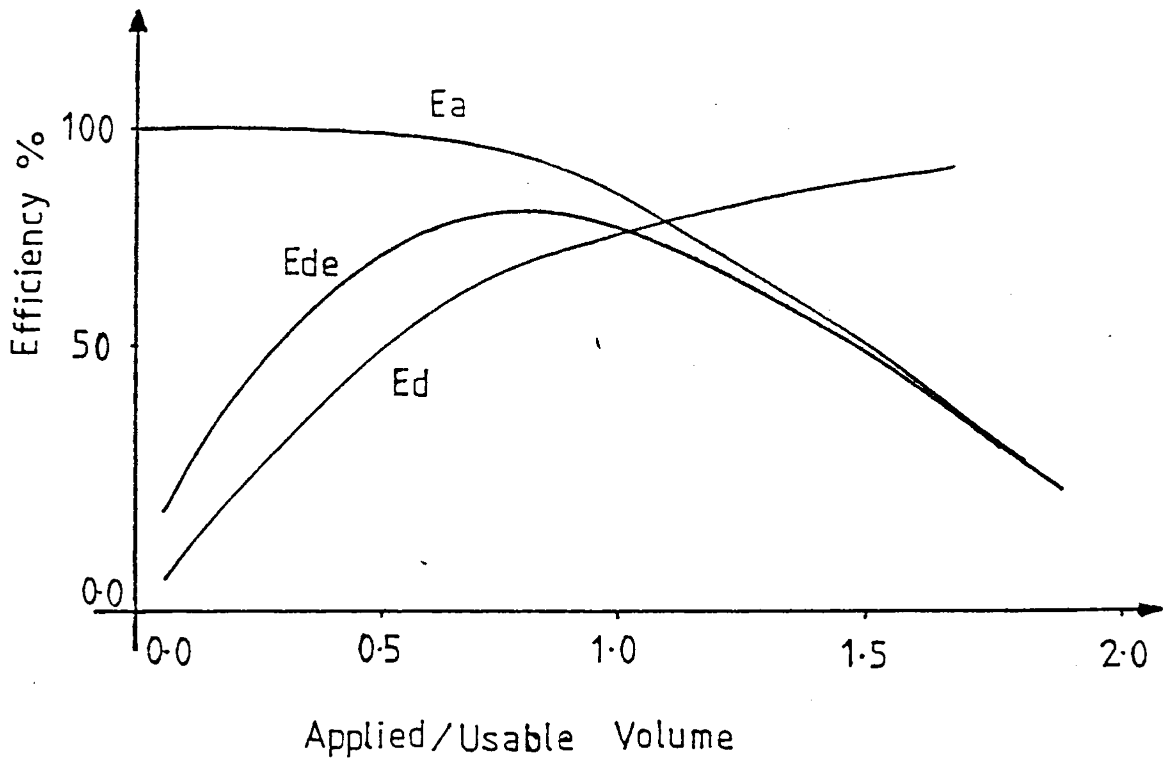

Fig. 2.4 Schematic diagram of the relation between deficit/excess (Ede), application (Ea) and distribution (Ed) efficiencies.

All four efficiency terms (Ea, Es, Ed and Ede), are evaluated every time an irrigation is scheduled. To investigate the effects of operational management practices (ie: allowable soil moisture deficit and inflow rate and duration) on these efficiencies, it is necessary that the water balance of the crop root zone is simulated. This task is undertaken in chapters 3 and 4. The antecedent soil moisture content, on the day of irrigation, determines the infiltration rate of the soil.

The processes of one and two dimensional infiltration are modelled in chapter 6. The infiltration process in turn effects the spatial and temporal movement and distribution of water on the field and in the soil. The simulation of the movement of water in border and furrow irrigation, for the determination of the actual and optimum operational efficiencies, is undertaken in chapter 7. Finally in chapter 9 a deterministic-statistical model is proposed for the evaluation of operational efficiencies under sprinkler irrigation.

CHAPTER 3 IRRIGATION SCHEDULING

3.1 Introduction :

Before any assessment of operational efficiencies can be made, it is necessary to establish the days on which irrigation is required, and estimate how much water should be applied to the field on each occasion. Many factors influence the timing and quantity of water required to replenish that consumed by the crop. The evapotranspiration rate, the soil hydraulic properties, the rooting depth and density and the species of the crop, all influence the rate at which water is removed from the soil. In this chapter an irrigation scheduling model is introduced as an aid to answering the questions of when and how much irrigation should be applied.

3.2 Review of existing models:

On-farm irrigation management is mainly concerned with the problems of applying water, at the right time and in adequate quantities, to ensure the optimal growth of crops. Traditionally irrigation periods were scheduled on the basis that every farmer received his appropriate share of the stream flow on rotation. The amount and frequency of irrigation depended on the number and size of the other farms. This practice is still prevalent in many parts of the world where water laws are handed down through generations (UNFAO 1954, UN 1968, UNFAO 1973, Biswas

1970, Lister 1978).

A study of the interactions between soil, water, plant and atmosphere soon demonstrates that the frequency and depth of irrigation has a marked effect on the final yield of crops. During the vegetative and flowering stages of growth adequate soil moisture is essential for optimum yield. Early in the season, while the roots are still shallow, frequent but light irrigation is required. As the roots extend to their maximum depth in the fruiting stage, larger quantities of water are required to fill the root zone.

Today the timing and amount of irrigation is chosen in response to atmospheric and vegetative demands. Irrigation can be scheduled on a demand basis since many of the operating constraints of a traditional irrigation system can be overcome by the proper control and management of the source of water and its conveyance to individual farms.

The use of mathematical models in irrigation was facilitated by the early hydrological simulation models developed in the early and middle 1960's . An extensive review of various hydrological models is provided by Fleming (1975, 1979). These models are mainly concerned with the simulation of the runoff process from rainfall on a watershed area. In contrast to rainfall-runoff models, irrigation water-balance is mainly concerned with the land-phase processes of the hydrological cycle and as such the established watershed models are often too broad in outlook for the detailed management of farm-scale irrigation systems.

The main objective in the deterministic modelling of irrigation is to simulate the changes in the water balance of the root zone in order to evaluate the quantity and time distribution of losses due to transpiration, evaporation and drainage. The early approach to quantifying these losses was the use of black-box models. Such models relate crop consumptive use to potential evapotranspiration, through a dimensionless growth-stage crop coefficient, by the equation (Withers & Vipond 1974):

$$Wc = Kc \cdot PET \tag{3.1}$$

where :

Wc = consumptive use of water (mm/d)
PET = potential evapotranspiration (mm/d)
Kc = crop coefficient.

The coefficient (Kc) has no physical meaning but represents the combined effects of growth stage, crop height, root depth and soil moisture depletion levels on the evapotranspiration process.

Jensen (1969) and Jensen etal (1970) developed the USDA Irrigation Scheduling Program, based on the function in Eqn. 3.1, to provide an irrigation scheduling system for subscribed farmers. Potential evapotranspiration is estimated for alfalfa by the

Penman method (section 3.5.4), and Kc is experimentally determined for each crop. Irrigation is scheduled for days when the cumulative consumptive use exceeds a critical level. Despite the empiricisms in the model it is still used on about 400000 hectares in the United States (Heerman 1980).

The pioneering works of Gardner (1960), Cowan (1965) and Molz and Remson (1970) on the mathematical analysis of soil water availability to plant roots, encouraged the numerical solution of the physically-based nonlinear partial differential equation of flow through porous media (chapter 6) with the addition of a root uptake term. Such a deterministic approach forms the basis of several soil water balance simulation models, eg : Nimah and Hanks (1973), Feddes etal (1976), Hillel etal (1976), Rowse etal (1978), and Jung and Taylor (1984).

Numerical models, although providing detailed and accurate results, do however suffer from two major disadvantages. First the physical relationships between soil, plant, water and atmosphere are very difficult and costly to measure and secondly the computing time required for numerical accuracy make such models impractical for conjunctive use with other hydrological processes (Stroosnijder 1982).

An alternative to the fully deterministic models is the parametric modelling technique. Stroosnijder (1982) defines parametric models as those models which simulate the various processes of the soil-water balance in a way that is a simplification of the fully physical processes. In this way processes which in reality take place on a continuous basis can be modelled on a longer time scale (eg: hourly or daily) by characteristic parameters which represent the physical properties of that process.

Infiltration, for instance, is the continuous process of water flux into the unsaturated soil. A parametric model allows the effects of moisture potential and hydraulic conductivity on the process of water flow in unsaturated soils, to be represented by such readily measurable soil parameters as field capacity, saturation moisture content, saturated hydraulic conductivity and wetting front pressure (chapters 5 and 6).

The use of parametric models in irrigation has evolved along side the developments in the mathematical modelling of the components of the hydrological cycle. The relationships between the irrigation-relevant hydrological processes is illustrated by the SPAW model of Saxton etal 1974, (Fig. 3.1).

Evapotranspiration, interception, runoff, infiltration and drainage form the basic hydrological processes that control the water balance in the root zone. Each process has seen continuous, independent mathematical development, with the result that it is

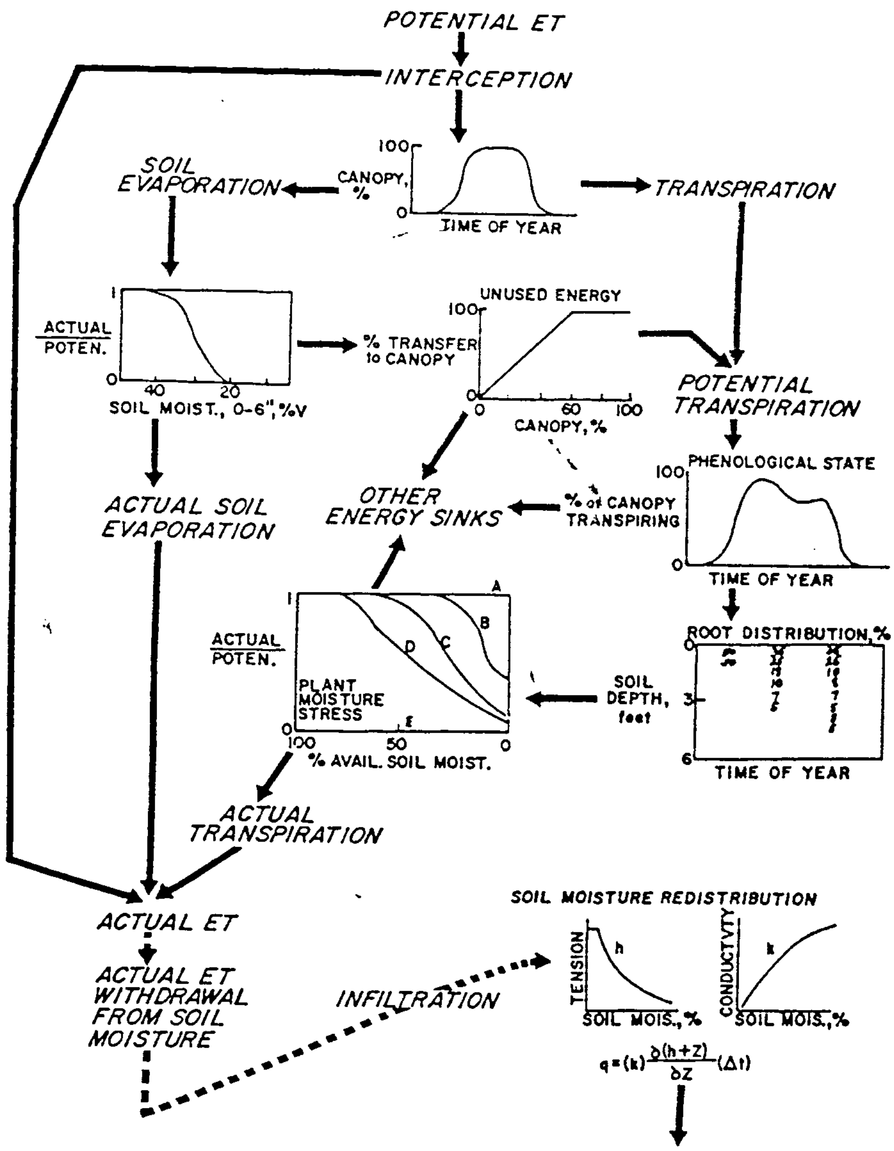

$$q = (k)\frac{\partial(h+Z)}{\partial Z}(\Delta t)$$

Fig. 3.1 Hydrological processes in the Soil-Plant-Atmosphere-Water continuum represented by the SPAW model of Saxton etal (1974).

difficult to undertake a critical, comparative categorization of the different irrigation models. Indeed some models used today in irrigation management were not originally designed for that purpose. A survey of reported irrigation-related models with some of their characteristics is shown in Table 3.1 .

The fully deterministic models assume that the entire soil profile has uniform properties. Some of the parametric models rely on empirical methods to simulate a process, while others fail to integrate the various hydrological components. From a modelling point of view none are adequate to fully describe the physical conditions that may exist in the field.

Nonuniformities in the soil hydraulic properties, the growing root zone and the constantly changing soil moisture content are shown in chapters 4 and 6 to influence the root zone water balance and the infiltration rate of the soil. These in turn effect the operational efficiencies of the surface and sprinkler irrigation systems (chapters 7 and 9 respectively).

The irrigation scheduling model, presented in this chapter and the next, aims to integrate, as much as possible, the component hydrological processes of irrigation and to incorporate such field characteristics as soil nonuniformity and dynamic, nununiform root zone storage, into a continuous soil water balance model.

Table 3.1 Hydrological characteristics of some irrigation models.

Model	PET method	Interception	Soil Water Balance	Actual ET method	Infiltration	Runoff method	Comment
USDA-ISP Jensen (1969)	Penman	-	-	Crop coef.	-	-	Black box scheduling model
Nimah & Hanks (1973)	Penman	-	Numerical model	Physically -based root extraction	Numerical model	-	Fully deterministic water balance model
Hanks (1974)	External input	-	Dynamic Uniform	Soil eva. & Transpiration	-	-	Parametric yield response model
USDAHL (1974)	Pan Eva.	-	Uniform Layered	Empirical	Empirical	Excess rain	Parametric rain-runoff model
SPAW Saxton etal 1974	Pan Eva. van Bavel	Constant	Dynamic Nonuniform Layered	Soil eva. & Transpiration	Rain less watershed runoff	-	Semi-empirical parametric model
CREAMS Knisel etal 1980	Penman	SCS implicit	Static Uniform Layered	Soil eva. & Transpiration	1D Uniform Green-Ampt model	1- SCS 2- Excess rain	Parametric rain-runoff model
MORECS Thompson etal 1981	Penman -Montieth	Empirical	Static Uniform	Resistance functions	-	Excess rainfall	Parametric water balance model
Martin etal 1984	Pan Eva.	SCS implicit	Static Uniform Layered	Soil eva. & Transpiration	SCS	SCS	Parametric yield response model
Jung & Taylor (1984)	Pan Eva. Jensen-Haise	-	Numerical model	Soil eva. & Transpiration	Numerical model	-	Deterministic water balance model

3.3 When to Irrigate ?

Crop yield depends on the transpiration rate, which is itself a function of the available soil water. When the supply of water is less than that necessary for unrestrained transpiration, the plant suffers stress and yield is reduced. In practical and economical terms, it is not always possible to provide enough water for maximum crop growth. A balance therefore must be struck between viable irrigation and desirable yield. To aid this decision an indication of the level of moisture stress developed in the plant is necessary.

Indicators of stress are varied in approach since many soil, plant and environmental factors effect the transpiration process. Haise & Hagan (1967) indicated that plant related factors such as stem and leaf growth, colouration and turgor pressures may be used as physical indicators of stress. On the modelling front Ahmed etal (1977) used the Stress Day Index (SDI), defined as the product of the plant water potential and an empirical yield sensitivity factor. Jackson etal (1976) used the plant canopy and air temperatures to define a Stress Degree Day (SDD) as the cumulative daily difference in the temperatures. This temperature-based crop stress model makes it particularly suitable for yield assessments by remote sensing thermal radiation measurements.

The moisture stress indicator used in this study is the widely used soil moisture deficit approach. The soil moisture deficit (SMD) is defined by Kruse (1978) as the difference between field capacity and actual soil moisture content in the root zone at any given time. It represents the amount of water removed by evapotranspiration and which is required to restore the soil to field capacity. The SMD is often expressed as a percentage of the total available soil moisture capacity (field capacity minus wilting point):

$$SMD = 100 \frac{(FC - SMC)}{(FC - WP)} \tag{3.2}$$

where :

SMD = soil moisture deficit (%)
FC = field capacity (cm3/cm3)
WP = wilting point (cm3/cm3)
SMC = actual soil moisture content (cm3/cm3)

The irrigation manager has to decide the maximum level of SMD at which irrigation must be applied. This level, defined as the management allowable soil moisture deficit (MNGSMD), is chosen to meet certain criteria. When water is in plentiful supply the priority is to obtain maximum crop yields, but when water supply is the limiting factor, the main objective would be to distribute the water to the maximum number of users for the optimum level of overall yield.

The yield response to moisture deficit

varies from one crop to another. This is reflected in the threshold of SMD at which irrigation should be applied to ensure maximium yields. Table 3.2 gives a general guide to this threshold level.

Table 3.2 Soil moisture deficit threshold levels for maximum crop yield (Welch & Granaham 1985).

Root Depth	Crop Type	MNGSMD (%)
Shallow (0.66-0.9 m)	Succulent crops harvested for the plant	45
Shallow	Fibrous crops	55
Moderate (0.9-1.5 m)	Perennial crops	58
Moderate	Annual crops	60
Deep (>1.5 m)	Perennial, succulent fruits	65
Deep	Perennial	70

3.4 How Much To Apply ?

Once the level of acceptable crop stress has been decided, the subsequent steps are the determination of exactly when this stress level is reached during the course of a drying cycle, and the quantity of water needed to replenish that lost from the soil by evapotranspiration. For this purpose a field scale water balance model is essential to keeping a continuous record of the inputs and outputs of water to and from the root zone moisture storage system.

The inputs to this system consist of precipitaion, irrigation and upward and lateral ground water flow into the root zone. The outputs are the interception loss, soil evaporation, plant transpiration, and both lateral and vertical drainage.

Neglecting the lateral and vertical ground water movements, the root zone soil moisture storage at the end of any day can be expressed by the following mass balance equation:

$$SMC(i) = SMC(i-1) + R(i) - T(i) - SE(i) - D(i) \qquad (3.3)$$

where :

- $SMC(i)$ = soil moisture storage (mm) on day i.
- $SMC(i-1)$ = soil moisture storage (mm) on on the previous day.
- $R(i)$ = net rainfall (gross rain minus runoff and interception) (mm)
- $T(i)$ = total transpiration on day i.
- $SE(i)$ = total soil evaporation on day i.
- $D(i)$ = total drainage (mm) from rootzone on day i.

The total root zone soil moisture content is calculated at the end of each day from Eqn. 3.3. The soil moisture deficit for that day is calculated by Eqn. 3.2. If this deficit is above the maximum allowable (MNGSMD) then the amount of irrigation required is evaluated as the depth of water necessary to fill the root zone to field capacity. The flow chart of the irrigation scheduling model (SCHEDULE) is shown in Fig. 3.2 .

A management factor (MNGIRG) defines the percentage of the required irrigation depth that is actually applied. This factor is useful in cases where deficit irrigation is practiced ,ie: where less water is applied to the soil deliberately to either maximize the limited resources or to maximize the land area cultivated.

Another use of MNGIRG is to include the 'leaching fraction' required to leach harmfull salts from the root zone. Since at this stage a soil salinity model has not been included in the simulation model, the MNGIRG factor can perform this function.

Considering that plants can differ in their response to soil moisture stress from one growth stage to another, both MNGSMD and MNGIRG can be defined for each growth stage, making the simulation model more flexible as a responsive management tool.

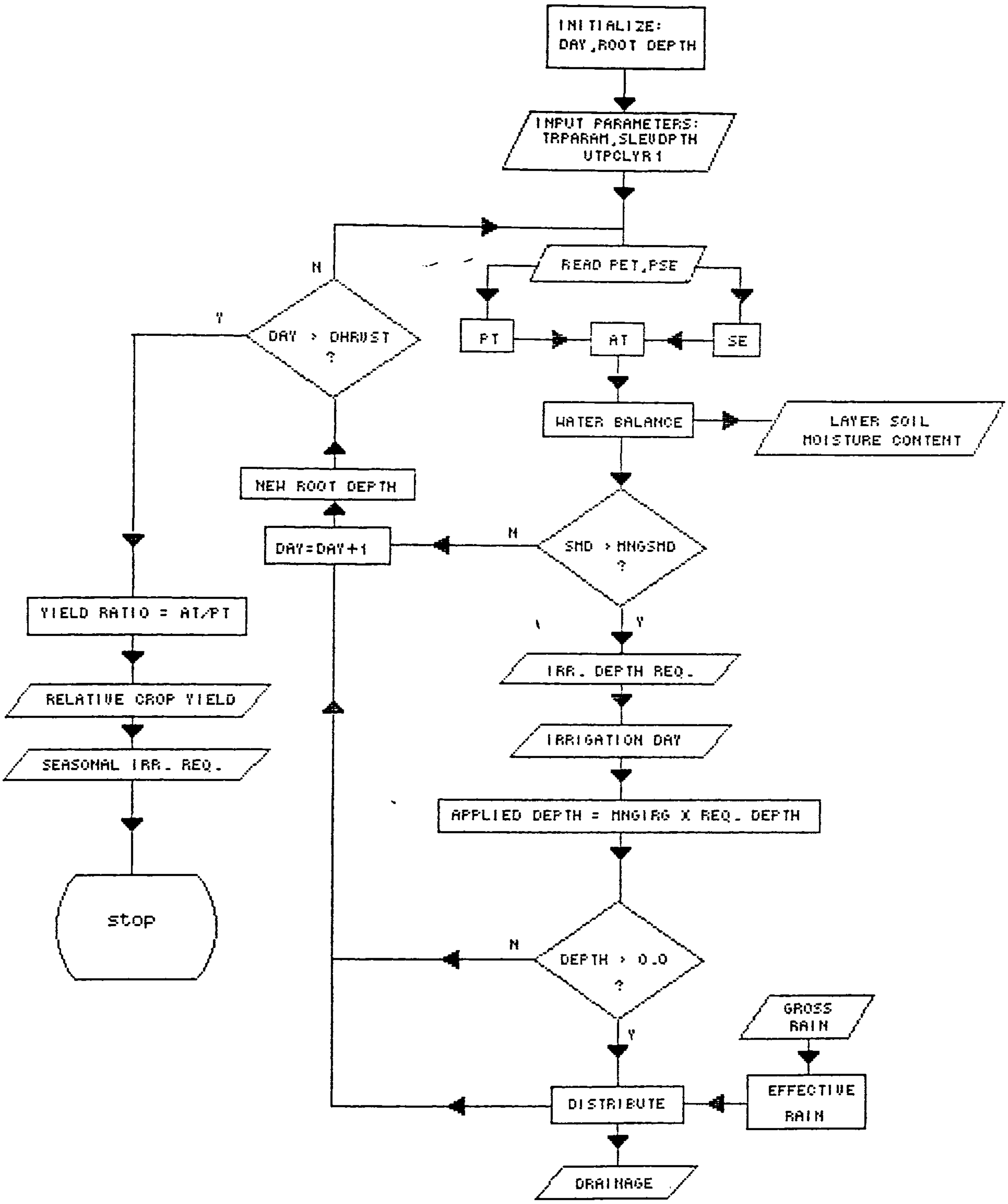

Fig. 3.2 Relational flow chart of the irrigation scheduling model (SCHEDULE).

3.5 Estimating root zone water gains and losses:

3.5.1 Rainfall, Runoff and Infiltration:

Runoff is that fraction of the rainfall that is not intercepted by vegetation or held in surface detention storage and which is not part of the rainfall that infiltrates into the soil. This "excess" or "effective" rain flows down the slope as "overland flow" and runs into the stream channel.

The determination of excess rainfall is of particular interest to the irrigation manager since it is an indication of the proportion of precipitation that does not infiltrate into the soil and is thus lost to the crop. A simplified mass balance approch is to consider infiltration to be the difference between rainfall and runoff volumes.

The methods used to estimate runoff (and therefore infiltration) from rainfall generally depend on the type of rainfall data available. Where break-point rainfall data are available, hydrological models of rainfall-runoff may be used (eg: PERM model of chapter 6). In the irrigation scheduling model however the water balance is kept on a daily basis and any recharge must be entered as a daily total. Where only daily rainfall depths are available then more empirical methods become necessary.

The Soil Conservation Service (SCS) method (US-SCS 1972) is used here to divide the gross rainfall into runoff, infiltration and initial losses such as interception. A method simillar to that of the CREAMS model (Knisel etal 1980) is used to include the effects of antecedent soil moisture contents on the runoff process.

The " SCS " method is a simple empirical model which relates the daily volume of runoff to rainfall and initial losses, according to the equation:

$$Q = \frac{(P - 0.2S)^2}{(P + 0.8S)} \tag{3.4}$$

where:

Q = daily runoff depth (mm)
P = daily rainfall depth (mm)
S = retention parameter (mm)

The retention parameter (S) embodies the soil type, vegetation cover and antecedent moisture conditions and is defined by (Knisel etal 1980):

$$S = Smx \left[1 - \sum_{j=1}^{N} P(j) \left(\frac{SM(j)}{UL(j)} \right) \right] \tag{3.5}$$

where:

P(j) = proportion of total roots in layer j.
j = root zone layer index.
N = number of rootzone layers.
UL(j) = upper limit of soil water storage in the root zone (mm).
SM(j) = actual soil water storage in the root zone prior to rain (mm).
Smx = maximum value of retention parameter.

Smx is defined as the maximum value of the retention parameter S , and is given by :

$$Smx = \frac{1000}{CN1} - 10 \qquad (3.6)$$

where:

CN1 = a 'dry conditions' curve number ranging from 0 to 100.

The values of CN1 are defined for different soil types and vegetation covers (Chow 1964, Bache & McCaskill 1984) .

Substitution of Eqn. 3.6 in Eqn. 3.5 enables the calculation of the infiltration and runoff depths (from daily rainfall) by the use of Eqn. 3.4 .

3.5.2 Drainage :

To distribute the applied water, wether from natural rainfall or scheduled irrigation, a simple cascading flow model is used to route the applied depth through each successive root zone layer, filling it up to field capacity before proceeding to the next. If the applied water is greater than the root zone storage capacity, the excess water is considered as drainage.

Assuming that the soil profile drains freely, the drainage depth at the end of the day is calculated according to the following mathematical expression:

$$D = Iv - \sum_{j=1}^{N} (FC(j) - SMC(j)) \qquad (3.7)$$

where:

- D = drainage depth (mm).
- Iv = infiltrated depth (mm).
- FC(j) = field capacity of layer j (mm).
- SMC(j) = soil moisture content (mm) of layer j.
- N = number of root zone layers.
- j = index of root zone layer.

The cascading flow model is described in more detail in a simillar model in chapter 6 .

3.5.3 Transpiration :

Water evaporates from all the outer and inner surfaces of the plant which come into contact with air. Evaporation from the outer plant cells is termed the cuticular transpiration and varies from 1% to 30% of the total depending on the species (Larcher 1983). The greatest part of transpiration however, occurs from the sub-stomatal air cavities where water is first converted to vapour before passing through the stomata opening. Guard cells around the stomata respond to turger pressure changes, caused by excessive water loss, by reducing or closing the stomata thus increasing the resistance to vapour diffusion from the plant to the atmosphere.

Cowan & Milthorpe (1968) state that "vapour transport is a function of differences of vapour pressure - not water potential ". This means the rate of transpiration is considered to be governed by the conditions of the atmospheric demand.

When water is in abundance, transpiration occurs at a rate limited only by the atmospheric conditions. Ignoring all other sinks of energy (eg into the soil and water) the available evaporative energy is assumed to be consumed in the processes of evaporation from the wet soil and plant surfaces. The transpiration rate can then be calculated from the energy balance equation :

$$PT(i) = PET(i) - PSE(i) \tag{3.8}$$

where :

PT(i) = potential transpiration on day i (mm).
PET(i) = potential crop evapotranspiration on day i (mm).
PSE(i) = potential soil evaporation on day i (mm).

Methods of estimating the potential evapotranspiration and the potential soil evaporation are given in sections 3.5.4 and 3.5.5 respectively.

Transpiration remains at the potential rate (PT), determined by the atmospheric demand, as long as the soil and vegetation are well supplied with water. When the soil begins to dry, water cannot be conducted to the evaporating surface fast enough and transpiration falls below it's upper limit of potential rate. This is referred to as the 'actual transpiration rate (AT)'. The rate of decline is controlled primarily by the level of soil moisture content and the evaporative potential of the atmosphere.

The reduction of transpiration from it's potential rate represents an important concept in irrigation management, particularly where deficit irrigation is practiced. The rate of dry matter production is directly related to the transpiration rate so that crop yield is reduced if the plant suffers stress due to water deficit in the root zone (Doorenbos & Pruitt 1977).

The rate at which AT falls below PT and the factors that influence it have been the subject of much recent research. Two approaches are commonly used to estimate AT : the physically-based and the parametric modelling techniques.

A) Physically Based Models :

One physically based approach is to solve the Penman-Montieth equation with the appropriate surface resistances. Experimental works by Szeicz & Long (1969) and Russell (1980) have shown that surface resistance increases as the soil moisture content decreases. Sheratt & Wheater (1984) used an empirical equation of surface resistance response to moisture content to determine the relative transpiration (AT/PT) .

The second physically based approach is based on the works of Van den Honert (1948), Gardner (1960), Cowan (1965) and Taylor & Klepper (1978) who expressed the rate of water flow through the plant as a product of the water potential gradient between the soil and the leaves, and the sum of the conductances of water in the soil and plant mediums. This method has been successfully used to model the water balance of cropped lands, eg: Zur & Jones (1981) for cotton, Rowse etal (1983) , Hillel etal (1976) and Jung & Taylor (1984) for soybeans.

The physically based models generally start with the equations of mass, heat and momentum transfer and derive expressions which relate AT to physical variables which can be measured on site. However as with most variables in the evaporation process, onsite measurements are labourious and complicated so that recourse to simpler parametric models is often more appropriate (Brutsaert 1982, Sherratt & Wheater 1984) .

B) Parametric Models :

Federer (1979, 1982), Feddes (1982) and Refsgaard (1981) have used the parametric approach in relating transpiration rate to variables such as soil moisture content, potential evapotranspiration and rooting characteristics. This is also the approach used in this study.

It is appropriate at this stage to define a coefficient of limiting soil water , Ksw , as the ratio of actual to potential transpiration rate:

$$Ksw = AT/PT \qquad (3.9)$$

where :

Ksw = coefficient of limiting soil water.
AT = actual transpiration rate (mm/day).
PT = potential transpiration rate (mm/day).

Many shapes have been proposed to describe the rate of fall of Ksw as a function of soil moisture depletion. Some of these are shown in Fig. 3.3. Curve A assumes no reduction in Ksw untill all available soil moisture has been removed. Curve B shows the reduction rate to be linear only beyond a threshold soil moisture depletion level, while curve D assumes the linear reduction to be immediate. Curves C & E take logarithmic and exponential forms respectively.

The mathematical models that describe these curves can be categorized into two main groups. The first group give Ksw as a function of a single variable, namely the soil moisture content. These models are often derived by fitting equations to relative transpiration and soil moisture contents as measured by lysimeters. Eagleman & Decker (1972) gave a regression equation of Ksw and soil moisture deficit (SMD) . Jensen etal (1971) fitted a logarithmic equation (curve C) to Ksw and the ratio of actual to maximum available moisture content.

The second group of models take into account other variables as well. The experimental works of Denmead & Shaw (1962), Holmes & Robertson (1963) and

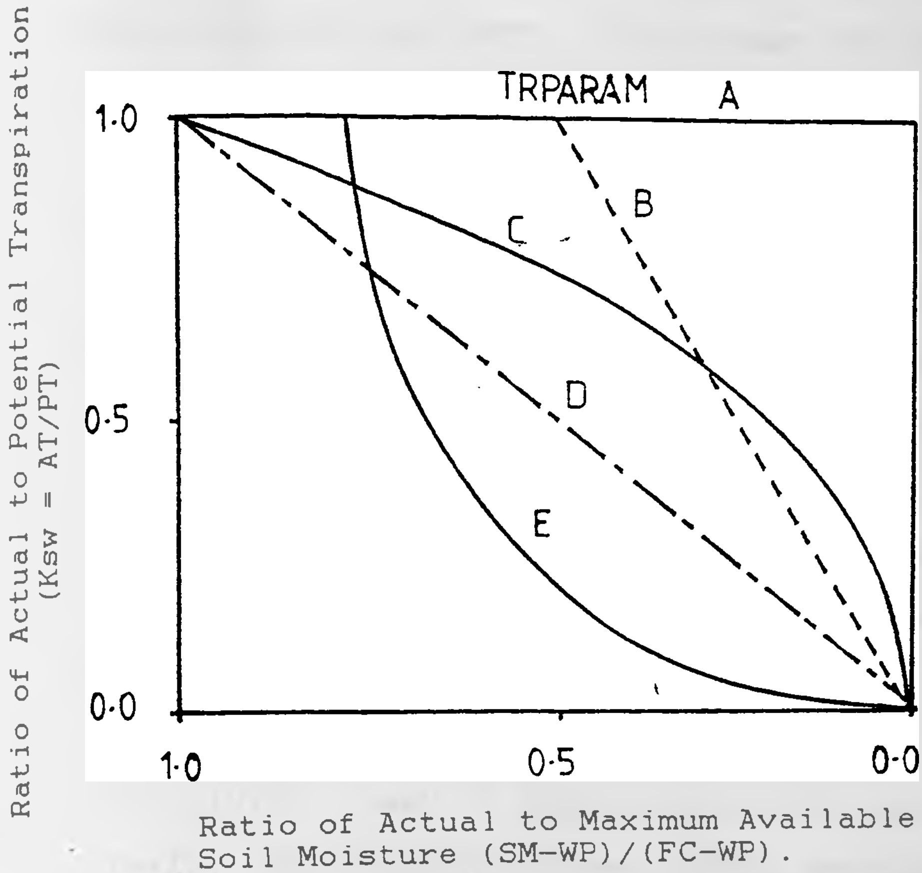

Fig. 3.3 Proposed shapes of transpiration response to depleting soil moisture, (AT and PT are actual and potential transpiration (mm); SM is actual soil moisture content (mm) ; FC is field capacity (mm); and WP is wilting point (mm)).

others indicate that the rate of fall of Ksw also depends on the magnitude of potential evapotranspiration (PET) . The higher the rate of PET, the steeper the slope of the curve.

Factors such as soil hydraulic conductivity, rooting density, rooting depth, soil moisture tension, also influence the response function to various degrees. These are however difficult to quantify and are assumed to be incorporated into the empirical parameters used in these models.

Norero etal (1972) developed a model taking into account PET and soil moisture potential . Boonyatharakul & Walker (1979) derived empirical functions relating Ksw to PET, soil hydraulic conductivity and a rooting-pattern parameter for alfalfa. Kristensen & Jensen (1975) developed a four parameter model incorporating functions of leaf area index, rooting pattern and PET . Calder etal (1983) used an exponential model (curve E), to relate Ksw to soil moisture deficit and TRPARAM (see below) , while Hanson (1976) related Ksw to the available soil moisture content and PET.

The method used in this case is the linear-response model (curve B), expressed mathematically as:

$$Ksw = (1/TRPARAM).(AW/AWM) \qquad (3.10)$$

where :

AW = available moisture (SMC − WP)
AWM = maximum available moisture (FC − WP)
TRPARAM = empirical parameter (0 < TRPARAM < 1.0)
SMC = antecedent soil moisture content (mm)
FC = field capacity (mm)
WP = wilting point (mm)

The constant TRPARAM is commonly taken as 0.5 (Ritchie etal 1972, Hanks 1974, Hanks & Hill 1980); others give 0.3 (Kanemasu etal 1976), and 0.25 (Ritchie etal 1976). Doorenbos & Pruit (1977) related the parameter TRPARAM to the crop type and PET rate.

The rate of actual transpiration is seen from Eqn. 3.10 and Eqn. 3.9 to depend on the soil properties (FC and WP). Where nonuniform soil properties exist, the transpiration rate must be evaluated for each root layer according to it's soil properties. Actual transpiration from layer j, is calculated with the aid of the linear-response model :

$$T(j) = PT(j) \cdot Ksw(j) \tag{3.11}$$

where :

T(j) = actual transpiration from root layer j.
PT(j) = potential transpiration from layer j.
Ksw(j) = coefficient of limiting soil water in layer j.

Assuming the root zone is divided into 4 equal layers, the fraction of the total potential transpiration assigned to each layer is equal to the product of the quarter potential rate and the proportion of roots P(j) in that layer:

$$PT(j) = (PT/4) . P(j) \qquad (3.12)$$

This function allows the assignment of more relative weight to transpiration from the top layers which contain a greater density of roots.

Substituting equations 3.10 and 3.12 in Eqn. 3.11 gives an expression for calculating the actual transpiration loss from a root zone layer :

$$T(j) = \frac{(PT/4) . P(j)}{TRPARAM} \left[\frac{SMC(j) - WP(j)}{FC(j) - WP(j)}\right] \qquad (3.13)$$

where:

T(j) = actual daily transpiration loss from layer j (mm).
PT = total daily potential transpiration (mm)
TRPARAM = transpiration-moisture deficit response parameter.
P(j) = proportion of total roots in layer j.
SMC(j) = soil moisture content in layer j (mm).
FC(j) = field capacity of layer j (mm).
WP(j) = wilting point of layer j (mm).

3.5.4 Potential Evapotranspiration:

The evaporation process is defined as 'the phenomenon by which a substrate is converted from the liquid or solid state into vapour' (Brutsaert 1982). The change of state of water molecules from liquid to gas requires an energy input equivalent to the latent heat of vapourization. In nature the source of this energy is the radiation emitted by the sun. Terrestrial factors such as wind, clouds, relative humidity and temperature help to maintain conditions for continuous evaporation.

Evapotranspiration (ET), is a term used to define the combined processes of evaporation from soil and water surfaces and transpiration from plants. In the field evaporation and transpiration are difficult to measure independently , and are thus often lumped together into a single descriptive term.

The upper limit of the evapotranspiration rate is referred to as the 'potential evapotranspiration rate (PET)'. The maximum rate of evapotranspiration is not only dependent on the atmospheric variables but also on the physical composition of the vegetation stand. The term 'reference-crop potential evapotranspiration (PETr)' has been used to define the water loss from a green crop, of uniform height, completely covering the ground and never short of water (Cuenca & Nicholson 1982).

Penman (1948) defined PETr for short grass and derived semi-empirical formulae for it's estimation. Subsequently other empirical relationships have been developed for the Penman formulae relative to alfalfa.

The common method of calculating the PET for any other crop is to estimate PETr relative to grass or alfalfa and to multiply this by a proportionality crop coefficient (Kc), derived from field lysimeter experiments (Doorenbos & Pruitt 1977):

$$PET = Kc \, . \, PETr \qquad (3.14)$$

The value of Kc varies throughout the growing season and represents the effects of factors such as crop height, root density, canopy cover and soil type. It's magnitude ranges from a low during early growth, to a peak at maximum crop development, and declines to a low after the onset of senescence. Some Kc values for various crops are tabulated in the appendix.

Effectively any crop can be used as the reference provided the physical requirements used in the definition of PETr are met. However the two most commonly used reference crops are grass and alfalfa.

Grass reference PETr is defined by Doorenbos & Pruit (1977) as " the rate of ET from an extended surface of 80-150 mm tall, green grass cover of uniform height, actively growing, completely shading the ground and not short of water".

Alfalfa reference PETr is defined by Jensen etal (1970) as "the rate of ET from a well-watered, actively growing, 300-460 mm tall, alfalfa crop with aerodynamically rough surface".

It is important that the values of Kc used in determining PET must be consistent with the grass or alfalfa reference used in the calculation of PETr (Cuenca & Nicholson 1982).

Over the years many empirical models have been proposed to estimate PETr . These models have been successfully used in the regions for which they were developed. The applicability of such models also depends on the level of data requirement. A summary of the input data for some more commonly used models are shown in Table 3.3 .

Since the amount of required input data for such models is normally less than that for the more physically based models, the empirical methods have proved usefull where meteorological data are scarce.

Care must be taken in the choice of model where climatic conditions deviate considerably from those for which the model was developed (Allen & Pruit 1986). In particular in arid and semi-arid regions where the effects of advective changes of temperature, humidity and wind speeds are greatest, some models can give spurious results. Hashemi & Habibian (1979) compared the Blaney-Criddle , Thornthwaite and the FAO-Blaney-Criddle models for the arid zone of southern

Table 3.3 Data requirements of some empirical potential evapotranspiration (PET) models.

Model / Input data	T	RH Va	Rn Rs	n	Uz	Lat. Ele.	Rain	Ref.	Comments
Blaney- Criddle	 *			 *				Hansen etal 1979	Temperate zones
FAO-Blaney -Criddle	 *	* 		 *	 *	* *		Doorenbos & Pruitt 1977	Correction factors
Jensen- Haise	* 	 *	 *					Jensen etal 1970	Summer and low Elev.
Thornthwaite	*			*				Shaw 1984	Monthly PET only
Linacre	* 	 *				* *		Linacre 1977	Temperate climates
Hargreves- Samani	*		*					Hargreaves & Samani 1987	Calibrated for S. Am
Turc	* 		 *				*	Shaw 1984	10 day PET only
Priestly- Taylor	*	*	*					Allen 1986	Humid, no advection

* Key :

T = temperature; RH = relative humidity; Va = atmospheric vapour pressure; Rn = net radiation; Rs = short wave radiation; n = number of sunshine hours; Uz = mean wind speed; (All values are mean daily); Lat. = latitude; Ele.= elevation.

Iran and concluded that temperature-based models tend to underestimate PET . The variability of PET estimates by several methods, under advective arid conditions, was also shown by Malek (1987) . Such site specific models are therefore considered inadequate for use in this study where generality of application is desired.

In this study reference crop evapotranspiration (PETr) is estimated by any one of three optional methods. These are the Pan Evaporation, the Penman, and the Penman-Montieth methods. The choice of method must be based on the availability of data.

3.5.4.1 The Pan Evaporation method (Option 1) :

Pan evaporation (Epan), is a measure of the water loss rate from an open water surface. The method requires that the rate of evaporation from a container (or pan) be measured on the site. The design of the evaporation pans do not follow any international standards, but all share common problems associated with external factors such as thermal transfers between the pan and the surrounds, albedo of water, boundary layer turbulances, temperature and humidity gradients above the pan and the composition of the surrounds, all effect the evaporation rate.

Generally all these factors are lumped into a 'pan coefficient, Kp ', from which reference crop evapotranspiration is estimated :

$$PETr = Kp \cdot Epan \quad (3.15)$$

where:

PETr = reference crop evapotranspiration (mm/d)
Epan = evaporation loss per day, mesured from a pan (mm).
Kp = pan coefficient.

For the US Class A pan, under average wind and humidity, a pan coefficient Kp = 0.7 is often used (Doorenbos & Pruit 1977), but calibration on site is deemed essential (Brutsaert 1982).

3.5.4.2 The Penman method (Option 2):

Penman (1948,1963) derived a physically based model of evapotranspiration from the consideration of the incoming and outgoing evaporative energies at an open surface of water (Fig. 3.4). While the principles are based on sound fundamental physical laws, some of the relationships used are empirical. The Penman equation is :

$$PETr = [S(Rn-G)/(S+C)] + [Ea.C/(S+C)] \quad (3.16)$$

where

PETr = reference evapotranspiration (mm/d)
S = slope of saturation vapour pressure-temperature curve at mean air temperature (mbar/ C)
C = psychrometer constant (mbar/ C)
Rn = net radiation (mm/d)
G = heat flux into the soil (mm/d)
Ea = aerodynamic vapour transfer term (mm/d)

The relationships defining the various terms

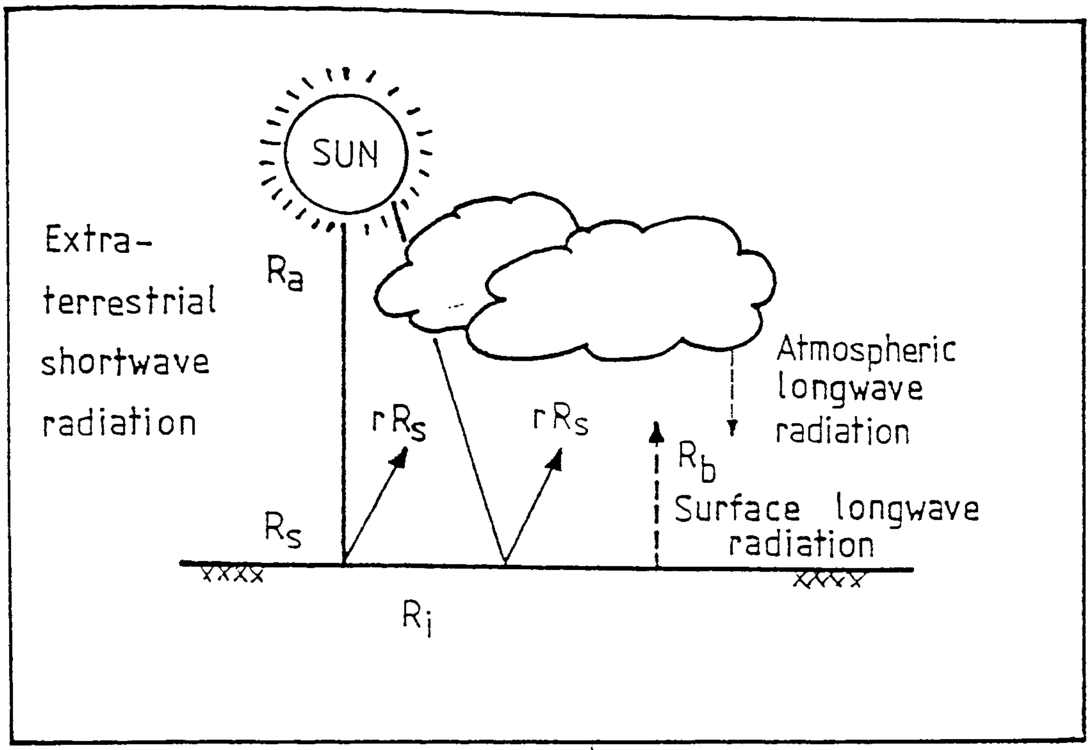

Fig. 3.4 Schematic diagram of incoming and outgoing radiations at the earth's surface. (Ra = extra-terrestrial shortwave radiation; Rs = atmoshperic shortwave radiation; Ri = incoming shortwave radiation at the surface; r = surface albedo; Rb = outgoing longwave radiation from surface).

in Eqn. 3.16 are listed in detail in the appendix. The Penman equation only requires knowledge of 4 meteorological factor. These are the mean daily temperature, the mean air vapour pressure , the degree of cloud cover, and the mean wind speed.

3.5.4.3 The Penman-Montieth method (Option 3):

Montieth (1965) modified the Penman formula to include terms describing the resistances to vapour diffusion from the evaporating surface and to the transfer of momentum in the canopy-atmosphere boundary layer. The Penman-Montieth equation of evapotranspiration ET , is given by :

$$L.ET = \frac{S\ Rn + pCp\ (Vs-Va)/ra}{S + C\ [1+ (rs/ra)]} \qquad (3.17)$$

where :

L.ET = evaporative energy (Watts/m2)
L = latent heat of vapourization (J/kg)
ET = evapotranspiration (Kg/m2/s)
Rn = net incoming radiation (mm/d)
S = slope of saturation vapour pressure-temperature curve (mbar/ C)
C = psychrometer constant (= 0.66)
p = air density (1.24 Kg/m3)
Cp = specific heat of air (= 1005 J/kg/ C)
Vs = saturated air vapour pressure (mbar)
Va = actual air vapour pressure (mbar)
ra = aerodynamic resistance (s/m)
rs = bulk surface resistance (s/m)

(Note that 1 mmH20 = 0.034 Watts/m2 .)

The advantage of the above equation to the the Penman equation is that it can be applied to any evaporating surface, wether fully or partially wet, by the inclusion of appropriate resistances. Expressions for estimation of the aerodynamic and bulk surface resistances are given in detail in the appendix.

3.5.5 Soil Evaporation :

3.5.5.1 Stages of Soil Evaporation Rate :

Direct evaporation from the soil represents a net loss to the atmosphere that is of no apparent benefit to the irrigator. In arid and semi-arid environments this loss may amount to over 50% of the annual precipitation. Efforts in irrigation management to reduce soil evaporation include the use of localised techniques such as trickle irrigation, mulching and tillage (Hillel 1980).

Evaporation from the soil involves a three stage process (Fig. 3.5). The first is the constant-rate stage during which the soil is wet and evaporation is controlled by the potential atmospheric demand. The second stage is the falling-rate, during which the movement of water is controlled by the conductivity of the drying soil . During this stage the evaporation rate progressively falls below the potential rate. The last stage is the slow-rate stage, and involves the process of water vapour diffusion through the soil medium. The last two stages merge together gradually and are often taken as a single falling-rate stage .

Idso etal (1979) derived equations for the three stages from incoming and reflected solar radiation, and the air and soil temperatures. Gardner & Hillel (1962) sought solutions to the vapour diffusion equation and derived equations for the transition time

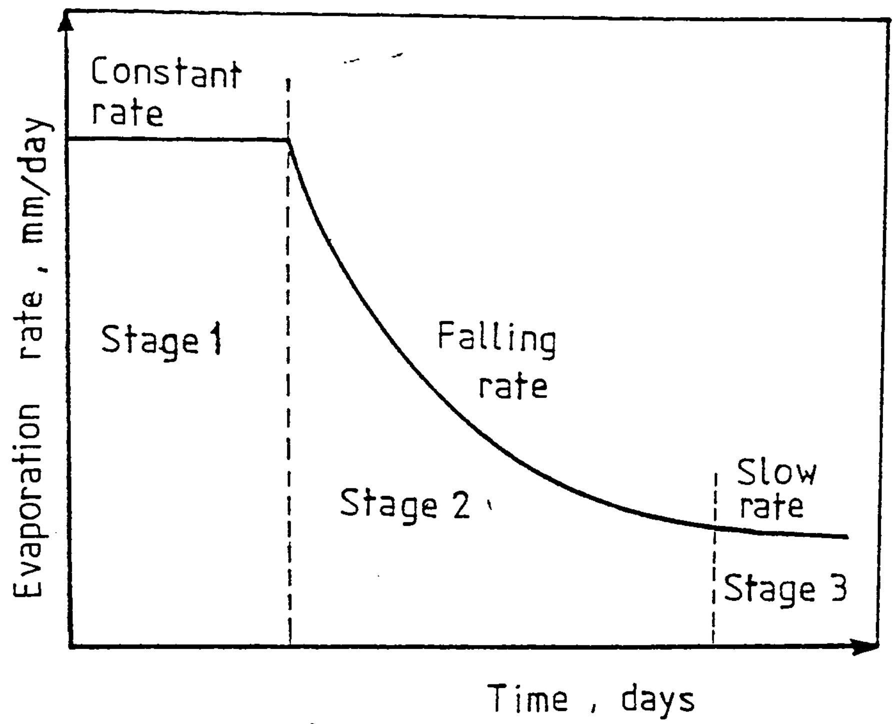

Fig. 3.5 Schematic diagram of the three stages of evaporation from soils.

from constant to falling rate stages.

The model used in this study is the empirical model of Ritchie (1972) and Ritchie etal (1976), given by :

Stage 1 :

$$PSE = PET \exp(-0.398\ (LAI + 2.5\ M)) \qquad (3.18)$$

Stage 2 :

$$SE = C.\ t^{1/2} - C\ (t-1)^{1/2} \qquad (3.19)$$

where:

PSE = soil evaporation at potential rate (mm/d)
SE = actual soil evaporation rate (mm/d)
M = fraction of soil covered by mulch
t = time since second stage initiation (days)
C = soil constant
LAI = Leaf area index

The transition from first to second stage occurs when a threshold amount of water is evaporated from the soil. This value , U , is a function of soil depth, hydraulic conductivity and evaporative conditions. This parameter is found by plotting the cumulative evaporation loss versus elapsed time for a soil drying-cycle test. The constant rate is represented by a straight line up to U , after which the curve gradually declines . A plot of cumulative evaporation above the threshold U versus square root of time will give a straight line , the slope of which is the parameter C .

3.5.5.2 Bare-Soil Lysimeter Tests :

To evaluate the parameters U and C for the soil under study (Auchincruive sand), an experiment was carried out in the laboratory on several containers filled with wet soil and allowed to dry. Two conditions of undrained and drained soils were looked at .

Undrained : Two plastic containers, 90 mm deep and 105 mm and 102 mm internal diameters, referred to as samples 1 and 2 respectively , were sealed at one end and filled with air dry soil . Water was added up to saturation (untill a thin layer of free standing water was visible on the surface). The containers were then left in the greenhouse (see chapter 4, section 4.3 for details) , and allowed to dry.

Two drying cycles were carried out , the first lasted 49 days, with initial moisture contents of 35.8 mm and 33.6 mm for samples 1 and 2 respectively. The second cycle was 18 days long with initial moisture content of sample 1 at 41.5 mm and sample 2 at 35.3 mm. The soil evaporation rate (SE) , was measured as the weight loss of the containers per day. Potential evaporation rate (Eo) , was taken to be that of free water evaporation from a container of 100 mm depth and 96 mm internal diameter. The weight loss of the water at daily intervals was measured and converted to the equivalent water depth of evaporation.

The relative soil evaporation (SE/Eo), is

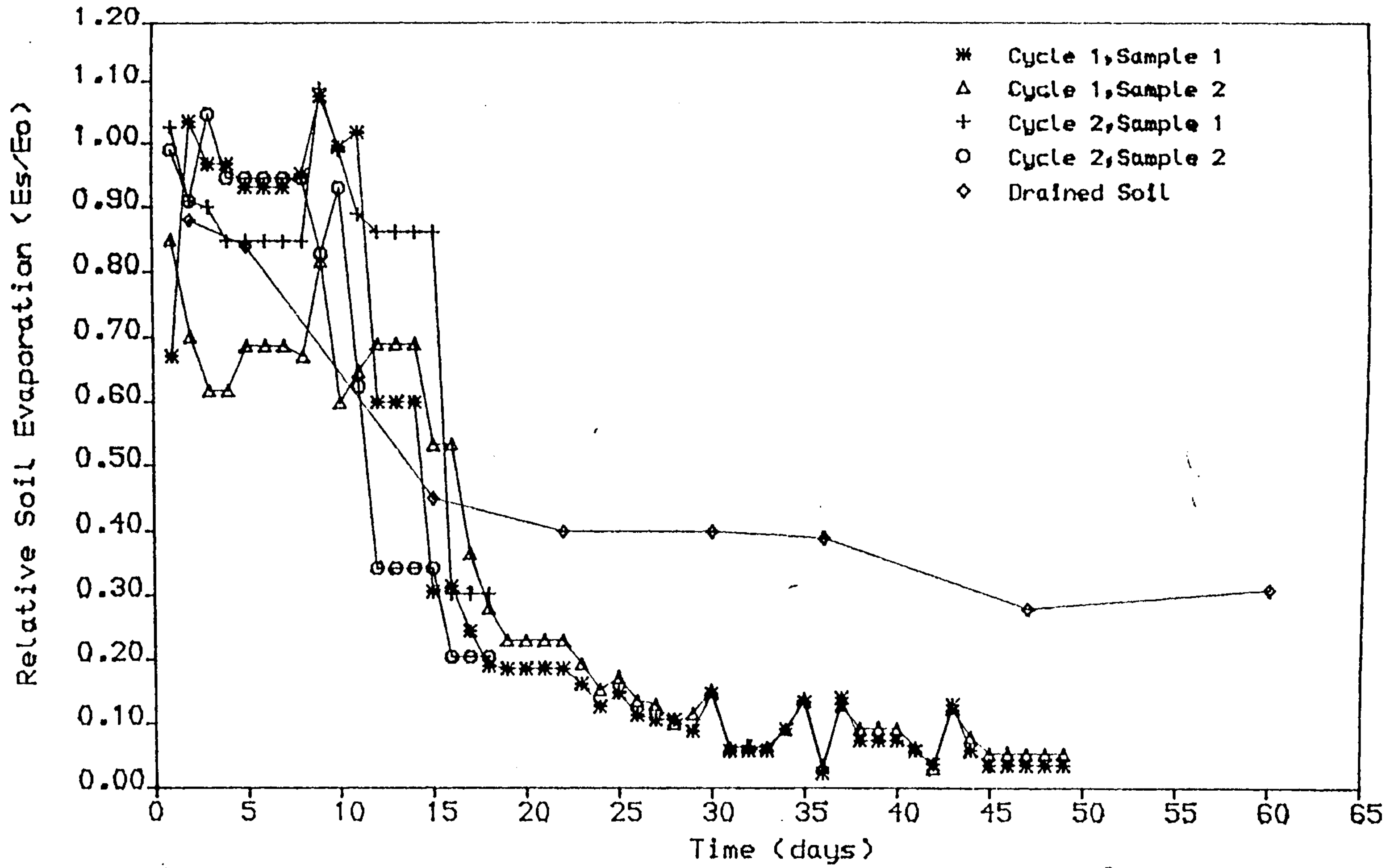

Fig. 3.6 Measured relative soil evaporation decay with time. (Es = actual soil evaporaton (mm); Eo = free water evaporation (mm)).

shown plotted against time in Fig. 3.6 . It can be seen that for all four tests there is an initial period when the relative evaporation is high. The fluctuations during this period may be due to the non-steady open water evaporation rates ; these ranged from 1.46 mm/d to 2.49 mm/d with an average of 1.91 mm/d over a 152 day period. Beyond about day 10 of the test, the relative evaporations drop rapidly, converging to near zero evaporation.

The response of relative soil evaporation to depleting soil moisture is shown in Fig. 3.7 . There is a fair degree of scatter but a downward trend is visible beyond about 0.15 cm3/cm3 moisture content. This is seen more clearly in Fig. 3.8 which represents the mean of moisture content classes (at 0.05 cm3/cm3 intervals). The standard deviations are shown as straight lines. Fig. 3.9 shows the plot of the fraction of cumulative soil evaporation and initial moisture content versus time. Initially the loss rate is constant but then gradually declines in time and the fractional water loss tends towards unity where all the soil moisture is lost .

From these tests it can be concluded that for the undrained case, the Auchincruive sand will loose water at the rate of the atmospheric demand, untill the moisture content reaches a critical value, about 0.15 cm3/cm3, below which the rate of evaporation declines

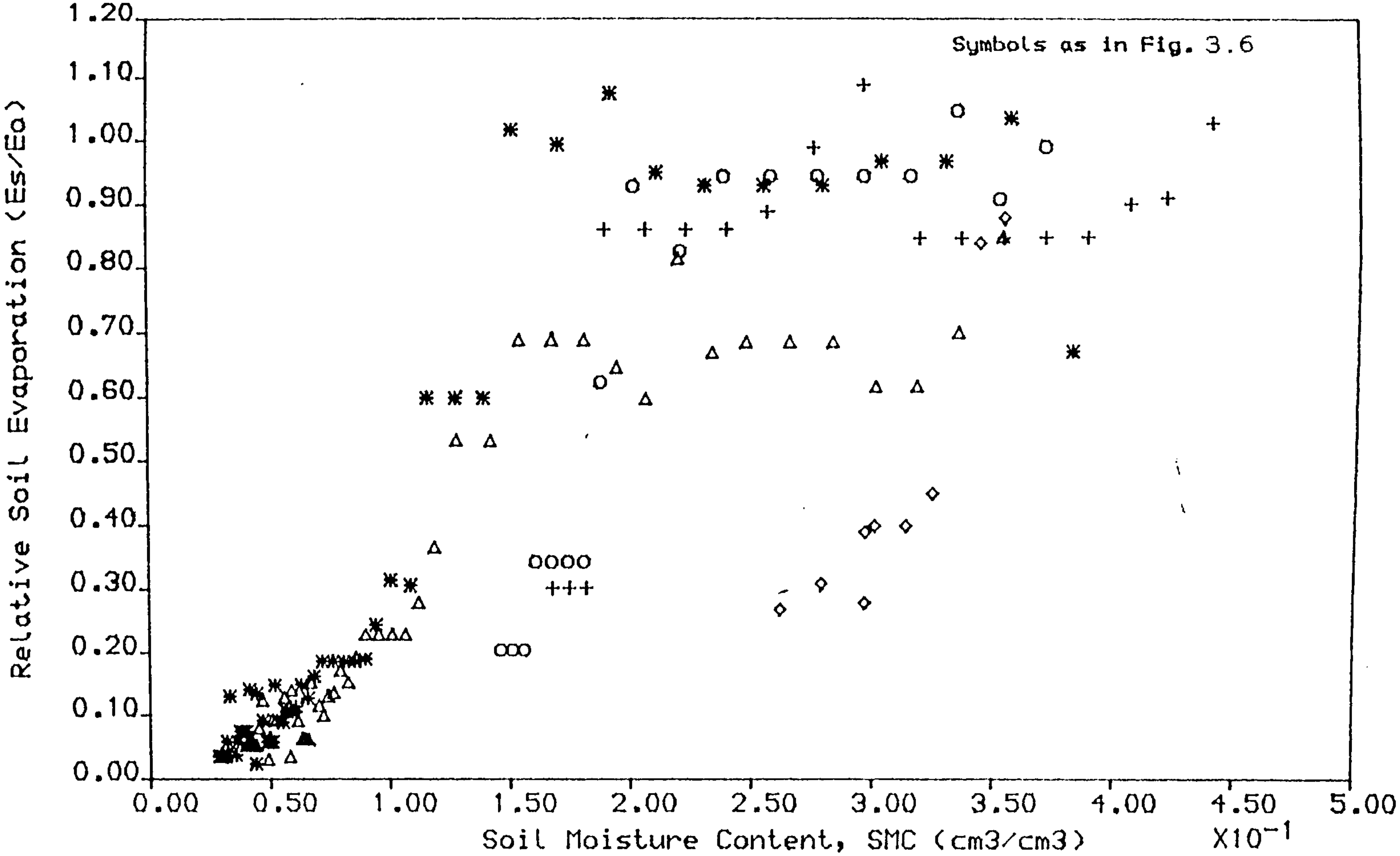

Fig. 3.7 Measured relation of relative soil evaporation (Es/Eo) to soil moisture content.

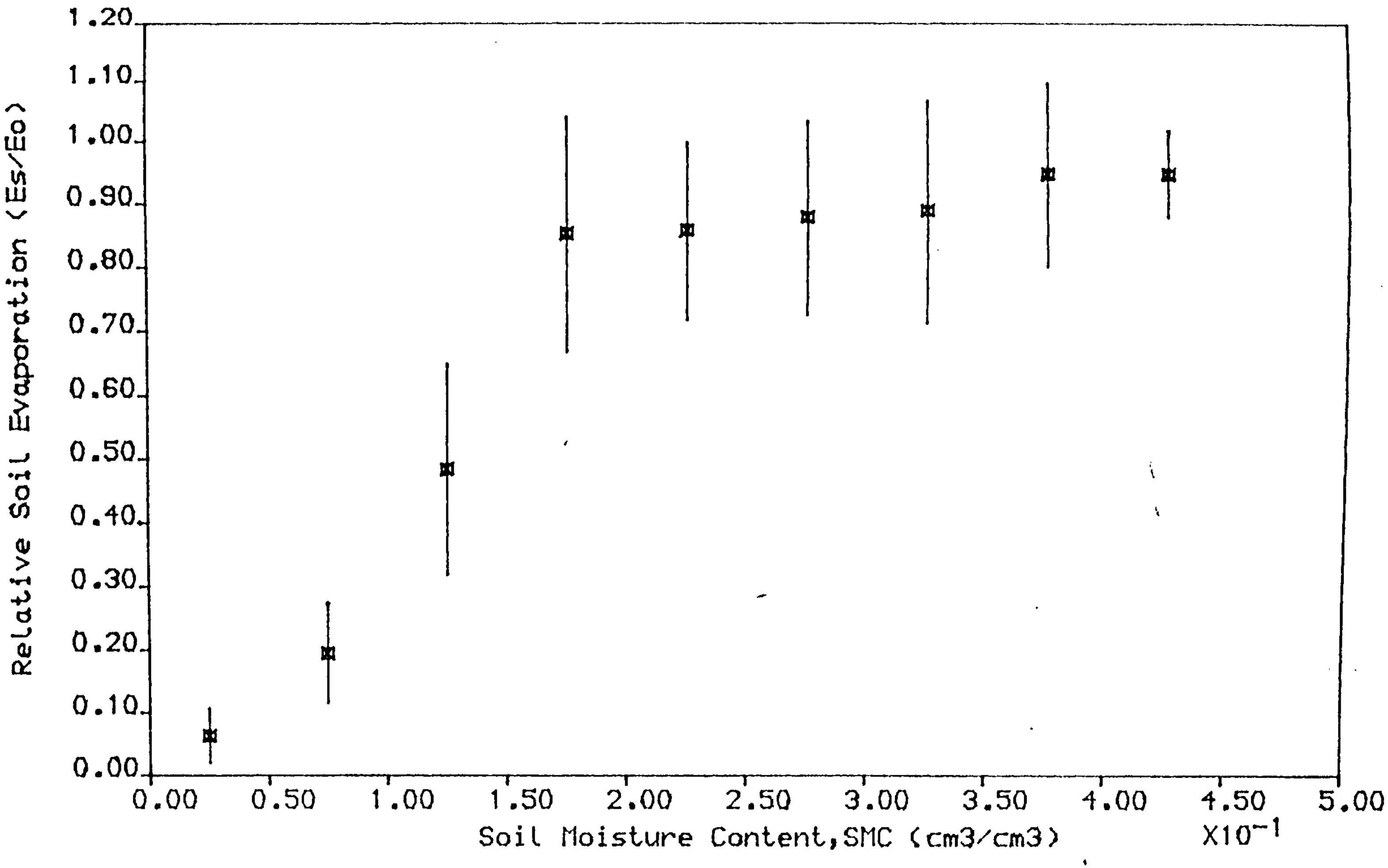

Fig. 3.8 Measured class means (squares) and standard deviations (vertical bars) of (Es/Eo) vs SMC for undrained soil evaporation tests.

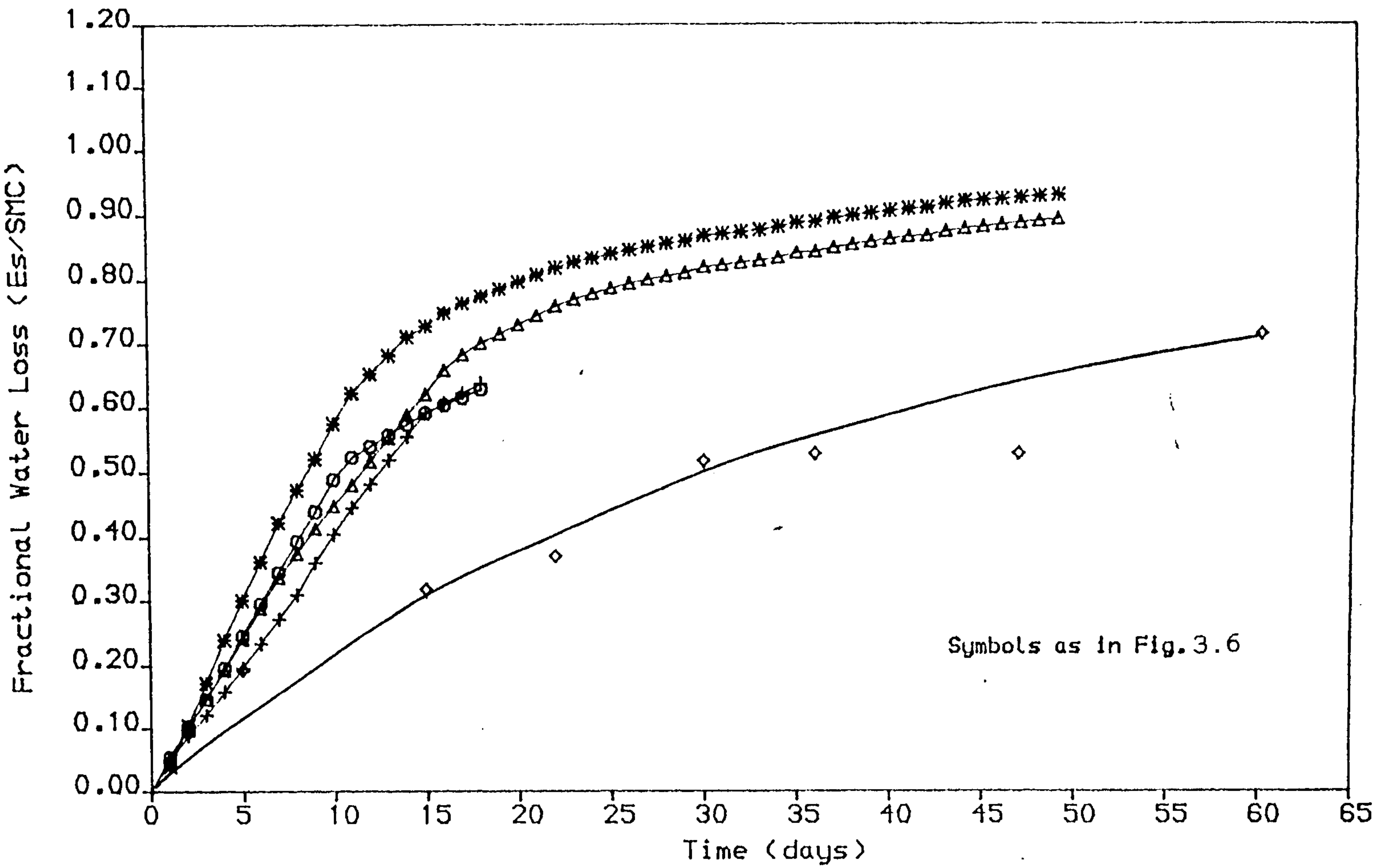

Fig. 3.9 Measured cumulative fractional water losses of the drying soils.

rapidly.

Drained : The drained-soil evaporation test consisted of a 1m length of plastic piping , 152 mm internal diameter, free draining at the bottom and filled with about 30 mm depth of grit to act as drains. The container was filled with the air dry sand and water was added untill continuous drainage was achieved. The soil was then covered and left for two days to allow gravitational drainage. Profile moisture content measurements were taken from access holes drilled on opposing sides of the lysimeter, at 100 mm intervals. Soil moisture contents were determined by the gravimetric method. Open water evaporation was measured as described in chapter 4. Evaporation from the soil was calculated from the changes of profile moisture contents. These changes are shown in Fig. 3.10.

The variations of relative evaporation with time and soil moisture content, are shown in Fig. 3.6 and Fig. 3.7 respectively. The relative evaporation declines after about 3 days . After 36 days of drying the average moisture content of the drained case had still not fallen below 0.26 cm3/cm3 . This would suggest that water was being conducted to the surface from deeper layers, helping to maintain a near steady evaporation rate . Fig. 3.10 confirms that even after 36 days of drying, the lower depths of the soil

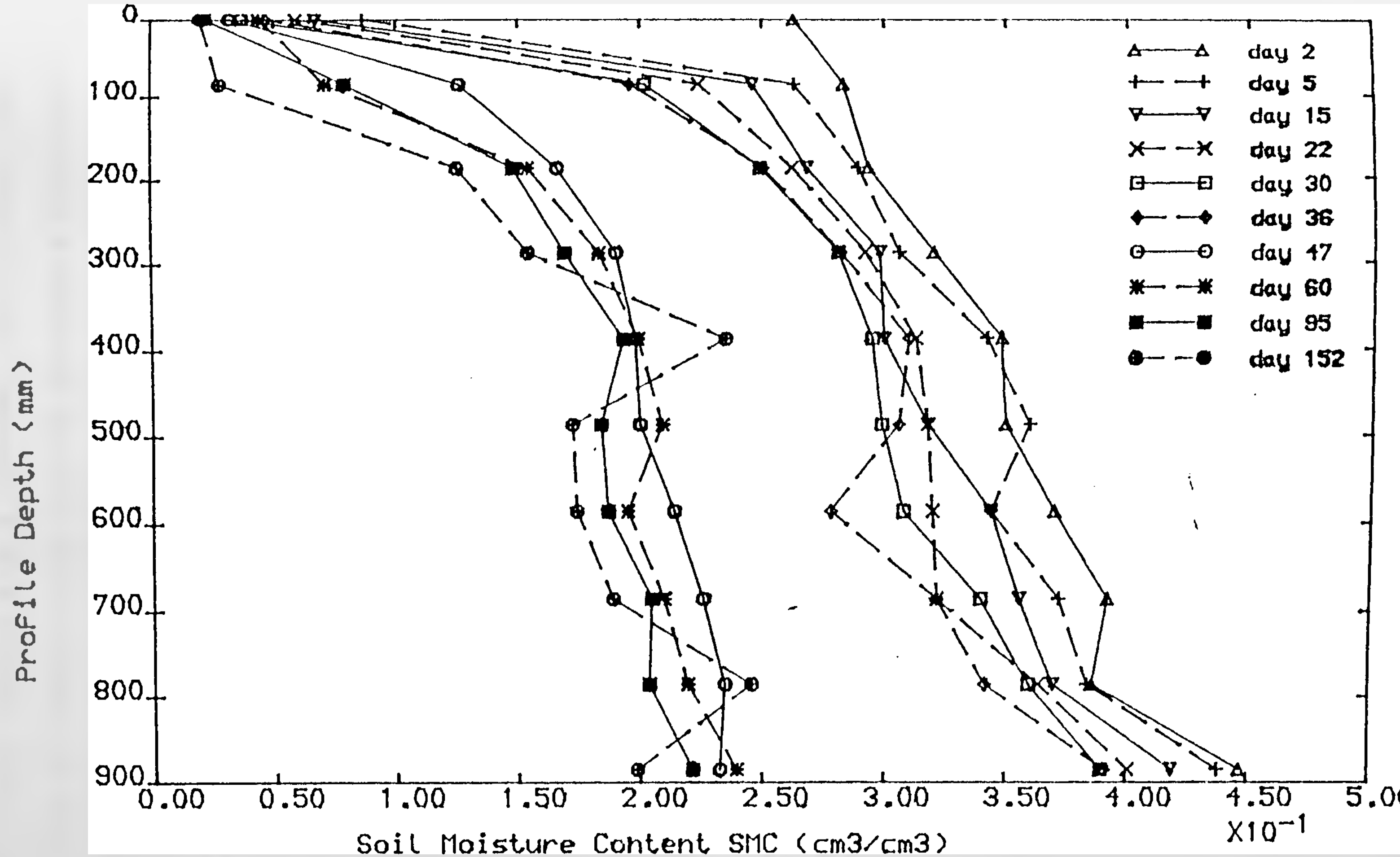

Fig. 3.10 Measured soil profile moisture changes due to evaporation from the bare-soil lysimeter.

remained above or near to field capacity (0.308 cm^3/cm^3). The fractional water loss of the top 100 mm of the column is shown for comparison to the undrained cases (Fig. 3.9). The decline is more gradual because water is transfered from lower depths to the evaporating surface.

3.5.5.3 Estimation of Model Parameters:

The parameters U and C, determined for the Auchincruive sand, are shown in Table 3.4.

Table 3.4 Experimentally determined values of the soil evaporation model parameters.

Experiment		C $mm/d^{-1/2}$	U mm
1) Undrained soils:			
Cycle 1,	sample 1	2.38	19.30
	sample 2	2.73	19.30
Cycle 2,	sample 1	3.57	18.61
	sample 2	2.03	18.61
	Mean	2.67	18.96
2) Drained soil:		2.38	5.7

The results of the undrained soil test show a fair degree of variation about the mean value. This is reflective of the non-steady open water evaporation rates and possibly of the differences in the container size and colour (sample 1 was placed in a light grey container while the second container was black in colour) . The causes for the discrepancies were not pursued further since the evaporation rate from the drained, deep soil lysimeter is much more representative of the state of the soil in the field compared to small, saturated soil samples. The top layers in the drained lysimeter are initially at field capacity and thus the cumulative water loss U, after which soil evaporation declines, is much lower than the saturated cases. The values of U and C for the drained lysimeter are within range of reported values for sandy soils (Table 3.5) .

Table 3.5 Soil evaporation parameters (C & U) for several soil types (Ritchie 1972, Kanemasu etal 1976).

Soil Type	C $mm/d^{-1/2}$	U mm
Carurle sand	1.68	5.0
Florence stony loam	2.89	5.8
Manter fine sandy loam	2.41	9.0
Mansic silty clay loam	3.53	9.2
Muir silty clay loam	3.27	10.2
Hays silt loam	3.36	11.2
Minneola silt loam	3.53	12.6
Lancaster clay loam	3.73	16.5
Adelanto clay loam	5.08	12.0
Yolo loam	4.04	9.0
Houston black clay	3.50	6.0
Plainfield sand	3.34	6.0
Auchincruive sand	2.40	5.7

3.6 Chapter Summary:

In this chapter the concept of irrigation scheduling is introduced. In order to indicate when and how much water should be applied to the crop, the daily water losses and gains to the root zone are evaluated. Gross rainfall is seperated into the rainfall and infiltration components, and the infiltrated water is routed through the root zone storage to determine possible drainage losses.

The Pan-evaporation method and the Penman and Penman-Montieth models are used to estimate the daily potential evapotranspiration rate . A mathematical expression is then derived for the estimation of the actual transpiration loss from a multi-layered root zone, taking into account the nonuniform root distribution. A two-stage empirical model is used to evaluate the actual soil evaporation rate. The parameters of the soil evaporation model are determined experimentally.

The actual rates of water loss estimated in this chapter are used in the chapter 4 to simulate the water balance of nonuniform soil profile with a growing, nonuniform root zone. The model is then used to establish the dates and the amounts of required irrigation, and to evaluate the antecedent soil moisture contents in the root zone layers, for use by the infiltration models in chapter 6.

CHAPTER 4 ROOT ZONE WATER BALANCE MODEL:

4.1 Introduction :

The methods of estimating the gains and losses of water in the root zone, described in the previous chapter, enable the calculation of the changes in root zone moisture storage from the mass balance equation (Eqn. 3.3). In this chapter a dynamic water balance model is proposed which incorporates such characteristics as a nonuniform soil profile and a growing root zone (with nonuniform root distribution), in the soil moisture accounting algorithm.

The model is then tested with actual soil moisture content and evapotranspiration data measured from a lysimeter experiment. The effects of different management practices on the irrigation schedules, end-of-season irrigation requirements and relative yield, are simulated.

4.2 Root zone water balance model.

4.2.1 Water balance of uniform soils with nonuniform, growing, root zones:

The common practice in irrigation modelling is to assume the root zone to be uniform in soil properties and of a constant depth. If the root depth development, particularly in the case of annual crops, is taken into consideration then the assumption of a static root zone storage capacity leads to the underestimation of the irrigation frequency and the over-estimation of the required irrigation quantities early in the growth season.

The rate of elongation of plant roots is subject to many factors which make its quantification difficult for modelling purposesd. Factors such as plant species, antecedent soil, water and nutrient conditions, the irrigation frequency and depth, tillage practices and the climate effect growth. Hansen etal (1979) recommend that as a rough guide the depth of rooting varies from 30 to 45 cm depth per month of active growth. Israelson & Hansen (1962) state that the maximum rooting depth is reached by the time fruiting occurs. Danielson (1967) categorised crops into shallow, moderate and deep rooted. A compilation of root depth developments, reported in the literature for several crops, is listed in the appendix. The root depth on any particular day can be obtained by interpolation between the observed values.

A simple approach to modelling the water balance of a growing root depth is to assume the rooting density to be uniform with depth, ie: at every point in the soil, water is taken up at the same rate as every other point. This approach is schematized in Fig. 4.1 . Consider the water balance algorithm :

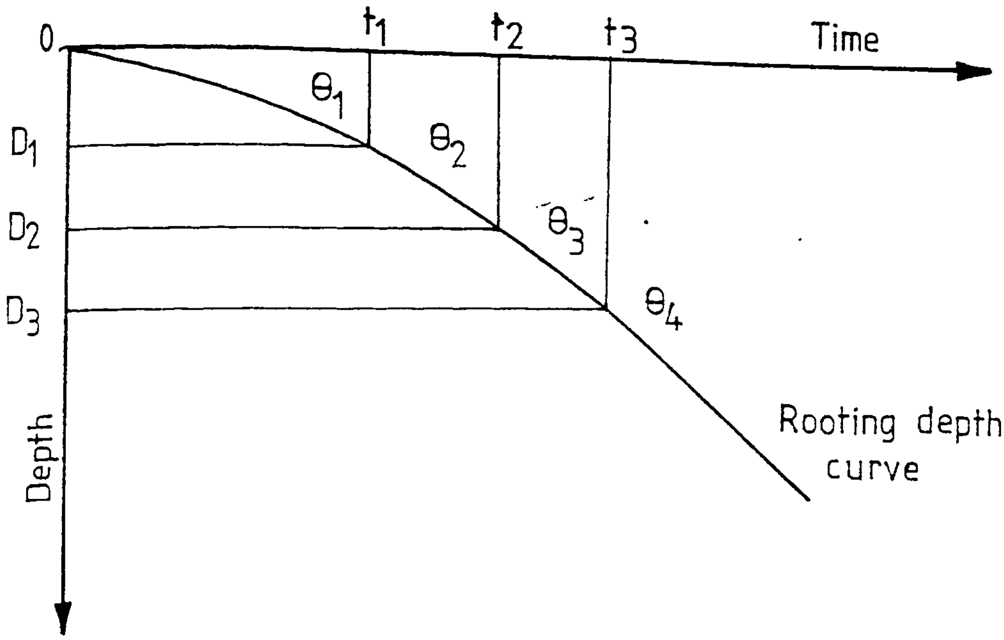

Fig. 4.1 Schematic representation of a dynamic, uniform root zone (θ = soil moisture content, cm3/cm3; D = root depth, mm; t = time, days).

At $t=1$ available water $= \theta 1\ D1 = \theta o\ D1$

$t=2$ $\theta 2\ D2 = \theta 1\ D1 + \theta o(D2-D1)$

$t=3$ $\theta 3\ D3 = \theta 2\ D2 + \theta o(D3-D2)$

etc ...

where θo is the initial moisture content; $\theta 1$ is the moisture content at time $t=1$; and D1 is the root depth at time $t=1$.

In general terms:

$$\theta(t+1).D(t+1) = [\theta(t) - T(t) - SE(t)].D(t) + \theta o[D(t+1) - D(t)] \qquad (4.1)$$

including the soil evaporation (SE) and transpiration (T) terms . D(t) is the maximum root depth on day t .

Rearranging :

$$\theta(t+1) = [(t) - T(t) - SE(t)].\left(\frac{D(t)}{D(t+1)}\right) + \theta o\ \left[1 \frac{D(t)}{D(t+1)}\right] \qquad (4.2)$$

This is the water balance equation for a growing root depth of uniform water uptake rate. The irrigation is scheduled for the condition when :

$$\sum_{t=0}^{t} [\theta o - \theta(t+1)] > \text{MNGSMD} \ (\theta o - \theta wp) \qquad (4.3)$$

where θwp is the wilting point moisture content.

θo is often set to field capacity by pre-season irrigation to ensure adequate moisture storage for germination and seedling development.

In the above analysis the uptake rate was assumed to be uniform with depth which suggests the rooting density is also uniform with depth. In reality this condition rarely exists since a greater proportion of roots develop near the surface. The rooting patterns of crops influence the water balance equation 4.2 in that more water will be removed from the surface layers. If the uptake rate is distributed uniformly with depth, all layers reach the critical moisture content (θc) at the same time, but when the surface layers loose water faster, they reach θc earlier and the plant will suffer stress.

The modelling solution to this problem is to divide the root zone into discrete soil layers with corresponding rooting densities. In general dividing the root zone into 4 equal layers is adequate to describe the root-distribution pattern. An average water extraction pattern, from top to bottom, is the

40, 30, 20 and 10% distribution. In the following water balance model, the aim is to develope an algorithm which responds to a wide range of root-distribution patterns.

The algorithm developed here is based on Fig. 4.2 . Consider at time t=1 :

at layer j=1 available water $= \theta(1,1).D(1,1) = \theta o(D1,1)$

j=2 $\theta(1,2).D(1,2) = \theta o(D(1,2)$

j=3 $\theta(1,3).D(1,3) = \theta o(D(1,3)$

j=4 $\theta(1,4).D(1,4) = \theta o(D(1,4)$

at time t=2 :

layer j=1 $\theta(2,1).D(2,1) = \theta(1,1).D(1,1) + \theta(1,2).[D(2,1)-D(1,1)] - T(1,1) - SE(1,1)$

layer j=2 etc ...

and at:

layer j=4 $\theta(2,4).D(2,4) = \theta(1,4).D(1,4) - \theta(1,4)[D(2,4)-D(1,4)] + \theta o[D(2,4)-D(1,4)] - T(1,4) - SE(1,4)$

In general therefore :

$$\begin{aligned}\theta(t,j).D(t,j) = {} & \theta(t-1,j).D(t-1,j) \\ & - \theta(t-1,j)[D(t,j)-D(t-1,j)] \\ & + \theta(t-1,j+1)[D(t,j)-D(t-1,j)] \\ & - T(t-1,j) - SE(t-1,j)\end{aligned} \tag{4.4}$$

Noting that $\theta(t,j>4) = \theta o$.

Rearranging :

$$\begin{aligned}\theta(t+1,j) = {} & \theta(t,j).[D(t)/D(t+1)] \\ & + [\theta(t,j+1) - \theta(t,j)].[1-(D(t)/D(t+1)] \\ & - [4.T(t,j)/D(t+1)] \\ & - [4.SE(t,j)/D(t+1)]\end{aligned} \tag{4.5}$$

Noting that $D(t,j)/D(t+1,j) = D(t)/D(t+1)$.

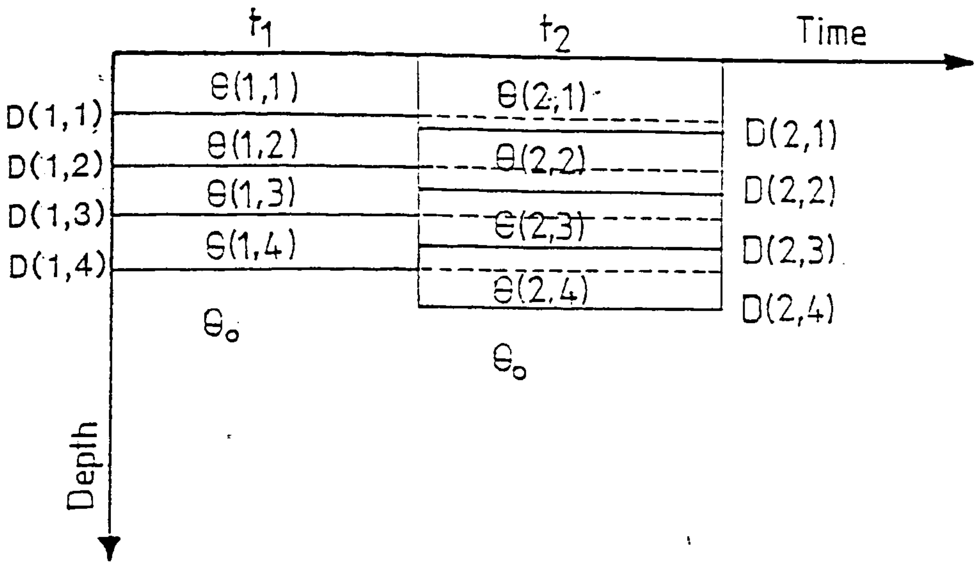

Fig. 4.2 Schematic representation of a nonuniform, dynamic root zone (θ(1,1) = soil moisture content, cm3/cm3, of layer 1 on day 1; θo = initial soil moisture content, cm3/cm3; D(2,4) = thickness (mm) of layer 4 on day 2; t1 = day 1; t2 = day 2).

Irrigation is timed for when the actual soil moisture deficit is greater than or equal to the maximum allowable soil moisture deficit :

$$\theta fc - \sum_{t=0}^{t} [\sum_{j=1}^{4} \theta(t+1,j)] > MNGSMD(\theta fc - \theta wp) \qquad (4.6)$$

4.2.2 Water balance of nonuniform soils with nonuniform, growing, root zones:

The water balance equation 4.5 , includes the transpiration rate term T(t,j), where t is the day number and j is the root layer index. Equation 3.13 indicates that the transpiration rate from any layer is dependent on the available moisture content in that layer. In nonuniform soils the water storage capacity of each soil profile layer will be different both in time and space. As the root depth increases so do the root layer thicknesses. Thus the soil related properties of any root layer are dependent on the profile layer or layers which are in contact with it.

An algorithm is developed here whereby, at any time (t) and root depth (RTDP), the hydraulic properties of the soil profile layer or layers are assigned to the root layer with which they are in contact. The notations used are defined in Table 4.1, for the soil profile example shown in Fig. 4.3.

In this example only the field-capacity

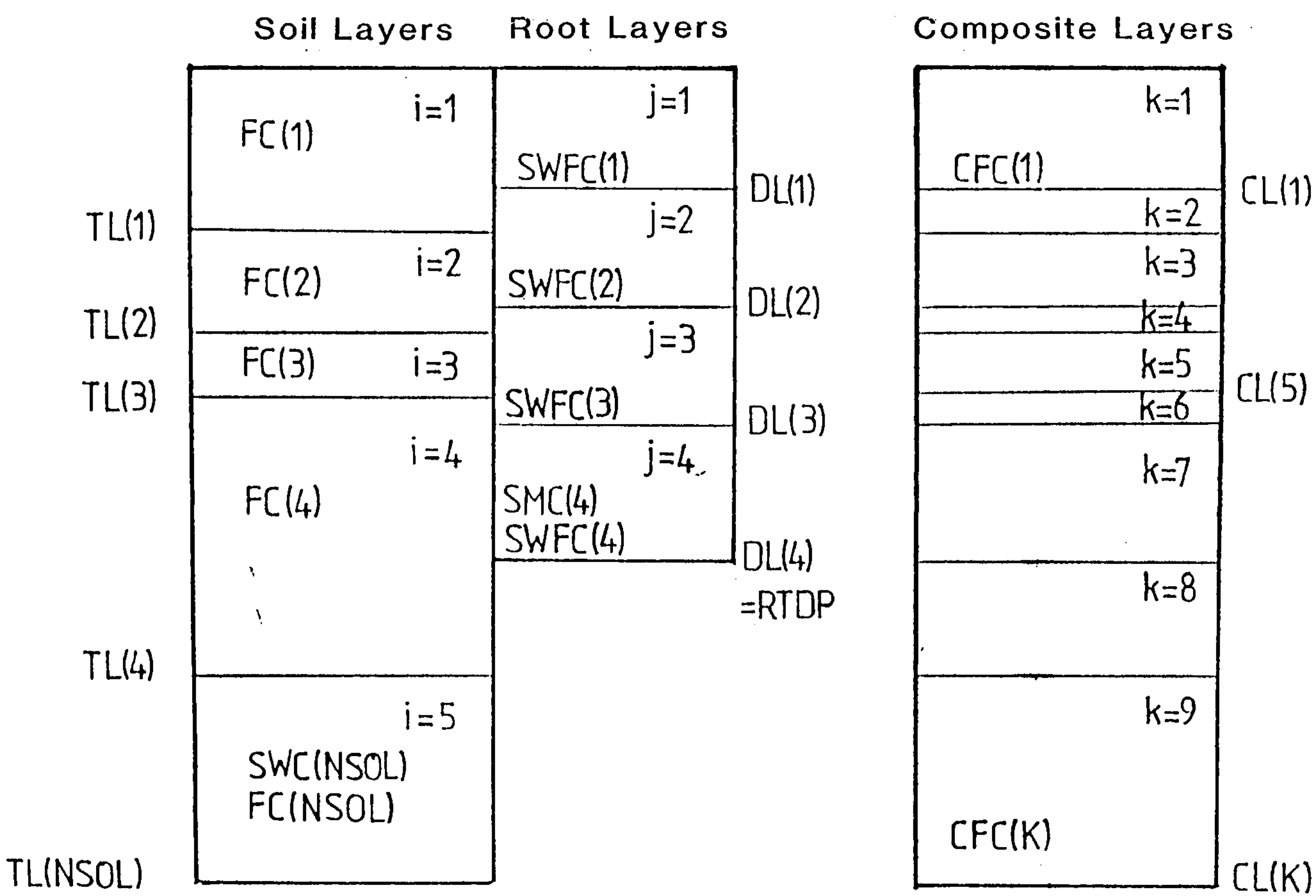

Fig. 4.3 Schematic diagram of discrete soil and root layers and the composite-layer profile (see Table 4.1).

Table 4.1 Definition of symbols used in the definition of soil, root and composite layer diagram (Fig. 4.3).

NSOL	=	number of soil layers.
RTDP	=	root depth, mm.
TL	=	thickness of soil layer, mm.
FC	=	soil layer field capacity, cm3/cm3.
SWC	=	soil moisture content, cm3/cm3.
SATK	=	soil saturated conductivity, mm/day.
SWFC	=	root layer field capacity, cm3/cm3.
SMC	=	root layer soil moisture content, cm3/cm3.
SKS	=	root layer saturated conductivity, mm/day.
DL	=	thickness of root layer, mm.
RTDP	=	rooting depth on the day, mm.
CFC	=	composite layer field capacity, cm3/cm3.
CL	=	thickness of composite layer, mm.
i	=	index of soil layer number.
j	=	index of root layer number.
k	=	index of composite layer number.

parameter is used to illustrate the algorithm. The same procedure also applies to other soil properties such as the wilting point WLTP(j), the saturated moisture content SWSAT(j), and the residual moisture content SWRESI(j).

A necessary assumption is that the soil profile properties (except antecedent moisture content) remain constant at all times. Depending on the position of RTDP the appropriate layer SWFC(j) must be determined from the corresponding FC(i) values. The analysis of Fig. 4.3 shows that two conditions can exist between the soil profile and root layers :

<u>Condition 1 :</u>

In this case a root layer is completely contained within one soil profile layer (eg. root layer j=1 in Fig. 4.3), and all the properties associated with that soil layer are assigned to the root layer :

$$SWFC(j) = FC(i) \tag{4.7}$$

<u>Condition 2 :</u>

In this case a root layer contains one or more complete soil layers plus one or more partial layers (eg. root layer j=3). A weighted averaging technique is used to calculate the hydraulic properties to be assigned to this root layer :

$$SWFC(j) = \frac{D1 + D2 + D3}{RTDP/4} \tag{4.8}$$

where:

$$D1 = DX1 \,.\, FC(i) \tag{4.9a}$$
$$D2 = TL(i+1) \,.\, FC(i+1) \tag{4.9b}$$
$$D3 = DX2 \,.\, FC(i+2) \tag{4.9c}$$

where DX1 and DX2 are the amounts (in millimeters) of overlap (Fig. 4.4) .

When the number of complete layers contained in layer j, NCOMPL(j), is greater than one , D2 is found by the summation :

$$D2 = \sum_{k=1}^{NCOMPL(j)} TL(i+k) \,.\, FC(i+k) \tag{4.9d}$$

The soil-root layer sorting subroutine (LYRSRT) is called at the beginning of each day with the new root depth as input. The complete sorting model flow chart is presented in Fig. 4.5 . The procedure can be summarized as follows :

1 - Find the soil layer within which the root depth bottom is located.

2 - Working backwards from this position, find for each root layer wether conditions 1 or 2 applies.

3 - For condition 1 , transfer the soil hydraulic properties according to equation 4.7 .

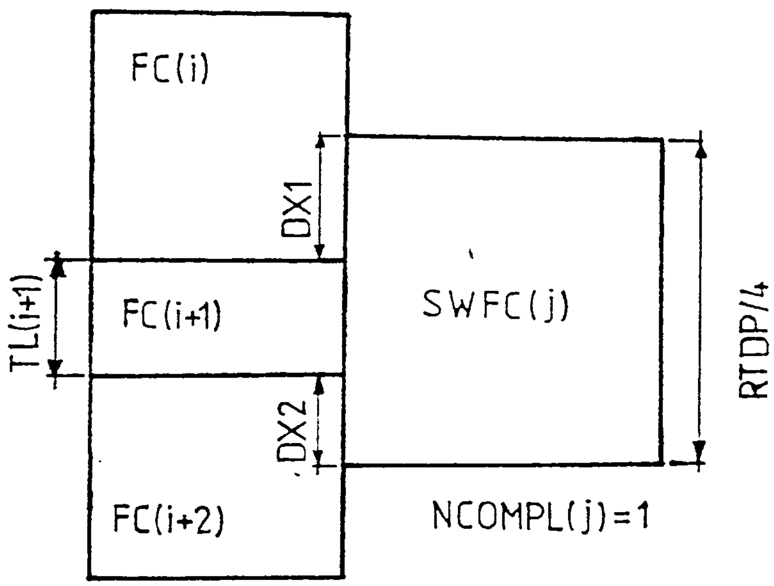

Fig. 4.4 Definition skech of overlapping soil and root layers (DX1 and DX2 are the amounts (mm) of overlap; see Table 4.1 for other symbols).

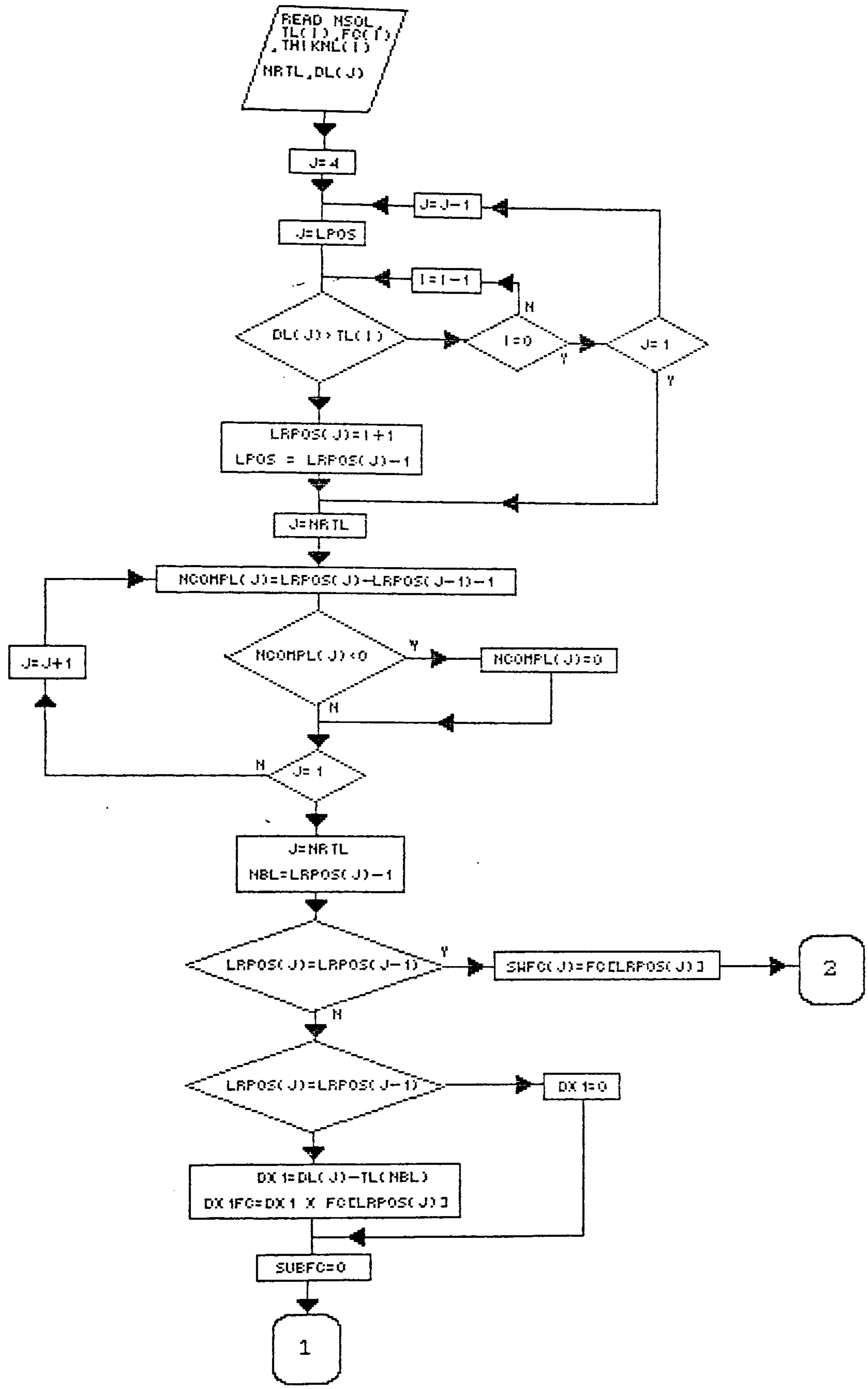

Fig. 4.5 Flow chart of composite-layer generation algorithm (see Table 4.2 for definition of terms).

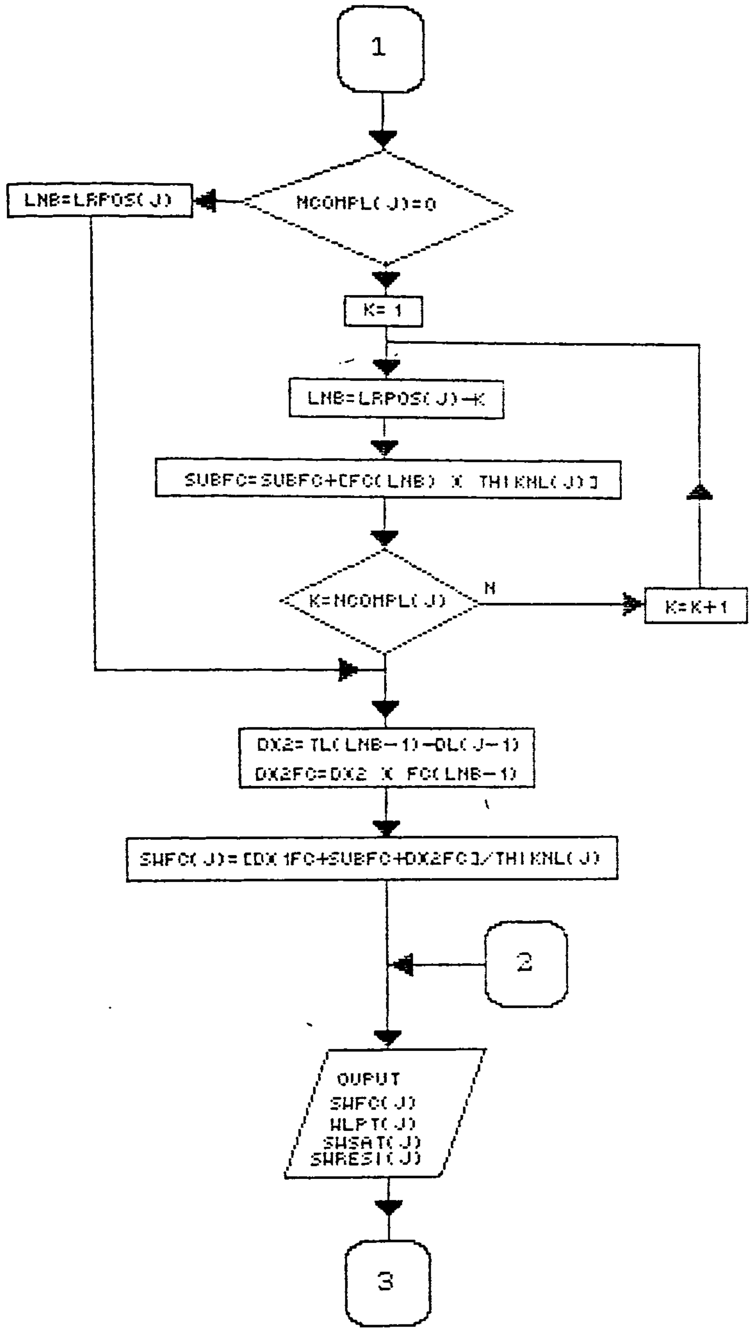

Fig. 4.5 Continued ..

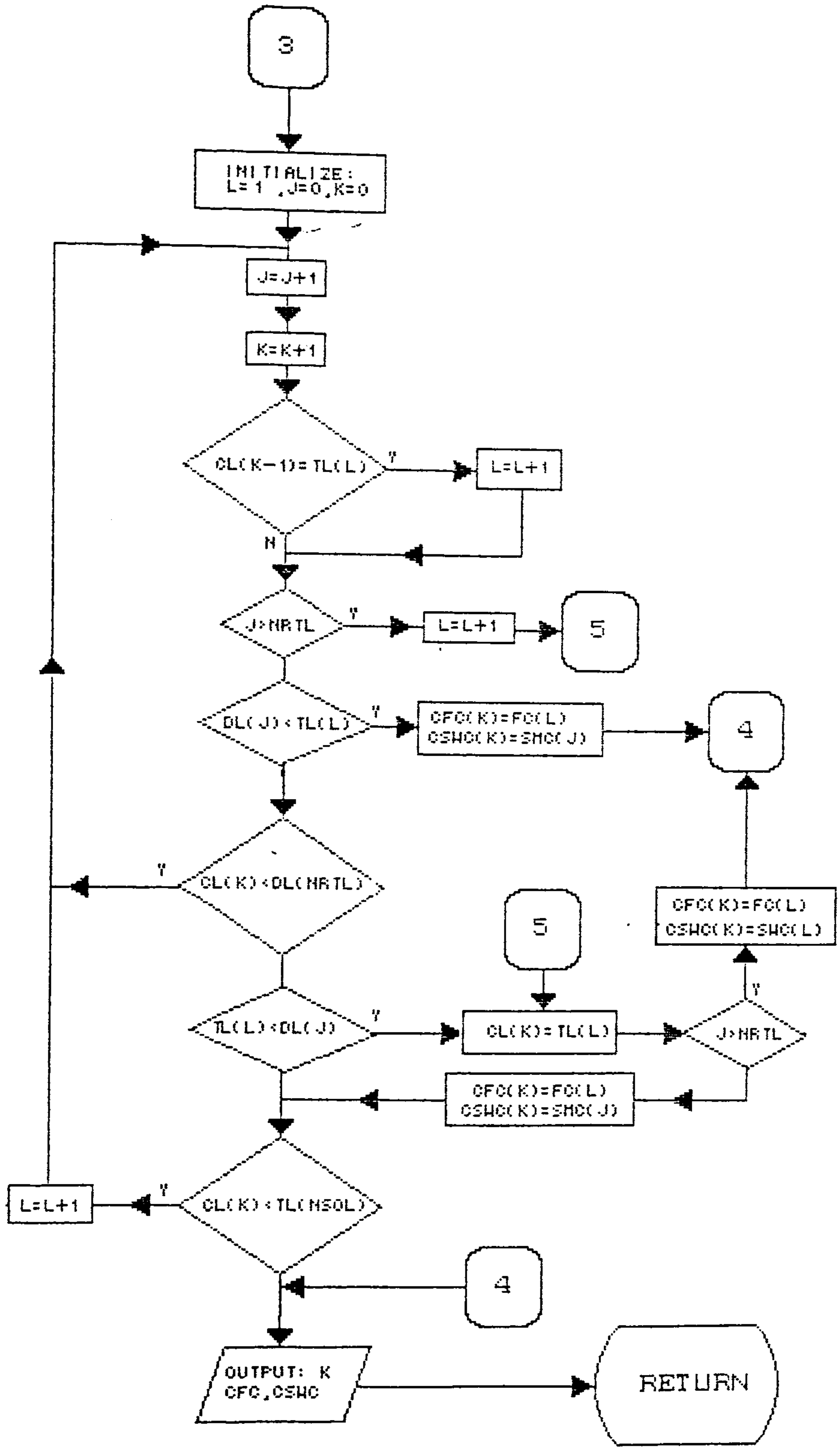

Fig. 4.5 Continued ..

Table 4.2 Definition of symbols used in the layer sorting algorithm (Fig. 4.5).

i	=	Index of soil layer.
j	=	Index of root layer.
k	=	Index of composite layer.
NSOL	=	Number of soil layers.
THIKNL(i)	=	Thickness of soil layer i (mm).
TL(i)	=	Depth to soil layer i (mm).
FC(i)	=	Field capacity of soil layer (cm3/cm3).
NRTL	=	Number of root layers.
DL(j)	=	Depth to root layer (mm).
LRPOS(j)	=	Position of root layer j, relative to soil the layers.
NCOMPL(j)	=	Number of complete soil layers in contact with root layer j.
SWFC(j)	=	Field capacity of root layer (cm3/cm3).
DX1	=	Distance of overlap between a root layer and the soil layer above it (mm).
DX1FC	=	Field capacity of segment DX1 (mm).
SUBFC	=	Field capacity of soil layer contained within a root layer (mm).
DX2	=	Distance of overlap between a root layer and the soil layer below it (mm).
DX2FC	=	Field capacity of segment DX2 (mm).
WLPT(j)	=	Wilting point of root layer j (cm3/cm3).
SWSAT(j)	=	Saturated moisture content of root layer j (cm3/cm3).
SWRESI(j)	=	Residual moisture content of root layer j (cm3/cm3).
CL(k)	=	Depth to composite layer k (mm).
CFC(k)	=	Field capacity of composite layer k (cm3/cm3).
CSWC(k)	=	Water content of composite layer k (cm3/cm3).

4 - For condition 2 , check if the root layer overlaps any soil layers, if so determine the amount of overlap and calculate new root layer properties according to equation 4.8 .

Composite Profile :

The composite layering, shown in Fig. 4.3 , is a superimposition of the soil and root layers' physical properties. The composite-layer diagram reflects the end-of-day physical properties of the nonuniform soil profile, under a nonuniform, growing, root zone. This composite-layer profile is required to assess the infiltration rate of the soil and the redistribution of the infiltrated water in the complex soil profile.

Whereas such properties as the soil moisture contents are directly transferable from the root layers across to the composite layer diagram, other properties, such as hydraulic conductivity, must be assigned from the soil layer diagram.

For instance consider the root layer j=2 . It's moisture content is determined by the transpiration from that layer and is thus independent of the soil layer it is in contact with. The other soil moisture properties (field capacity etc) are determined by the procedure outlined above. Root layer j=2 overlaps two soil layers i=1 and i=2 , and therefore must reflect two different soil hydraulic conductivities SKS(i=1) and SKS(i=2) .

One method would be to estimate the root layer hydraulic conductivity SATK(j=2) as a weighted average of SKS(1) and SKS(2) . A more representative method is to form a composite-layer profile which maintains the soil hydraulic conductivity properties and which also reflects the changing root layer moisture content. For example the composite layers k=2 and k=3, (Fig. 4.3), have the same moisture contents (from root layer j=2), but layer k=2 has a conductivity value of SKS(i=1) and layer k=3 has a value of SKS(i=2). The flowchart of the algorithm used for this composite-layer model is shown as the third part of Fig. 4.5 .

The composite-layer profile is a prerequisite to the running of the nonuniform infiltration model (chapter 6). The only requirements of the subroutine LYRSRT are that each day the new root depths and the new root layer moisture contents are passed on from the root zone water balance model. In the interest of reducing unnecessary data storage, the composite-layer output is limited to days for which irrigation have been predicted or planned.

It should finally be emphasized that the layer configurations shown in the example of Fig. 4.3 are not static (except for the soil profile), but change every day in response to the dynamic rooting depth and the differential water uptakes from the root layers. In this way much of the real processes of the field can be dynamically modelled without the need for gross assumptions concerning the spatial and temporal characteristics of a cultivated soil profile.

4.2.3 Crop Rooting Pattern :

The development of the rooting pattern of crops is not only dependent on the species but also on the physical properties of the soil medium and the irrigation and fertilizer management practices. The distribution of the rooting density (expressed as cm root length per cm3 volume of soil), is influenced by such factors as soil shear strength, pore size distribution, moisture and nutrient distribution and the frequency and depth of irrigation (Milthorpe & Moorby 1979).

Boonyatharakol & Walker (1979) provide functional relationships for several rooting patterns. In modelling, it is desirable that, as far as possible, a single function should describe a process, with the function parameters reflecting the variations in the inputs and outputs.

In general the shape of the rooting pattern of crops can be described by an exponential function:

$$R(z) = a \exp(b.z) \tag{4.10}$$

where R(z) is the percentage of roots at depth z ; and 'a' and 'b' are the exponential shape constants.

Assuming the root zone is divided into NL number of layers, we can write:

$$R(j) = a \exp[\, b.z(j)] \tag{4.11}$$

where

$$z(j) = [2(j-1)+1]/2NL \tag{4.12}$$

and j is the layer index (1 at top).

Gerwitz & Page (1974) presented an empirical function based on the exponential distribution:

$$R(z) = 100[\, 1- \exp(- f.z)\,] \tag{4.13}$$

From the analysis of a number of crop rooting patterns, they proposed that the factor 'f' be defined as :

$$f = 1/ Z63 \tag{4.14}$$

where Z63 is the depth that contains 63% of the total root mass, and must be determined experimentally.

Rowse & Barnes (1979) proposed the following function :

$$C = (R^{1/2}/b)\ .\ \exp[- z/(b.R^{1/2})] \tag{4.15}$$

where

C = mean concentration of roots (cm/cm3) at depth z (cm)

b = shape parameter

R = total root length beneath 1cm2 of soil

But with a little rearrangement Eqn. 4.15 can be shown to be very simillar to Eqn. 4.13 :

$$R(z) = 100[\ 1-\exp(\ -z/(b.R^{1/2}\ )\ ] \tag{4.16}$$

where:

$$1/(b.R^{1/2}\ ) = f \tag{4.17}$$

The advantage of using Eqn. 4.13 is that it describes the rooting pattern function through the single parameter Z63 . In many instances this value may not be available since its determination involves the excavation of the entire root zone. A more desirable parameter is the percentage uptake in the first layer only.

Assuming the root layer is divided into 4 equal layers, Eqn 4.13 can be rearranged to give an expression for Z63 :

$$Z63 = \frac{-\ Z}{\ln[\ 1-\ R(z)/100\ ]} \tag{4.17}$$

Thus if Z = RTDP/4 for the first layer (where RTDP is the root depth) then:

$$Z63 = \frac{-\ RTDP}{4\ \ln[\ 1 - P(1)/100\ ]} \qquad (4.18)$$

where P(1) is the percentage of roots in the first quarter root layer.

In this way the rooting-pattern function is described by the single variable P(1) and equations 4.18 , 4.14 and 4.13 .

In the scheduling model two options are available. In the first, given the percentage of roots in all four layers, the shape constants 'a' and 'b' are determined for Eqn. 4.10 by regression analysis. The second option only requires the percentage of roots in the first layer to describe the rooting-pattern function as described above. This latter option , although more parameter efficient, does have a disadvantage in that for P(1)=35% the total percentage of roots accounted for, is only 82.15% . This value improves to 87% for P(1)=40% and to 94% for P(1)=50% . This small error implies that the assumption of an exponential distribution will not hold true for small values of P(1), ie: more evenly distributed rooting patterns.

4.3 Lysimeter Experiment :

To test the validity of the algorithms developed for equation 4.5 , it was necessary to undertake an experiment primarily to obtain data on the changes of soil moisture content within the root zone. These data are then used to test the viability of the root zone water balance model.

The experiment was set up in a laboratory-based glasshouse . The source of artificial solar light was a set of three 400 watt high pressure sodium plant irradiators. The lysimeter container (Plate 4.1), was made of clear perspex with width, breadth and depth dimensions of 25 x 25 x 100 cm respectively. The outer surfaces were covered with aluminium foil to insulate the soil profile from direct radiation. Access holes (of 20 mm diameter), were drilled, on three sides of the container, in two columns and at 10 cm vertical intervals. These holes, normally closed with rubber or cork bungs, acted as access holes from which soil samples could be taken at any time during a drying cycle . The base of the container was drilled with holes to allow free drainage.

The lysimeter was filled with a sandy soil obtained from Auchincruive in Ayrshire, Scotland, (see chapter 5 for properties). The soil was wetted and allowed to settle naturally before the container was topped up with more soil. This was repeated untill the

Plate 4.1 The lysimeter used in the experiment.

container was full. The entire profile was then wetted, the surface covered to prevent evaporation, and allowed to drain for two days to simulate field capacity moisture conditions. The lysimeter was then planted with 6 soyabean seeds and the surface covered with absorbant tissue paper which was kept constantly moist to speed up the germination process. The seeds emerged after 12 days. The cover was then removed and the number of plants was reduced to 4 . The water accounting procedure was then started.

Free water evaporation was measured by taking note of the loss in weight of an open container filled with water. The temperature was measured by a mini-max thermometer and relative humidity by a whirling wet and dry bulb aspirated psychrometer. The evaporation, temperature and humidity were measured daily (except weekends). The mean daily variations of these variables are shown in Figs. 4.6 , 4.7 and 4.8 .

Two methods of water loss accounting were employed . In the first, refered to as the 'drainage method', water loss at the end of a drying cycle was determined as that volume retained in the soil after the addition of a fixed volume of water to the lysimeter. The amount of drainage plus the free water evaporation after two days, was subtracted from the applied water to give the water retained in the soil. This represents the water lost by evapotranspiration during the previous drying cycle.

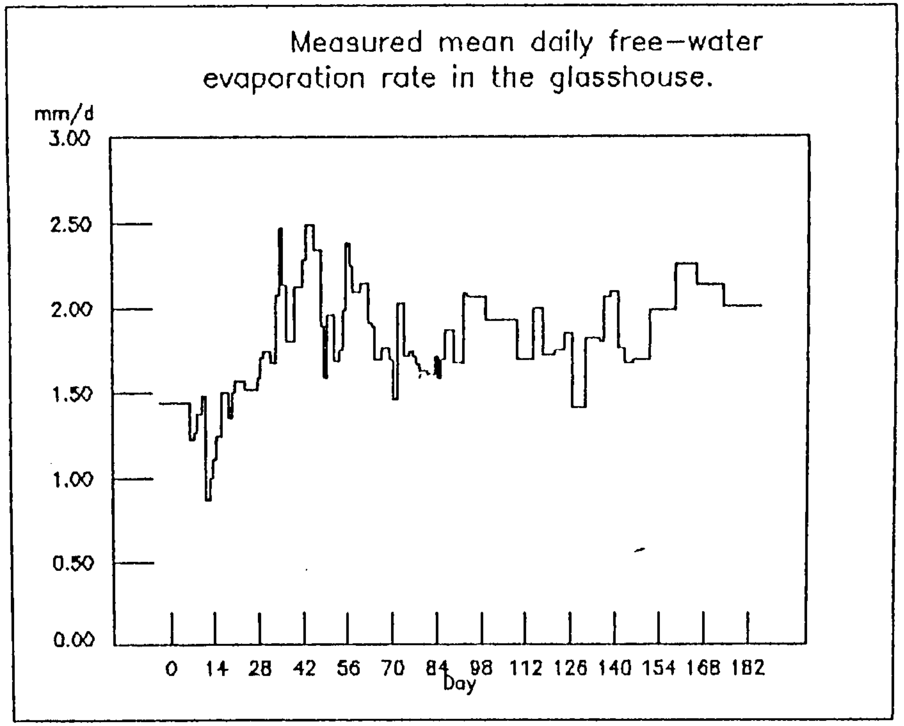

Fig. 4.6 Measured mean daily free-water evaporation rate in the glasshouse.

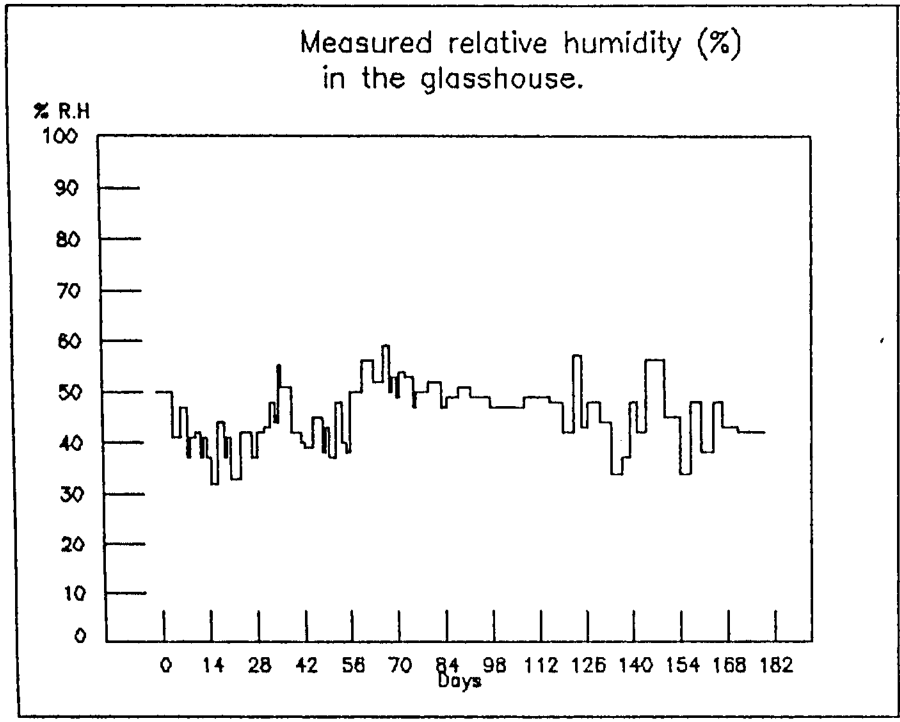

Fig. 4.7 Measured mean daily relative humidity in the glasshouse.

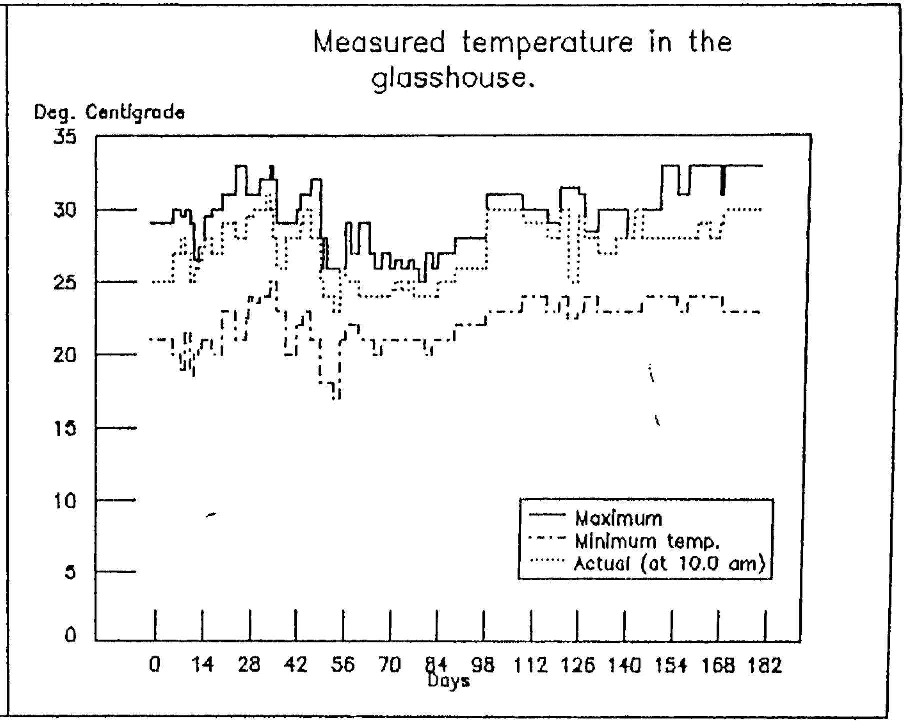

Fig. 4.8 Measured mean daily temperature of the glasshouse.

The second method, called the 'profile method', involved the taking of small soil samples from the array of access holes in the profile, and determining their moisture contents by the oven-drying gravimetric method. At each depth increment three soil samples were taken and the moisture contents averaged to give the soil moisture content in that layer.

At the end of each drying cycle, water was applied to the surface and the profile was assumed to have been restored to field capacity. Overall 9 drying cycles were simulated extending over a period of 180 days. Details of the cycle lengths and sampling dates are given in Table 4.3 .

The variations in the profile soil moisture contents, during the two longest drying periods 4 & 9 , are shown in Figs. 4.9 and 4.10 .

The water loss between samplings was calculated as the cumulative weight loss of all the samples taken from the vertical arrays. This loss represents the actual evapotranspiration (AET) . Fig. 4.11 shows the cumulative AET measured during cycles 4 and 9 .

Plotting the ratio of the cumulative potential (free water) evaporation (PET) and the AET (Fig. 4.12), for cycles 4 and 9 , shows the general downward trend which is consistent with the theory that AET reduces as the soil dries .

Table 4.3 Lysimeter experiment sampling dates and water balance.

Drying cycle	Dura. (days)	Sampling on day	Irrig. mm	Drain. mm	ET mm	ET mm/d
1	5	5	40	32.8	3.28	0.66
2	7	3,5,6	64	54.96	5.70	0.81
3	14	3,8,9,14	80	56.00	18.97	1.36
4	27	1,6,9,14,20, 22,27	112	59.68	45.71	1.69
5	15	1,8,14	64	31.68	27.14	1.81
6	13	1,9,13	64	35.76	21.38	1.64
7	21	10,21	64	25.44	33.25	1.58
8	22	10,22	64	25.12	32.04	1.46
9	56	10,17,31,42, 53	80	39.20	36.57	0.65

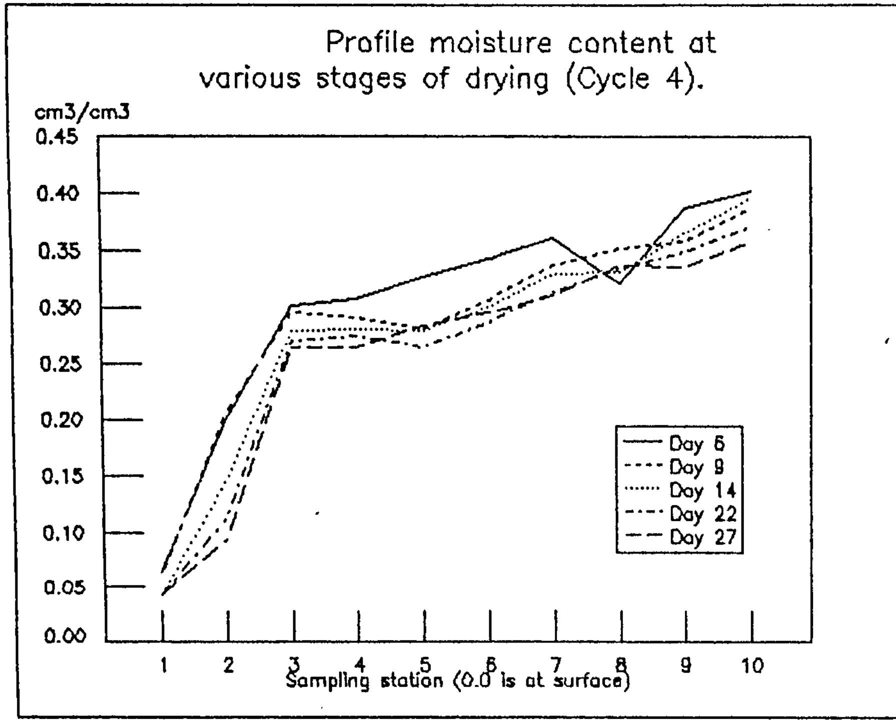

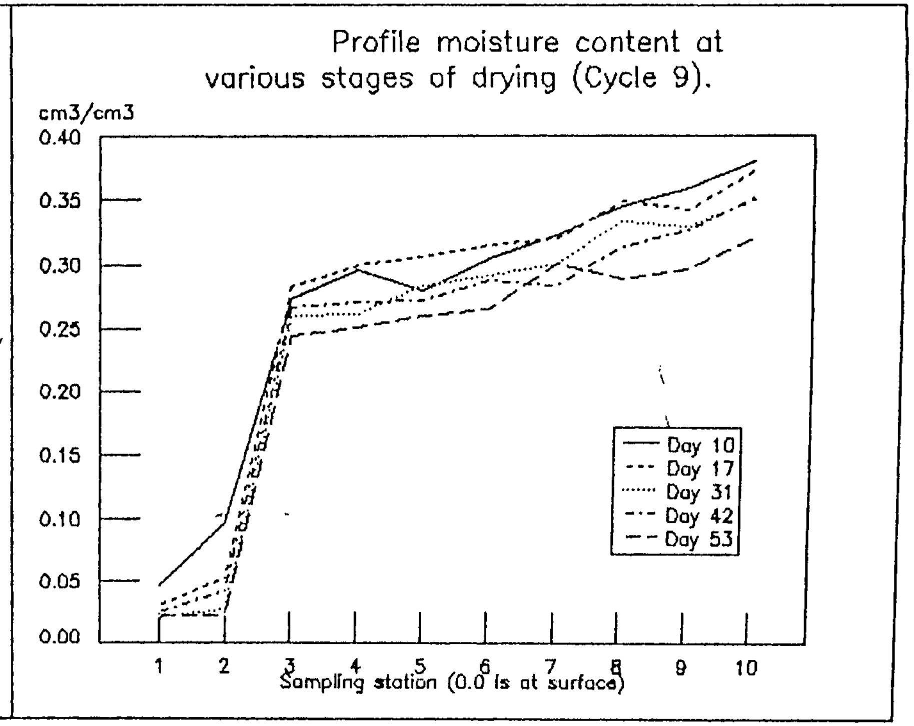

Fig. 4.9 Profile moisture content changes during drying cycle 4.

Fig. 4.10 Profile moisture content changes during drying cycle 9.

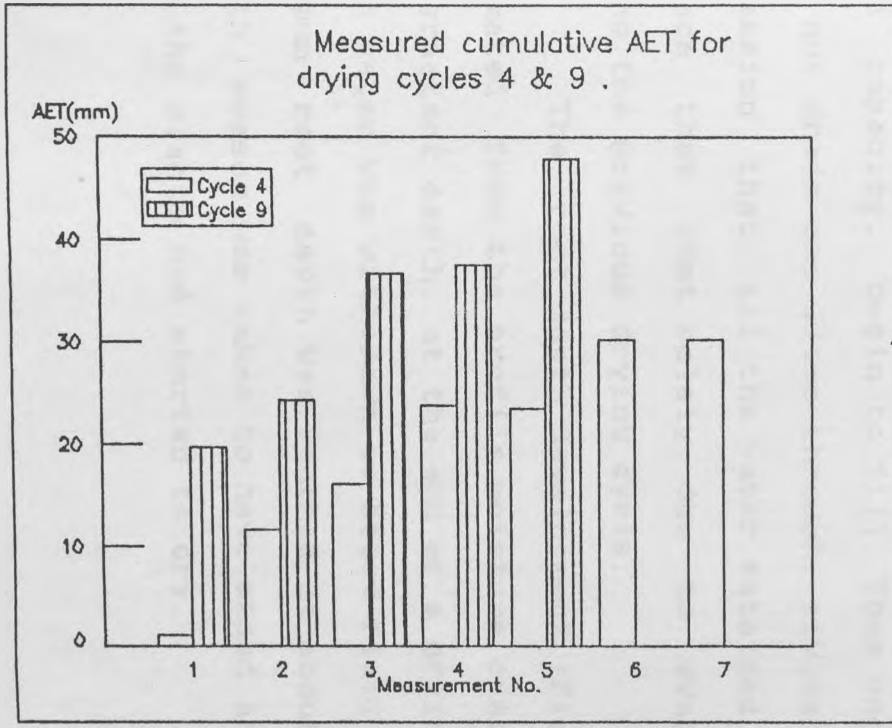

Fig. 4.11 Measured cumulative actual evapotranspiration (AET) for drying cycles 4 & 9.

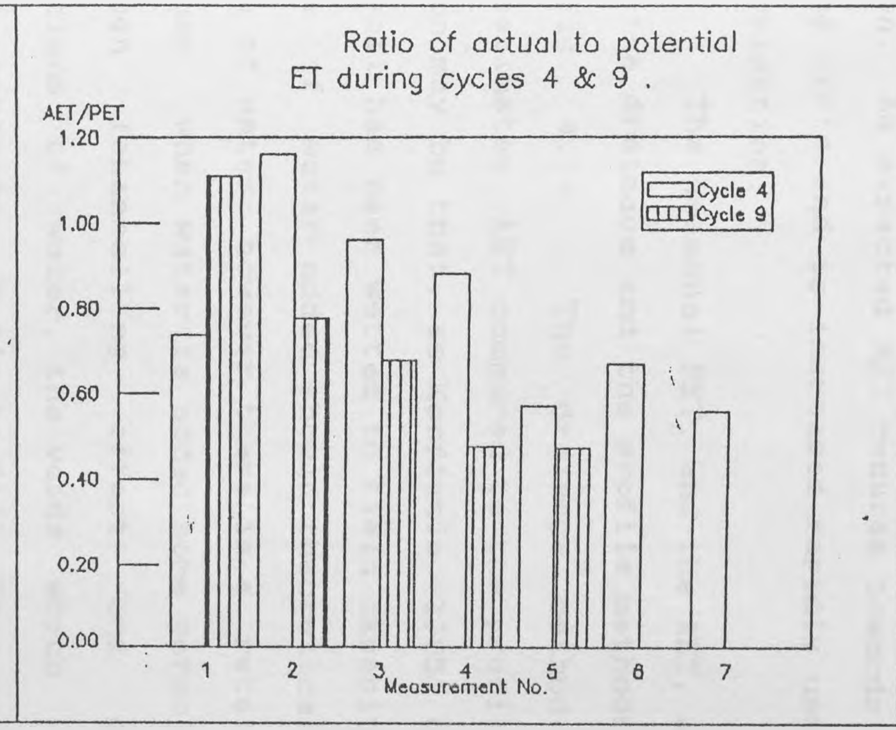

Fig. 4.12 Ratio of actual (AET) to potential (PET) evapotranspiration during drying cycles 4 & 9.

Figure 4.13 illustrates the cumulative AET, measured by the profile method, for the whole growth season. As expected AET reduces towards the end of a drying cycle and is increased rapidly upon application of irrigation.

The seasonal PET, and the AET, as measured by both the drainage and the profile methods, are compared in Fig. 4.14 . The drainage method consistently overestimates AET compared to the profile method. The reason may be that, as Korfiatis (1985) observed, once the soil has been wetted to field capacity, then every litre of water added should theoretically drain one litre of water; however there is a 'retained moisture' because when water is added some percolates directly through (channelling effect) and on subsequent additions of water, the voids which remained below field capacity, begin to fill. Then one litre added will not drain one litre through, giving the misleading impression that all the water retained was used to replace that lost solely due to evapotranspiration during the previous drying cycle.

The root depth development (Fig. 4.15), was estimated from the profile moisture content curves as the greatest depth, at the end of a drying cycle, from which water was withdrawn to below field capacity. The maximum root depth was reached at about day 72. The growth season was taken to have ended after 160 days when the plants had started to dry.

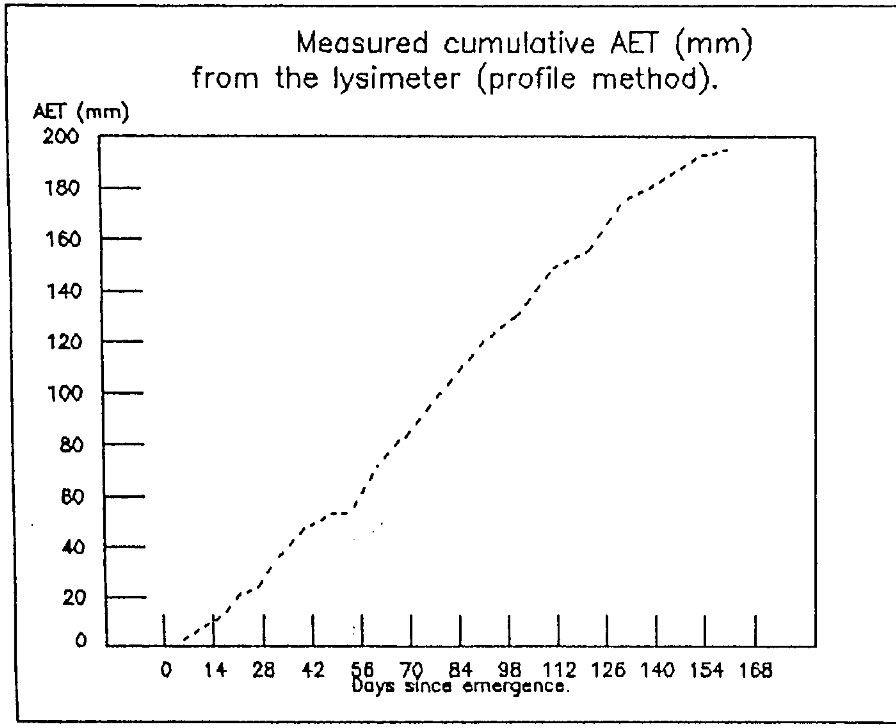

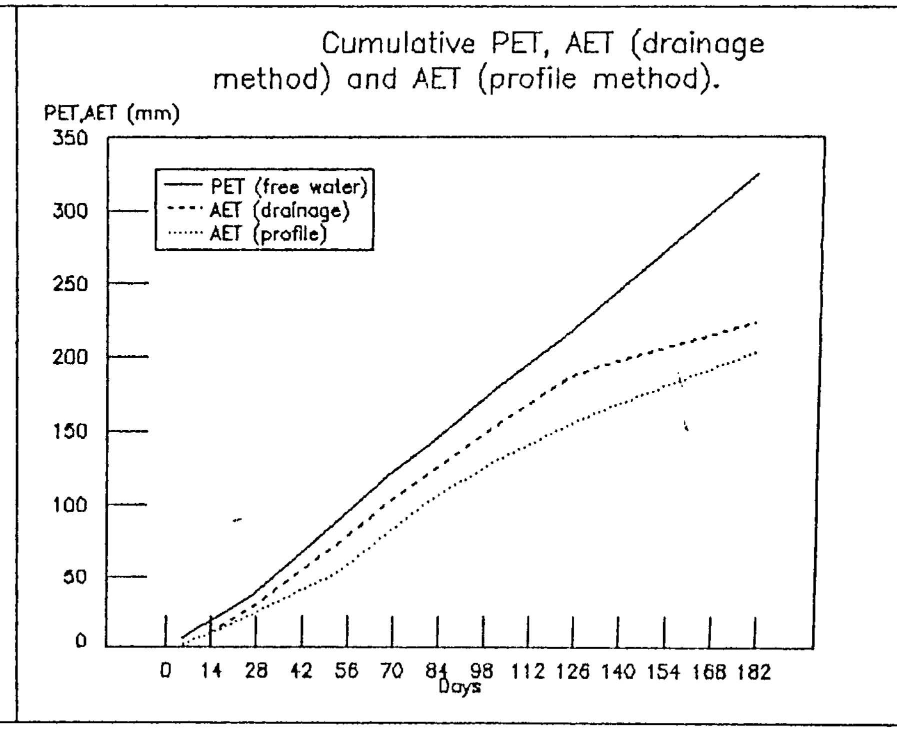

Fig. 4.13 Measured cumulative actual evapotranspiration (AET) from the lysimeter by the profile method.

Fig. 4.14 Comparison of cumulative potential (PET) with actual (AET) evapotranspiration as measured by the profile and drainage methods.

The leaf area index, Fig. 4.16 , was estimated by the direct measurement of the area of the leaves relative to the surface area of the lysimeter. The crop height development curve (Fig. 4.17), was also measured during the growth period. The maximum average height was reached at about day 50 .

Fig. 4.15 Measured soyabean root depth developement.

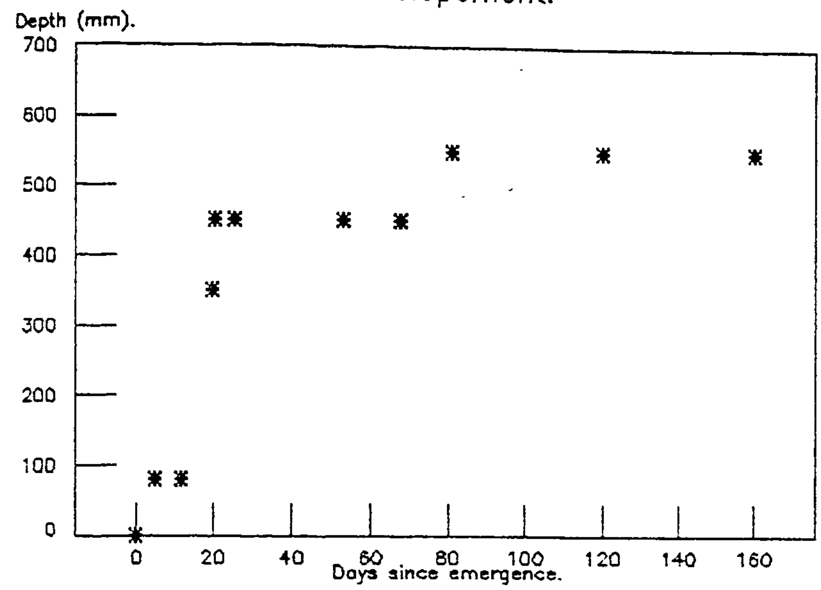

Fig. 4.16 Measured Leaf Area Index of the soyabean stand.

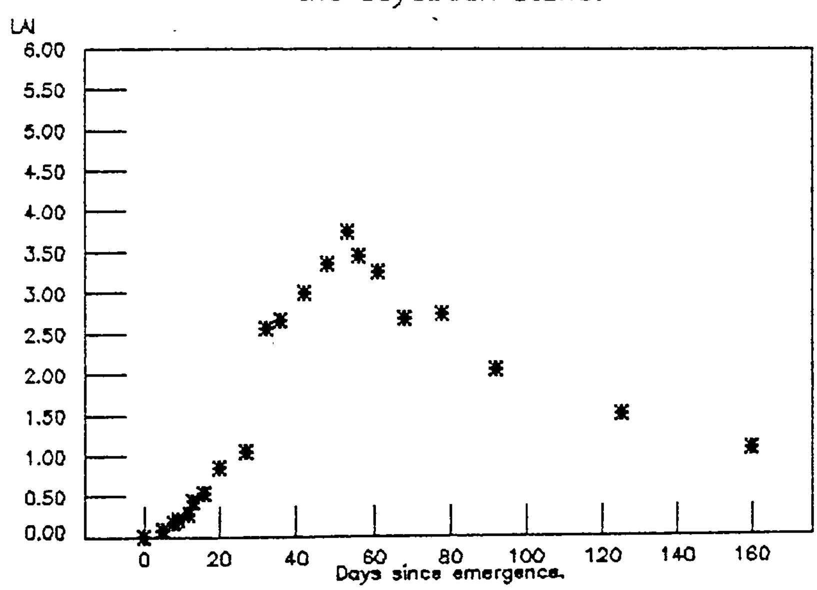

Fig. 4.17 Measured height developement of the soyabean stand.

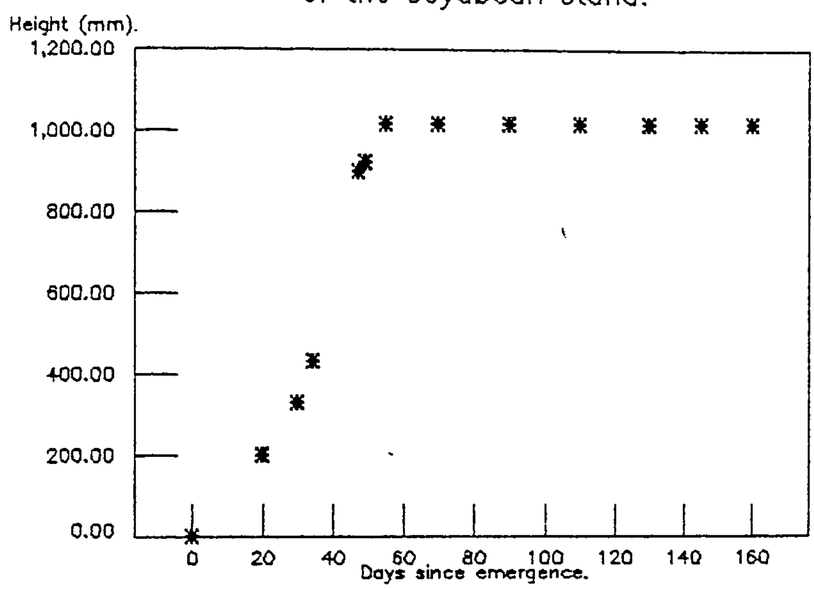

4.4 Testing the Model :

The root zone water balance model was developed with the aim of scheduling irrigations for nonuniform soils with dynamic, nonuniform, root zones. To test the predictive potentials of the model and to verify the algorithms used, the model was tested with the data obtained from the lysimeter experiment. Only the dynamic, nonuniform, root zone aspect of the model could be simulated since the soil in the lysimeter was uniform; although a uniform soil profile represents a special case of nonuniformity in soils and is a valid test of the model algorithm.

4.4.1 Criterion for Calibration :

Apart from the physically determinable soil, crop and meteorological parameters, the model requires three semi-empirical parameters defined below:

1 - TRPARAM: This is the transpiration response factor and reflects the sensitivity of the plant transpiration rate to depleting soil moisture. It's value ranges from zero to one (see chapter 3, section 3.4.3).

2 - SLEVDP: This is the soil depth of evaporation, ie the maximum depth from which evaporation takes place. A range of values from 50mm to the maximum root depth is assumed here.

3 - UTPCLYR1: This parametrer is the percentage of roots in the first layer and characterises the water uptake distribution pattern. It's magnitude is assumed

to range from 30% to 90% .

The last two parameters have physical existance and can be measured in the field. It is however recognised that the magnitudes of all three parameters are less likely to be available from routinely measured field properties since they relate to conditions below the soil surface and vary according to crop, soil and moisture conditions. For instance a crop with a dense rooting system will be less susceptible to soil moisture depletion than a sparse-rooting plant, and the corresponding TRPARAM value will be higher. The SLEVDP parameter is soil based, with coarser soils having a higher value than finer soils.

The calibration procedure selects values of the above three parameters, within user specified lower and upper boundaries and size increments, and compares the simulated cumulative actual evapotranspiration (AETs) and the corresponding recorded values (AETm), for which the mean of the absolute relative deviations is minimum.

The mean absolute relative deviation (MARD) is defined by Yaron etal (1973) as :

$$MARD = \frac{100}{N} \sum_{i=1}^{N} . \frac{OBS(i) - SIM(i)}{OBS(i)} \qquad (4.19)$$

where N is the number of observations; OBS(i) is the observed variable (AETm) in period i ; SIM(i) is the simulated variable (AETs) in period i .

Yaron etal (1973) suggest that this statistic is preferable to the conventional standard deviation because it reduces the relative weight of some extraordinary and out of range measurement that could be the result of errors in the soil moisture measurement. A maximum MARD value of about 15% is considered compatible with likely experimental errors.

Table 4.4 shows the simulated results for the optimum, upper and lower boundary values of the three parameters. Optimization increments of 50mm , 0.05 and 5% were chosen for SLEVDP, TRPARAM and UTPCLYR1 respectively. The resultant comparisons between simulated and recorded actual evapotranspiration are shown in Figs. 4.18 , 4.19 and 4.20 , for the three respective cases. The simulated seasonal AET is overestimated by about 4% compared to the measured AET for the optimum case but the overall error (between observed and simulated AET) does not exceed 15% .

Figures 4.19 and 4.20 show that for either the upper or the lower boundary values of the three parameters (SLEVDP, TRPARAM, and UTPCLYR1), the water balance model consistently underestimates the cumulative evapotranspiration. This may not be desirable in practice since crop water stress will be predicted later than it may occur. An assessment, by

Table 4.4 Scheduling model simulation results for optimum, upper and lower boundary parameter values.

a) Parameters:	Optimum	Upper	Lower
SLEVDP (mm)	300.0	550.0	50.0
TRPARAM	0.4	1.0	0.0
UTPCLYR1 (%)	50.0	90.0	30.0
b) Results:			
MARD (%)	15.71	22.29	17.96
AT (mm)	121.03	85.41	103.18
AETs (mm)	202.94	167.32	185.10
AT/PT	0.86	0.61	0.74
% MARD change	-	+ 41.88	+ 14.32
% AET error	+ 4.07	- 14.19	- 5.07

* Key:

SLEVDP = soil depth of evaporation.
TRPARAM = transpiration rate decay parameter.
UTPCLYR1 = percentage of root in first layer.
MARD = mean absolute relative deviation.
AT = simulated actual transpiration.
AETs = simulated actual evapotranspiration.
PT = simulated potential transpiration.

USER: CMAV71 PLOTFILE: CPET6F3 ENTRY NO. 69692 QUEUED ON 14/09/88 AT 17:13 PLOTTED ON 14/09/88 AT 20:21

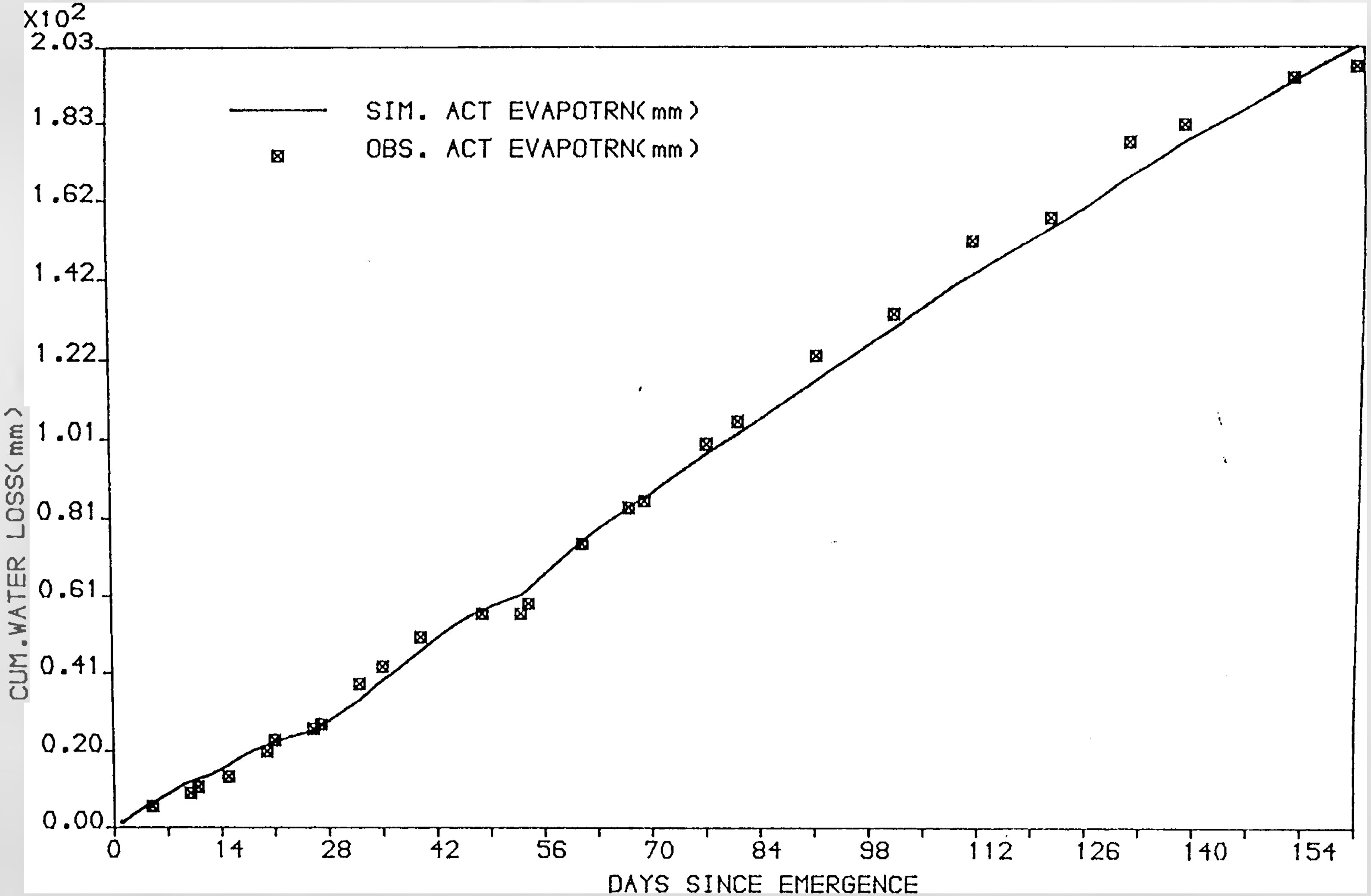

Fig. 4.18 Simulated and observed cumulative water loss (actual evapotranspiration, AET) under optimum model parameter values (see Table 4.4).

USER: CMAV71 PLOTFILE: CPETGF2 ENTRY NO. 89697 QUEUED ON 14/09/88 AT 18:12 PLOTTED ON 15/09/88 AT 09:48

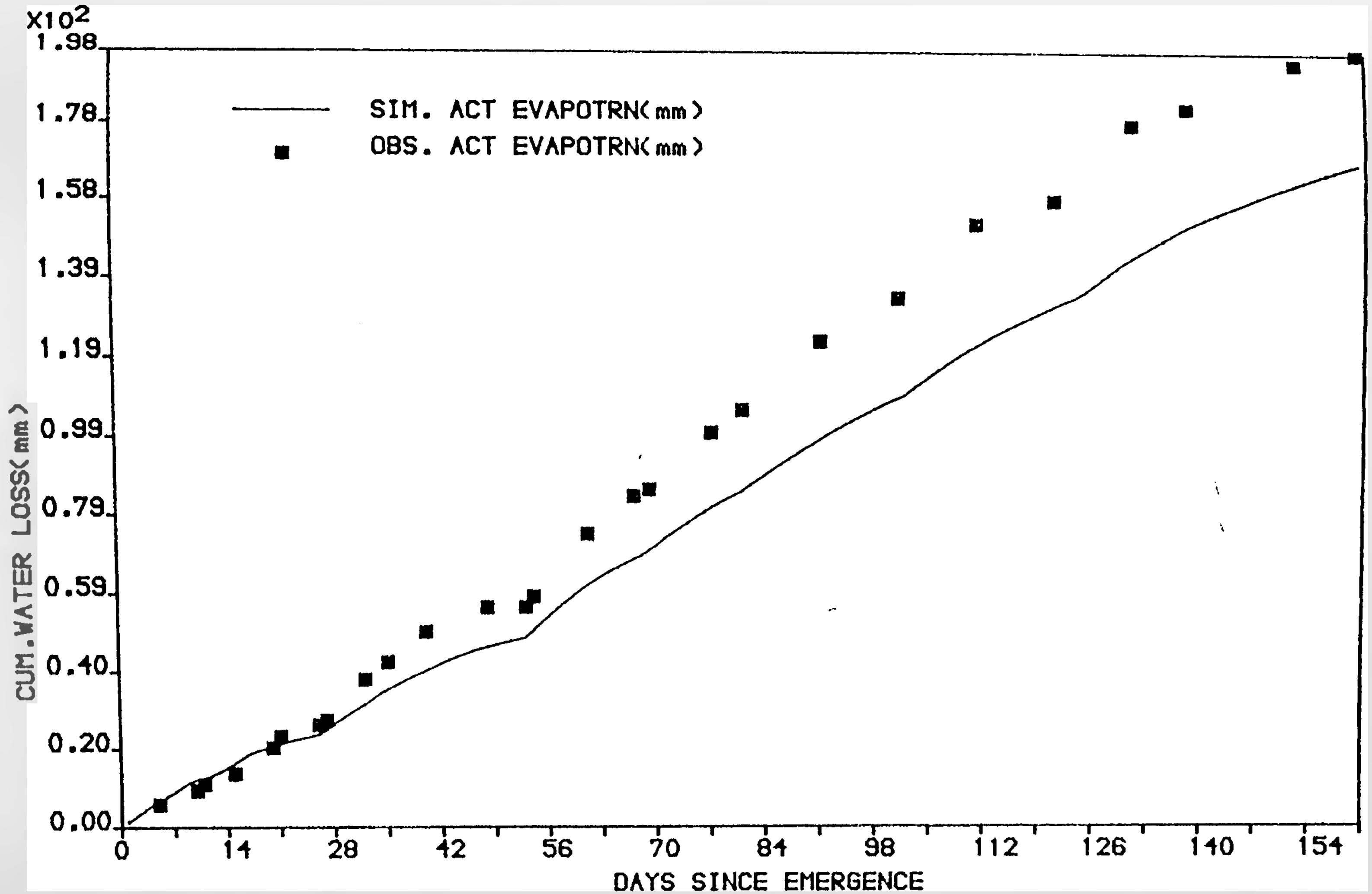

Fig. 4.19 Simulated and observed cumulative water loss (actual evapotranspiration, AET) under upper boundary model parameter values (see Table 4.4).

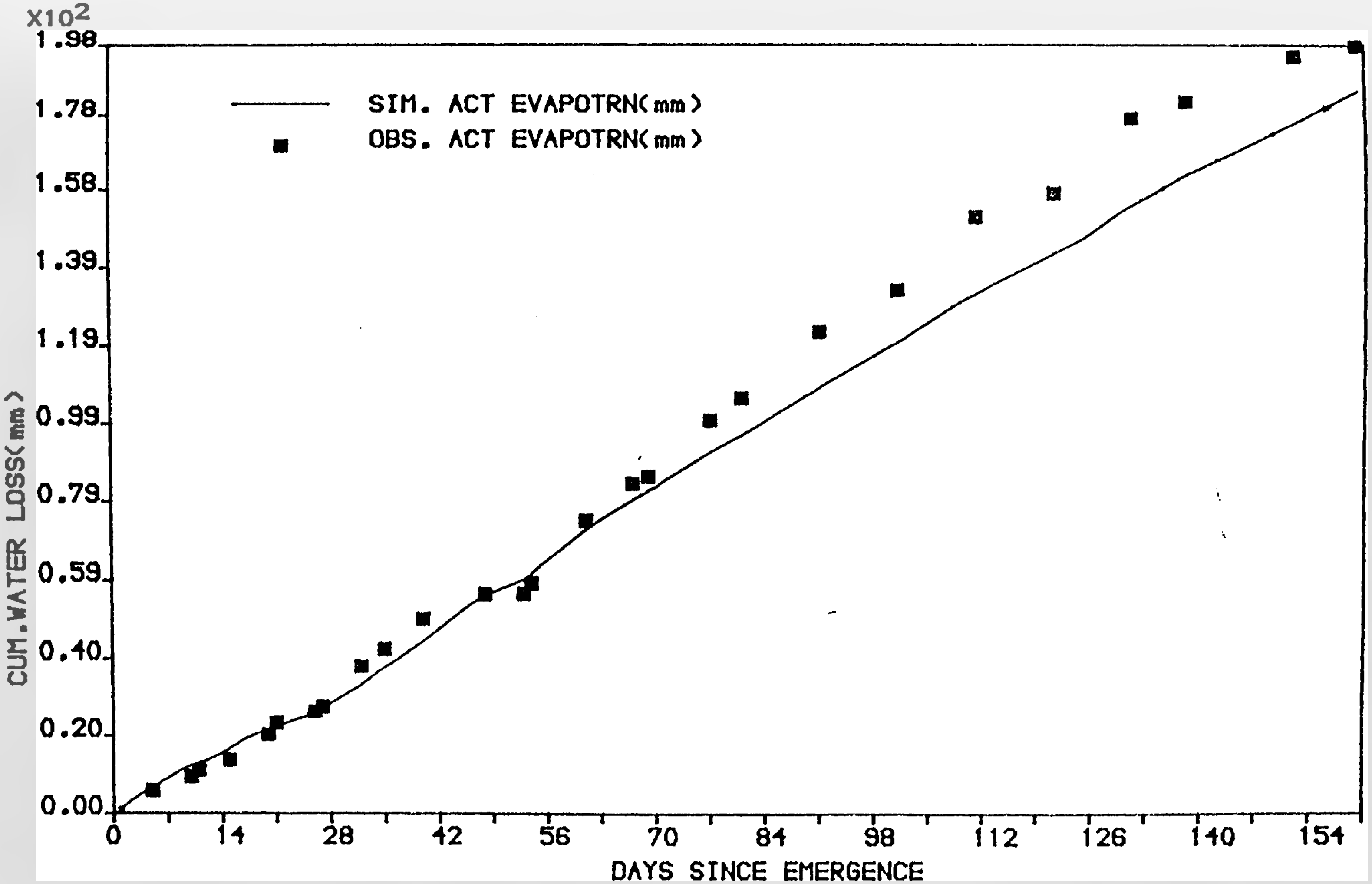

Fig. 4.20 Simulated and observed cumulative water loss (actual evapotranspiration, AET) under lower boundary model parameter values (see Table 4.4).

further lysimetric experiments, will determine wether this characteristic of the model is case-specific or occurs generally.

4.4.2 Model sensitivity:

The sensitivity of the SCHEDULE model to the soil related parameters is shown in Table 4.5 . The simulations are for data of the lysimeter experiment. The model showed no sensitivity to the residual and saturated moisture contents. The highest sensitivity was shown to the parameter U , which is the threshold cumulative soil evaporation after which the transition from the first to second stage soil evaporation occurs. A reduction of 10% in the value of U caused the MARD to be reduced by 11.2% . The model is otherwise not sensitive to any individual parameter but rather to a combination of parameters (eg. 41% change in MARD in Table 4.4).

Some values of MARD, for the first three parameters, are lower than the minimum MARD value obtained by the automatic optimization routine. This anomaly is attributable to the limited value increments specified in the optimization routine. Manual optimization of the parameters, although time consuming, may yield slightly better results. But since the model shows no overt sensitivity to any one particular parameter this task is best carried out by the automatic optimization technique.

The results of the simulation model are shown in Figs. 4.21 and 4.22 for the daily and cumulative water balance. Soil evaporation is dominant untill about day 45 when transpiration exceeds evaporation.

Table 4.5 Sensitivity analysis of the scheduling model to input parameters.

Parameter change	value	MARD %	AT mm	AETs mm	AT/PT	% MARD change
-20 %	240	15.56	119.80	203.99	0.86	-0.95
SLEVDP	300	15.71	121.03	202.94	0.86	0.0
+20%	360	15.86	122.07	203.99	0.87	+0.94
-20%	0.32	16.21	123.10	205.01	0.88	+3.18
TRPARAM	0.40	15.71	121.03	202.94	0.86	0.0
+20%	0.48	15.33	118.90	200.81	0.85	-2.42
-20%	40	16.10	115.05	196.96	0.82	+2.48
UTPCLYR1	50	15.71	121.03	202.94	0.86	0.0
+20%	60	15.53	122.18	204.09	0.87	-1.14
-10%	0.277	15.38	116.33	198.25	0.83	-2.10
FC	0.308	15.71	121.03	202.94	0.86	0.0
+10%	0.339	16.23	124.28	206.19	0.89	+3.31
-10%	0.095	16.12	122.74	204.65	0.88	+2.60
WLPT	0.105	15.71	121.03	202.94	0.86	0.0
+10%	0.116	15.34	118.87	200.79	0.85	-2.36
-10%	0.036	15.71	121.03	202.94	0.86	0.0
SWRESI	0.04	15.71	121.03	202.94	0.86	0.0
+10%	0.044	15.71	121.03	202.94	0.86	0.0
-10%	0.4	15.71	121.03	202.94	0.86	0.0
SWSAT	0.445	15.71	121.03	202.94	0.86	0.0
+10%	0.489	15.71	121.03	202.94	0.86	0.0
-10%	5.4	13.95	122.42	201.76	0.87	-11.2
U	6.0	15.71	121.03	202.94	0.86	0.0
+10%	6.6	16.97	119.63	204.13	0.85	+ 8.0
-10%	2.16	15.33	122.85	201.57	0.88	-2.42
C	2.4	15.71	121.03	202.94	0.86	0.0
+10%	2.64	16.11	119.20	204.30	0.85	+2.55

* Key:

FC = soil field capacity (cm3/cm3).
WLPT = soil wilting point (cm3/cm3).
SWRESI = soil residual moisture content (cm3/cm3).
SWSAT = saturated moisture content (cm3/cm3).
U = soil evaporation model parameter (mm).
C = soil evaporation model parameter.
(for other definitions see Table 4.2)

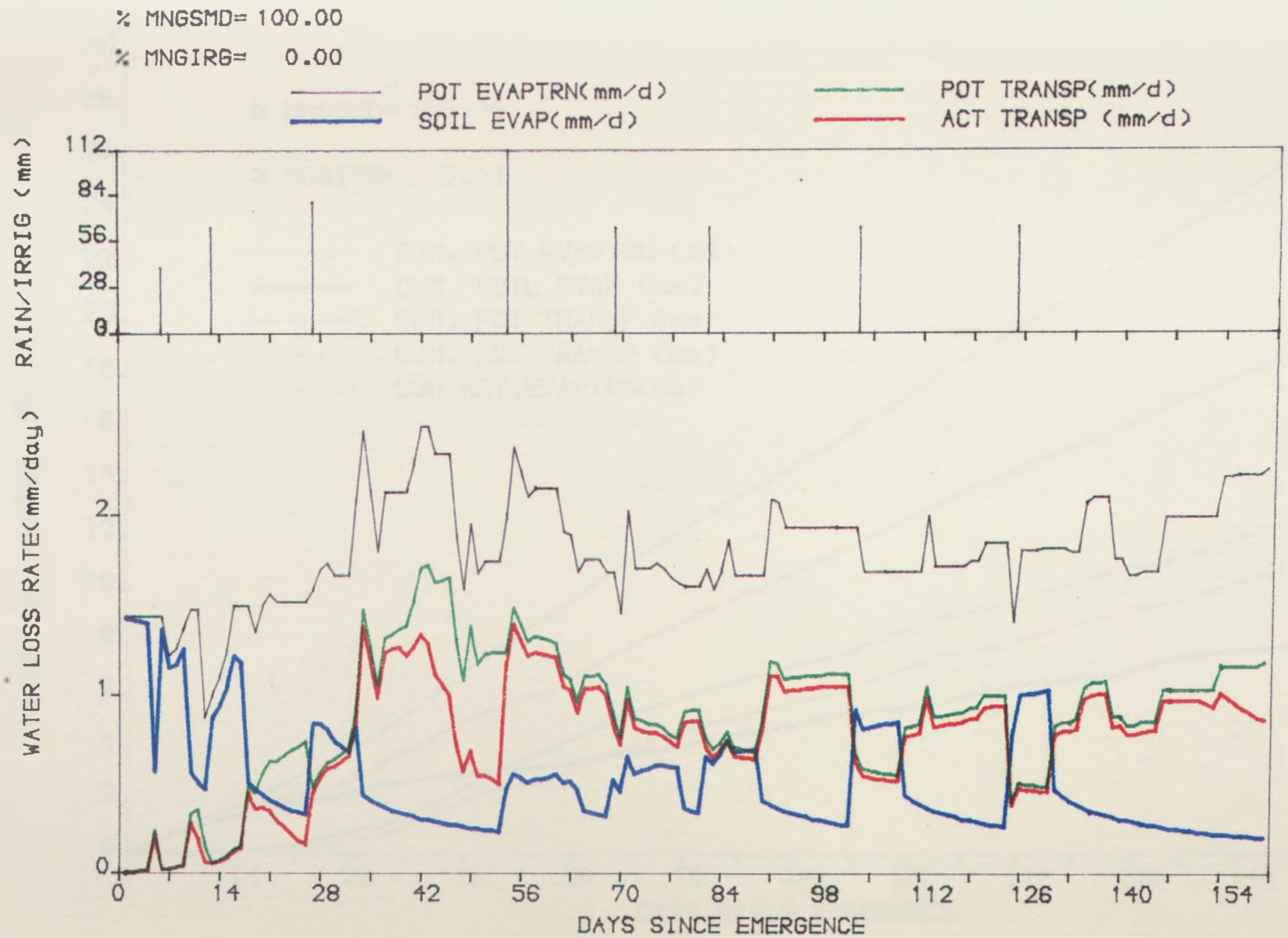

Fig. 4.21 Simulated daily water losses from the lysimeter.

USER: CMAV71 PLOTFILE: SIMN8100IO ENTRY NO. 70221 QUEUED ON 16/09/88 AT 16:49 PLOTTED ON 16/09/88 AT 16:57 FRAME 2/7

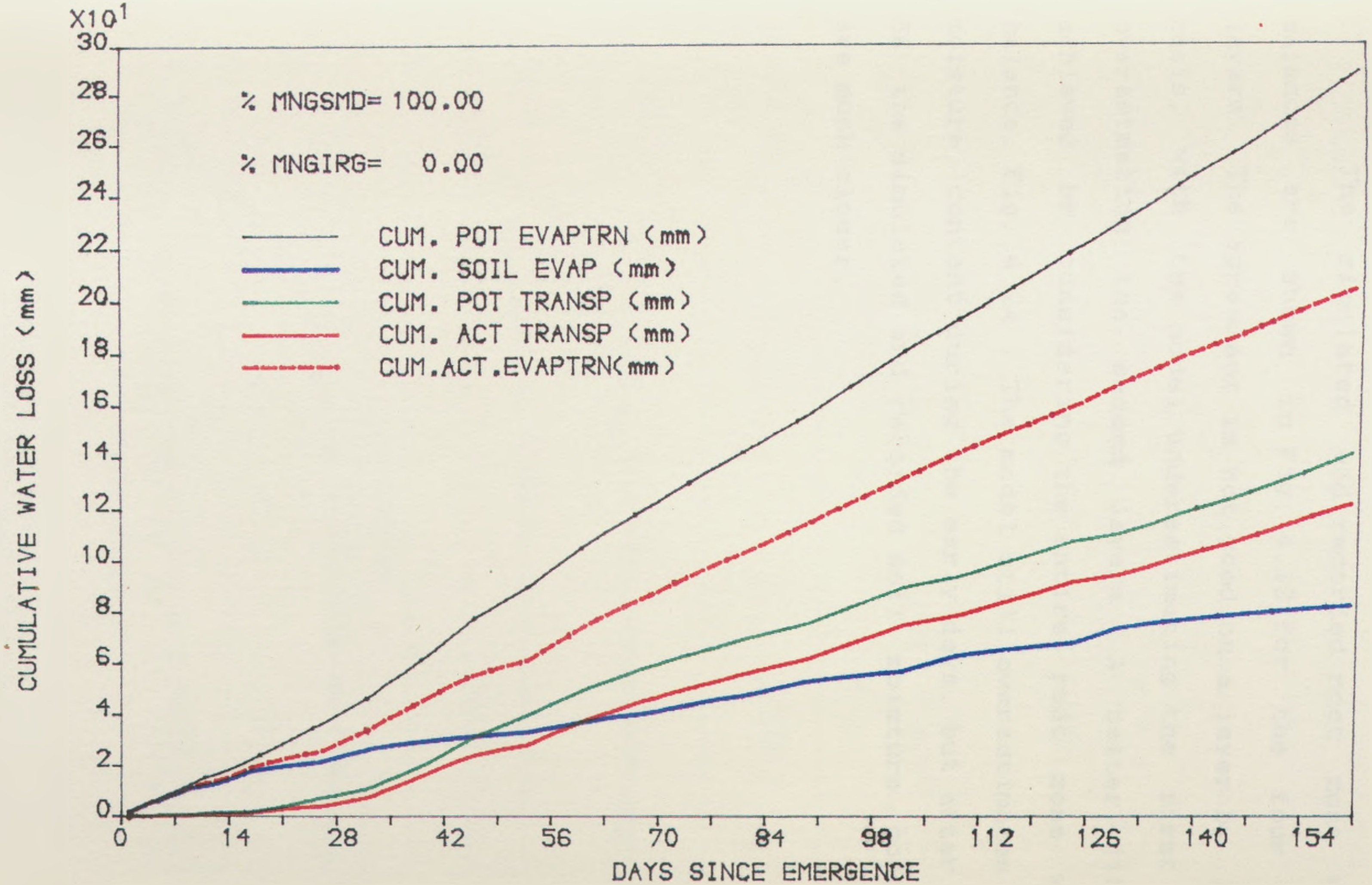

Fig. 4.22 Simulated cumulative water losses from the lysimeter.

The initially high soil evaporation is due to the low transpiration rate and the small leaf area index early in the season.

The simulated and recorded root zone water balances are shown in Fig. 4.23 for the four root layers. The agreement is not good on a layer by layer basis, with the model underestimating the first and overestmating the second layers. A better fit is achieved by considering the entire root zone water balance, Fig. 4.24 . The model still overestimates the moisture content during the early days, but after day 56 the simulated and recorded soil moisture contents are much closer.

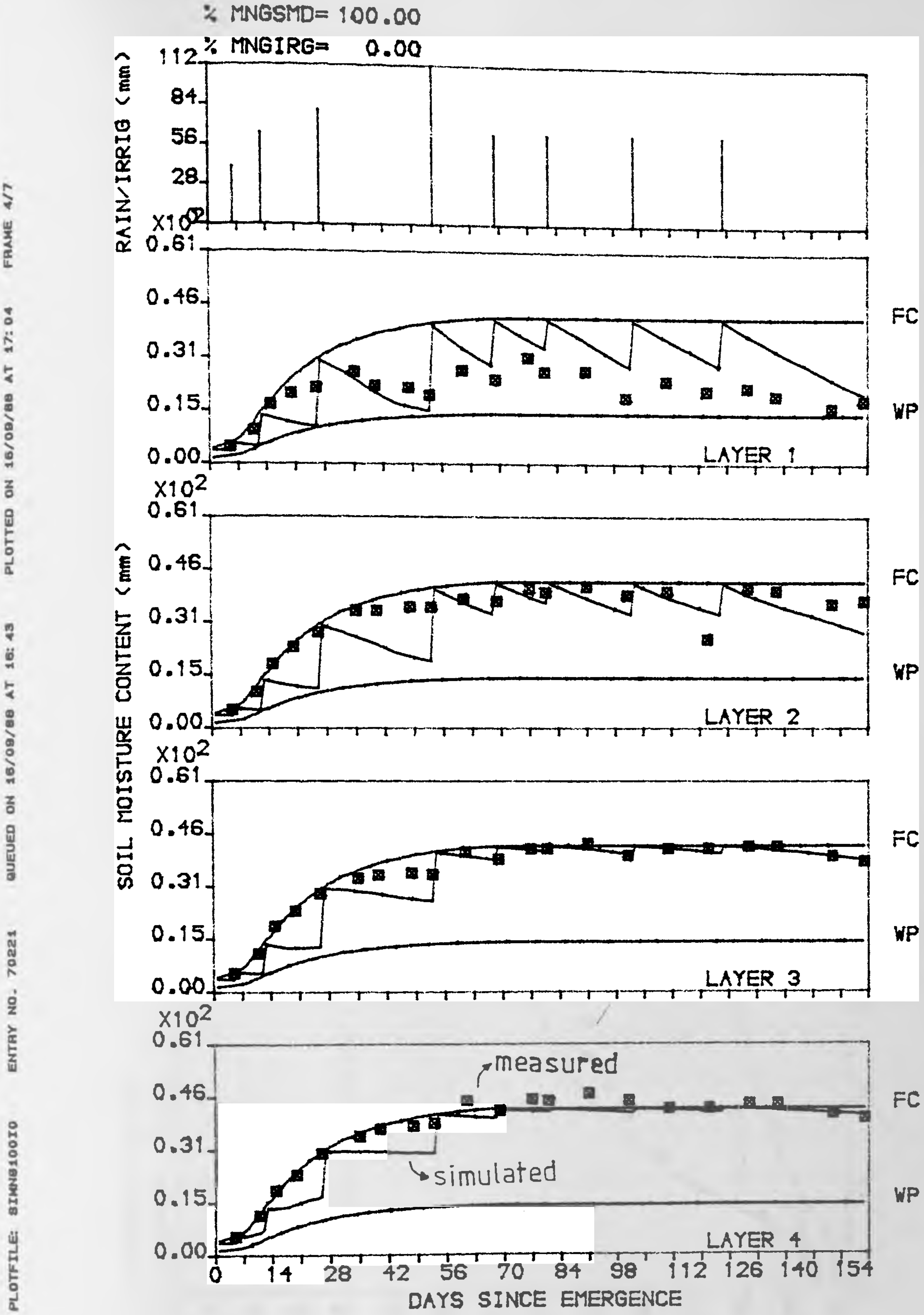

Fig. 4.23 Comparison of measured and simulated moisture contents in the root layers (FC is the field capacity, and WP is wilting point).

USER: CMAV71 PLOTFILE: SIMN6100IO ENTRY NO. 70221 QUEUED ON 16/09/88 AT 16:43 PLOTTED ON 16/09/88 AT 17:09 FRAME 5/7

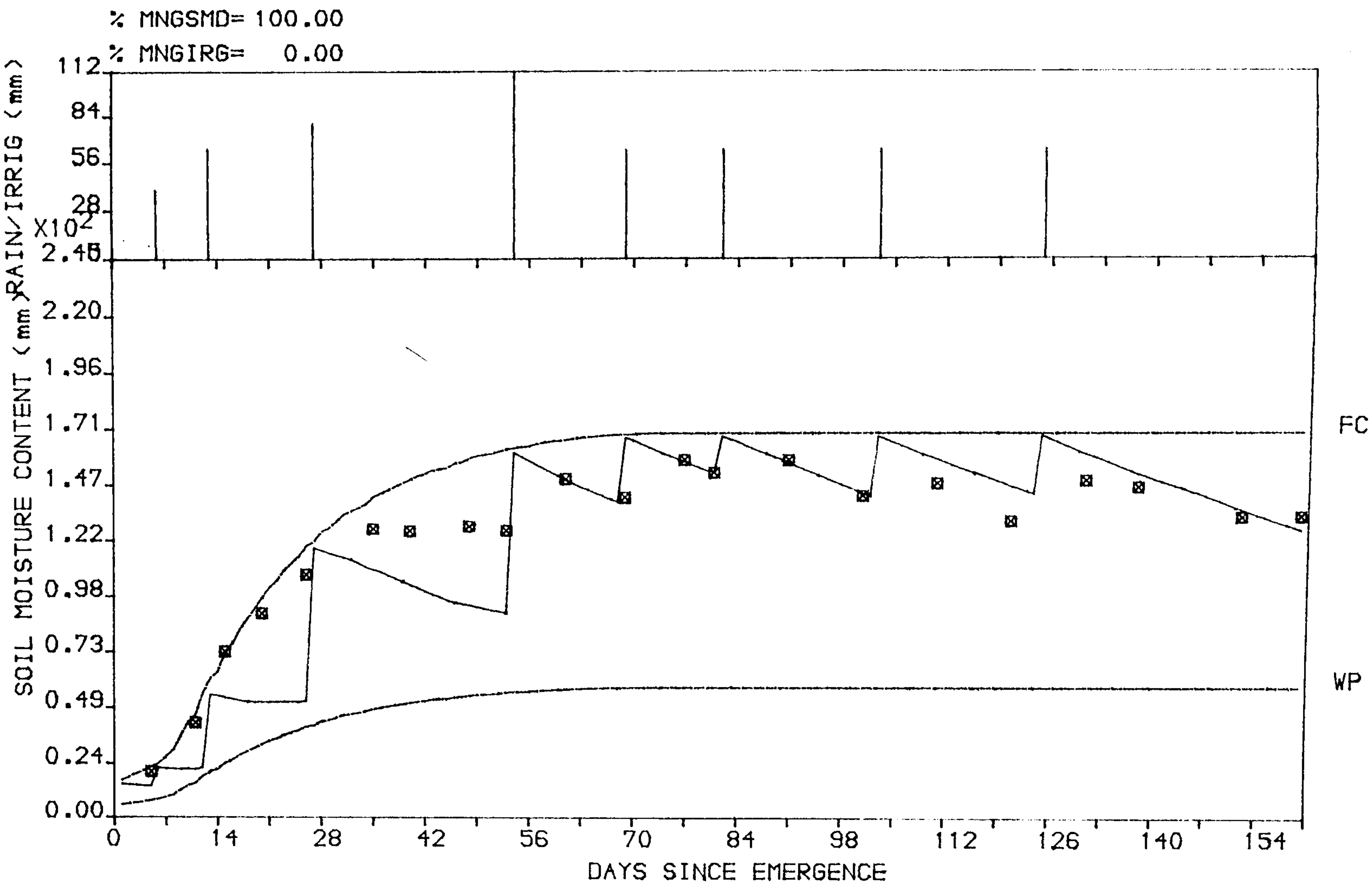

Fig. 4.24 Comparison of measured and simulated moisture contents in the root zone (FC is field capacity and WP is wilting point).

4.5 Management Practices :

The two management factors MNGSMD and MNGIRG are the basic tools available for controlling the predicted irrigation dates and amounts.

The scheduling model response to changes in the above factors is shown in Table 4.6. The combination of MNGSMD = 50% and MNGIRG = 50% offers the best management option since it requires the least seasonal irrigation quantity and the yield response ratio is similar to the more heavy irrigation practices.

A more widely ranging simulation of the effects of MNGSMD and MNGIRG on the predicted yield ratio and required seasonal irrigation, is shown in Table 4.7 and Figs. 4.25 to 4.28. Two cases were studied: case one where rainfall is included (pre-planned irrigations, Table 4.3, are treated as rain), and case two when no rain is taken into account. The high yield ratio values (Figs. 4.25 and 4.26) for the first case, irrespective of the values of MNGSMD and MNGIRG, suggest that the pre-planned irrigations are enough to replenish the soil and keep transpiration near optimum. For the no-rain simulations the effect of MNGSMD on yield ratio is as expected, with the ratio reducing as allowable moisture deficit is increased (Fig. 4.25). The effect of MNGIRG on this ratio (Fig. 4.26) shows that higher applications need not necessarily result in higher yields.

Table 4.6 Simulated irrigation schedules (days and depths) for different management practices.

MNGSMD MNGIRG	50 100		50 75		50 50		25 100	
	Day	Depth mm	Day	Depth mm	Day	Depth mm	Day	Depth mm
	4	7.21	4	5.41	4	3.6	2	3.62
	9	15.01	9	11.26	9	7.5	4	3.73
	12	19.61	12	17.52	10	7.2	7	5.34
	17	31.18	17	23.39	12	10.22	9	10.09
	26	42.61	26	28.46	17	15.59	11	10.38
	42	51.86	42	38.91	21	18.42	12	9.79
					26	20.36	15	18.88
					42	25.94	18	18.38
							22	19.73
							33	24.64
							41	25.86
							52	27.71
							67	27.97
							148	28.95
AT/PT	0.955		0.955		0.954		0.974	
Total Depth	162.4		124.5		109.4		232.9	

* Key:

MNGSMD = management allowable soil moisture deficit (%).

MNGIRG = percentage of actual irrigation application.

AT/PT = ratio of actual to potential transpiration.

Table 4.7 Simulated effects of MNGSMD and MNGIRG on the yield ratio and total required irrigation depth.

MNGSMD (%)	MNGIRG (%)	With Rain AT/PT	With Rain IRR. (mm)	Without Rain AT/PT	Without Rain IRR. (mm)
10	100	0.974	308.5	0.974	329.6
25	100	0.974	232.9	0.974	312.9
35	100	0.960	222.4	0.946	300.3
50	100	0.955	162.4	0.830	278.8
60	100	0.931	113.5	0.733	233.5
75	100	0.900	77.0	0.574	188.5
80	100	0.886	100.5	0.509	220.3
100	100	0.886	0.0	0.399	145.5
50	10	0.947	72.8	0.856	266.5
50	25	0.949	90.8	0.924	283.3
50	35	0.952	106.8	0.951	283.4
50	50	0.954	109.4	0.952	295.9
50	75	0.955	124.5	0.923	294.7
50	85	0.955	140.5	0.892	271.1
50	100	0.955	162.4	0.830	278.8

* Key:

MNGSMD = management allowable soil moisture deficit.

MNGIRG = percentage of actual irrigation application.

AT/PT = ratio of actual to potential transpiration.

IRR. = total seasonal irrigation requirement.

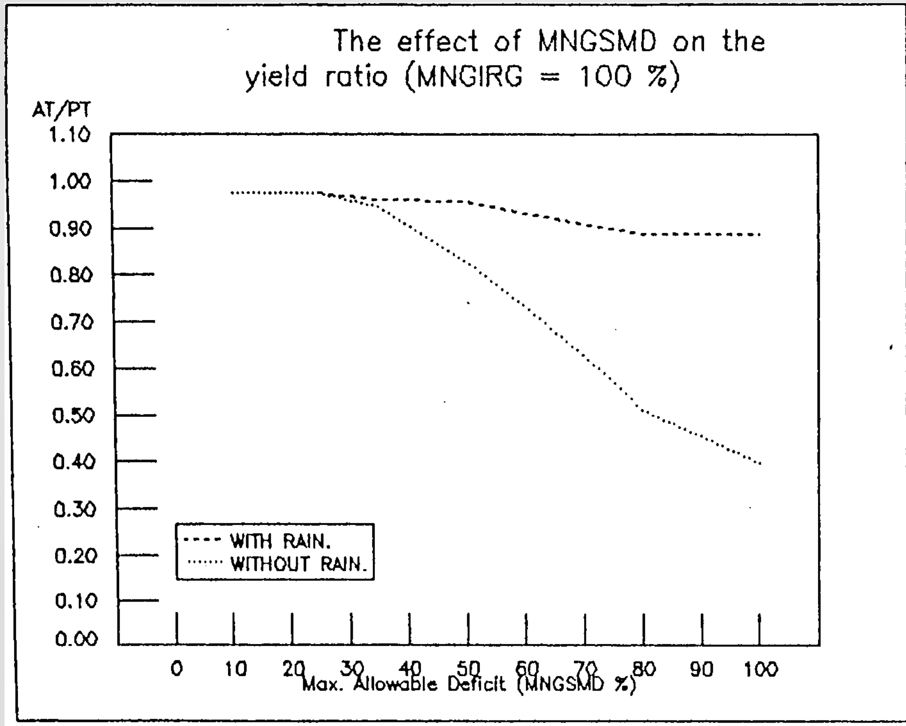

Fig. 4.25 The effect of MNGSMD on the yield ratio (AT/PT), MNGIRG = 100% .

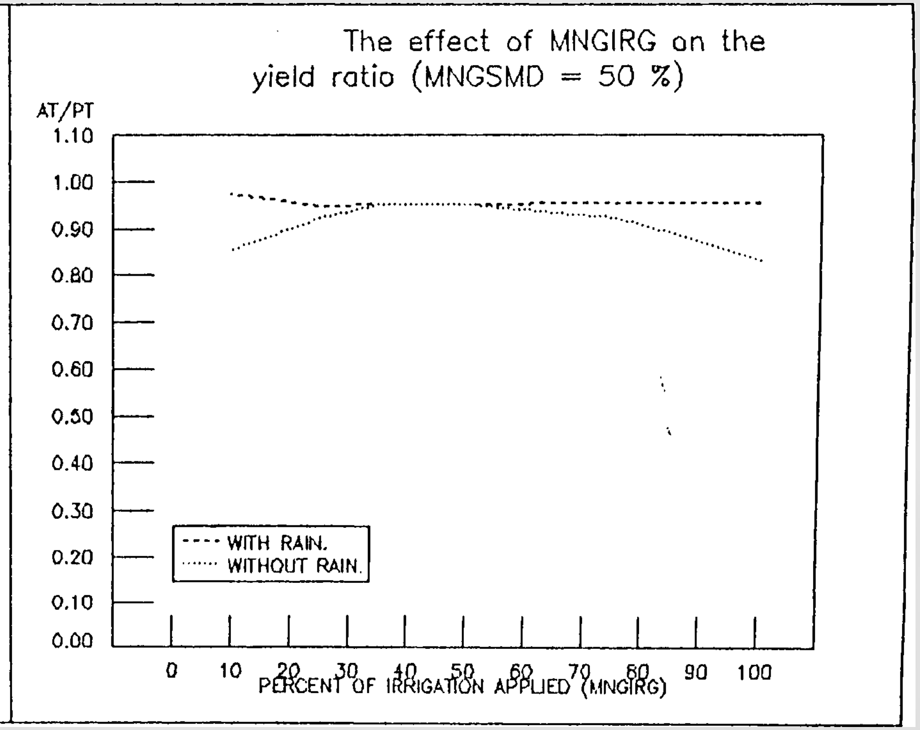

Fig. 4.26 The effect of MNGSMD on the yield ratio (AT/PT), MNGIRG = 50% .

In Figure 4.27 the effect of MNGSMD on the total required irrigation depth is shown. As maximum allowable soil moisture deficit is increased there is a corresponding decrease in the required irrigation since the frequency of irrigations is less. The case of no-rain simulation shows that more irrigation is required at every MNGSMD level since the soil is allowed to dry for longer uninterrupted periods.

The effect of MNGIRG on the required irrigation (Fig. 4.28) shows that as this factor is increased , required irrigation also increases. In the case of no-rain simulation the required irrigation at all MNGIRG levels is seen to be much higher than when the rain is taken into account since the soil moisture level is allowed to reduce without periodic recharges by rain. The change in the required irrigation is not large with respect to the change in the MNGIRG levels, suggesting that required irrigation depth is primarily controlled by the MNGSMD factor. This is reasonable since at low MNGIRG values the frequency of irrigation will be higher thus resulting in high total irrigation.

The decision as to which management factors are most suitable for an irrigation system depend on the level of desirable yield and the available irrigation water. Table 4.6 and Fig. 4.25 suggest that assuming MNGIRG is at a constant 100 % and no rainfall, the best MNGSMD level is around the 35 % level since

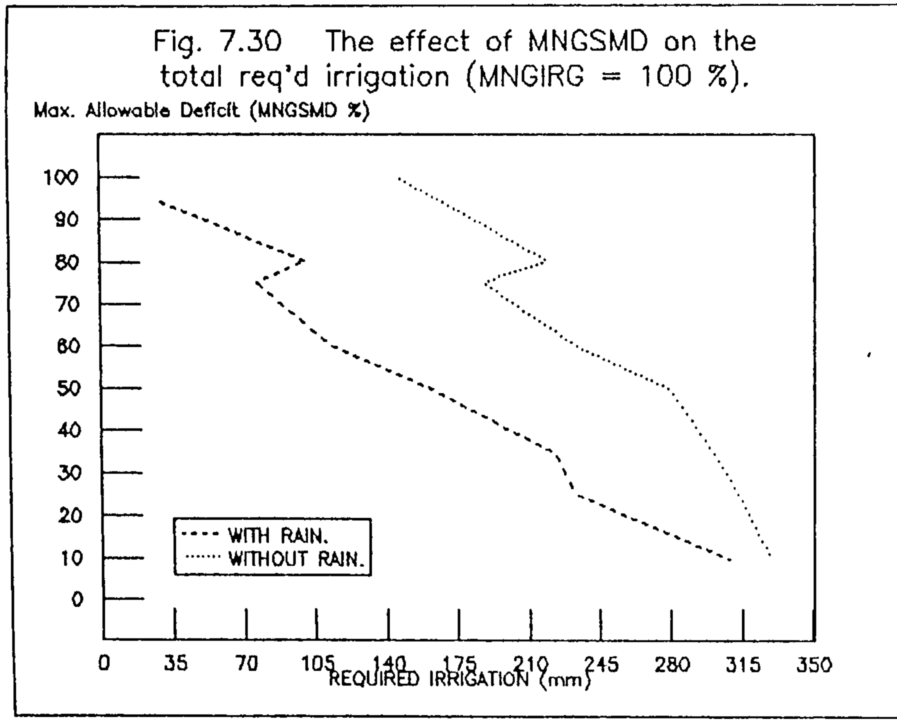

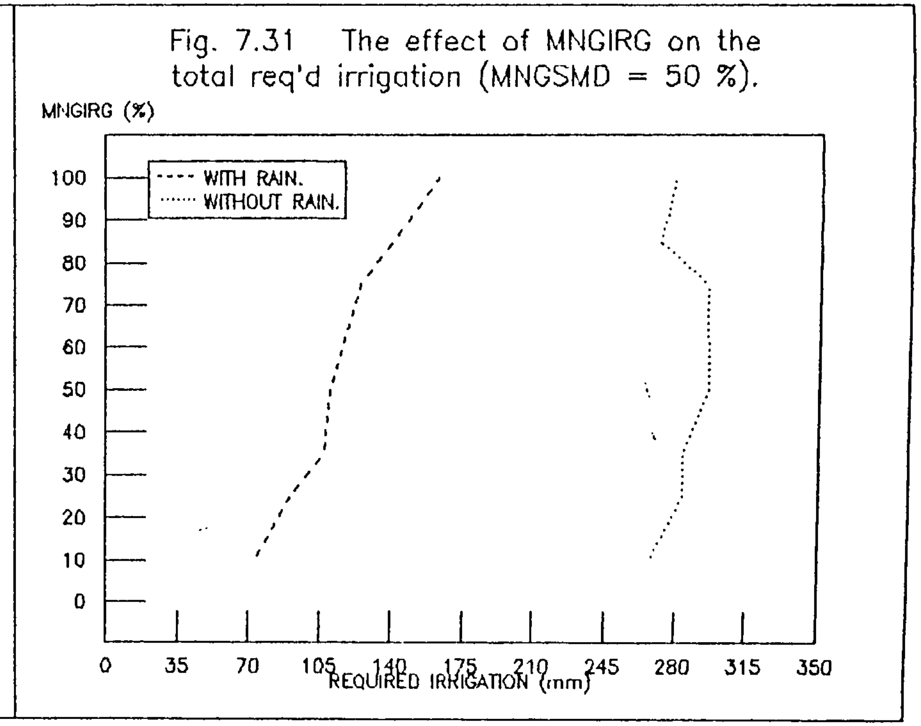

Fig. 4.27 The effect of MNGSMD on the total req'd irrigation (MNGIRG = 100%).

Fig. 4.28 The effect of MNGIRG on the total req'd irrigation (MNGSMD = 50%).

the reduction in yield is not severe untill MNGSMD increases above this level.

4.6 Chapter Summary:

In this chapter the water balance of a nonuniform soil profile, with a growing, nonuniform root zone, is simulated. The water balance model was tested with data generated by a lysimeter experiment. The soil was taken to be uniform in hydraulic properties, but the moisture content in the growing root zone, was treated as nonuniform during the growth period. The model predicted the changes in root zone moisture content well, and the simulated and recorded cumulative actual evapotranspiration showed close agreement.

The lysimeter data is used to simulate the effects of various management practices on the irrigation quantities and schedules, and on the total seasonal irrigation requirement and relative crop yield.

An algorithm is developed whereby, at the end of each day, the soil and root zone layer thicknesses, hydraulic properties and moisture contents are sorted into a composite-layer soil profile. This new profile reflects changes in root zone moisture contents and the changes in soil properties as the growing root zone extends into nonuniform soil layers.

The composite-layer soil profile is used by the one and two dimensional infiltration models of chapter 6, to simulate the infiltration process in nonuniform soils, taking into account the antecedent soil moisture conditions.

In the following chapter (chapter 5) the physical properties of the sandy soil used in the lysimeter, are evaluated and methods are compared for the determination of those soil parameters required by the root zone water balance and infiltration models for general application.

CHAPTER 5 DETERMINATION OF SOIL-WATER PROPERTIES

The purpose of irrigation is to fill up the depleting root zone soil moisture storage . The quantity and duration of recharge necessary to refill the storage up to the field capacity depends on the rate of water loss and the infiltration characteristics of the soil.

It was shown in chapter 3 that the rate at which water is lost from the soil by evapotranspiration depends to some extent on soil-specific parameters. The soil also controls the amount and the rate of infiltration following rain or irrigation (chapter 6). In this chapter those physical properties of the soil which effect the evapotranspiration and infiltration processes are determined.

5.1 Soil Physical Properties:

The following tests were undertaken to determine some of the properties of the soil which influence the status of water in that medium. The details of the tests can be found in such laboratory test manuals as the British Standards (BS 1377: 1975) and Head (1984). Only a brief outline of the tests perfomed on the Auchincruive sand and the results are reprted here.

a) Saturated Moisture Content (θs):

This property of the soil is determined by passing water through a sample of the soil to replace the air in the voids. The moisture content of the soil sample is then measured by the gravitational method. The average for 3 tests was found to be 0.445 cm3/cm3.

b) Residual Moisture Content (θr) :

This property of the soil is taken to be the same as the oven-dry moisture content of the soil. The sample of soil is heated in an oven, set at 105 degrees celcius, and weighed periodically untill no change in weight is observed. The residual moisture content was thus measured for the sandy soil and found to be 0.05 cm3/cm3 .

c) Bulk Density (B.D) :

This is found by measuring the weight in grammes (g) of an air dry sample of the soil, occupying a 50 cubic centimeter (cm3) volume. The B.D of the sandy soil was found to be 1.498 g/cm3 .

d) Organic Matter Content (OMC) :

This is determined by heating a sample of the oven-dry soil to a temperature of 450 degrees celcius. The loss in weight of the sample is a measure of the amount of organic matter present. This was found to be 2.0% for the Auchincruive sandy soil.

e) Particle Size Distribution :

The dry sieve and the pipette analysis methods were used to determine the textural composition of the soil. The percentages of sand, silt and clay were found to be 86.25, 11.16 and 2.59 respectively.

f) Saturated Hydraulic Conductivity (Ks) :

The standard 'falling head permeameter' method was used to determine Ks. The average of 12 tests showed Ks to be 0.31 cm/min .

5.2 Soil-Water Potential:

The absorption and redistribution of water in an unsaturated soil medium involves the replacement of air voids in the soil by water. The speed and amount by which this replacement takes place is dependent on the particle size distribution and in particular the degree of fine materials present. Coarse soils have larger voids thus water enters and leaves the soil faster and in larger amounts.

Hydrogen ions in the water are attracted to the oxygen ions of the minerals and form hydrogen bonds . The amount of water absorbed onto the surface of soil particles by hydrogen bonding depends on the available surface area of the particles. Finer soils have larger surface areas and so absorb more water (Donahue etal 1983) .

The strength by which water is held in the soil is termed the 'matric potential'. Other forces such as osmotic, gravitational and pressure also contribute to varying degrees to this force. The combination of all these forces is the 'soil water potential'. The units of potential are those of force and may be expressed in terms of tension or pressure depending on the point of reference.

The water potential of a soil sample varies with the amount of water present in the soil (Fig. 5.1). The less water remaining, the stronger is the tensile force between the soil particles and the water molecules. This variation is unique to each soil and is termed the soil moisture 'characteristic' or 'retention' curve.

Three essential soil-water parameters can be derived from the characteristic curve. These are defined below:

5.2.1 Field Capacity (FC) :

The soil moisture content at a tension of 0.33 bars is termed the 'field capacity', and represents the upper limit of moisture held in the soil without gravitational drainage . Water added above this upper limit is considered lost to the crops, either as drainage or waterlogging.

5.2.2 Wilting Point (WP):

The soil moisture content at which the plant can no longer extract water, is the 'wilting point' or the 'permenant wilting point', and corresponds to about 15 bars of tension.

The amount of water held between the field capacity and the wilting point is the 'plant available water', from which storage, the plant uptakes water.

5.2.3 Wetting Front Pressure (Pw) :

The wetting front pressure is an indicator of

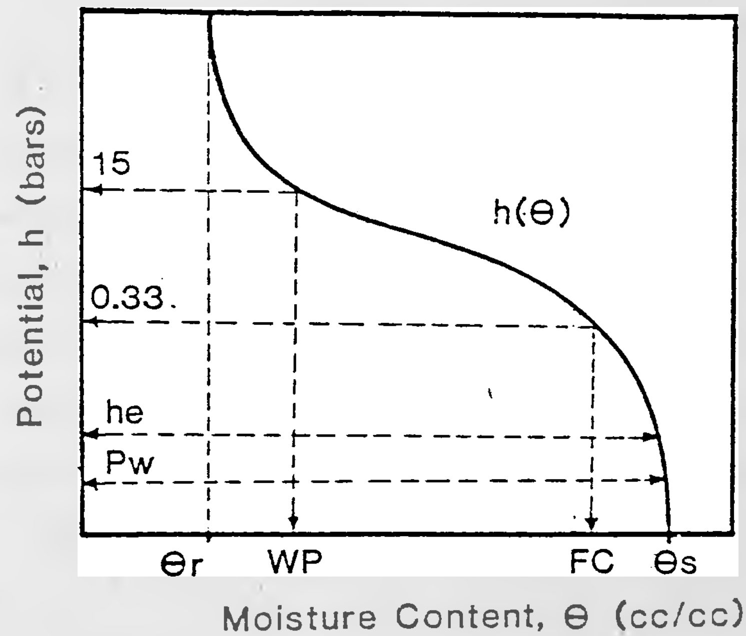

Fig. 5.1 Typical soil moisture characteristics curve. (Θs = saturated moisture content; Θr = residual moisture content; FC = field capacity ; WP = wilting point; he = air entry pressure; and Pw = wetting front pressure. Note the vertical scale has logarithmic scale.)

the ease with which the air in the soil is replaced with water. Bouwer (1969) defines Pw as 'the soil-water potential whereby the soil is essentially wetted to it's maximum water content'. The wetting front pressure is a required parameter of the Green-Ampt model of infiltration (see Chapter 6).

The point of departure from saturation in Fig. 5.1 is referred to as the 'air exist' or 'bubbling' pressure (he). Bouwer (1969) suggested that the wetting front pressure may be taken to be half the bubbling pressure, ie: Pw = 0.5 he . Others have proposed complicated mathematical expressions based on the retention curve and the unsaturated hydraulic conductivity-moisture content relationship (Neuman 1976, Brakensiek & Onstad 1977, Panikar & Nanjappa 1977).

The next step is the evaluation of the soil moisture characteristics curve. Some methods are reviewed below and the results are compared.

5.2.4 Methods of Evaluating the Soil Moisture Characteristic Curve.

5.2.4.1 Experimental Methods :

The magnitude of the tension by which a quantity of water is held in the soil medium can be measured both in the field and in the laboratory. Methods such as the tensiometer, suction plate, pressure plate, osmotic membrane, nuclear techniques, and gypsum blocks are widely used (Marshal & Holmes 1979, Hillel 1980, Schmugge etal 1980).

Field and laboratory methods require accurate and often expensive instrumentation which may not always be readily available or even economically viable (Arya & Paris 1981). Laboratory methods, although yield more detailed information, can however give spurious results due to the disturbance of the soil sample (Marshal & Holmes 1979), while field measuring techniques are restricted to a small range of matric potentials above the 1.0 bar tension and require calibration with laboratory methods (Schmugge etal 1980). This limits the use of field methods to the monitoring of soil moisture changes rather than the evaluation of the characteristic curve.

The method utilized here to evaluate the soil moisture characteristic of the Auchincruive sandy soil, is the pressure plate technique (Hillel 1980). The apparatus consists of a pressure chamber, an air compressor and pressure regulators (Plate 5.1). The saturated soil samples are placed on porous ceramic plates and pressure is applied to drain out the soil water. The constant pressure is maintained for at least 7 days to allow equilibrium outflows. The soil is then removed and it's moisture content measured by the gravitational method. This process was repeated for a number of pressures ranging from 0.5 to 15 bars .

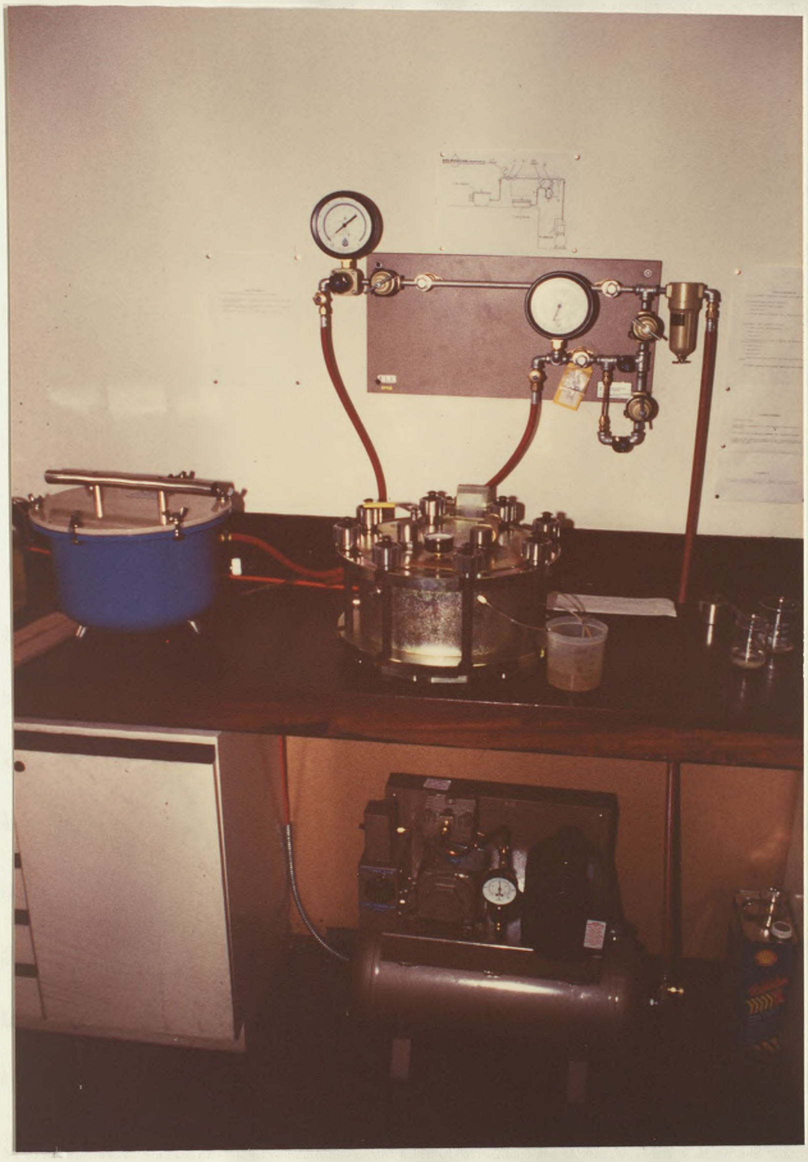

Plate 5.1 Pressure Plate apparatus.

Overall 13 pressure intervals were tested and the resultant moisture content-pressure data, averaged for three tests per pressure, is plotted in Fig. 5.2 . For comparative purposes a plot of the characteristic curve of a clayey soil is also plotted.

5.2.4.2 Empirical Models :

In instances where detailed laboratory or field measurement of soil properties is not possible or economically desirable, then empirical methods can provide approximate information for most engineering applications.

These empirical approaches can be divided into two general groups. The first are those which predict moisture contents at specific matric potentials, by relating the two with measured textural soil properties (Salter & Williams 1969, Gupta & Larson 1979, Arya & Paris 1981, Rawls & Brakensiek 1982, Schulze etal 1985, Haverkamp & Parlange 1986). The second group of models assume a closed-form power equation of the moisture characteristic curve and statistically derive the curve fitting parameters for various soil textural groups (Clapp & Hornberger 1978, Ghosh 1980, McCuen etal 1981, Gregson etal 1987).

Gupta & Larson (1979) developed regression equations relating moisture contents at specific matric potentials, to soil texture, organic matter content and bulk density:

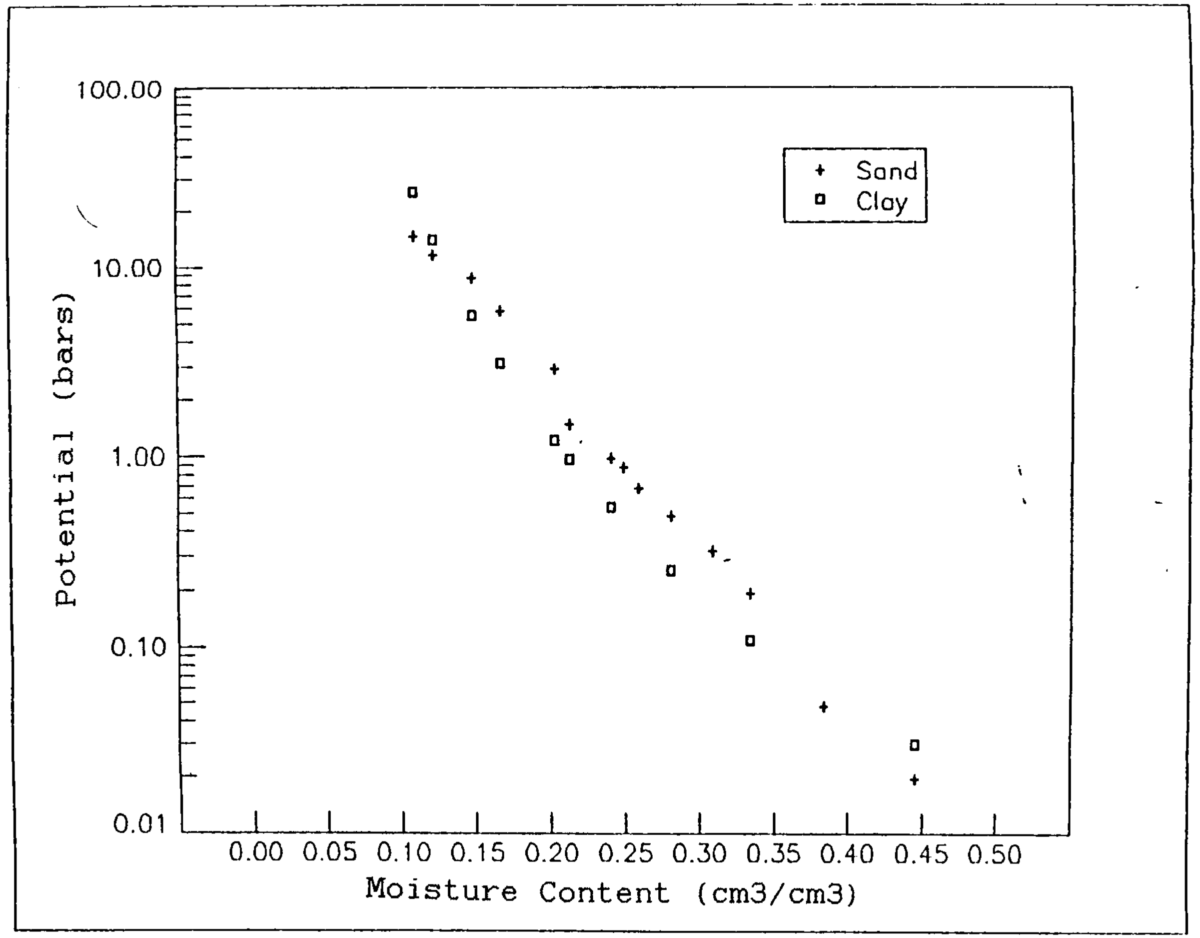

Fig. 5.2 Moisture characteristic of the Auchincruive sand measured by the pressure plate test (clay soil data from Zur & Jones 1981).

$$\theta p = a.Sand(\%) + b.Silt(\%) + c.Clay(\%) + d.OMC(\%) + e.BD(g/cm3) \quad (5.1)$$

where θp is the predicted moisture content (cm3/cm3) at a given potential; OMC is the organic matter content; BD is the bulk density; and regression coefficients 'a' to 'e' are statistically derived for a particular potential. The range of matric potentials considered are 0.04 to 15.0 bars.

Rawls & Brakensiek (1982) extended the above method to the analysis of about 500 soils and developed the following regression model :

$$\theta p = a' + b'.Sand(\%) + c'.Silt(\%) + d'.Clay(\%) + e'.OMC(\%) + f'.BD(g/cm3) + g'.\theta(0.33) + h'.\theta(15) \quad (5.2)$$

where 'a' to 'h' are regression coefficients for specific matric potentials (0.04 to 15 bars); and $\theta(0.33)$ and $\theta(15)$ are moisture contents (cm3/cm3) at 0.33 and 15 bar tensions respectively.

Arya & Paris (1981), from the observation of the similarity between the shape of the particle size distribution curve and the characteristics curve, developed a method by which the soil moisture tensions and moisture contents at discrete pore size intervals can be estimated.

The particle size distribution curve is divided into a number of discrete fractions, for each of which the moisture content ($\Theta(i)$, cm3/cm3) is related to the pore volume by :

$$\Theta(i) = \sum_{1}^{i} BD \cdot V(i) \qquad (5.3)$$

where BD is the soil bulk density (g/cm3); and V(i) is the pore volume per unit mass of fraction i (cm3/g).

The volumetric moisture content for a particle size fraction is averaged for two successive fractions. The corresponding matric potential is found from the pore radius according to the capillarity equation (Marshal & Holmes 1979):

$$h(i) = \frac{2\ t}{BDw \cdot g \cdot r(i)} \qquad (5.4)$$

where t is the surface tension of water (N/m2); g is acceleration due to gravity (m/s2); BDw is density of water (kg/m3); and r(i) is the pore radius (m).

Haverkamp & Parlange (1986) similarly related the soil moisture retention curve to the particle size distribution curve to derive expressions for the wetting and drying curves (based on the Brooks-Corey equation , see below) , taking into account air entrapment and hysterisis. Their model is limited to non-organic sandy soils.

The next group of empirical models base their analysis upon the assumption of a power curve representing the shape of the moisture characteristic curve. The diverse nature of the retention curve has led to several forms for the power function (Brooks & Corey 1966, Rogowski 1972, Van Genuchten 1980, Stephens & Rehfeldt 1985, and Gregson etal 1987).

Brooks & Corey (1966) expressed this equation as :

$$Se = \left(\frac{he}{h}\right)^{k} \qquad \text{for } h>he \qquad (5.5)$$

where :

$$Se = \frac{\theta - \theta r}{\theta s - \theta r} \qquad (5.6)$$

where

- Se = effective saturation
- θr = residual moisture content (cm3/cm3)
- θs = saturated moisture content (cm3/cm3)
- θ = actual moisture content (cm3/cm3)
- h = actual water potential (bars)
- he = air entry or bubbling pressure (bars)
- k = index of pore size distribution

The residual moisture content can be taken to be zero (Haverkamp & Parlange 1986), or assumed to be the moisture content at 15 bar tension (Rogowski 1972, Van Genuchten 1980), while others suggest elaborate methods for it's estimation (Stephens & Rehfeldt 1985, Mualem 1976, Van Genuchten 1980).

The assumption of zero residual moisture content transforms Eqn. 5.5 into the equation given by Campbell (1974) :

$$\theta = \theta s \left(\frac{h}{he}\right)^{1/b} \quad \text{for } h>he \qquad (5.7)$$

This is simply a rearrangement of the modified Brooks-Corey equation with $k = 1/b$. Both models assume $\theta=\theta s$ for $h<he$ (ie a sharp decline at air entry pressure).

McCuen etal (1981) undertook a statistical analysis of the Brooks-Corey parameters (θs, θr, he and k), for 1085 soils and derived values for the parameters across 11 soil texture classess (Table 5.1). This method only requires knowledge of the USDA textural classification of the soil.

Clapp & Hornberger (1978) similarly derived values for the parameters in Eqn. 5.7 for USDA soil texture classes (Table 5.2).

Ghosh (1980) derived an empirical expression for the parameter 'b' in Eqn. 5.7 , from the percentage of sand, silt and clay content of the soil. The air entry pressure 'he', is then estimated from the slope and one measured value of the retention curve.

Gregson etal (1987) modified Eqn. 5.7 and reduced the number of parameters from two (he & b) to one (b), by statistical analysis of a number of soils :

$$h = 0.00374\ (1.8\ \theta\ )^{b} \qquad (5.8)$$

Table 5.1 Representative Values for the Brooks-Corey Parameters (After McCuen etal 1981), (see key for definition of symbols).

Soil Texture	θs cc/cc	θr cc/cc	he cm	b	Ks cm/min
Sand	0.345	0.016	15.78	3.41	0.408
Loamy sand	0.410	0.024	9.70	2.23	1.32
Sandy loam	0.423	0.048	16.78	2.64	3.0×10^{-4}
Silt loam	0.484	0.018	43.33	4.83	1.2×10^{-6}
Loam	0.452	0.034	23.20	4.06	0.096
Sandy clay loam	0.405	0.075	25.86	2.90	1.4×10^{-5}
Silty clay loam	0.473	0.054	36.86	6.10	4.6×10^{-7}
Clay loam	0.476	0.087	27.25	3.86	0.06
Sandy clay	0.405	0.171	40.53	2.29	0.021
Silty clay	0.476	0.085	27.17	5.38	0.030
Clay	0.475	0.106	32.92	5.36	0.018

* key : θs = saturated moisture content (cm3/cm3).
θr = residual moisture content (cm3/cm3).
he = air entry pressure (cm).
b = slope of log-log retension curve.
Ks = saturated hydraulic conductivity (cm.min).

Table 5.2 Representative Values for the Brooks-Corey Parameters (After Clapp & Hornberger 1978) (see key for definition of symbols).

Soil Texture	θs cc/cc	θr cc/cc	he cm	b	Ks cm/min
Sand	0.395	0.0	4.66	4.05	1.056
Loamy sand	0.410	0.0	2.38	4.38	0.938
Sandy loam	0.435	0.0	9.52	4.90	0.208
Silt loam	0.484	0.0	75.30	5.30	0.043
Loam	0.451	0.0	20.00	5.39	0.042
Sandy clay loam	0.420	0.0	11.70	7.12	0.038
Silty clay loam	0.477	0.0	19.70	7.75	0.010
Clay loam	0.476	0.0	48.10	8.52	0.015
Sandy clay	0.426	0.0	8.18	10.4	0.013
Silty clay	0.492	0.0	23.00	10.4	0.006
Clay	0.482	0.0	24.30	11.4	0.008

* key : θs = saturated moisture content (cm3/cm3).
θr = residual moisture content (cm3/cm3).
he = air entry pressure (cm).
b = slope of log-log retension curve.
Ks = saturated hydraulic conductivity (cm.min).

This model seems to be promising and certainly parameter efficient, although it's validity for a greater range of soils needs evaluation.

A comparison of some of the empirical models with the measured data of the Auchincruive sand is shown in Fig. 5.3 .

The empirical models exhibit a fair degree of variation. The discrete-potential prediction models show that the Arya-Paris and Gupta-Larson models underestimate the potentials. The latter model was derived from analysis of mainly fine, dredged soils. The Rawls-Brakensiek model shows very close agreement with measured data especially near the drier end. This is due to the inclusion of measured matching points of moisture contents at 0.33 and 15 bar tensions in the model. Of the closed-form equations, the one-parameter Gregson etal model came closest to measured data with simillar slope but lower air entry pressure, followed by the Clapp-Hornberger model. All these closed-form models were matched at saturation with measured data. The Ghosh model overpredicted potential at the wet end while underestimating it at the drier end. In the McCuen etal model all the parameters were estimated from the statistical data and do not show much promise.

The parameters 'b' and 'he' are respectively determined from the slope and intercept of the log-log plots of the retention curves (Figs. 5.4a & 5.4b). These are listed in Table 5.3 (Note that 1 bar =

USER: CMAV71 PLOTFILE: SMCHARSF ENTRY NO. 62179 QUEUED ON 09/08/88 AT 10:57 PLOTTED ON 10/08/88 AT 18:40

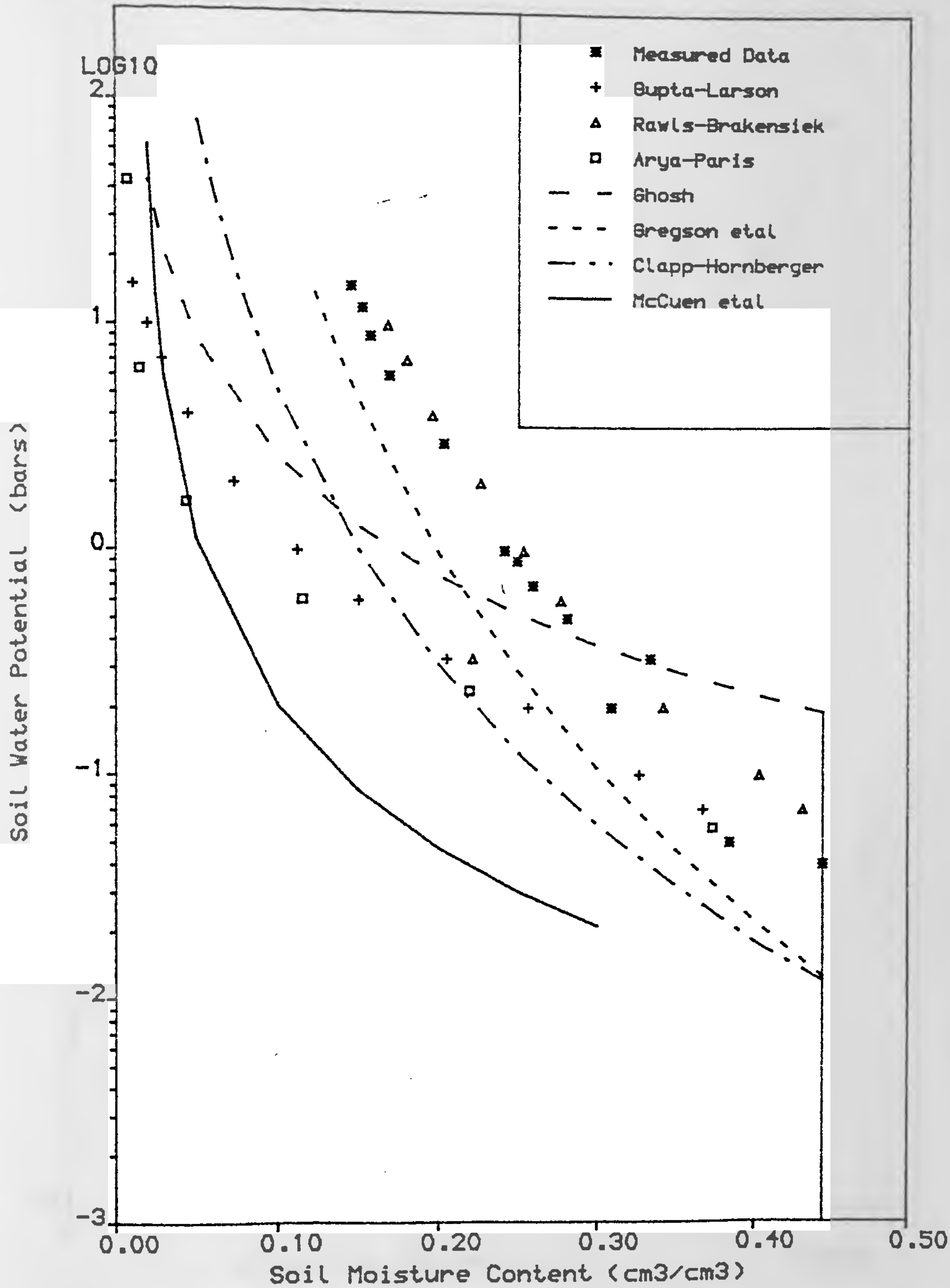

Fig. 5.3 Comparison of empirical models with measured moisture characteristic curve. (see text for details of models).

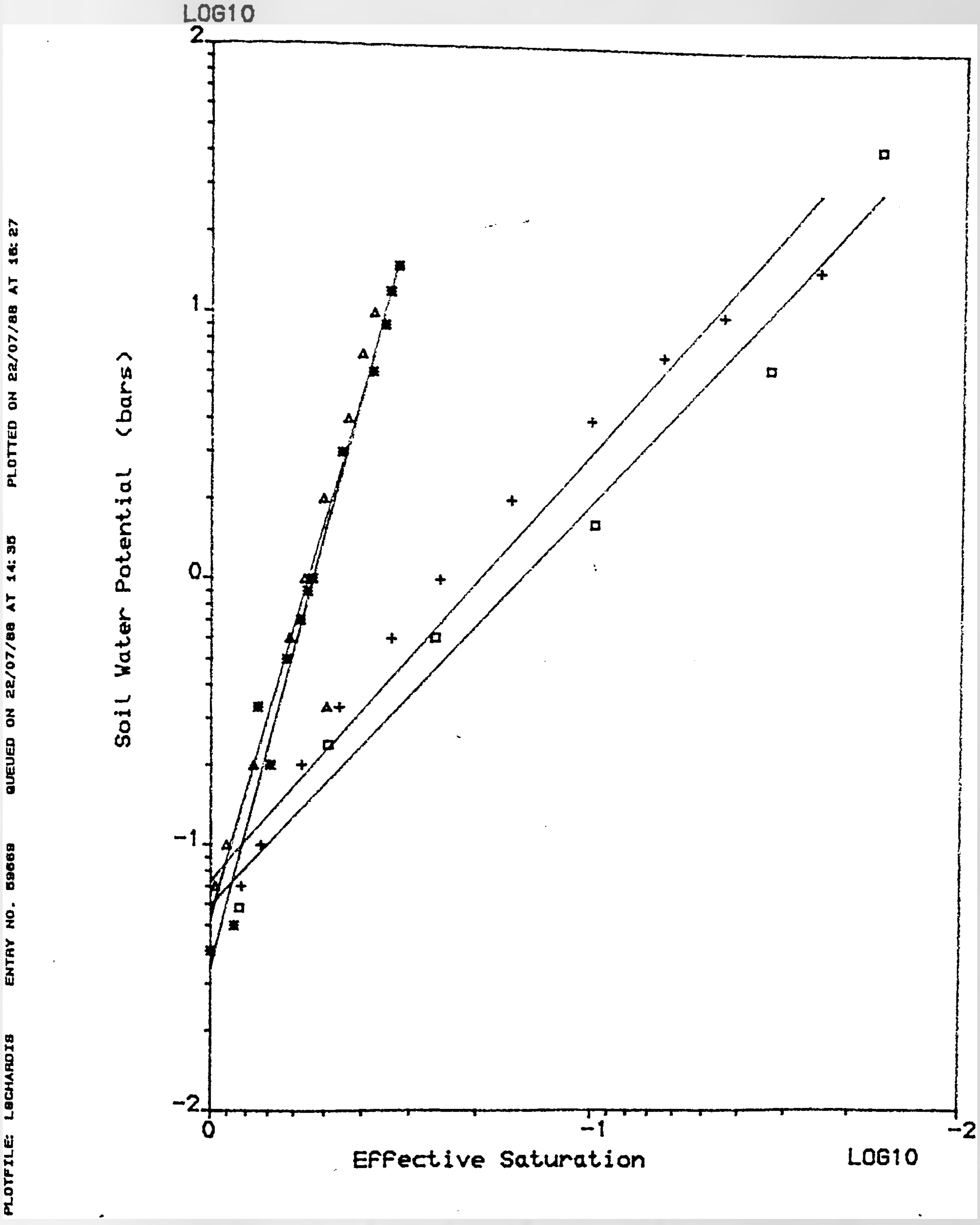

Fig. 5.4a Log-Log plot of discrete-form models of moisture characteristic.
(NB/ Effective saturation is the ratio of actual to saturated moisture content).

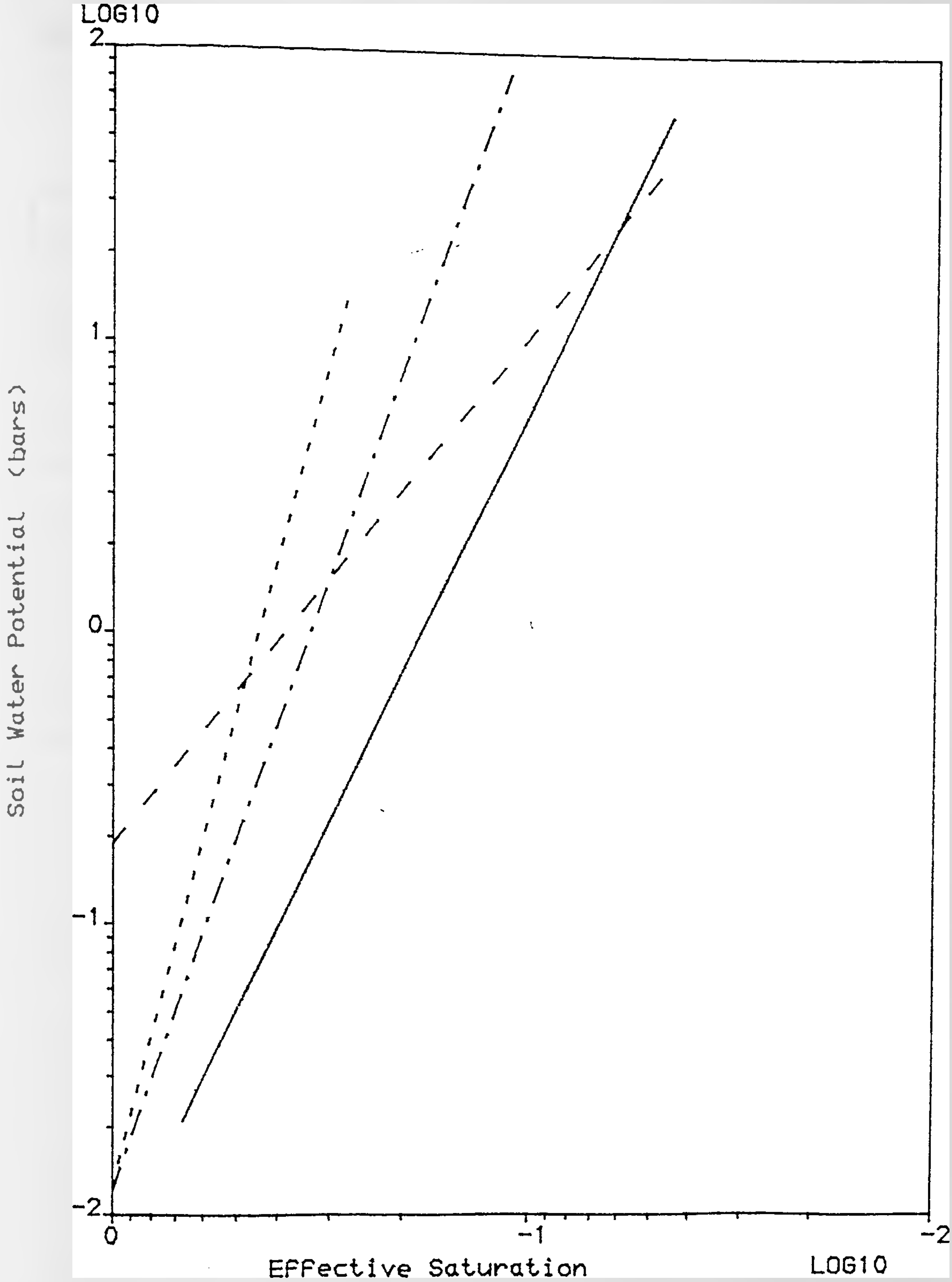

Fig. 5.4b Log-Log plot of closed-form models of moisture characteristic.
(NB/ Effective saturation is the ratio of actual to saturated moisture content).

TABLE 5.3 Retention curve parameters estimated by various methods for Auchincruive sand ('b' is the slope of log-log retention curve; and 'he' is the air entry pressure. For details of methods see text).

Method	'b'	'he' (cm)	r
1- Measured data	-5.44	34.6	0.990
2- Gupta-Larson	-1.619	73.0	0.964
3- Rawls-Brakensiek	-4.988	53.2	0.884
4- Arya-Paris	-1.521	59.0	0.976
5- Ghosh	-1.750	190.0	-
6- Gregson etal	-5.440	3.7	-
7- Clapp-Hornberger	-4.050	12.1	-
8- McCuen etal	-1.876	15.8	-

1000 cm).

The soil-water parameters (FC, WP and Pw) can now be estimated by substituting the values of 'b' and 'he' in equation 5.7 . The results are summarized in Table 5.4. These show a fair degree of variability between the methods. This suggests that great care must be taken in the use of such empirical methods for determination of FC, WP and Pw . Either indirect laboratory-based methods (eg: pressure plate) or direct insitu methods (eg: 2 day drainage tests) would be preferble.

Table 5.4 Estimated field capacity (FC), wilting point (WP) and wetting front pressure (Pw) Parameters for the Auchincruive sand. (For details of methods see text).

Method	FC cm3/cm3	WP cm3/cm3	Pw cm
1- Measured data *	0.308	0.105	20.1
2- Gupta-Larson	0.175	0.017	36.5
3- Rawls-Brakensiek	0.309	0.144	26.6
4- Arya-Paris	0.143	0.012	29.5
5- Ghosh	0.325	0.037	95.0
6- Gregson etal	0.195	0.097	1.9
7- Clapp-Hornberger	0.197	0.077	6.1
8- McCuen etal	0.088	0.012	7.9
Mean	0.216	0.068	27.6

* Measured data are from Fig. 5.2 .

5.3 Summary of Measured Soil Properties :

The results of the various measured properties of the Auchincruive sandy soil are summarized in the table below :

Table 5.5 Summary of the measured properties of the Auchincruive sandy soil.

Property	Symbol	Value	Units
Bulk Density	BD	1.498	g/cm3
Organic Matter Content	OMC	2.0	%
Particle Size Distribution	Sand	86.25	%
	Silt	11.16	%
	Clay	2.59	%
Residual Moisture Content	θr	0.05	cm3/cm3
Saturated Moisture Content	θs	0.445	cm3/cm3
Field Capacity	FC	0.309	cm3/cm3
Wilting Point	WP	0.105	cm3/cm3
Saturated Hydraulic Conductivity	Ks	0.31	cm/min
Wetting Front Pressure	Pw	20.10	cm

CHAPTER 6 INFILTRATION INTO NONUNIFORM SOILS

6.1 Introduction :

Infiltration is the process of water absorption and distribution in the unsaturated soil medium. This involves the replacement of air voids in the soil by water. The speed and amount by which this replacement takes place is dependent on the particle size distribution and in particular the degree of fine materials present. Coarse soils have larger voids thus water enters and leaves the soil faster and in larger amounts. The opposite is true for soils containing mostly fine materials.

Infiltration controls the land-phase processes of the hydrological cycle. The amount of runoff that occurs from rainfall is primarily dependent on the infiltration rate of the soil. The seperation of rainfall or irrigation water into the runoff and infiltration components is of particular interest to the irrigation managers since the infiltrated water fills the root zone moisture storage and an idea of its magnitude helps determine the adequacy of irrigation practices.

The infiltration rate of the soil also determines the amount of time a field needs to be inundated with water to ensure adequate recharge of the root zone moisture storage. The infiltration process therefore conveys information about the spatial and temporal movement and distribution of water on the irrigated field.

The irrigation scheduling model developed in chapters 3 and 4 enables the prediction of the days and the amounts of irrigation required for a particular field and crop. To determine the duration of each irrigation event an evaluation of the infiltration rate of the soil, under conditions of changing root zone moisture contents, is necessary.

In this chapter the process of infiltration and the factors which effect it are examined. Mathematical models are suggested for the simulation of one and two dimensional infiltration into nonuniform soils. These models form the links between the continuous water balance model and the event-based surface and sprinkler irrigation operational management models.

6.2 Existing Infiltration Models :

The physically-based infiltration models are based on the solutions of the partial differential equation of water movement in unsaturated soils, often referred to as the Richards equation (Richards 1931) . The equations of mass continuity and Darcy's law on water flow through porous media (Darcy 1856), are used to derive the equations of flow in unsaturated soils (Marshall & Holmes 1979, Hillel 1980):

Horizontal flow :

$$\frac{\partial \theta}{\partial t} = \frac{\partial}{\partial x} \left(K \frac{\partial h}{\partial x} \right) \qquad (6.1)$$

Vertical flow :

$$\frac{\partial \theta}{\partial t} = \frac{\partial}{\partial z} \left(K \frac{\partial h}{\partial z} \right) - \frac{\partial K}{\partial z} \qquad (6.2)$$

where:

θ = volumetric moisture content (cm3/cm3)
h = soil water potential (cm)
K = hydraulic conductivity (cm/hr)
t = time (hr)
x = horizontal distance (cm)
z = vertical distance (cm)

The major disadvantages of solving such non-linear partial differential equations are the complexities of the numerical solutions and the requirement for accurate soil moisture characteristics and hydraulic conductivity functions. The small time and distance increments necessary in the numerical solutions also incur high computing costs (Van Keulen 1982).

To overcome such difficulties several empirical infiltration models, derived mainly from observations of the decay of infiltration rates with time of ponded soils, have been proposed . More recently efforts have been made to derive models with physically-based parameters so as to broaden the limited range of the empirical models' applicability.

Philip (1957) solved Eqn. 6.2 analytically and derived an infiltration function based on the soil sorptivity and saturated conductivity. Horton (1940) proposed a parametric model based on an exponential function fitted to the infiltration-rate decay curve. Kostiakov (1932) used a simillar procedure but fitted a linear allometric function to the curve. Holtan etal (1974) used an empirical model with parameters based on surface porosity, available storage and vegetation cover.

All the models mentioned above assume that the surface is initially ponded and that the antecedent soil moisture conditions play no part in the infiltration process. To overcome these shortcomings, Smith (1972) solved Eqn. 6.2 analytically and derived a model with physically-based parameters which incorporates rainfall intensity and antecedent soil moisture conditions.

An infiltration model, which was developed in the year 1911 but whose potential has only recently been realized, is the so called Green-Ampt model. Green & Ampt (1911) derived an equation for the rate of infiltration of water into suddenly ponded soils :

$$i = Ks\ (H + L - Pw)/\ L \tag{6.3}$$

where Ks is the saturated hydraulic conductivity (mm/min) ; H is the depth of water on the surface (mm);

L is the vertical depth of the saturated zone (mm); and Pw is the capillary pressure at the wetting front (mm).

The concept of this model can best be described as a piston-type flow. The wetting front is assumed to be sharp (Fig. 6.1). The Green-Ampt model has been used successfully in the hydrological simulation of infiltration from rainfall (Mein & Larson 1973, Swartzendruber 1974, Morel-Seytoux 1976, Knisel 1980).

The major disadvantage of the Green-Ampt model is that the infiltration rate is not a direct and simple function of time. Infiltration rate, is an implicit function of time which must be solved by iteration, numerical methods, or graphical aids (Chu 1978). The advantages of this model are that all it's parameters are physically based, and the piston-type flow concept makes it particularly suitable for modelling infiltration into stratified soils where the soil properties vary from layer to layer.

The Green-Ampt model forms the basis of the one and two dimensional models of infiltration into nonuniform soils, developed in the following sections and used in chapters 7 and 8.

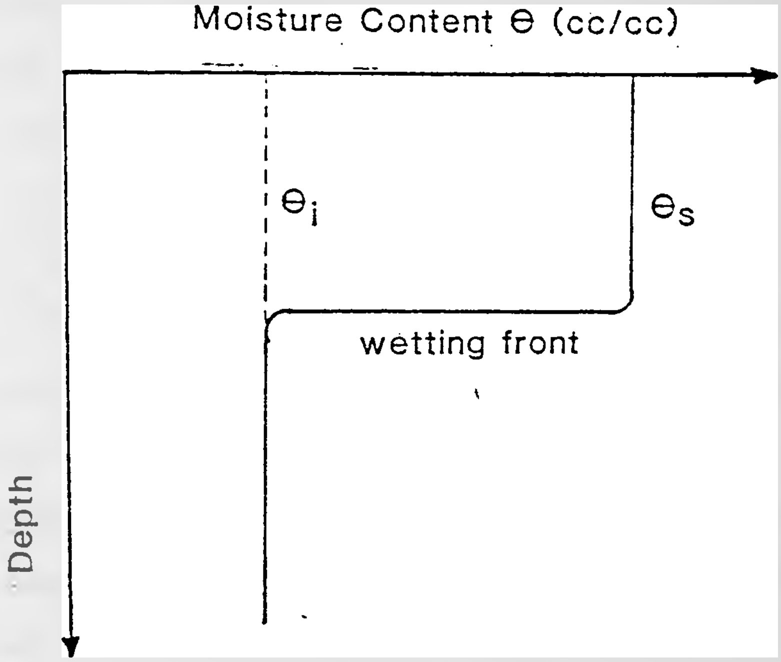

Fig. 6.1 Schematic diagram of piston-type flow with sharp wetting front in the Green-Ampt model. (θs = saturated moisture content, cm3/cm33; θi = initial moisture content, cm3/cm3).

6.3 Infiltration Into Nonuniform Soils:

Nonuniformity in soils is taken here to mean that either soil moisture content θ, or hydraulic conductivity K, or both, change spatially within the soil profile. While moisture content is independent of directions, hydraulic conductivity can vary directionally depending on the structure of the soil minerals. Hillel (1980) defines the case where K varies from point to point as hydraulically 'inhomogeneous'. Where K varies for different directions, the soil is said to be 'anisotropic'.

The models presented in this section are applicable to either uniform or nonuniform soils. In the latter case it is assumed that the soil is non-homogeneous in moisture content and hydraulically homogeneous but anisotropic only in the horizontal and vertical directions.

6.3.1 Bouwer's One Dimensional Model :

Natural rain, sprinkler irrigation, and surface irrigation by the border and flooding methods can be considered as cases for the one dimensional infiltration of water into the soil.

The one dimensional vertical flow of water in uniform soils can be simulated from the solution of Eqn. 6.2 or approximated by the various empirical and semi-empirical models reviewed in the previous section. The assumption of uniformities in soil hydraulic properties may not be representative of the field conditions. In reality the soil profile is seldom uniform in hydraulic properties. Where uniformity exists in the root zone, the differential root water extraction with depth, ensures the soil is not uniform in moisture content, although the saturated conductivity and wetting front pressure parameters remain constant.

The modelling of one dimensional water flow in nonuniform soils has been undertaken by Childs & Bybordi (1969) and Bouwer (1969,1976). The model used in this study is that of Bouwer (1969). The original tabular method of solution has been translated into an algorithm for the purpose of computer simulation . The model utilizes the equation of Green-Ampt to follow the spatial and temporal movement of water through a stratified soil profile of decreasing saturated hydraulic conductivity Ks, and/or moisture content θ.

In the Green-Ampt model (Eqn. 6.3) the infiltration rate is not a direct function of the elapsed time. Introducing the rate of advance of the wet front (dL/dt) as:

$$\frac{dL}{dt} = \frac{i}{(\theta s - \theta i)} \qquad (6.4)$$

where:

L = depth of wetting front (mm) at time t (min)
θs = saturated moisture content (mm)
θi = initial moisture content (mm)
i = infiltration rate at time t (mm/min).

and substituting into Eqn. 6.3 yields a relationship between the depth of wet front L , and time t :

$$t = \frac{(\theta s-\theta i)}{Ks} \left[L-(H-Pw) \ln \frac{H + L - Pw}{H - Pw} \right] \qquad (6.5)$$

where 'ln' is the natural logarithm; and all other terms are as previously defined.

The method involves routing the infiltrated water through each discrete soil layer, using the appropriate moisture contents. By assuming that the entire soil profile above a wetting front is uniform in θ , two fictitious times are calculated as the times that the wet front would reach the top and bottom of any layer (j) :

$$t' = \frac{f(j)}{Ks} \left(Ks.t / f \right)_{j-1} \qquad (6.6)$$

and

$$t'' = \frac{f(j)}{Ks} \left(Ks.t / f \right)_{j} \qquad (6.7)$$

where

$$f(j) = \theta s(j) - \theta i(j) \qquad (6.8)$$

The difference between these two times gives the true time taken for the wet front to move through layer j :

$$t = t'' - t' \tag{6.9}$$

If the saturated conductivity of the soil is decreasing with depth also, then at each layer, the harmonic mean of the conductivities above it must be used (Brakensiek 1970) :

$$Ks = L / \left(\sum_{1}^{j} [\, d(j)/Ks(j) \,] \right) \tag{6.10}$$

where L is the vertical depth to wetting front; d(j) is the thickness of layer j ; and Ks(j) is the saturated conductivity in layer j .

The flow chart in Fig. 6.2 shows the steps involved. The output of the model is a set of values of time versus cumulative infiltration. Table 6.1 shows the input parameter requirements of the model. The values are those of Bouwer's example. The result of the model run is shown in Fig. 6.3 .

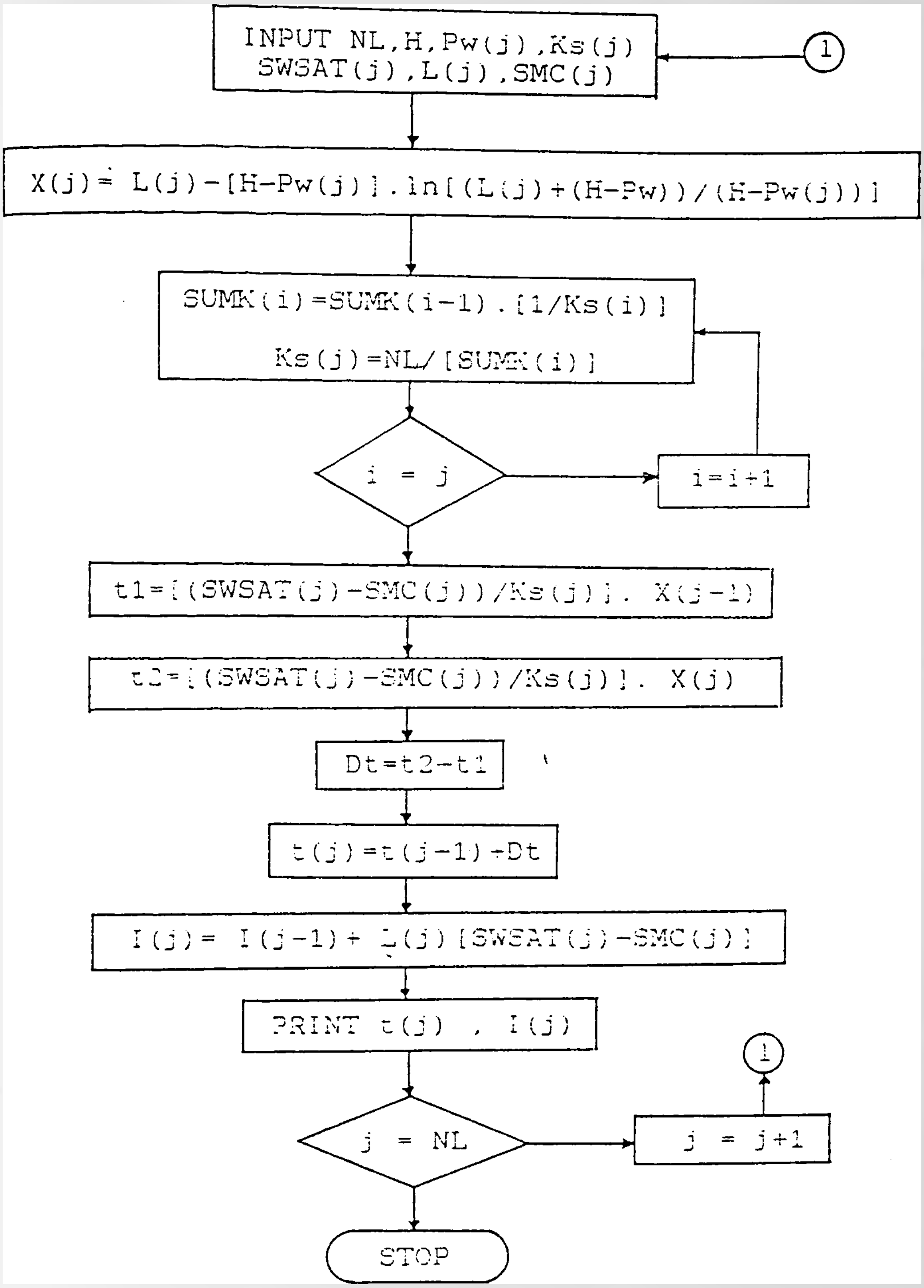

Fig. 6.2 Flow chart of the Bouwer infiltration model for nonuniform soils, after Bouwer 1969, (see text for definition of terms).

Table 6.1 Example of Input Parameters Required for the 1D model of Bouwer (assuming H=0.0 cm).

Layer No.	Thickness cm	Ks cm/hr	θs cc/cc	Pw cm	θi cc/cc
1	10.0	0.416	0.40	20.0	0.178
2	10.0	0.333	0.40	20.0	0.194
3	10.0	0.250	0.40	20.0	0.210
4	10.0	0.166	0.40	20.0	0.226
5	10.0	0.166	0.40	20.0	0.242
6	10.0	0.125	0.40	20.0	0.258
7	10.0	0.125	0.40	20.0	0.274
8	10.0	0.083	0.40	20.0	0.290
9	10.0	0.083	0.40	20.0	0.306
10	10.0	0.083	0.40	20.0	0.322

* Key :

Ks = saturated hydraulic conductivity (cm/hr)
θs = saturated moisture content (cm3/cm3)
Pw = pressure at wetting front (cm)
θi = initial moisture content (cm3/cm3)

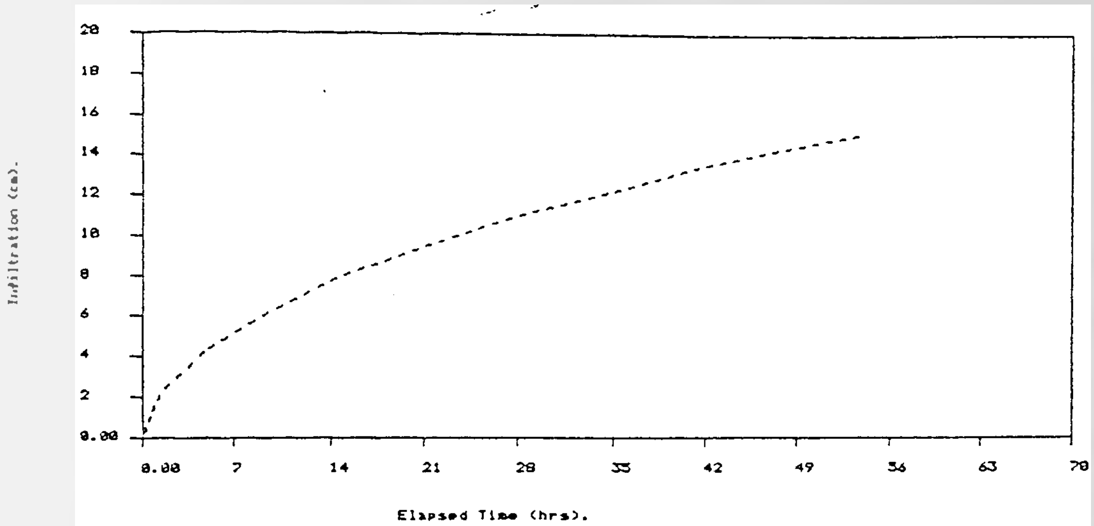

Fig. 6.3 Simulated cumulative infiltration curve by Bouwer's model.

The shape of the infiltration curve can be expressed mathematically by the Kostiakov (1932) equation :

$$I = c\, t^{n} \tag{6.11}$$

where:
I = cumulative infiltration (cm)
t = elapsed time (hours)
c & n = infiltration-curve fitting parameters.

The infiltration parameters (c and n), reflect the hydraulic properties of the soil profile and incorporate the changes in the soil moisture content in the root zone of crops. These parameters are derived by fitting a straight line to the log-log plot of the infiltration curve.

The influence of changes in the antecedent moisture content and hydraulic properties, on the infiltration parameters is analysed next.

Sensitivity of the model :

The input parameters required for the Bouwer infiltration model are the head of water on the surface (H), the layer thickness (L) and the corresponding saturated hydraulic conductivity (Ks), saturated moisture content (Θs), wetting front pressure (Pw), and the initial moisture content (Θi). All are physically measureable properties which effect the infiltration process to varying degrees. To assess the effect of each parameter, the rest were kept constant (see Table

6.1) and the target parameter was changed by $\pm 10\%$. The results of this sensitivity analysis are shown in Figs. 6.4 to 6.9 .

The point of interest in this analysis is the variation in the degree of departure from the central curve on the infiltration axis. The relative changes in the slopes of the curves determine the magnitude of the parameters 'c' and 'n' in Eqn. 6.11 . These variations are shown in Table 6.2 .

The model shows less variation in the parameter 'n' than the 'c' parameter. In the latter case, the model is most sensitive to Ks and θs , and moderately sensitive to Pw and θi . Pw is perhaps the most difficult soil property to determine . The other parameters are readily measureable in the field (see chapter 5). The lack of sensitivity to the thickness of the soil layers suggests accurate determination of the boundaries between different soil layers is not essential.

The sensitivity of the model to the soil-specific parameters, Ks, θs, θi and Pw, shows the importance of defining each irrigated field unit primarily by it's soil properties. This ensures that the root zone water balance model and the infiltration model, and hence the surface and sprinkler irrigation operations models, are accurate representations of the conditions in that field alone.

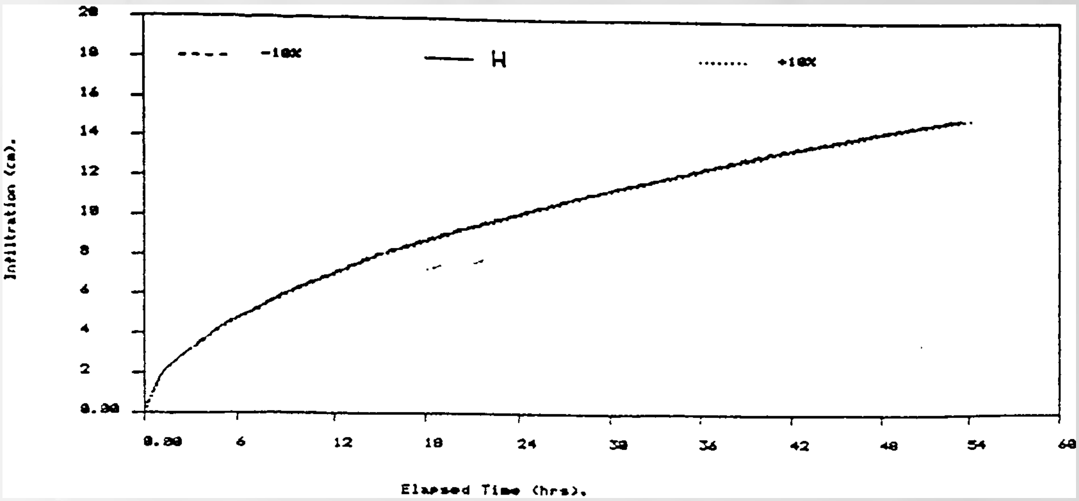

Fig. 6.4 Model sensitivity to depth of water on surface (parameter H).

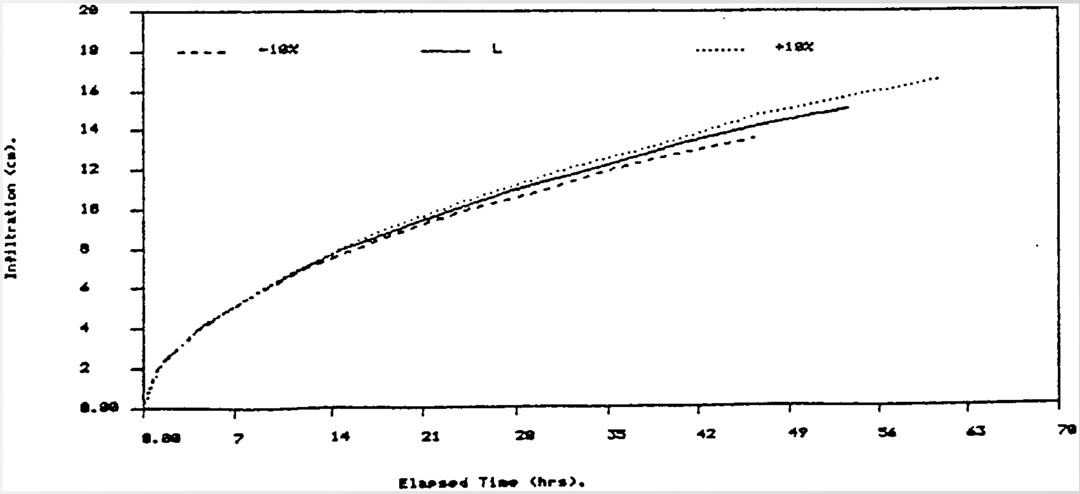

Fig. 6.5 Model sensitivity to soil layer thickness (parameter L).

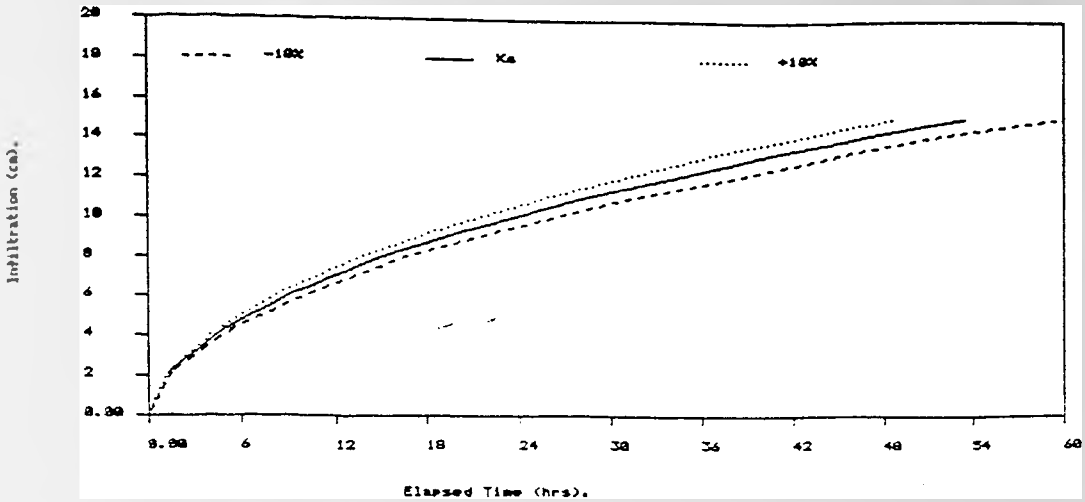

Fig. 6.6 Model sensitivity to saturated hydraulic conductivity (parameter Ks).

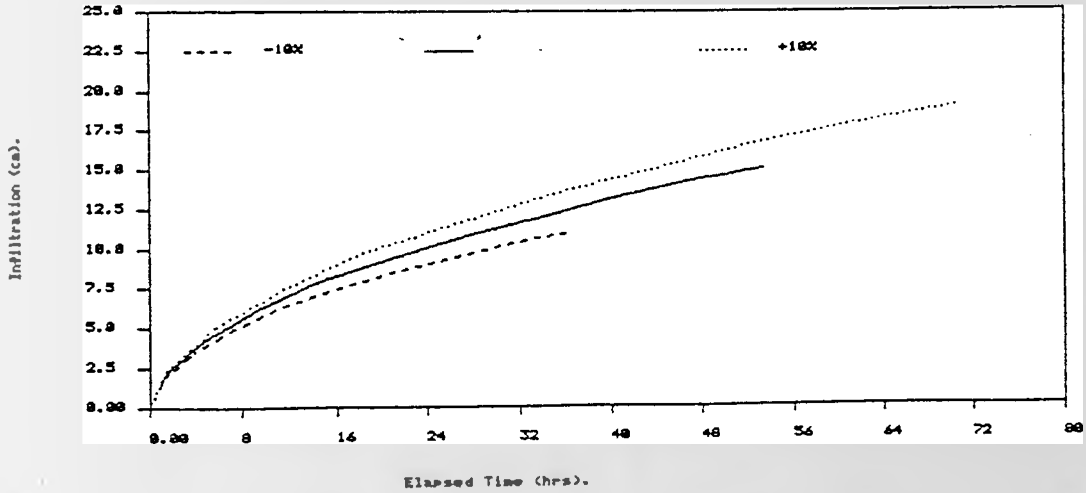

Fig. 6.7 Model sensitivity to saturated moisture content (parameter Θs).

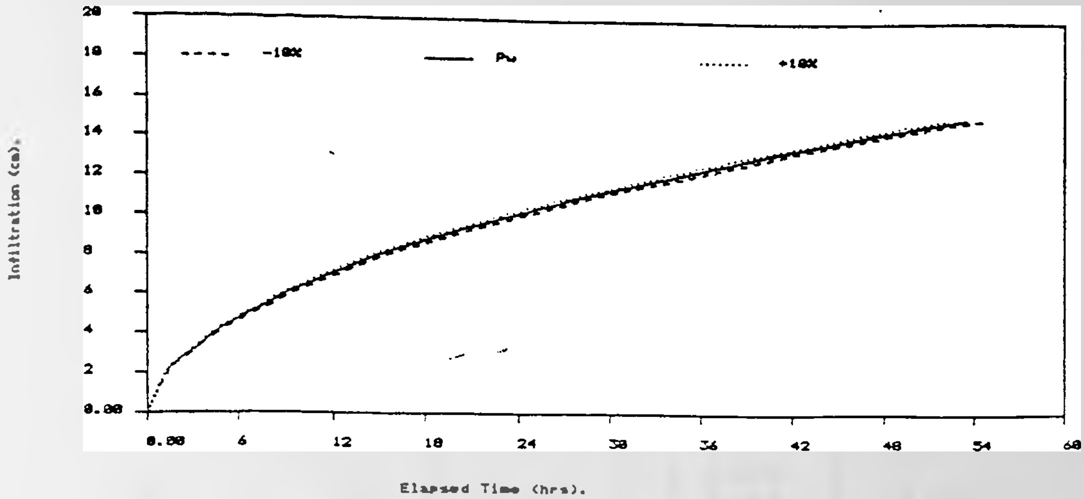

Fig. 6.8 Model sensitivity to wetting front pressure (parameter Pw).

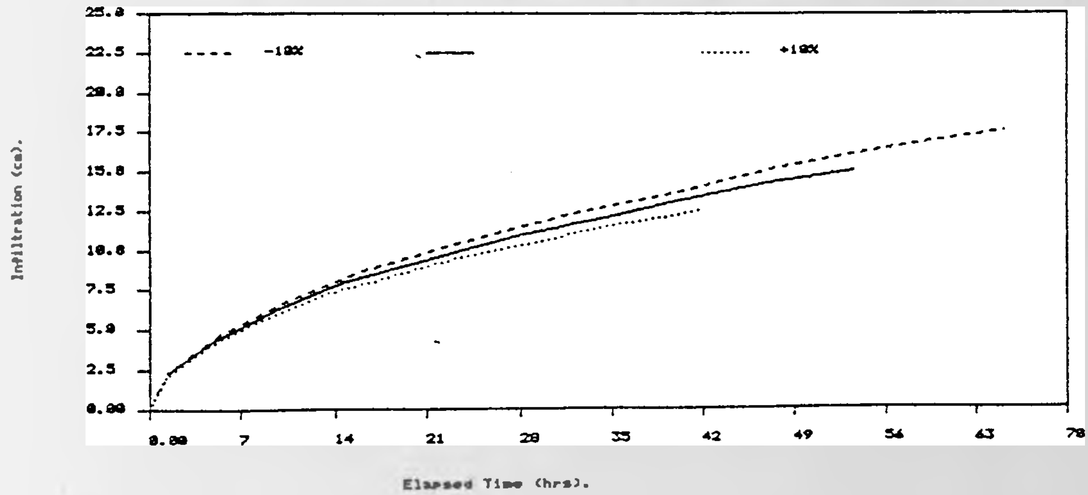

Fig. 6.9 Model sensitivity to initial soil moisture content (parameter Θi).

Table 6.2 Sensitivity of the infiltration parameters 'c' and 'n' to the soil physical properties.

Parameter	'c' (cm)	% change	'n'	% change
-10%	1.88	+1.62	0.5296	-0.45
H	1.85		0.5320	
+10%	1.82	-1.62	0.5346	+0.49
-10%	1.85	0.00	0.5244	-1.43
L	1.85		0.5320	
+10%	1.84	-0.54	0.5393	+1.37
-10%	1.75	-5.40	0.5319	-0.02
Ks	1.85		0.5320	
+10%	1.95	+5.40	0.5321	+0.02
-10%	1.69	-8.65	0.5274	-0.86
θs	1.85		0.5320	
+10%	1.99	+7.56	0.5355	+0.66
-10%	1.79	-3.24	0.5372	+0.98
Pw	1.85		0.5320	
+10%	1.91	+3.24	0.5273	-0.88
-10%	1.91	+3.24	0.5358	+0.71
θi	1.85		0.5320	
+10%	1.78	-3.78	0.5280	-0.75

* Key :

Ks = saturated hydraulic conductivity (cm/hr)
θs = saturated moisture content (cm3/cm3)
Pw = pressure at wetting front (cm)
θi = initial moisture content (cm3/cm3)
L = thickness of soil layer (cm)
H = depth of water on surface (cm)

6.3.3 Two Dimensional Model (2DVAR):

6.3.3.1 Development of the 2DVAR model:

In furrow irrigation practice, water is released into narrow channels and allowed to infiltrate both in the vertical and the horizontal directions. This process can be simulated by the solution of the complex equations 6.1 and 6.2, of flow through porous media (Selim & Kirkham 1973).

Empirical models, which can express the two dimensional (2D) infiltration process by simple mathematical functions, are more desirable for inclusion in larger simulation models. Toksoz etal (1965) studied the 2D infiltration process by a number of field tests, and fitted simple power functions to the infiltration-time curve.

Fok etal (1982) derived 2D exponential infiltration equations from the solution of the Green-Ampt model. These were presented as explicit functions of time for four successive time domains, each with a range dependent on the soil hydraulic properties. Their 2D model was applied to the case of furrow irrigation (Fok & Chiang 1984). The assumptions made in their model were : 1) the soil is homogeneous and isotropic; 2) the vertical flow region is bound by the width of the water surface in the furrow; 3) the furrow is of a rectangular cross section; and 4) the locus of a wetting front from a point is semi-elliptical.

The challenge here is to overcome the above assumption that the soil is homogeneous. The procedure used here is to simultaneously solve the horizontal and vertical flow equations. Fig. 6.10 schematically illustrates the simultaneous movement of the wetting front in the two directions. The furrow is assumed to be rectangular in cross section and symmetry about the furrow centre line is also assumed.

The vertical flow was simulated using the Bouwer model of one dimensional infiltration into nonuniform soils (see previous section). The soil profile is divided into discrete layers, each characterized by it's respective hydraulic properties. The vertical infiltration model essentially calculates the time that the wetting front takes to travel through each successive layer . The depth of water required to fill layer j to saturation is found from :

$$y(j) = [\ SWSAT(j) - SMC(j)\ ] \cdot L(j) \qquad (6.12)$$

where y(j) is the storage capacity of layer j (mm); SWSAT(j) and SMC(j) are the volumetric saturated and initial moisture contents respectively (cm3/cm3); and L(j) is the thickness of layer j (mm).

During the time that the water front is moving through layer j, horizontal infiltration is also taking place in that layer. Tolikas etal (1980) derived a simple model for horizontal infiltration which

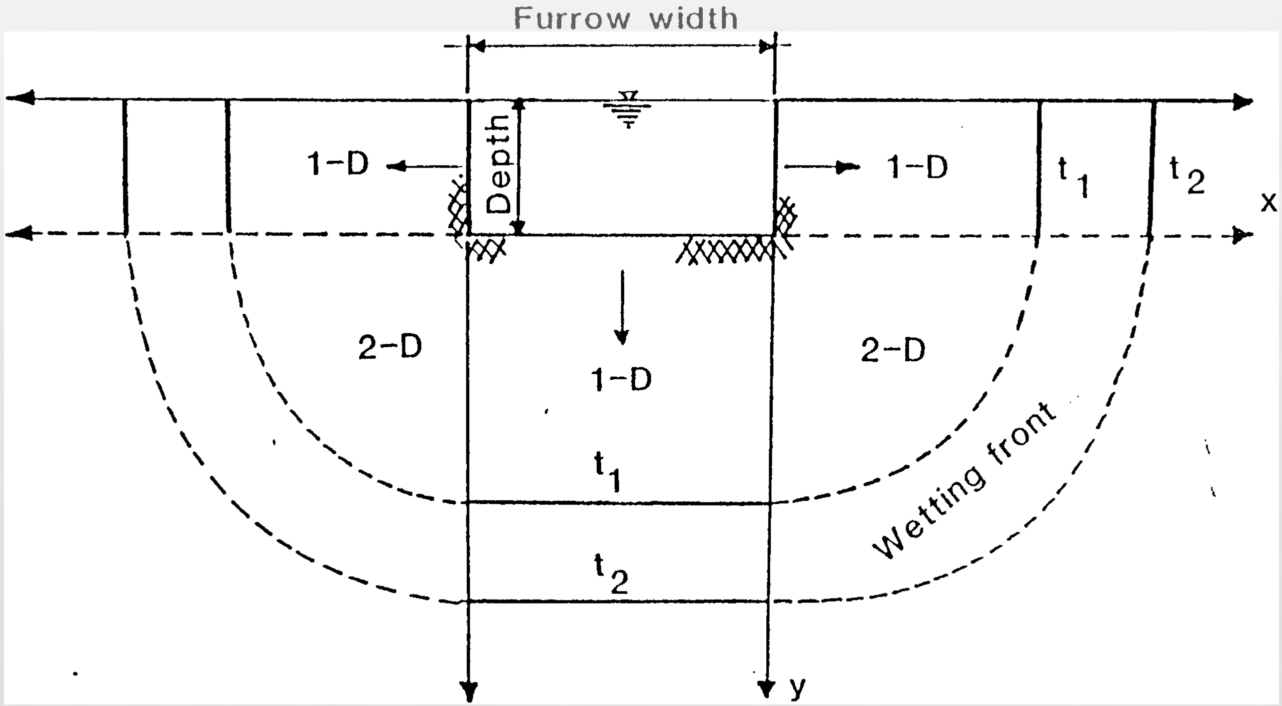

Fig. 6.10 Schematic representation of wetting fronts in two dimensional infiltration. (1-D and 2-D are zones of one and two dimensional infiltration; t= index of time).

requires knowledge of the diffusivity function of the soil. Toksoz etal (1965) observed that the horizontal advance distance was proportional to the square root of time. Fok etal (1982) derived an expression for horizontal advance rate, based on Darcy's law of flow through porous media :

$$x = \left[\frac{2.HKs.HPw}{L.\ SWSAT(SWSAT-SMC)} \right]^{0.5} .\ t^{0.5} \qquad (6.13)$$

where HPw is the horizontal wetting front pressure (mm); HKs is the saturated horizontal hydraulic conductivity (mm/min); and L is soil thickness (mm).

Thus for a stratified soil Eqn. 6.13 can be written as :

$$x(j) = \left[\frac{2.HKs(j).HPw(j)}{L(j).\ SWSAT(j)(SWSAT(j)-SMC(j)} \right]^{0.5} .\ t^{0.5} \qquad (6.14)$$

As the water front travels through deeper layers, horizontal movement of water still continues in the layers above, at a rate dependent on the latest time t . So at each new time step Eqn. 6.14 must be re-evaluated for the layers above the current layer.

The cumulative infiltration volumes (mm3 per unit furrow length), at time t, for the vertical (Iv), and horizontal (Ih), directions respectively, are thus :

$$Iv(t) = Fw \sum_{j=1}^{k} y(j) \qquad (6.15)$$

and

$$Ih(t) = 2 \sum_{j=1}^{k} [\ x(j).(SWSAT(J)-SMC(J)).L(j)\ ] \qquad (6.16)$$

where:

Iv(t) = cumulative vertical infiltration at time t (mm3 per unit furrow length)
Fw = furrow width (mm)
Ih(t) = cumulative horizontal infiltration at time t (mm3 per unit furrow length)
k = layer number containing the wetting front at time t.

The volume of water that infiltrates horizontally above the furrow bottom, into the sides, is found from the following :

$$Is(t) = 2\ Fd\ .\ x(1).\ [SWSAT(1)-SMC(1)] \qquad (6.17)$$

where:

Is(t) = cumulative infiltration into the sides of the furrow ridge, at time t (mm3 per unit furrow length)
Fd = depth of water in furrow (mm).
(NB: the number 1 in brackets referes to layer one).

Thus the total cumulative infiltration is thus the sum of the three volumes :

$$I(t) = Iv(t) + Ih(t) + Is(t) \qquad (6.18)$$

where I(t) is the total infiltration volume (mm3 per unit furrow length) at elapsed time 't' minutes.

This represents the total infiltration volume per unit furrow length. In reality the shape of the furrow will be parabolic in cross section. The effect of the shape on the infiltration characteristics is not clear (Fok etal 1982). It will be assumed here that whatever the shape of the furrow, the effective width and depth are those of the water surface width and water depth in the furrow.

The water depth is small at the beginning of irrigation and increases with time to a peak before receding. Freyberg etal (1980) studied the effect of time-dependent surface water depths on the Green-Ampt infiltration model and showed that the effect is of marginal significance. The analysis in Table 6.2 showed little sensitivity to water depth H. The change in water depth will also effect Eqn. 6.17 , but is not expected to be a major error of calculation since the volume of 'Is(t)' is relatively small.

The boundary conditions for the advancing wetting fronts are considered to be the profile bottom at an impermeable boundary, where vertical infiltration ceases, and mid-way between two furrows, where the horizontally moving wet front is assumed to stop. The time variation of total cumulative infiltration is expressed in the form of the Kostiakov power equation (Eqn. 6.11).

6.3.3.2 Validation of the 2DVAR model :

A) Uniform soils :

The 2DVAR model was tested with the experimental data and simulation results of the models presented by Fok etal (1982) and Fok & Chiang (1984). The latter author's tests consisted of tracing the movement of water in a large container, with controlled inundation of a rectangular furrow. Two soils (A & B) were tested. The properties and dimensions of the soils and apparatus are presented in Table 6.3 . In their tests the soil profile was taken to be uniform and homogeneous. The 2DVAR model presented here is tested with measured data for this soil condition only. Simulation runs for hypothetical nonuniform soils will also be presented.

For soils A & B , the profile depth was taken to be 21.0 inches and of uniform properties. For the simulation a depth increment of 0.5 in was chosen. For each successive depth increment, the elapsed time was calculated from Eqn. 6.13 as the time the wet front takes to travel through the storage represented by Eqn. 6.18 . The corresponding horizontal advance is calculated from Eqn. 6.21 . Thus the total infiltration at successive time t is determined from Eqn. 6.25.

The simulated wetting patterns of the two soils are shown in Fig. 6.11 and Fig. 6.12 . The

Table 6.3 Soil parameters used in the testing of the two dimensional infiltration model.

Parameter	Soil A	B	C	D
SMC (cm3/cm3)	0.071	0.104	0.107	0.179
SWSAT (cm3/cm3)	0.258	0.369	0.377	0.389
Pw (inches)	27.3	27.6	21.3	19.7
Ks (inches/min.)	0.00156	0.00224	0.00143	0.00213
Fw (inches)	4.17	4.12	0.40	0.40
Fd (inches)	1.20	1.75	0.40	5.90
Fl (inches)	4.0	4.0	0.40	5.90

* Key:

SMC = initial soil moisture content
SWSAT = saturated soil moisture content
Pw = wetting front pressure
Ks = saturated hydraulic conductivity
Fw = furrow width
Fd = furrow depth (or depth of water in furrow)
Fl = furrow length.

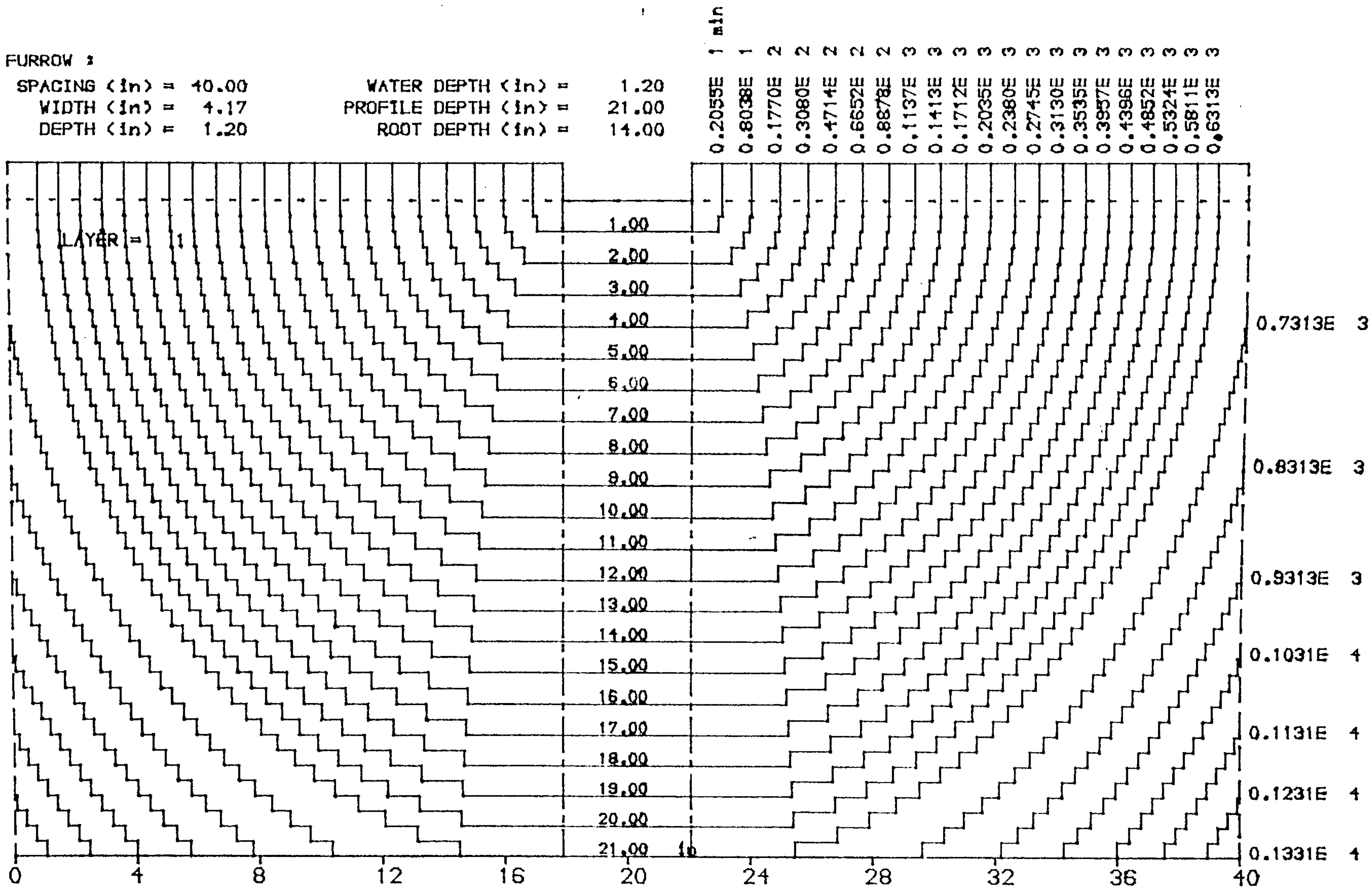

Fig. 6.11 Simulated 2-D wetting pattern for soil A, Table 6.3.

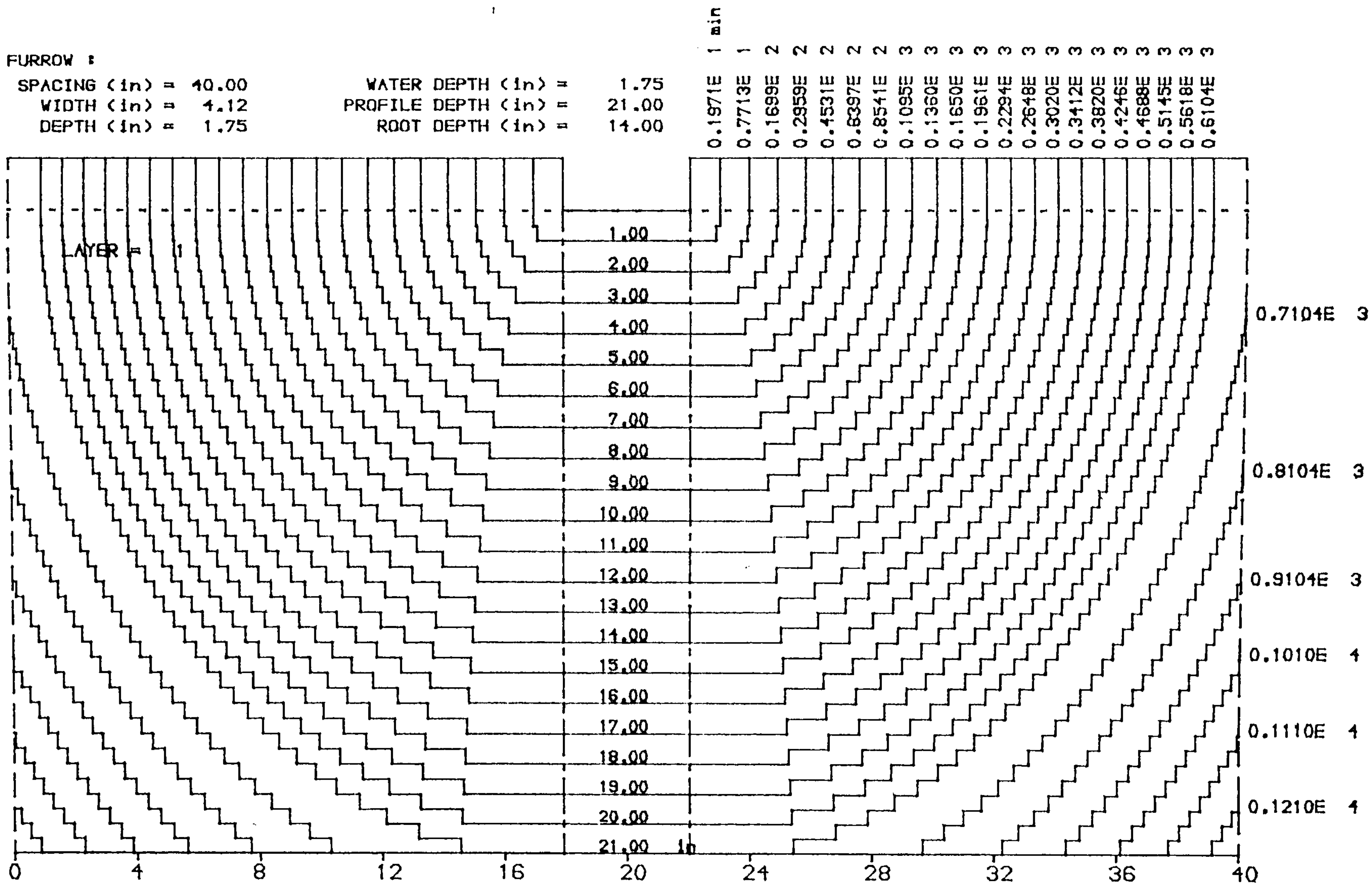

Fig. 6.12 Simulated 2-D wetting pattern for soil B, Table 6.3.

advance times for the wetting fronts are also shown. In soil A, the wetting front reaches the profile bottom in 631.3 minutes and the entire profile is wetted in about 1331 minutes. For soil B, the profile depth was reached in about 610 minutes, and the entire profile was wetted in 1210 minutes.

The infiltration-time curves, simulated for the two soils by the 2DVAR model, are compared with the measured and computed data, as reported by Fok & Chiang (1984), and presented in Figs. 6.13 and 6.14 . The prediction for soil A shows close agreement with measured data at early times, but over estimation at longer times (11.4% at 70 minutes). The deviation from measured data is larger for soil B , where at 80 minutes the overestimation is 20.5% .

The tests carried out by Fok etal (1982) were under simillar conditions to the above tests, but water was applied as a line source on the soil surface. Table 6.3 shows the soil properties and test dimensions for soils C and D . It is assumed here that the line source has an equivalent furrow depth and width of 0.4 in (1cm). This effectively results in a very small value of vertical infiltration, Iv, in Eqn. 6.22.

For these two simulations, the profile depth was taken to be uniform to a depth of 14 inches. A depth increment of 0.2 in was chosen. The simulated wetting patterns are shown in Figs. 6.15 and 6.16

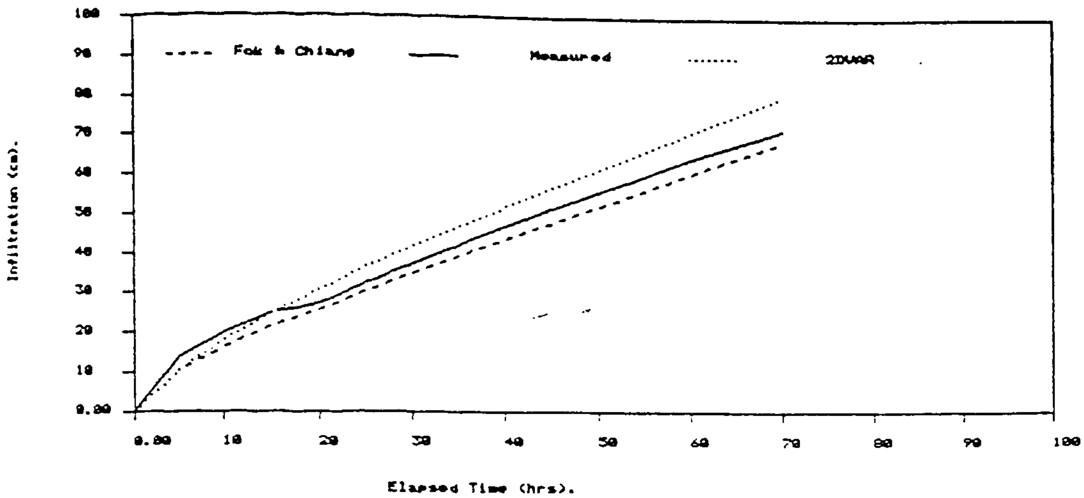

Fig. 6.13 Measured and predicted 2-D infiltration in soil A, Table 6.3.

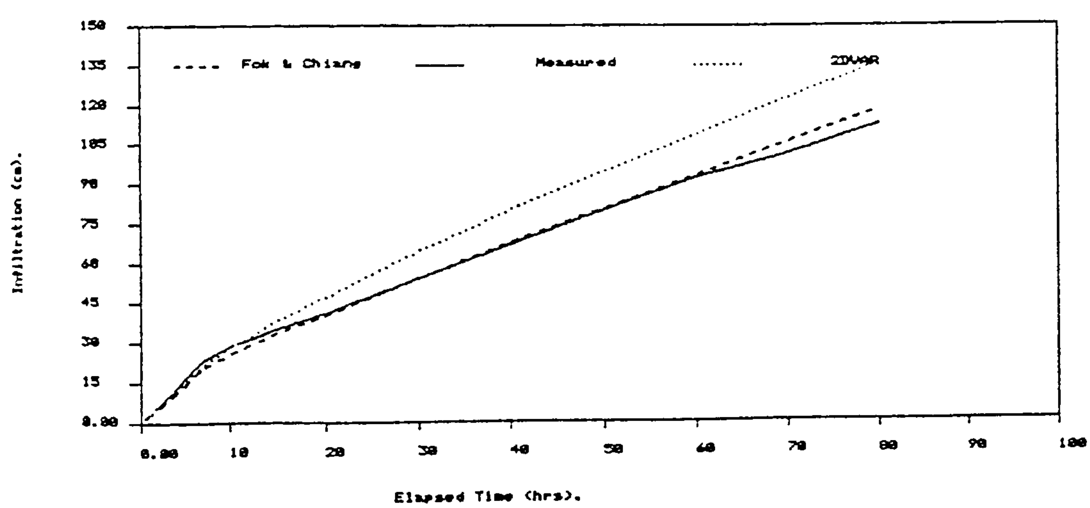

Fig. 6.14 Measured and predicted 2-D infiltration in soil B, Table 6.3.

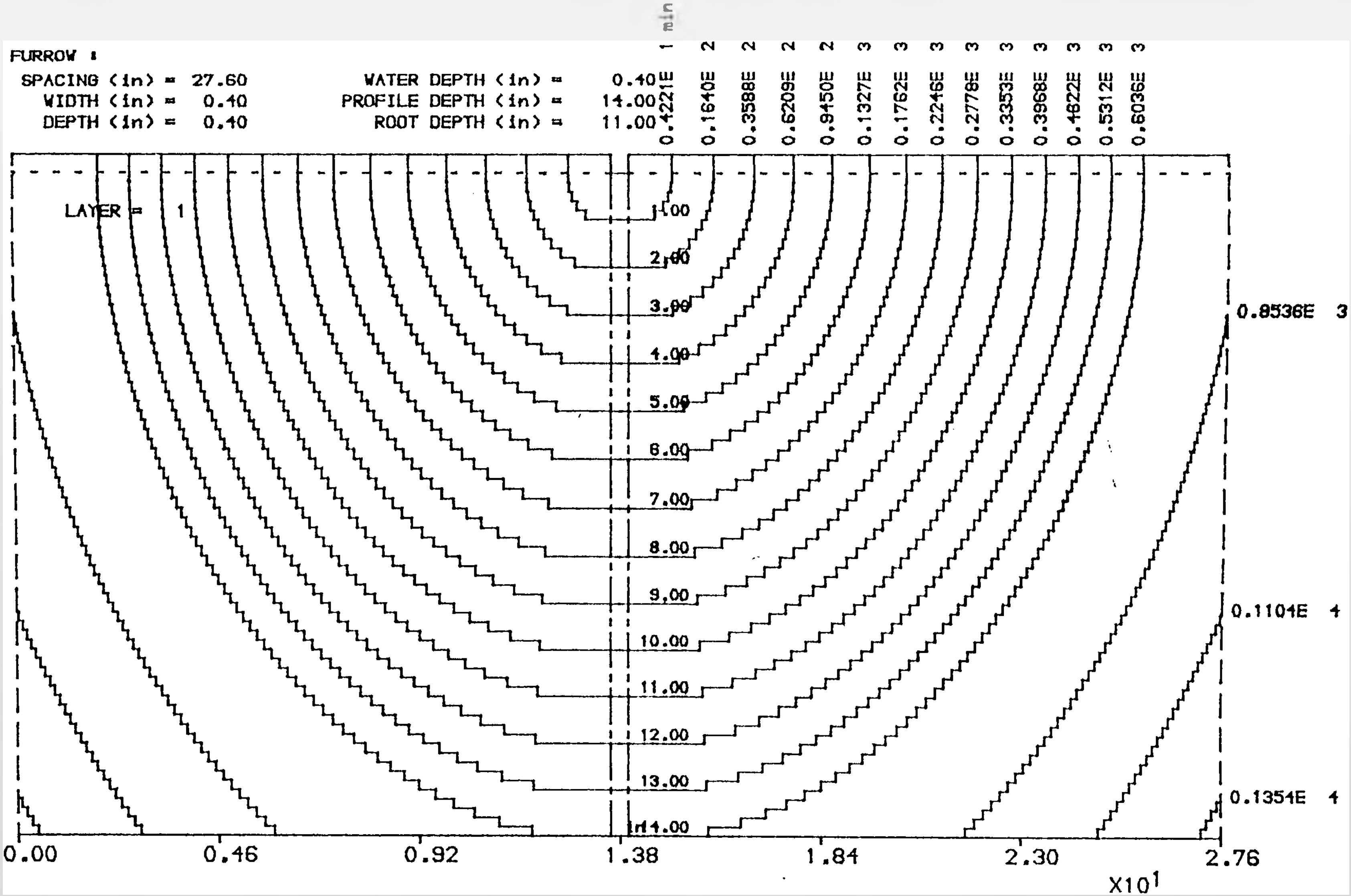

Fig. 6.15 Simulated 2-D wetting pattern for soil C, Table 6.3.

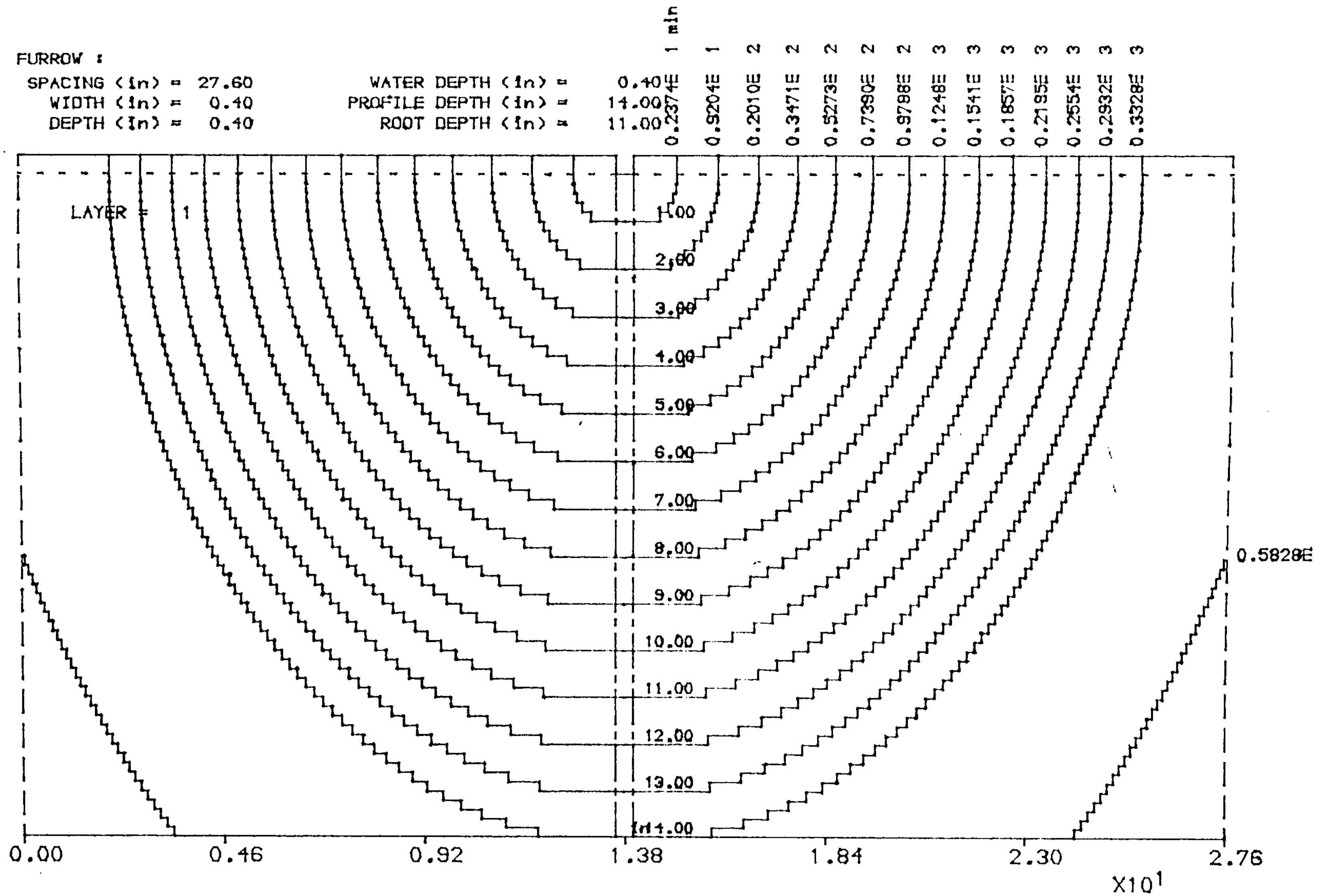

Fig. 6.16 Simulated 2-D wetting pattern for soil D, Table 6.3.

respectively. For soil C the wet front reaches the profile depth in 603.6 minutes and the entire profile is wetted in 1354 minutes. The corresponding predictions for soil D are 332.8 minutes and 582.8 minutes.

The infiltration curves for soils C and D are shown in Figs. 6.17 and 6.18 respectively. These show the comparisons between the present model (2DVAR), the Fok etal model , and the measured data. The present model shows a consistent overestimation of infiltration for soil C. The Fok etal model begins with close agreement but gradually departs from the measured curve. The deviation of both predictive models at 391 minutes is about 11% . The prediction for soil D is more encouraging . The 2DVAR model follows the measured curve closely throughout the test duration. The departure at 330 minutes is only 5.8% , while that of Fok etal model is 14% .

For the four simulations (soils A, B, C & D), the maximum deviation of the 2DVAR model is below 12% for 3 out of 4 soils, and about 20% for the other. For the four soils tested the results are on the whole acceptable. It is evident from the infiltration curves that the model developed by Fok etal (1982), and used by Fok & Chiang (1984), makes better predictions, but is limited in application to uniform soils. The 2DVAR model is capable of simulating the infiltration process for nonuniform, anisotropic soils.

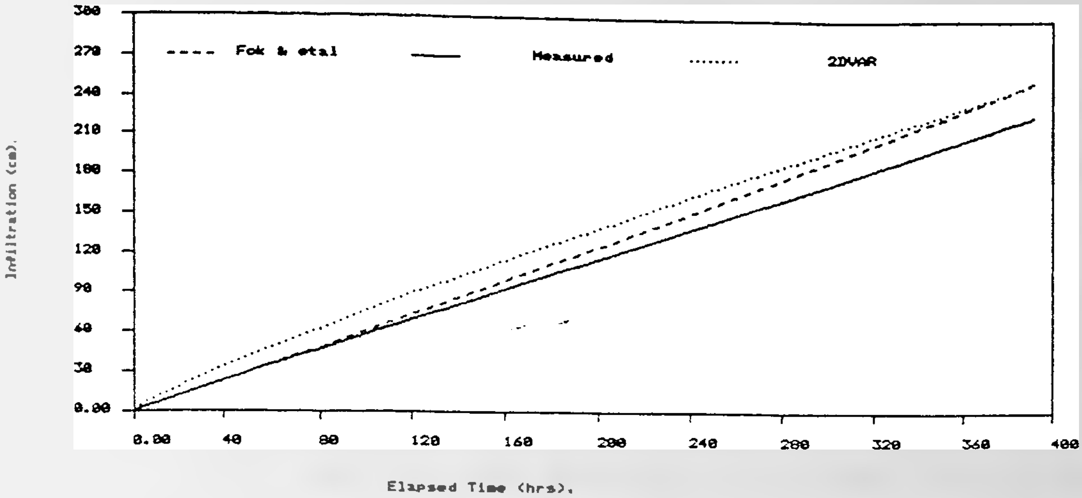

Fig. 6.17 Measured and predicted 2-D infiltration in soil C, Table 6.3.

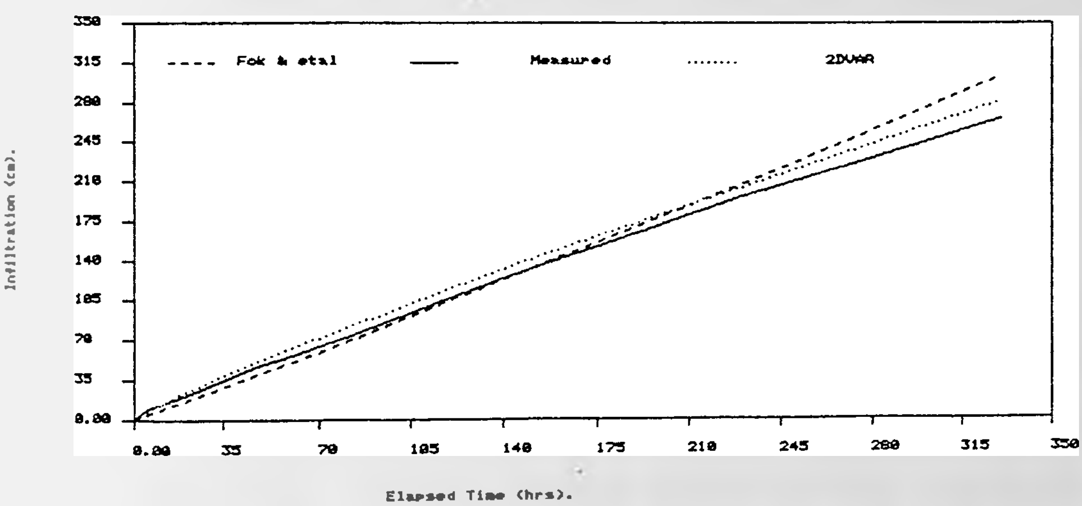

Fig. 6.18 Measured and predicted 2-D infiltration in soil D, Table 6.3.

B) Nonuniform soils :

As previously defined, nonuniformity refers to either soil moisture content and/or hydraulic conductivity variations in the spatial sense. Detailed infiltration data and wetting pattern developments for nonuniform soils was not available so hypothetical cases are simulated based on the data of soil A in Table 6.3 . The 21 inch profile is divided into 7 equal layers, the properties of which are varied and the response of the model to the simulated nonuniformities is observed.

Case 1 - The effect of anisotropy :

Profile 1 : In this simulation the same data as for soil A are used, but the vertical saturated conductivity is assumed to be successively reduced,from top to bottom, by 10% at each layer (ie: 1.56E-3, 1.4E-3, 1.25E-3, 1.09E-3, 9.4E-4, 7.8E-4, 6.2E-4 inches per minute). Horizontal Ks is kept constant at 1.56E-3 (in/min).

The resultant wetting pattern is shown in Fig. 6.19 . It can be seen that as expected, the vertical advance of the wet front is slower than the isotropic case (soil A, Fig. 6.11). The wetting front reaches the profile bottom (depth of 21 inches) in 713.7 minutes . For soil A this value is 631.3 minutes (Fig. 6.11).

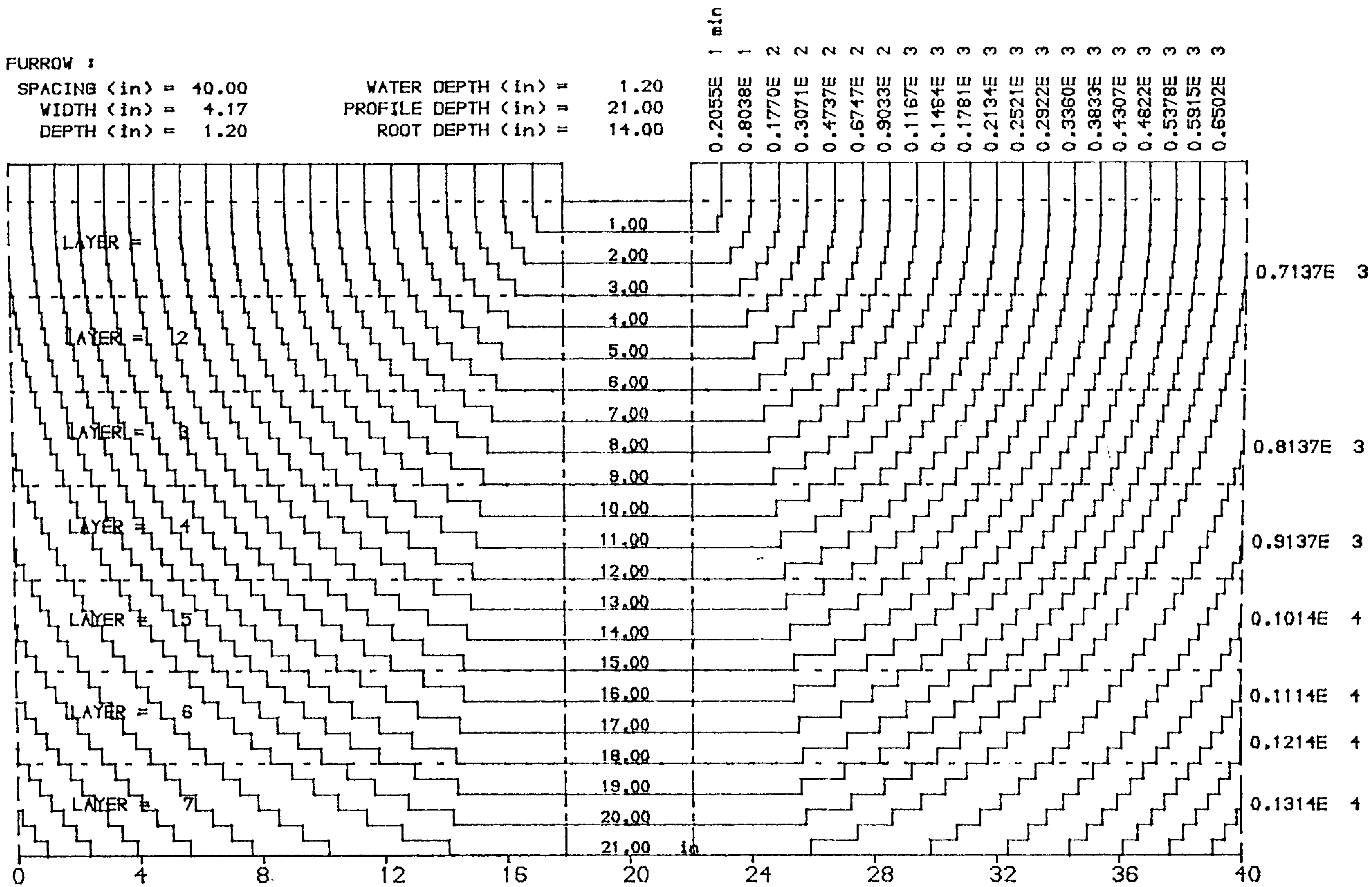

Fig. 6.19 Simulated 2-D wetting pattern for soil A, Table 6.3, under reducing vertical Ks.

Profile 2 : Figure 6.20 shows the wetting pattern for a soil profile where the anisotropy is the reverse of the above case, ie: the horizontal conductivity is reduced successively by 10% (same values as above). In comparison to soil A in Fig. 6.11, the wet front reaches the bottom at the same time (631.3 minutes), but the horizontal advance at each successive layer becomes progressively slower. All infiltration after 631.3 minutes is in the horizontal direction, and the time taken to entirely fill the profile is 2331 minutes.

Profile 3 : Figure 6.21 shows the simulated wetting pattern for a complex soil profile of uniform moisture content and decreasing conductivity from top to bottom of 1.56E-3, 1.4E-3, 1.25E-3, 1.09E-3, 9.4E-4, 7.8E-4, and 6.2E-4 (in/min), in the horizontal direction and half of these values for the corresponding vertical direction. The wet front reaches the vertical boundaries well before the profile bottom is reached in 1527 minutes. This means that the soil is saturated thoroughly down to a depth of 12 inches by the time the vertical infiltration ceases. The time taken for the entire profile to be saturated is 3027 minutes.

Profile 4 : Figure 6.22 shows the case of a soil in which the horizontal Ks is half the vertical Ks for all the layers, ie : Hks = 0.5Ks = 7.8E-4 (in/min) for all layers. In comparison to Fig. 6.11, the time of the wet front reaching the bottom is the same 631.3 minutes,

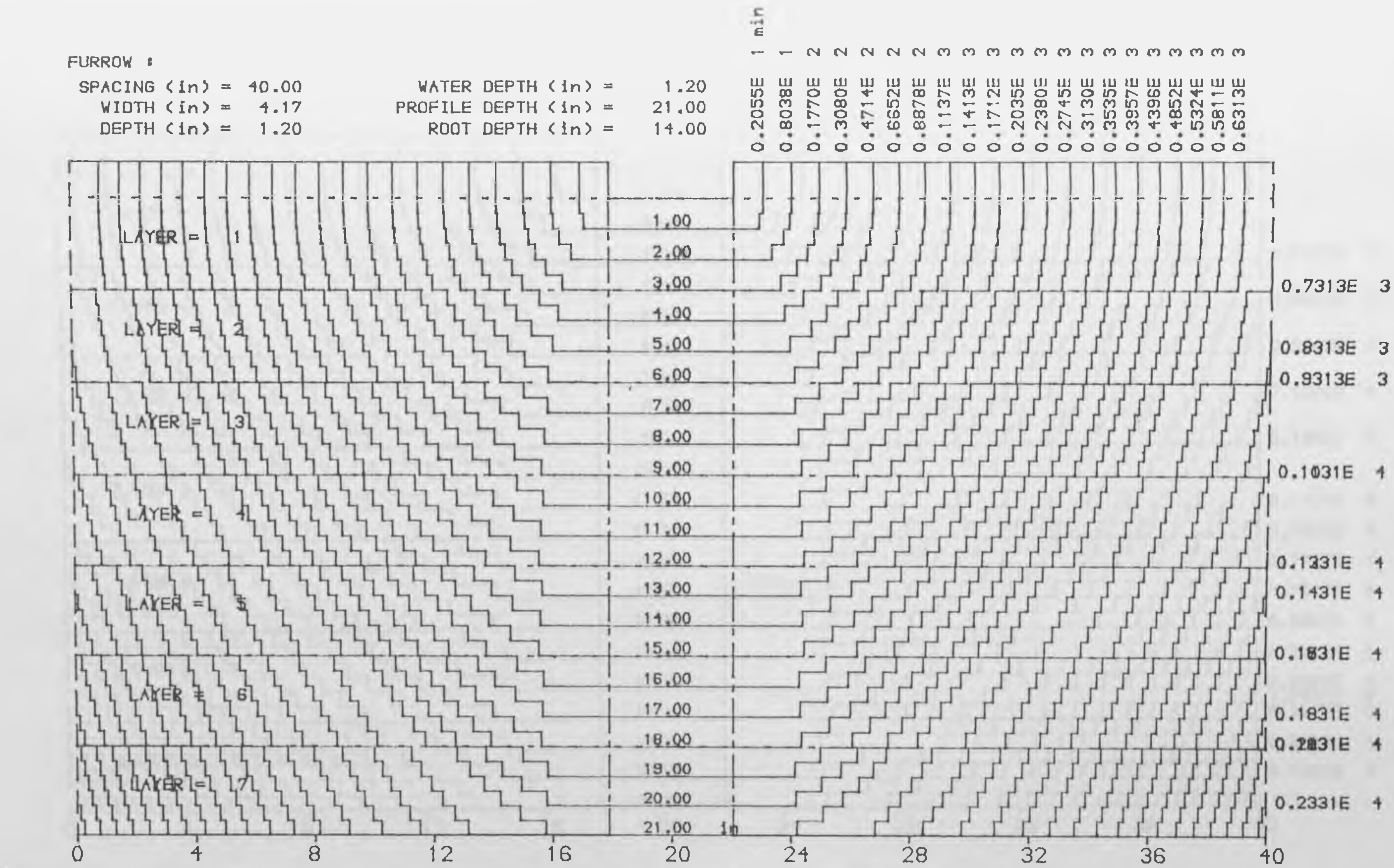

Fig. 6.20 Simulated 2-D wetting pattern for soil A, Table 6.3, under reducing horizontal Ks.

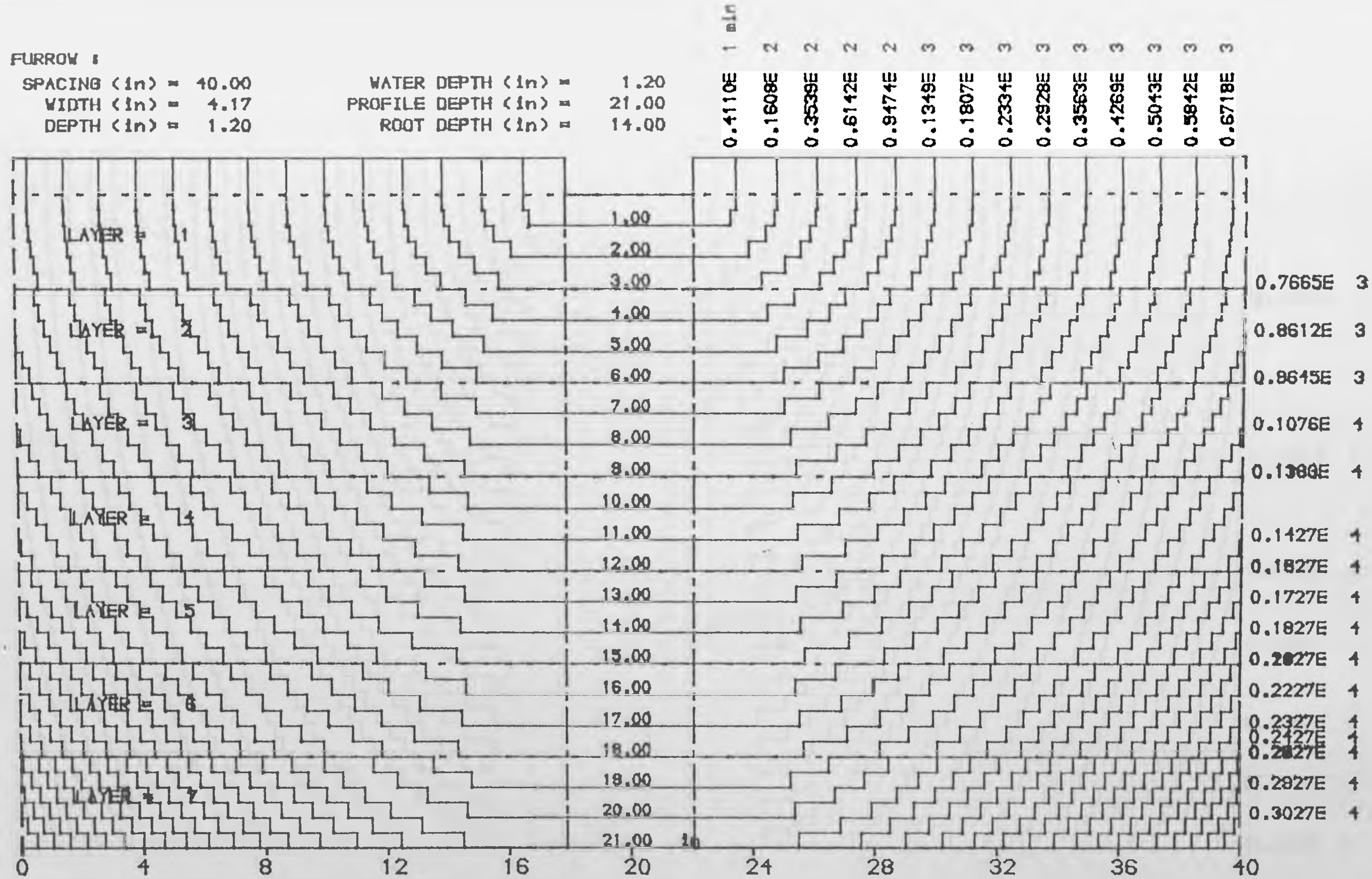

Fig. 6.21 Simulated 2-D wetting pattern for soil A, Table 6.3, with horizontal Ks > vertical Ks.

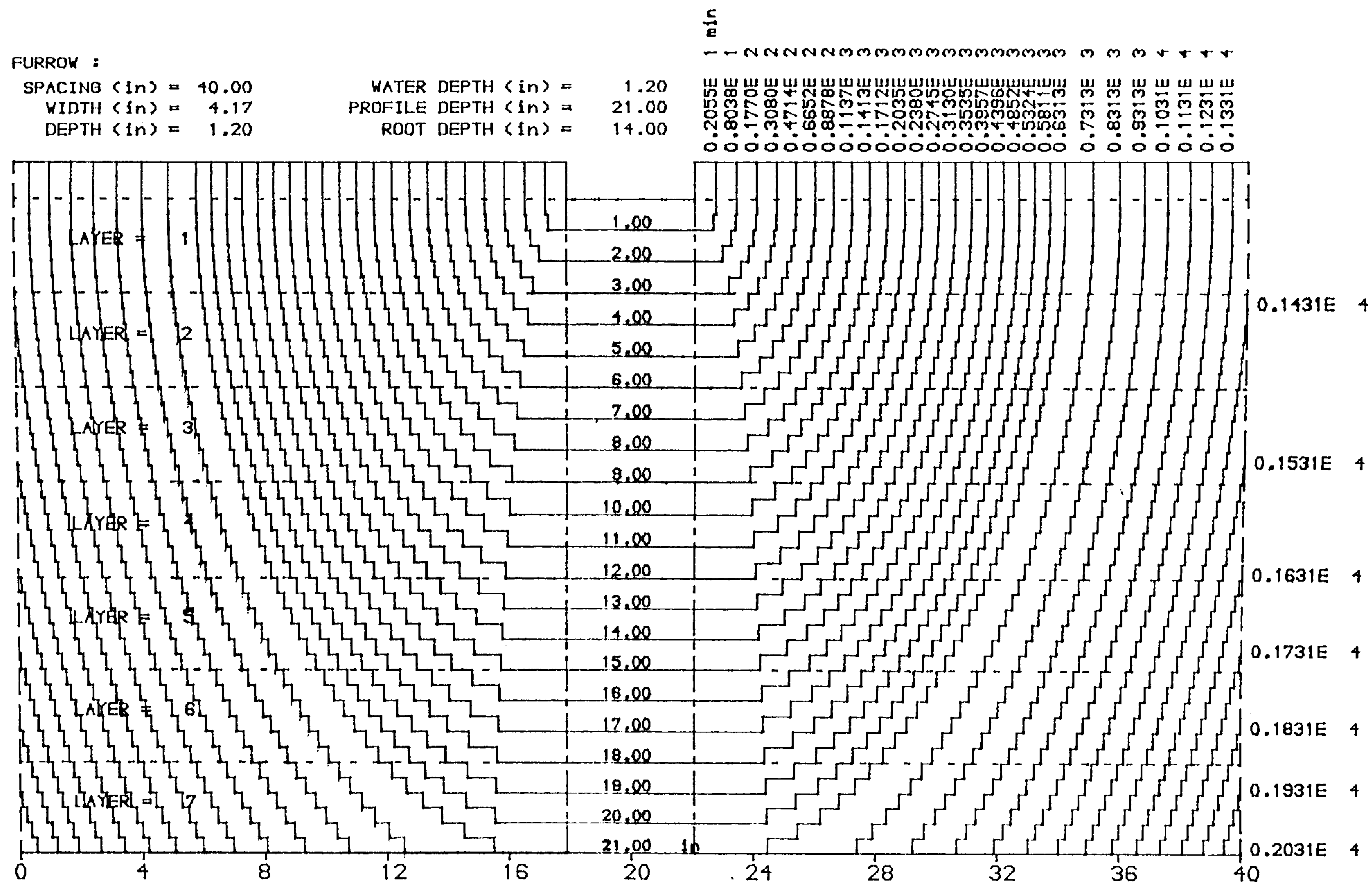

Fig. 6.22 Simulated 2-D wetting pattern for soil A, Table 6.3, with vertical Ks > horizontal Ks.

but the maximum horizontal advance distance at this time is less. The profile is completely saturated in 2031 minutes.

Case 2 - The effect of moisture nonuniformity :

To simulate the effect of moisture content nonuniformity, the profile of soil A is divided into 7 equal layers as before. All the parameters, except moisture content, are kept constant for all layers. The following moisture contents : 0.071, 0.078, 0.086, 0.094, 0.104, 0.114, 0.126 (cm3/cm3) , are assigned to the layers from top to bottom (ie: each layer increases by 10% of the previous layer). This condition simulates a soil profile of increasing moisture content with depth, as would exist in the rootzone of crops.

The wetting pattern generated from this profile is shown in Fig. 6.23 . Since the moisture content is decreasing with depth, the wetting front advances faster, both vertically and horizontally. The time to reach the bottom is 517.9 minutes, while 1018 minutes are required for the complete wetting of the profile.

Case 3 - Nonuniform and anisotropic soil profile :

This case is a combination of the decreasing layer conductivity properties of case 1 (profile 3), and the moisture contents of case 2. The wetting pattern is shown in Fig. 6.24 . Compared to Fig. 6.21, the effect of increasing moisture content with depth is

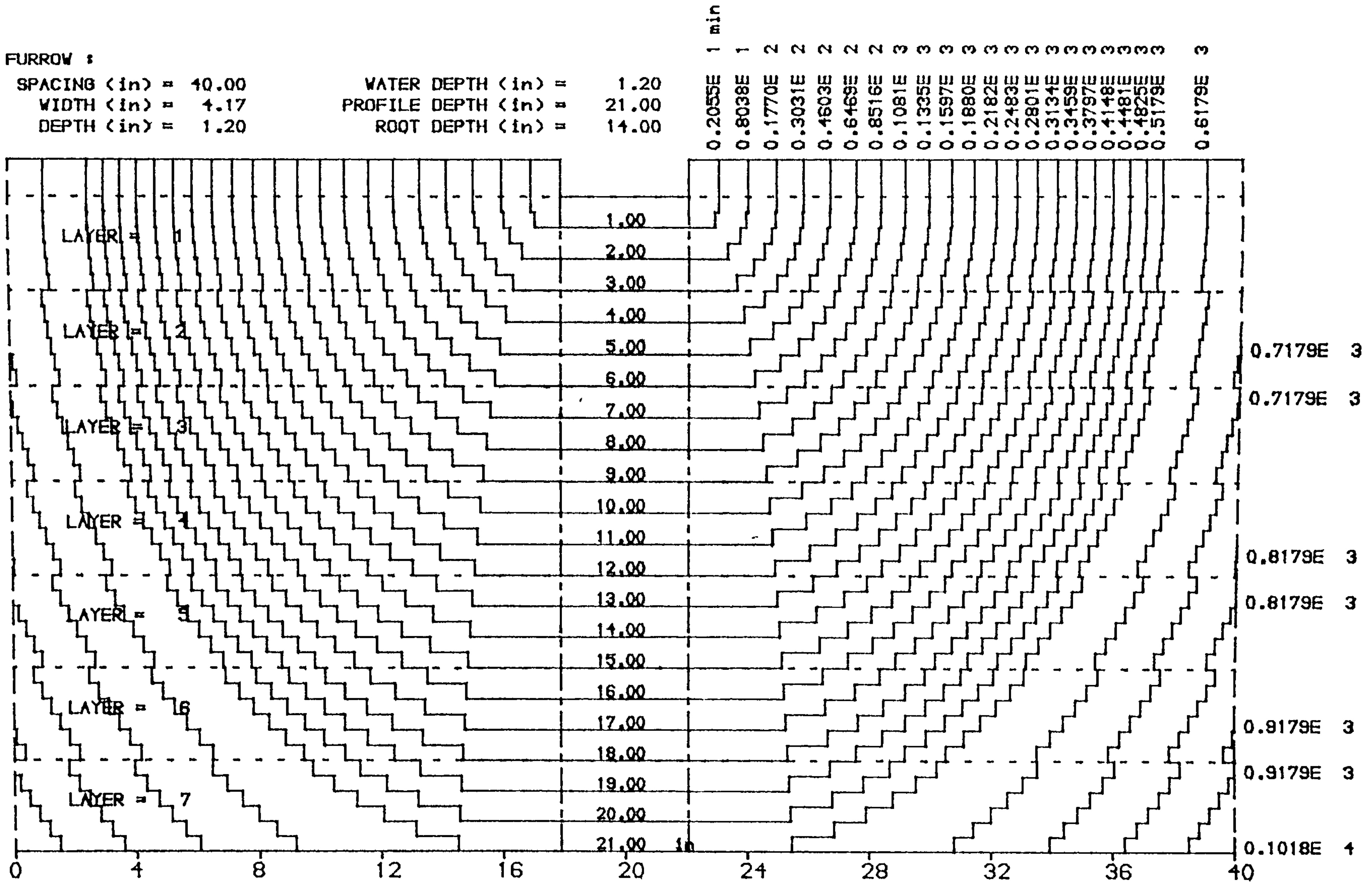

Fig. 6.23 Simulated 2-D wetting pattern for soil A, Table 6.3, with nonuniform moisture contents.

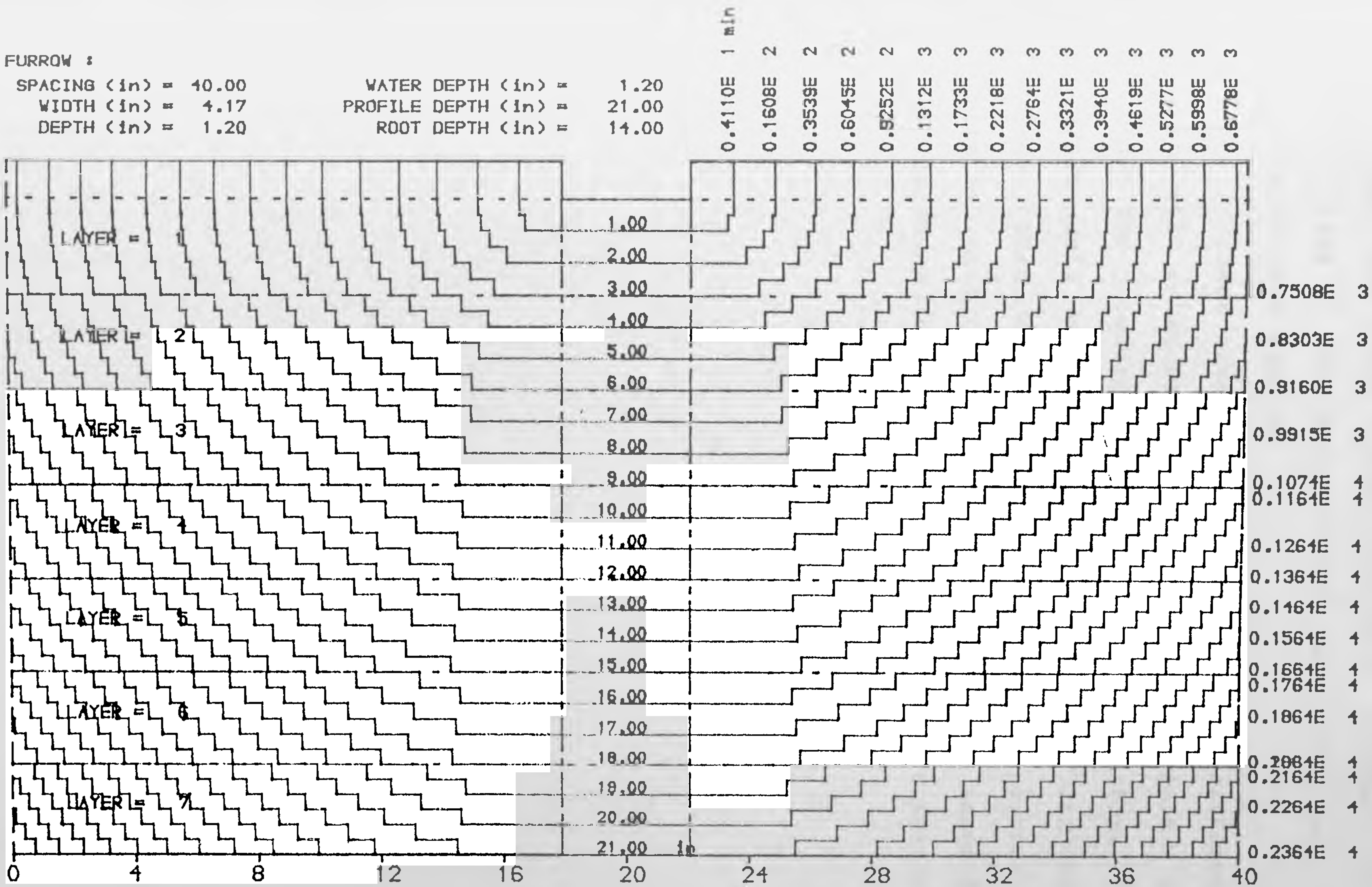

Fig. 6.24 Simulated 2-D wetting pattern for soil A, Table 6.3, with nonuniform & anisotropic profile.

that the wet front reaches the lower boundary in a faster time of 1164 minutes, and completely wets the profile in 2364 minutes.

These simulations illustrate the differences which will exist between the irrigation models that assume the rooting distribution to be uniform (ie: uniform soil moisture change with depth), and those models that assume nonuniform water extraction patterns, and incorporate the nonuniform antecedent soil moisture contents, in the infiltration function.

6.4 Chapter Summary

The process of infiltration of water into the soil is investigated in this chapter. Mathematical models are developed for one dimensional infiltration (such as from rainfall, sprinkler irrigation and border and flooding irrigation methods), and for two dimensional infiltration (such as from furrow irrigation).

The effects of nonuniform soil moisture content and saturated hydraulic conductivity on the infiltration process are simulated.

The infiltration functions form the links between the continuous root zone water balance model (chapters 3 and 4) and the event-based surface and sprinkler irrigation models.

For each successive scheduled irrigation, the parameters of the infiltration function are evaluated for that day, based on the antecedent soil moisture conditions. The subsequent respective uses of the one dimensional and two dimensional infiltration functions in the surface irrigation model (chapter 7) and the sprinkler irrigation model (chapter 8), ensure that the evaluated operational efficiencies are representative of the dynamic soil moisture conditions in the crop root zone.

CHAPTER 7 MODELLING THE OPERATIONAL EFFICIENCIES OF SURFACE IRRIGATION SYSTEMS.

7.1 Introduction :

In the introductory chapter to this thesis the need for improved irrigation efficiencies at the farm level was recognized. It was also recognized that a major reason for the inefficient use of water is the improper operational management of on-farm irrigation systems.

In surface irrigation methods water is released at one end of the field and wets the soil as it flows down the slope. The infiltration rate of the soil and the root zone soil moisture deficit determine the necessary flow rate and duration required to refill the root zone .

It was shown in chapter 6 that the infiltration rate of the soil is dependent not only on the soil properties but also on the antecedent soil moisture conditions. In the context of this study, for each scheduled irrigation, the infiltration rate of the soil is determined, based on the antecedent root zone moisture contents, using the one dimensional or the two dimensional infiltration models of chapter 6. The irrigation dates and the corresponding root zone soil moisture contents and deficits are determined by the irrigation scheduling model of chapter 3 and the dynamic water balance model of chapter 4.

Operationally, the irrigator has under his control the rate and duration of flow. He must ensure that the water is applied uniformly and with as little losses as possible. The movement and distribution of water on the field involves complex hydraulic principles. Simulation of the movement of water on an infiltrating surface will enable the irrigation manager to assess the relative qualities of various operational practices (ie: inflow rates and durations) and so choose the best operating policy .

In this chapter the processes of water flow in border and furrow irrigation methods are simulated and the distribution of the applied water on the field is modelled and various irrigation efficiencies are evaluated. The potential uses of the surface irrigation simulation model in the design and operational management of irrigation systems is also discussed.

7.2 Surface Irrigation :

Surface irrigation can be categorized into wild flooding, border, basin, corrugation and furrow methods (Hansen etal 1979). Wild flooding involves the spreading of large volumes of water, over large areas of land, during periods of high stream flow. This method is suitable for regions where water is cheap and in plentiful supply since the efficiency of application is low.

Border irrigation systems consist of long parallel earth ridges which guide the water down the strip of land between the levees. This method can be applied to a wide range of soil types, although for shallow rooted crops on sandy soils drainage losses can be high (Booher 1974).

In basin irrigation the field is divided into small, level units into which water is released in controlled quantities and retained untill it is infiltrated. The level land means that the process of water application is static, ie much of the infiltration occurs after the water advance is complete (Dedrick etal 1982).

Corrugation irrigation is described by Booher (1974) as being suitable for close-growing crops, particularly pastures, and where free movement of machinary is required. The narrow corrugations are formed, after the field has been seeded, by indenting the surface rather than forming furrows.

Furrow irrigation involves releasing water into regularly spaced small channels to allow infiltration in the lateral and vertical directions. This method requires carefull land grading for uniform application of water. One advantage of this method is that the reduced surface of open water reduces evaporation losses, although less land becomes available for cultivation (Hansen etal 1979).

A more detailed analysis of the limitations, advantages and conditions of use of the various methods described above are given by Booher (1974) and Bishop etal (1967).

Hydraulically speaking surface irrigation methods can be categorized into processes subject to one dimensional or two dimensional infiltration. Methods such as basin, wild flooding and border involve the one dimensional, vertical infiltration of water into the soil, whereas in the corrugation and furrow methods water infiltrates both laterally and vertically. In this study, the term 'border' is used to characterize the one dimensional infiltration process. The border model also applies to basin and flooding methods. Similarly the term 'furrow' applies to both furrow and corrugation irrigation methods, and is associated with the 2D infiltration process.

The hydraulic behaviour of water flow over a permeable medium is complex . The flow is a case of unsteady, nonuniform, gradually varied, free-surface open channel flow over a porous bed, with variable infiltration rate (Sherman & Singh 1978). The mathematical models are based on the Saint-Venant equations of conservation of mass and momentum (French 1986). The mass conservation equation is :

$$-\frac{\partial q}{\partial x} - f = \frac{\partial h}{\partial t} \tag{7.1}$$

and the conservation of momentum is expressed as :

$$\frac{1}{g}\frac{\partial v}{\partial t} + \frac{v}{g}\frac{\partial v}{\partial x} + \frac{\partial h}{\partial x} = So - Sf + \frac{vf}{gh} \tag{7.2}$$

where

- h = depth of water (m)
- t = time (min)
- q = flux per unit width (m/min)
- x = distance down the reach (m)
- f = infiltration rate (m/min)
- g = acceleration due to gravity (m/min2)
- v = flow velocity (m/min)
- So = bed slope (m/m)
- Sf = friction slope (m/min)

The methods of solution of the above equations are categorized into the volume-balance, fully-dynamic, kinematic, and zero-inertia models (Jaynes 1986). The volume-balance models solve the mass conservation equation from assumptions regarding the surface and sub-surface water profile shapes. Methods used in this category include algebraic models (Strelkoff 1977, Levien & de Souza 1987) and Muskingum models (Singh & HE 1988, Singh etal 1988).

The fully-dynamic models slove the complete Saint-Venant equations (Katopodes & Strelkoff 1977), but the high level of accuracy is offset by the increased computational complexity and running time. The kinematic models assume the acceleration terms and the change in water depth to be negligible in the momentum equation (Smith 1972, Sherman & Singh 1978). Zero-inertia models only assume the acceleration terms to be negligible (Strelkoff & Katopodes 1977, Rama 1982, Jaynes 1986, Walker & Skogerboe 1987).

The process of surface irrigation follows several phases (Fig. 7.1). In the advance phase water moves down the field as a sharply defined wetting front untill it reaches the downstream end. If inflow continues water will accumulate on the field, and for unblocked borders, flow out at the downstream end. This is the storage phase and lasts untill the inflow is shut off when the depletion phase begind. This phase lasts untill the depth of water at the upstream end is zero, when the recession phase begins. During this phase a recession front is formed which travels downstream untill all the water has been removed from the surface by infiltration and runoff (evaporation assumed negligible), at which time the irrigation

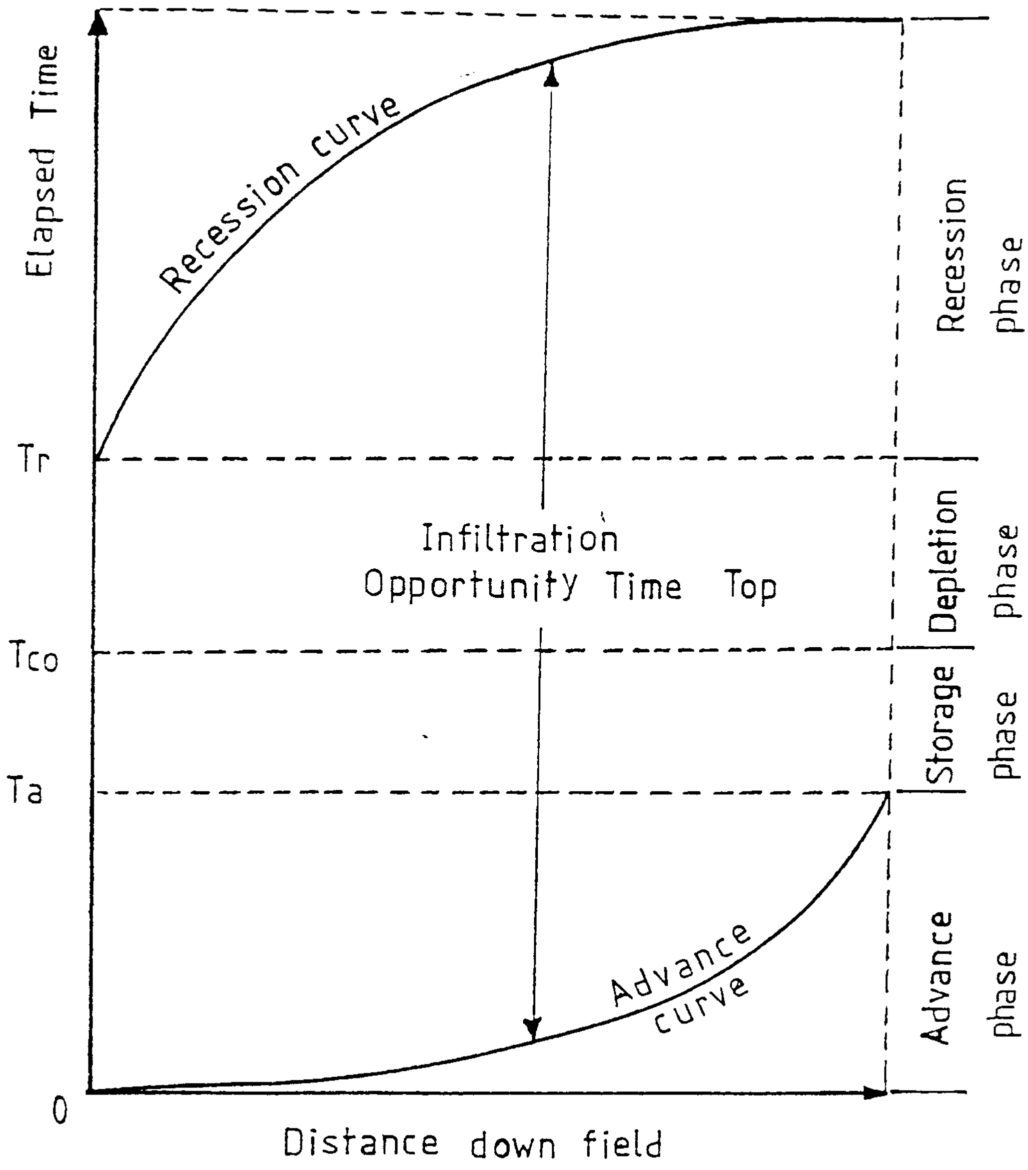

Fig. 7.1 Phases of surface irrigation flow process (Ta = advance time; Tco = irrigation cutoff time; Tr = recession time).

process is over.

Depending on the inflow cutoff time (Tco) the storage and depletion phases may not exist and if cutoff time is less than the advance time, recession will occur concurrently with advance (Sherman & Singh 1978). The differences between the advance and recession curves at any point on the field represents the infiltration opportunity time. As Sherman & Singh point out : " any influence designers have on the depth and uniformity of water application must be exerted through the control of these two curves ".

The factors which effect the shape of the advance and recession curves include the land slope, soil infiltration rate, inflow rate, irrigation cutoff time, surface roughness and field dimensions. At the design stage most of these factors can be altered to suit the design purpose. At the operational level, however, only the inflow rate and the cutoff time (irrigation duration) are directly controllable.

7.2.1 Surface Irrigation Model :

The model used here is an integrated and modified version of the algebraic border and furrow irrigation models described by Strelkoff (1977) and Levien & de Souza (1987). The model is only applicable to sloping, open-ended fields assuming uniform flow during irrigation. The two major phases of irrigation, ie: the advance and recession phases, are dealt with seperately.

A) Advance Phase :

The volume balance of flow during the advance phase can be described mathematically if the assumptions are made that flow rate is constant and at normal depth at the inlet, and that the surface and sub-surface water profiles (Fig. 7.2) are described by two shape factors. Referring to Fig. 7.2 , the volume balance equation can be written thus :

$$Q1.t = x\ (Ao\ Za + Azm\ Zb) \qquad (7.3)$$

where Q1 = inflow rate during advance phase (m3/min); t = elapsed time since inflow began (min); x = advance distance in time t (m) ; Ao = cross-sectional area of surface flow (m2); Azm = cross-sectional area of sub-surface flow (m2); Za = surface profile shape factor; Zb = sub-surface profile shape factor.

The shape factors are described by Hart etal (1968) as " the ratio of the area of pertinent storage profile to that of its cicumscribing rectangle ". Referring to Fig. 7.2, these are defined as :

$$Za = \frac{\text{Area AFCO}}{\text{Area ABCO}} \qquad (7.4)$$

and

$$Zb = \frac{\text{Area OCGE}}{\text{Area OCDE}} \qquad (7.5)$$

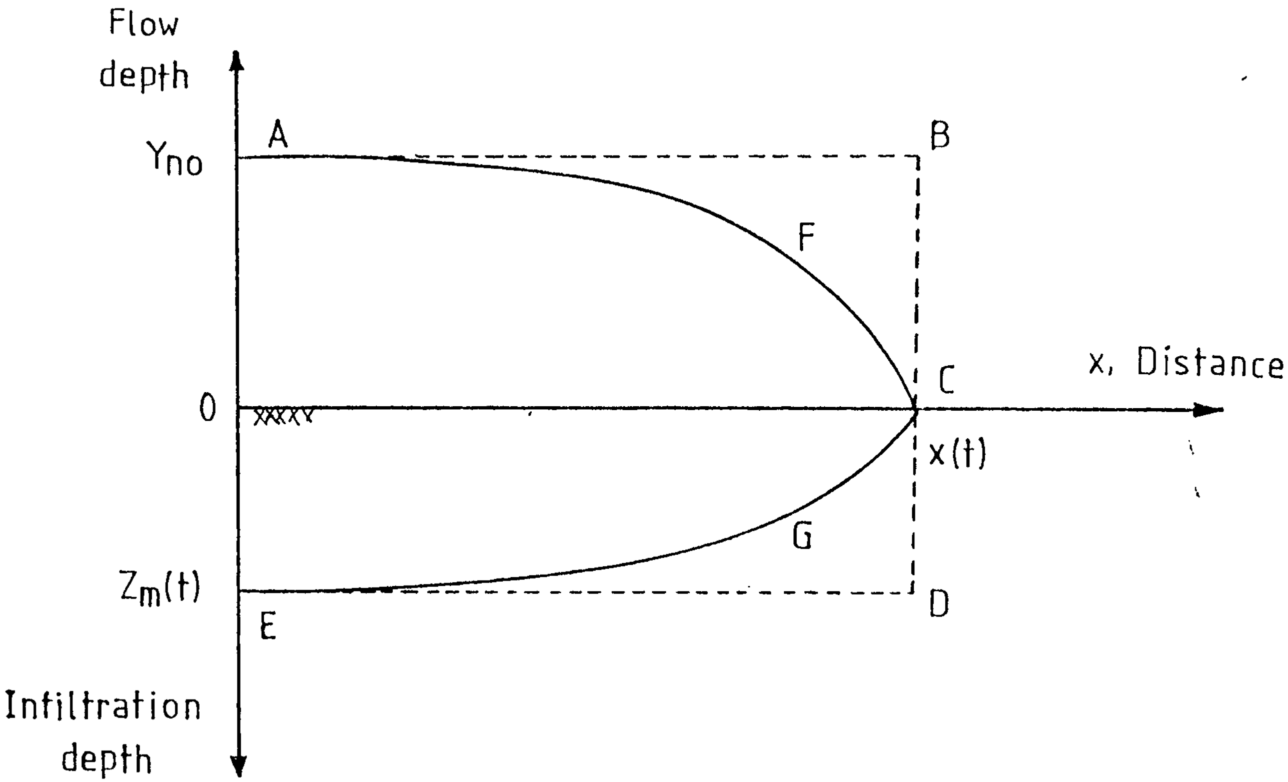

Fig. 7.2 Schematic diagram of surface and subsurface flow profiles (Yno = normal depth of flow; Zm(t) = maximum infiltration depth at time t; x(t) = advance distance at time t).

The advance curve can now be determined by solving Eqn. 7.3 for the advance distance 'x' at a known time 't' . All the other terms are known or estimated as described next.

Assuming the cross-sectional shape of the furrow is parabolic , Ao can be expressed as :

$$Ao = (B.Yno)/(M+1) \qquad (7.6)$$

where Yno = normal depth of flow (m); and the furrow cross-sectional water surface width (B, m) is given by:

$$B = C\ (Yno)^{M} \qquad (7.7)$$

where C and M are parabolic shape constants.

For border irrigation the values of C and M are 1.0 and 0.0 respectively, reducing Eqn. 7.7 to unit width and Eqn. 7.6 to an expression for the border cross-sectional area per unit width. In the following analysis the assignment of C=1.0 and M=0.0 will make the equations applicable to the case of border irrigation.

The cross-sectional area of the infiltrated water profile (Azm) is expressed as :

$$Azm = B\ .\ Zm(t) \qquad (7.8)$$

where Zm(t) is the depth of infiltration at time t (m), and is approximated by the Kostiakov equation :

$$Zm(t) = k \; t^{d} \tag{7.9}$$

where 'k' and 'd' are the infiltration constants. These two coefficients are determined for each irrigation day, using the one dimensional infiltration model for border irrigation, and the two dimensional infiltration model for furrow irrigation (see chapter 6) .

The normal depth of flow is calculated by Manning's formula :

$$Yno(Q) = \left[\frac{Q1 \; . \; n}{Cu. \;\; So^{1/2}} \; \frac{(M+1)^{5/3}}{C} \right]^{3/(3M+5)} \tag{7.10}$$

where n = Manning's roughness; So = bed slope; Cu = unit coefficient (Cu=60 [m,min], Cu=1.486 [ft,s]); C and M are the cross-sectional shape parameters (Eqn. 7.7) .

The shape factors (Za & Zb) are estimated according to the method of Singh & Chauhan (1972). The surface shape factor is given by :

$$Za = 1 - \frac{1}{\ln(t/a + 1)} + \frac{a}{t} \tag{7.11}$$

and the sub-surface shape factor by :

$$Zb = \frac{1}{\ln(t/a + 1)} \sum_{j=1}^{100} \frac{1}{(d+j)} \left(\frac{1}{1+ a/t} \right)^{j} \qquad (7.12)$$

where t = elapsed time (min); d = infiltration coefficient; and the factor 'a' is an empirical parameter found from:

$$a = \frac{(t')^{2}}{t'' - 2.0\ t'} \qquad (7.13)$$

The times t' and t'' are the times that the advance wave takes to reach two arbitrary distances x' and x'' such that x''= 2 x' . These two times (t' and t'') are found by solving the following empirical equation iteratively :

$$Q1 \,.\, t = x\ (\ 0.665\ Yno + 0.744\ Zm(t)\ ) \qquad (7.14)$$

Two iterative techniques were utilized for the solution of the above equation. These were the Newton-Raphson preocedure and the method of False Position (Cope etal 1982). During the testing of the model it was observed that when the rate of advance was very slow, both the techniques failed to converge. It was decided therefore to resort to more approximate methods of determining Za and Zb when the iterative procedures failed. These methods are described next.

Singh & Chauhan (1972) showed that Za and Zb are functions of both time (t) and infiltration coefficient (d). Fok & Bishop (1965) on the other hand, related Za only to the constant (d) by the expression :

$$Za = \frac{1}{1 + \exp(-0.6\ d)} \tag{7.15}$$

Singh & Chauhan showed this equation predicted Za values in the middle range of those of equation 7.11 for different times.

The sub-surface factor Zb is determined by the solution presented by Hart etal (1968) where :

$$Zb = \frac{1}{1 + d} \qquad \text{for} \quad t^* \ll 1.0 \tag{7.16}$$

and

$$Zb = \frac{(1-d)\ \pi d}{\sin\ \pi d} \qquad \text{for} \quad t^* \gg 1.0 \tag{7.17}$$

where

$$t^* = \frac{t}{(Yno/k)^{1/d}} \tag{7.18}$$

Singh & Chauhan suggest that up to values of d=0.55 the method of Hart etal gives similar results to Eqn. 7.12 .

B) Recession Phase :

The method used in this study to evaluate the recession curve is the algebraic model presented by Strelkoff (1977) and further developed by Levien & de Souza (1987).

The recession distance is calculated as an implicit function of recession time according to the following equation :

$$t = Tco + \frac{Sy}{(M+1)\ Ia\ G^{3/2}} \left[3.(F')^{1/3} - 3.\tan^{-1}(F')^{1/3} \right] - \left[3.(F'')^{1/3} - 3.\tan^{-1}(F'')^{1/3} \right] \qquad (7.19)$$

where

$$F' = G^{3/2} . L \qquad (7.20)$$

and

$$F'' = G^{3/2} . x' \qquad (7.21)$$

where:

- Tco = time of inflow cutoff (min).
- Sy = slope of water surface (m/m).
- Ia = average infiltration rate (m/min).
- G = a factor (see below).
- M = parabolic furrow cross-section parameter.
- L = length of field (m).
- x' = the length , from the downstream end, that is still inundated .

The water surface slope (Fig. 7.3) is given by :

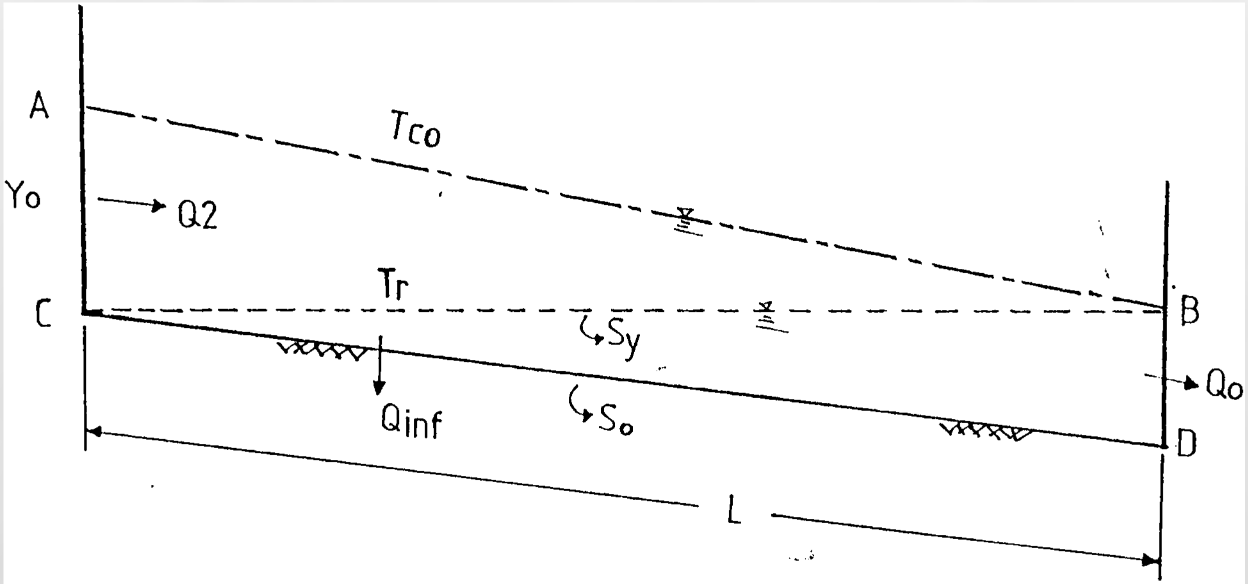

Fig. 7.3 Assumed water surface profile at cutoff and recession times (Yo = upstream depth; Q2 = upstream inflow rate; Tco = cutoff time; Tr = recession time; Qinf = infiltration rate; Qo = downstream outflow rate; Sy = water surface gradient; So = bed slope).

$$Sy = Yno(Q2) / L \qquad (7.22)$$

and the average infiltration rate is found as:

$$Ia = \frac{I(Tr) + I(Tr-Ta)}{2} \qquad (7.23)$$

where:

- Ia = average infiltration rate (average of upper and lower ends)
- Ta = time for advance wave to read end of plot.
- I(Tr) = infiltration rate at upstream end, at recession time Tr.
- I(Tr-Ta) = infiltration rate at downstream end.

Note that the infiltration rate is simply the time derivative of Eqn. 7.9 :

$$I = d\ k\ (t)^{d-1} \qquad (7.24)$$

The recession time, Tr, is calculated as the sum of the cutoff time and the time taken for volume ABC in Fig. 7.3 to be removed by infiltration and runoff. The mathematical expression is given as:

$$Tr = Tco + \frac{Ao\ L}{(M+2)\ Q2} \qquad (7.25)$$

The factor 'G' is given as :

$$G = \frac{Cu.(So)^{1/2}.(Sy)^{1/2}}{(M+1)^{5/3} . n . Ia} \qquad (7.26)$$

The recession-wave travel time, as it moves down the plot, is calculated from Eqn. 7.19.

C) Runoff prior to recession :

The runoff volume, before recession starts, Vro(Tr) , is calculated by the balance equation of inflows and outflow volumes :

$$Vro(Tr) = Vo - Vy(Tr) - Vz(Tr) \qquad (7.27)$$

where Vo is the total volume applied to the field :

$$Vo = (Q1 . Ta) + Q2 (Tco - Ta) \qquad (7.28)$$

and the volume remaining on the surface Vy(Tr) :

$$Vy(Tr) = \frac{C}{(M+1)(M+2)} Sy^{M+1} . L^{M+2} \qquad (7.29)$$

and the infiltration volume Vz(Tr) is found from :

$$Vz(Tr) = \frac{Zm(Tr) + Zm(Tr-Tl)}{2} . B. L \qquad (7.30)$$

Equation 7.28 requires that Tr > Ta , ie: the cutoff time (Tco) must be greater than the advance time (Ta). This constraint means that in the operation of the system, water must be allowed to reach the end of the plot before the supply is cut off.

D) Runoff during recession :

The runoff volume during recession Vdr(Tr) is given by :

$$Vdr(Tr) = \frac{B\ Sy}{(M+1)\ G^{3}} \left[\frac{1}{2} (F')^{2} - \frac{3}{4} (F')^{4/3} + \frac{3}{2} (F')^{2/3} - \frac{3}{2} \ln \left(1 + (F')^{2/3} \right) \right] \qquad (7.31)$$

where all the terms have been defined previously.

The results of the model, for the border irrigation method, is shown in Fig. 7.4 , for the data of Strelkoff (1977). The modified approach (model 1) is compared to the results of Strelkoff's algebraic model (model 2) and observed data. The present model underestimates the advance curve slightly but predicts the recession curve better than model 2, especially near the end of irrigation. The border irigation option was also tested with the data of Jaynes (1986). Model 2 is the result of Jaynes' zero inertia model. The present model (model 1) underestimates the advance rate but the recession curve is better predicted (Fig. 7.5). The third comparison (Fig. 7.6), also reported in Jaynes (1986), shows model 1 to slightly underestimate the advance rate but grossly underestimate the

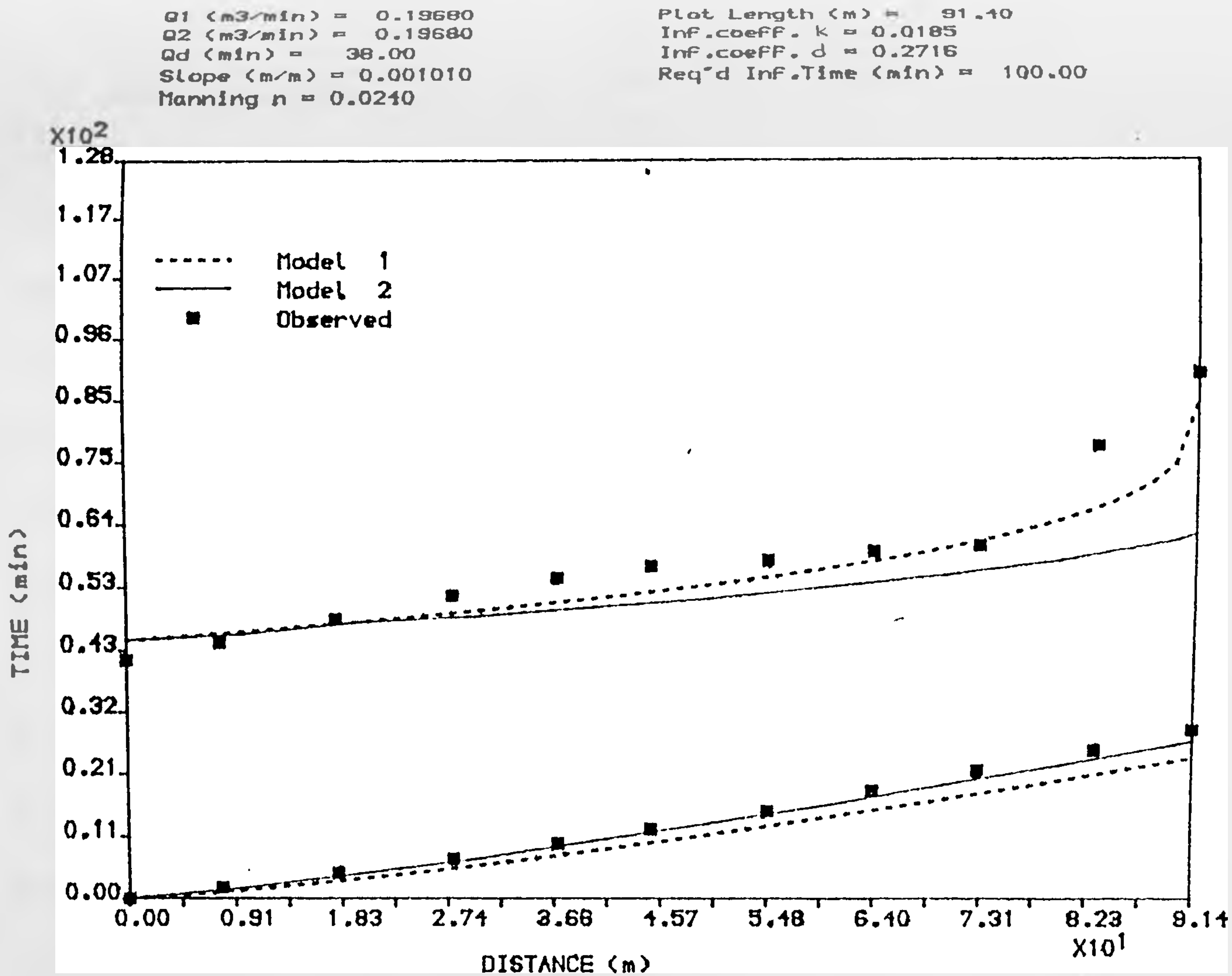

Fig. 7.4 Comparison of observed and simulated advance and recession curves for the border case of Strelkoff. (Model 1 is by present model; Model 2 is the reported Strelkoff simulation).

Q1 (m3/min) = 0.19680
Q2 (m3/min) = 0.19680
Qd (min) = 38.00
Slope (m/m) = 0.001000
Manning n = 0.0240

Plot Length (m) = 91.44
Inf.coeff. k = 0.0020
Inf.coeff. α = 0.2716
Req'd Inf.Time (min) = 100.00

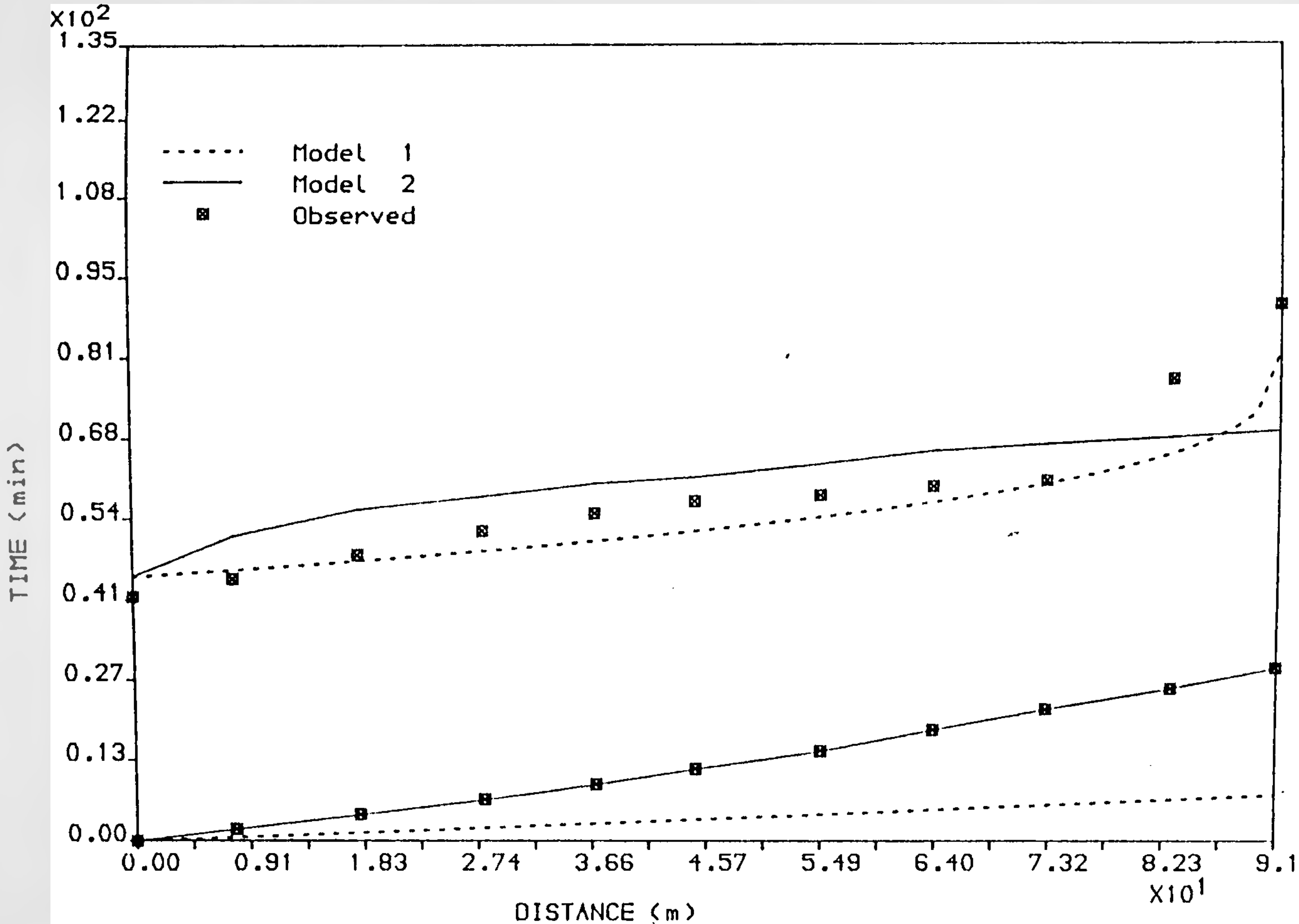

Fig. 7.5 Comparison of observed and simulated advance and recession curves for the border case of Jaynes (1). (Model 1 is by present model; Model 2 is the reported Jaynes simulation).

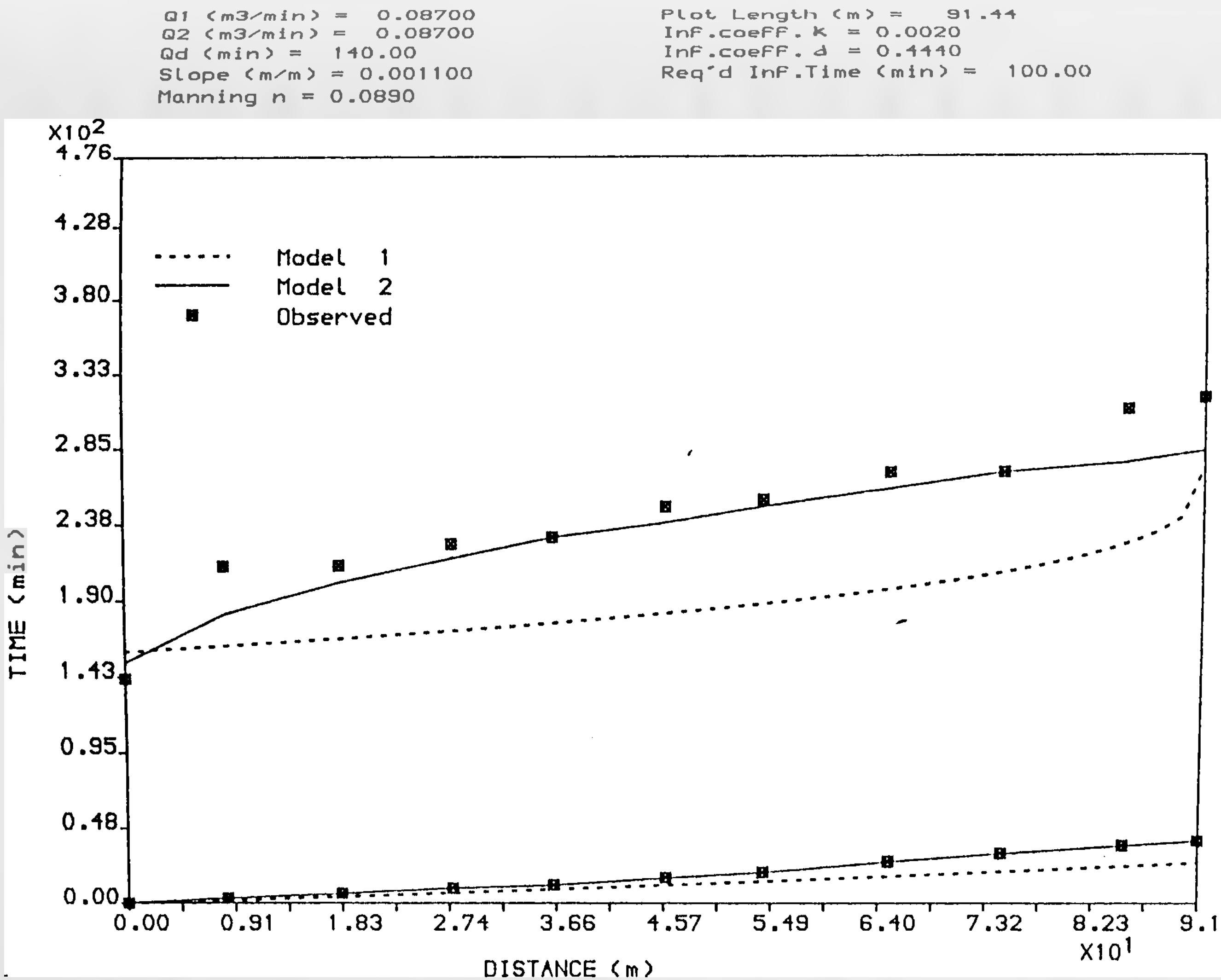

Fig. 7.6 Comparison of measured and simulated advance and recession curves for the border case of Jaynes (2). (Model 1 is by present model; Model 2 is the reported Jaynes simulation).

recession curve.

For the case of furrow irrigation, the predictive model (model 1) shows very close comparison with both the algebraic model (model 2) of Levien & de Souza (1987) and their reported observed data (Fig. 7.7).

On the whole the integrated surface irrigation model predicts the advance and recession curves well. The sensitivity of the model to variables that are prone to errors of measurement will help identify likely sources of errors in the prediction. The parameters tested for are the inflow rate, slope, Manning's roughness, infiltration coefficients (k & d), and the flow cross-section shape constants (C & M). The data set for the furrow case (Fig. 7.7) is used as the basis for the analysis. The results are shown in Figs. 7.8 to 7.14. In all cases little sensitivity is shown by the recession curve to all but the infiltration coefficient (d). The advance curve shows maximum sensitivity to the infiltration power coefficient (d) and the inflow rate.

As expected increasing the inflow rate speeds up the advance, and increasing the infiltration coefficients slows the advance. Little sensitivity is shown to changes in the slope and roughness parameters, while the furrow shape parameters effect the advance curve moderately. Increasing the parameter C increases

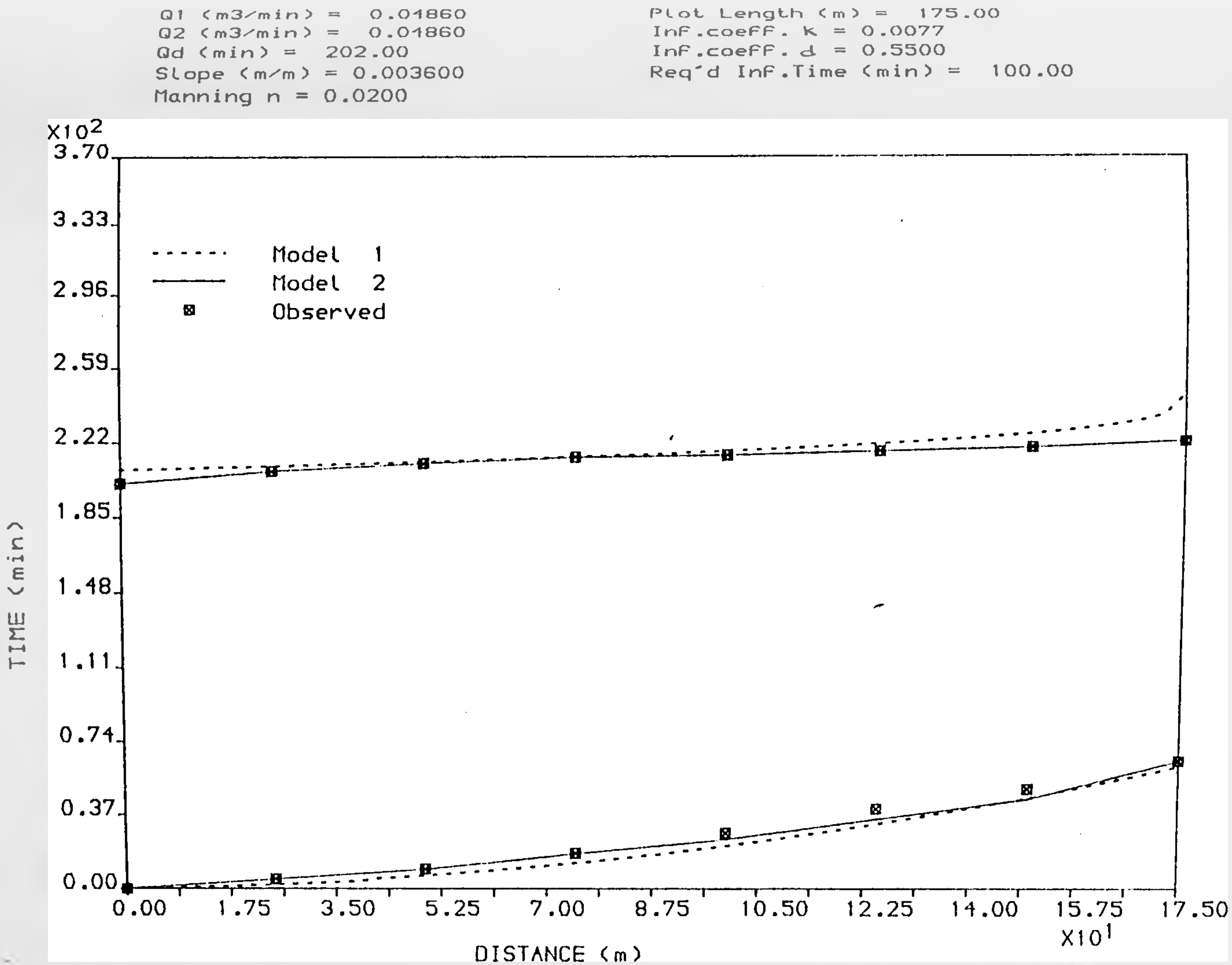

Fig. 7.7 Comparison of measured and simulated advance and recession curves for the furrow case of Levien & de Souza. (Model 1 is by present model; Model 2 is the reported Levien & de Souza simulation).

Q1 (m3/min) = 0.04860
Q2 (m3/min) = 0.04860
Qd (min) = 202.00
Slope (m/m) = 0.003600
Manning n = 0.0200

Plot Length (m) = 175.00
Inf.coeff. k = 0.0077
Inf.coeff. d = 0.5500
Req'd Inf.Time (min) = 100.00

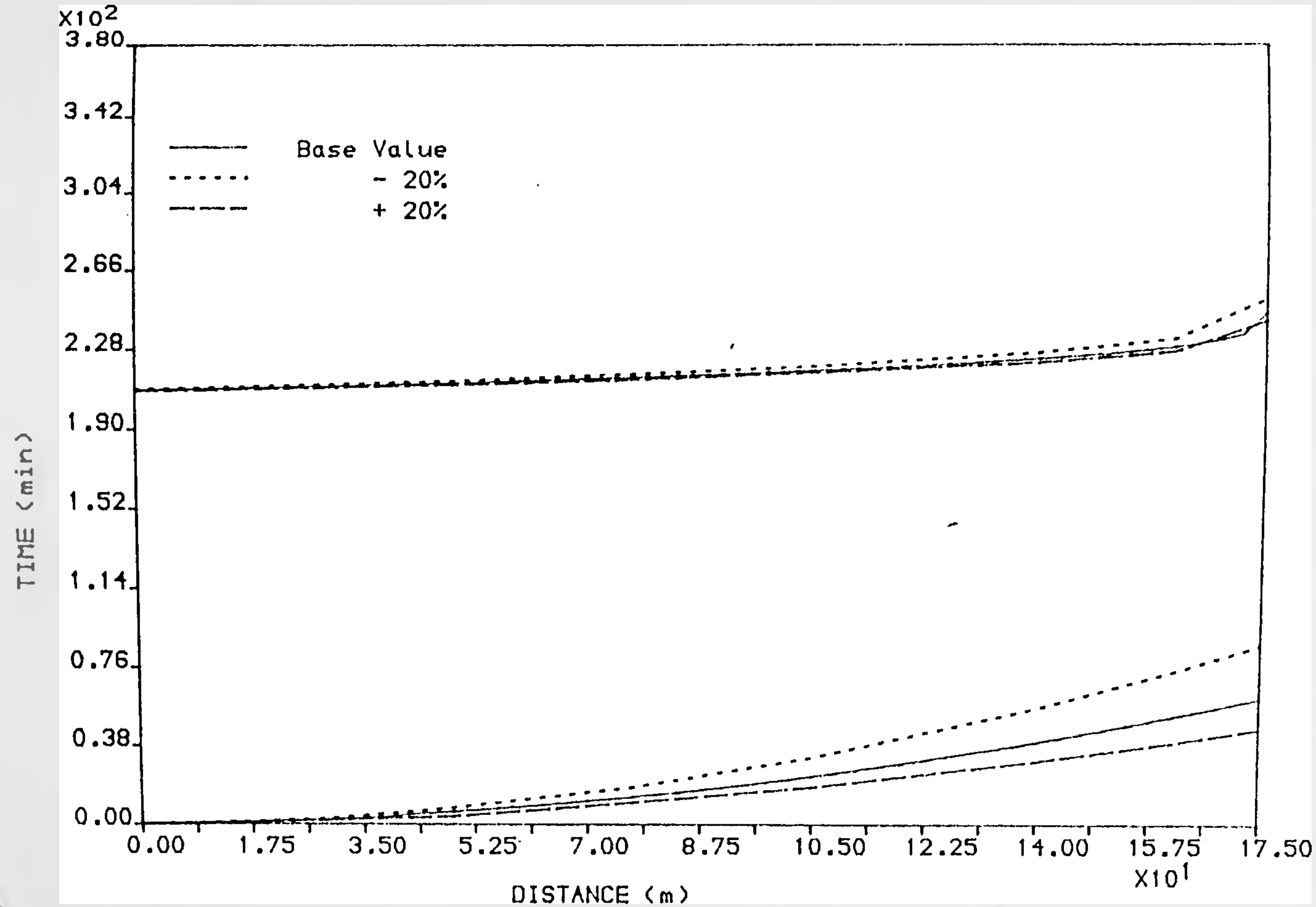

Fig. 7.8 Sensitivity of surface irrigation model to inflow rate (for data of Levien & de Souza 1987).

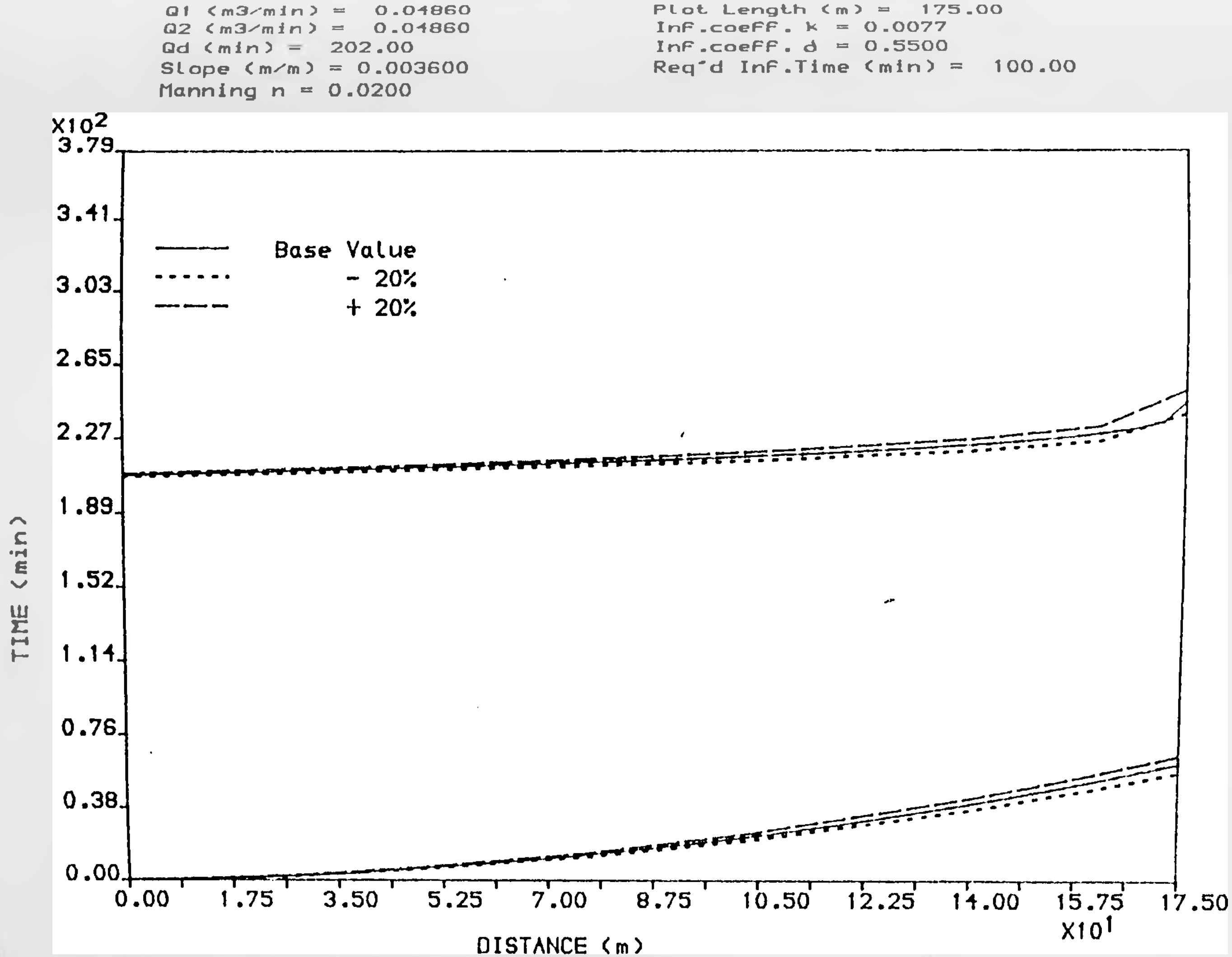

Fig. 7.9 Sensitivity of surface irrigation model to Manning's roughness (for data of Levien & de Souza 1987).

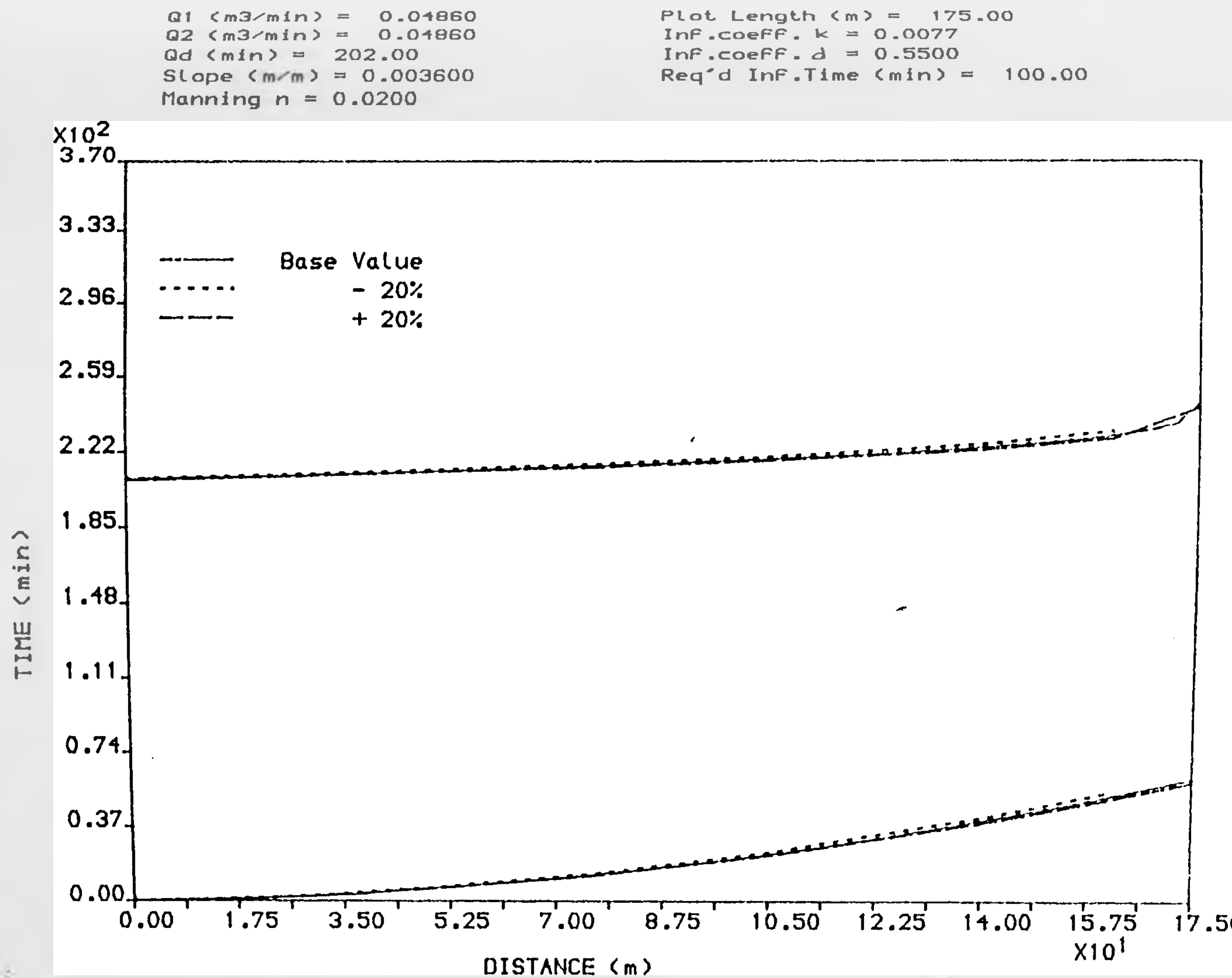

Fig. 7.10 Sensitivity of surface irrigation model to field slope (for data of Levien & de Souza 1987).

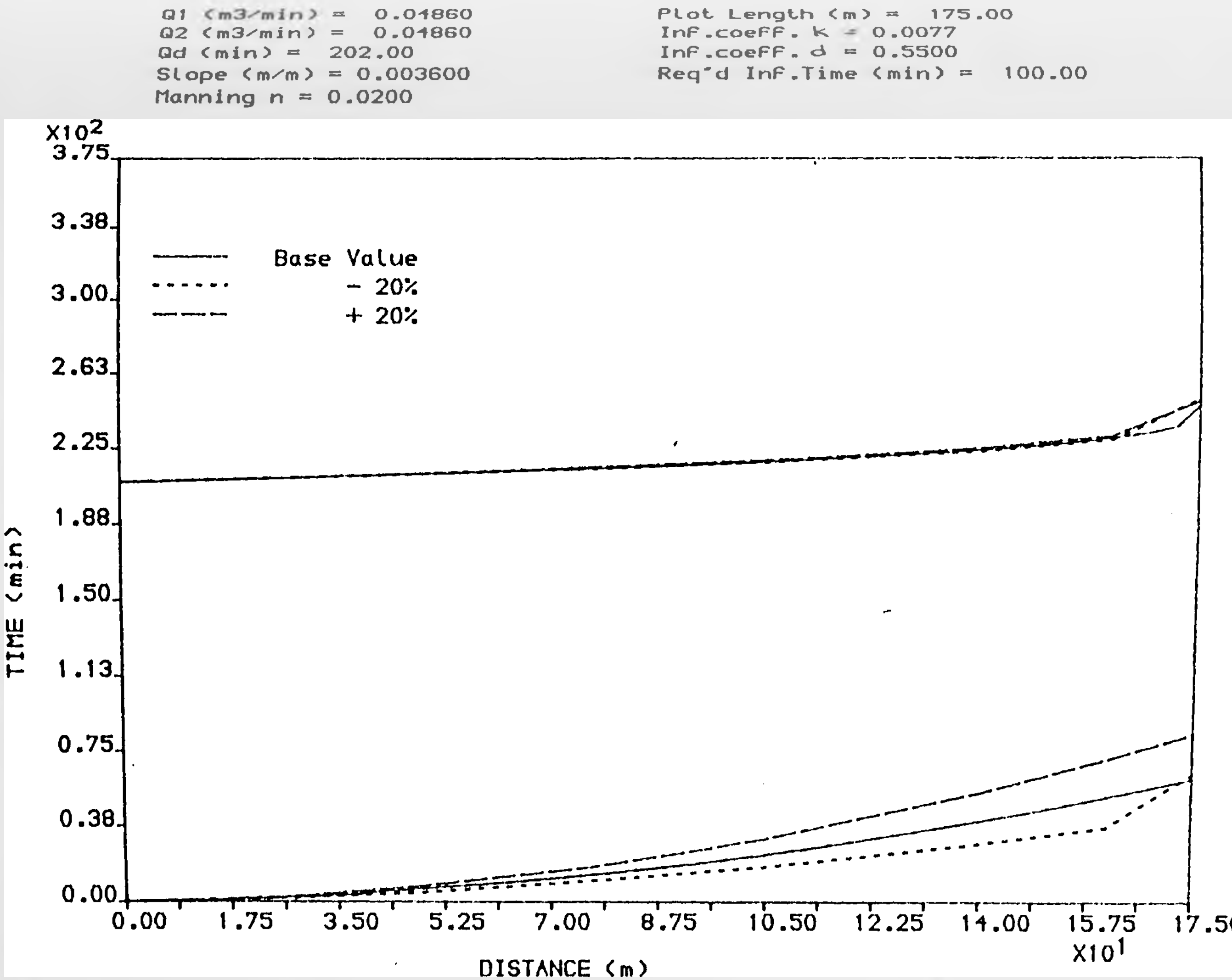

Fig. 7.11 Sensitivity of surface irrigation model to infiltration coefficient (k),(for data of Levien & de Souza 1987).

Q1 (m3/min) = 0.04860
Q2 (m3/min) = 0.04860
Qd (min) = 202.00
Slope (m/m) = 0.003600
Manning n = 0.0200

Plot Length (m) = 175.00
Inf.coeff. k = 0.0077
Inf.coeff. d = 0.5500
Req'd Inf.Time (min) = 100.00

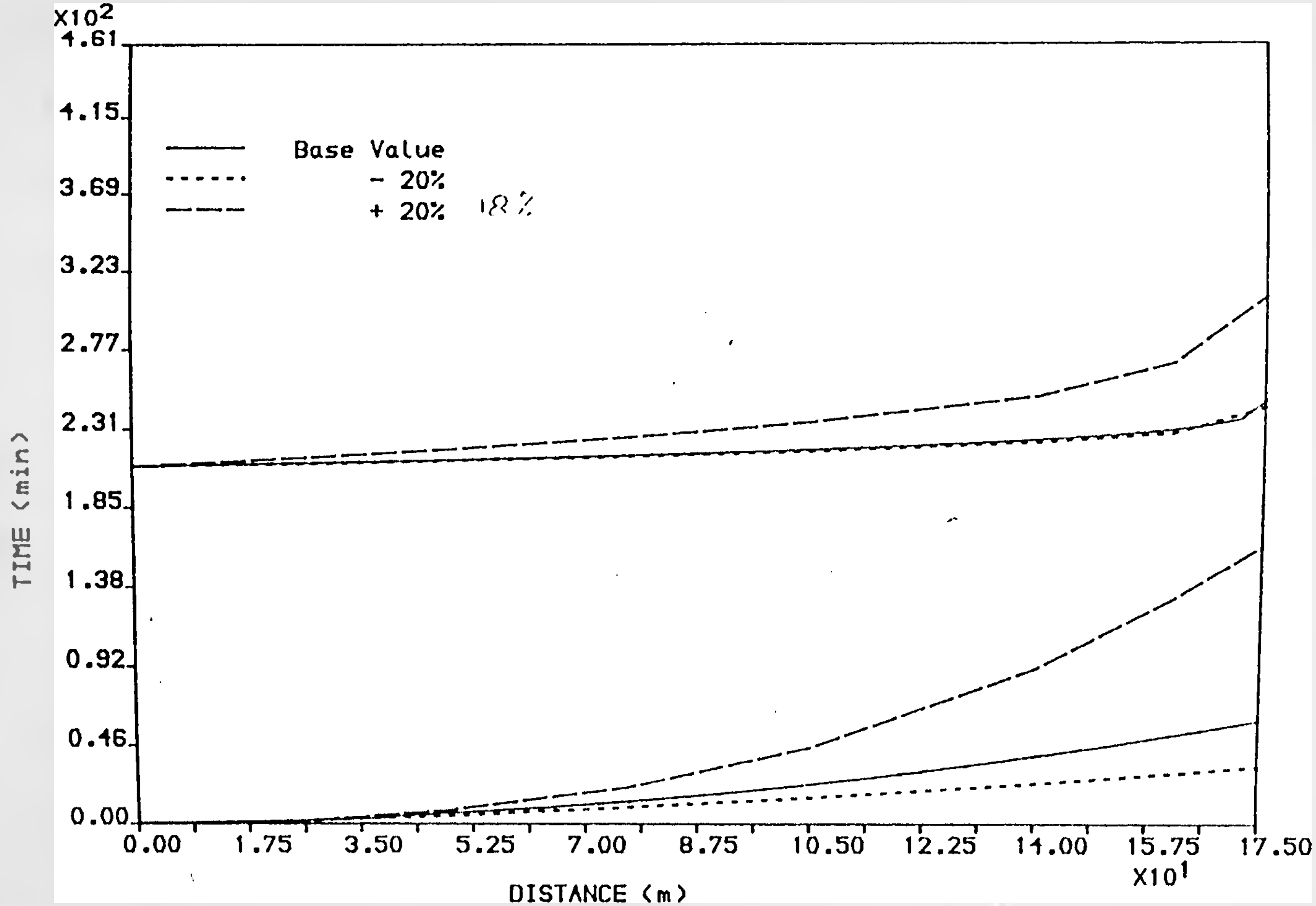

Fig. 7.12 Sensitivity of surface irrigation model to infiltration coefficient (d), (for data of Levien & de Souza 1987).

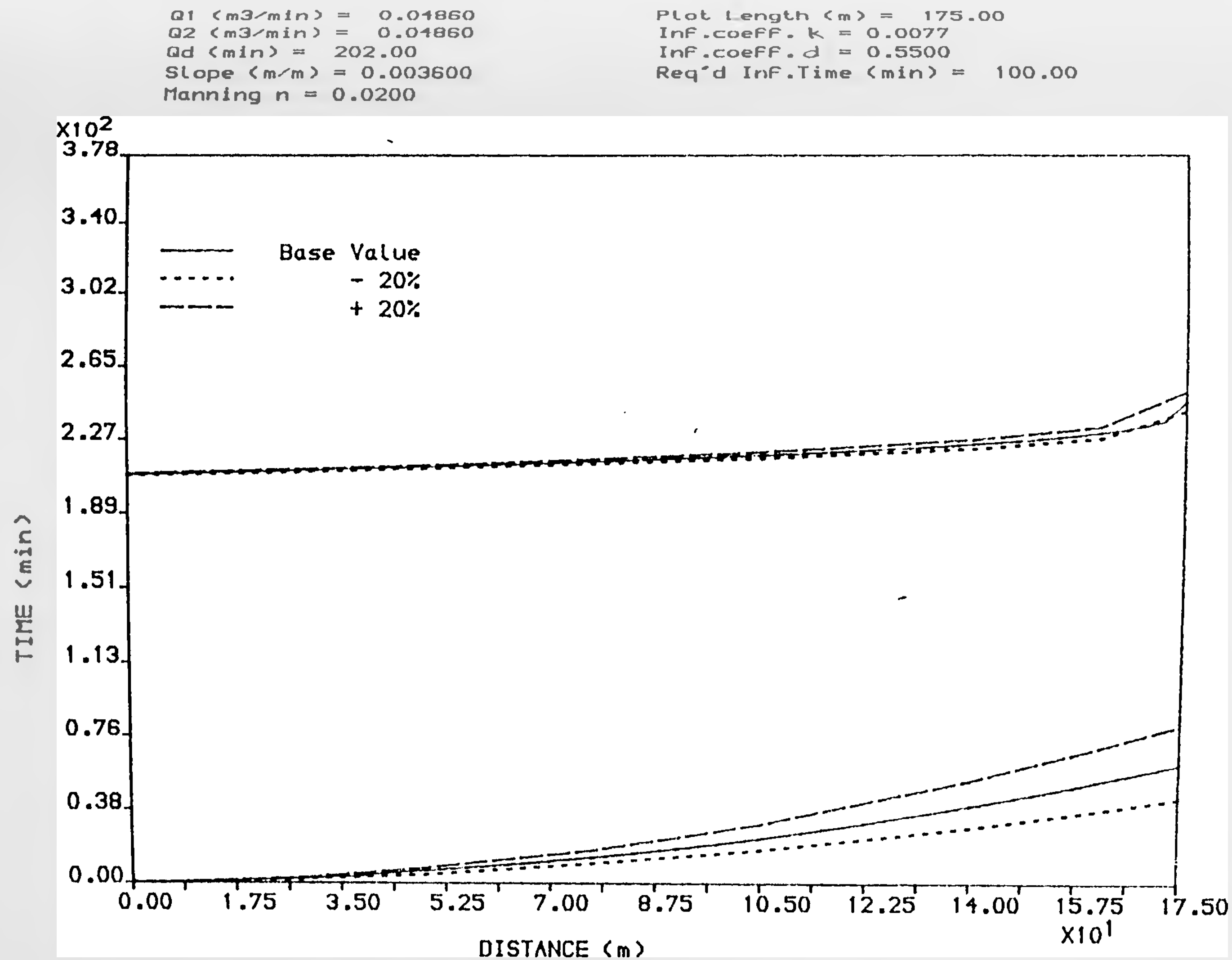

Fig. 7.13 Sensitivity of surface irrigation model to furrow shape factor (C), (for data of Levien & de Souza 1987).

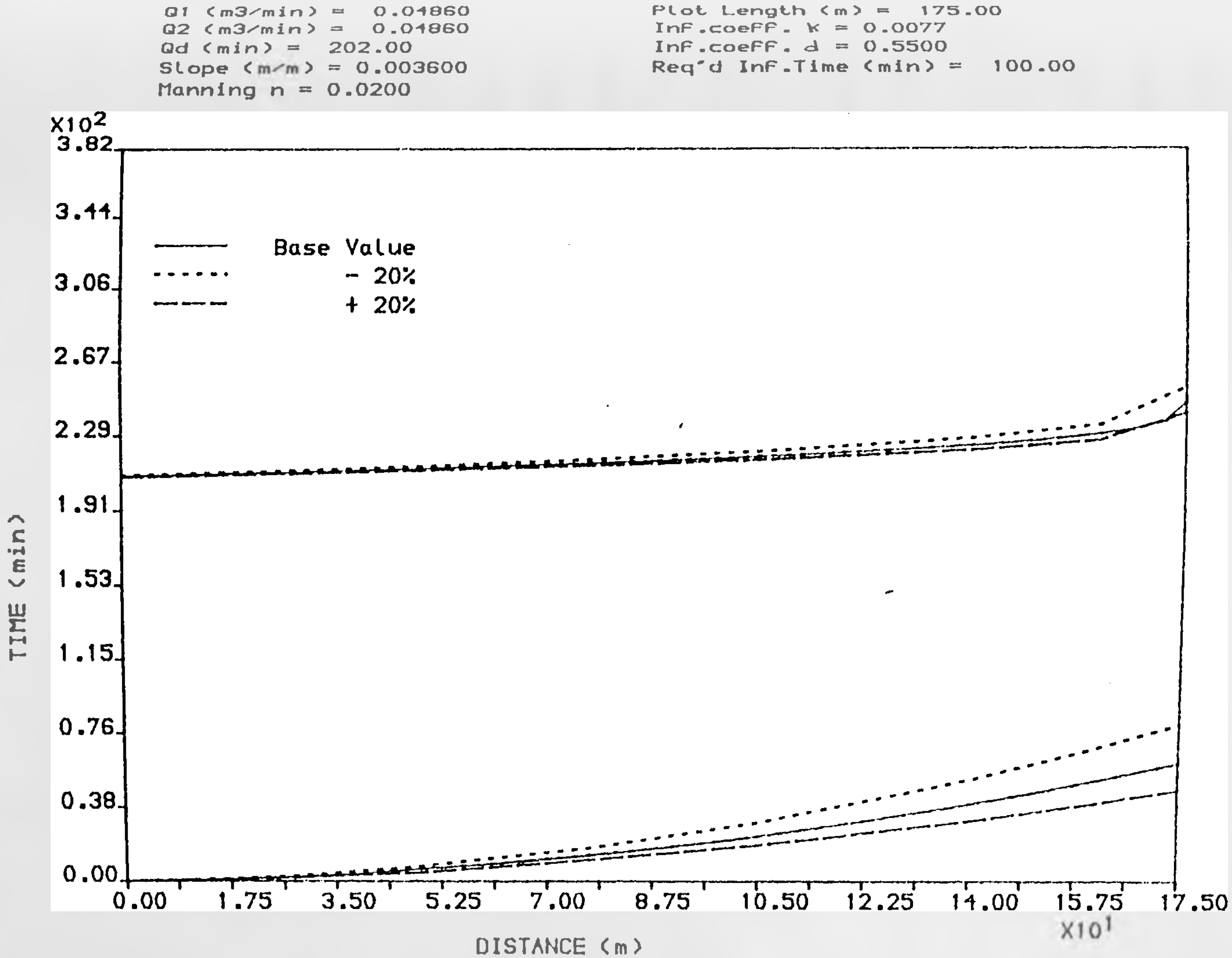

Fig. 7.14 Sensitivity of surface irrigation model to furrow shape factor (M), (for data of Levien & de Souza 1987).

the cross-sectional area of flow thus reducing the advance rate. Conversely increasing the power coefficient M reduces the cross-sectional area of the furrow, leading to more rapid advance.

A point of interest which arose out of the sensitivity analysis is that the infiltration coefficient (d) in Eqn. 7.9 , could not be increased beyond a value of 0.65 for the given inflow rate. The reason is that the calculated average infiltration rate during the recession phase exceeded the inflow rate. An infiltration parameter of d=0.65 represents a high intake rate, eg: in sandy soils. The performance of the model is therefore suspect when the infiltration rate is high and the inflow rate low.

The sensitivity of the model to the infiltration coefficients only reaffirms the need for an infiltration function which responds to changes in antecedent soil moisture conditions and irrigation practices. The surface irrigation model is used in the next section to evaluate various irrigation efficiencies for optimal operational management.

7.2.2 Surface Irrigation Efficiency Evaluation :

The concepts of efficiencies usefull to the irrigation manager were reviewed in chapter 2 . In this section the application (Ea), distribution (Ed), storage (Es) and deficit-excess (Ede) efficiencies, are determined from the advance and recession curves simulated by the surface irrigation model.

The vertical distance between the recession and advance curves represents the inundation time, or the infiltration opportunity time (Top) at any distance down the field :

$$\mathrm{Top}(x) = \mathrm{Tr}(x) - \mathrm{Ta}(x) \qquad (7.32)$$

where Tr(x) and Ta(x) are the ordinates of the recession and advance curves respectively at distance x.

For the purpose of calculating the infiltrated volumes, the length of the plot is divided into N equal reaches. Referring to Fig. 7.15 , the infiltration opportunity time for reach (j) is calculated as the average opportunity time:

$$\mathrm{Top}(j) = \frac{\mathrm{Tr}(j) + \mathrm{Tr}(j-1)}{2} - \frac{\mathrm{Ta}(j) + \mathrm{Ta}(j-1)}{2} \qquad (7.33)$$

and infiltrated volume per unit width, in reach j, is :

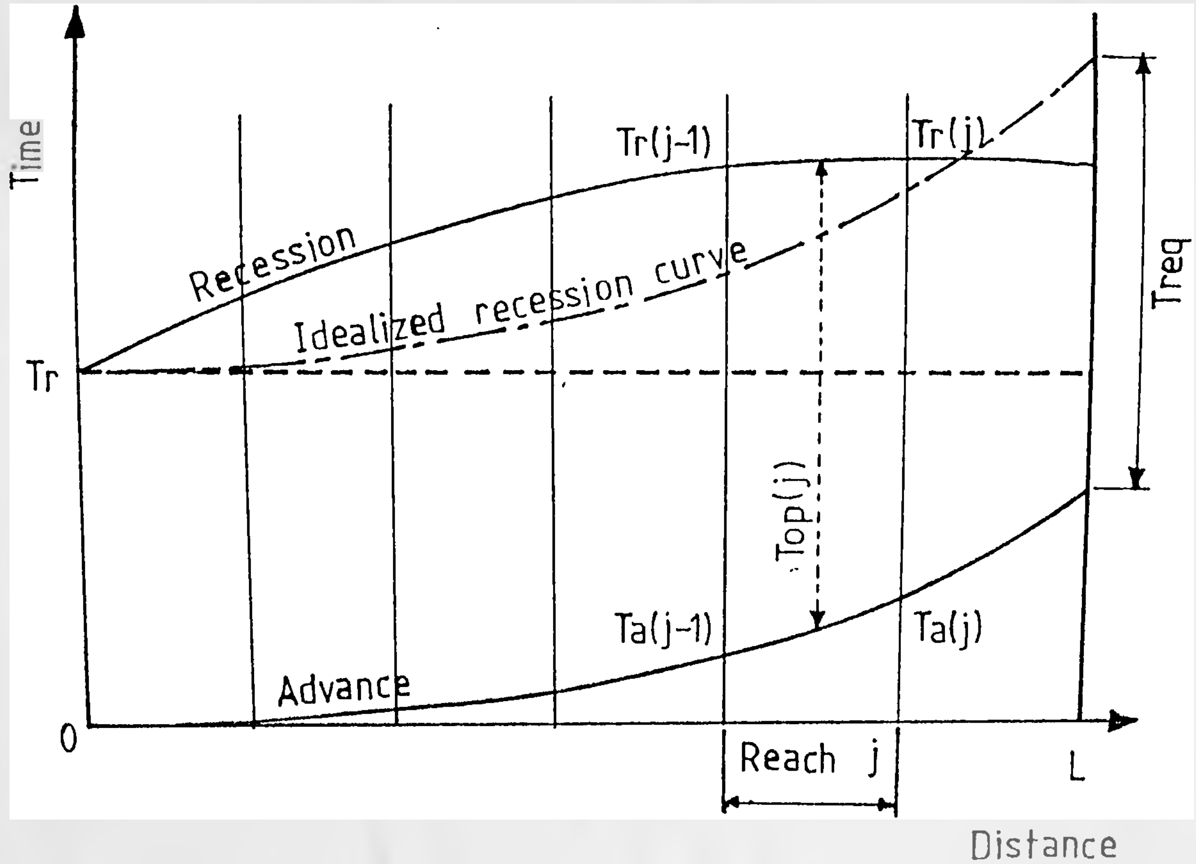

Fig. 7.15 Diagram of discretization of advance-recession curve for volume calculations (Tr = recession time, min.; Ta = advance time, min.; Treq = required inundation time ,min.; L = plot lenght, m)

$$F(j) = k\,[Top(j)]^{d} \,.\, (L/N) \tag{7.34}$$

The total infiltrated volume over the whole plot is :

$$Vz = \sum_{j=1}^{N} F(j) \tag{7.35}$$

The required irrigation volume (Freq), in any reach, is calculates by:

$$Freq = k\,(\,Treq\,)^{d} \,.\,(L/N) \tag{7.36}$$

where Treq = the required inundation time to fill the root zone moisture storage to field capacity. Treq is constant for all reaches and represents the vertical distance between the advance curve and the ideal recesion curve.

For each reach the difference, Fd(j), between the actual and required infiltration volumes is found from the following :

$$Fd(j) = F(i) - Freq \tag{7.37}$$

Where there is an excess of infiltration (ie drainage from root zone), the cumulative excess volume (Vxs) is determined by :

$$Vxs = \sum_{j=1}^{N} Fd(j) \qquad \text{for } Fd(j) > 0 \qquad (7.38)$$

and when infiltration is less than the root zone capacity, the deficit volume (Vdf) is :

$$Vdf = \sum_{j=1}^{N} Fd(j) \qquad \text{for } Fd(j) < 0 \qquad (7.39)$$

The volume infiltrated before recession starts (Vzbr) is represented by the vertical distance between the time of recession (Tr) and the advance curve. This is calculated by:

$$Vzbr = \sum_{j=1}^{N} k \left[Tr - Ta(j) \right]^{d} . (L/N) \qquad (7.40)$$

The total runoff (Vt) at the end of the irrigation is thus found from the following volume balance equation :

$$Vt = [Vo - Vy(Tr) - Vzbr] + Vdr(Tr) \qquad (7.41)$$

where Vo = total inflow volume; Vy(Tr) = volume remaining on surface at cutoff time (Eqn. 7.29); and

Vdr(Tr) = runoff volume during recession (Eqn. 7.31).

The various irrigation efficiencies can now be determined :

a) Application Efficiency (Ea) :

This is the percentage of total water that remains in the root zone , and is calculated by :

$$Ea = 100 \; (Vrz \; / \; Vo) \qquad (7.42)$$

where Vrz is the volume remaining in the root zone:

$$Vrz = Vo - Vt - Vxs \qquad (7.43)$$

b) Storage Efficiency (Es) :

This is a measure of the percentage of the roots zone that is actually filled by infiltration :

$$Es = 100 \left(1 - \frac{Vdf}{N \,.\, Freq}\right) \qquad (7.44)$$

The storage efficiency is 100% when no irrigation deficit exists.

c) Distribution Efficiency (Ed) :

This is calculated by determining the relative deviation from average infiltration throughout the length of the plot.

The average infiltration volume per reach Fave(j) is :

$$Fave(j) = Vz/N \tag{7.45}$$

where Vz is defined by Eqn. 7.39.

The deviation from average infiltration, Fdev(j) is calculated by :

$$Fdev(j) = F(j) - Fave(j) \tag{7.46}$$

Thus the sum of the volumes of deviations from average (Vdev) is the sum :

$$Vdev = \sum_{j=1}^{N} Fdev(j) \tag{7.47}$$

The distribution efficiency is now found by the following :

$$Ed = 100 \left(1 - \frac{Vdev}{Vz} \right) \tag{7.48}$$

d) Deficit-Excess Efficiency (Ede) :

This is found directly from Eqn. 2.4 as :

$$Ede = \frac{Es \, . \, Ea}{Ea + Es - (Ea.Es)} \tag{2.4}$$

Taking the data set of Strelkoff (1977) for a border irrigation plot (Fig. 7.4 and Table 7.1), the irrigation efficiencies obtained in the simulation are given in Table 7.2 .

Table 7.1 Border irrigation example used in the simulation (after Strelkoff 1977).

Inflow rate	=	0.1968	(m3/min)
Inflow duration	=	38.0	(min)
Plot slope	=	0.00101	(m/m)
Plot length	=	91.4	(m)
Manning's roughness	=	0.024	
Infiltration coef. (k)	=	0.0185	(m/min)
Infiltration coef. (d)	=	0.2716	
Req. inundation time	=	100.0	(min)

Table 7.2 Simulated efficiencies for the border irrigation data of Table 7.1.

ADVANCE PHASE INFLOW RATE		(m3/min)	=	.19680D+00
ADVANCE PHASE FLOW DURATION		(min)	=	24.0
STORAGE PHASE INFLOW RATE		(m3/min)	=	.19680D+00
STORAGE PHASE FLOW DURATION		(min)	=	14.0
TOTAL FLOW DURATION		(min)	=	38.0
TOTAL FLOW VOLUME		(m3)	=	.74784D+01
TOTAL RUNOFF VOLUME		(m3)	=	.28089D+01
APPLICATION EFFICIENCY	: Ea	(%)	=	62.44
STORAGE EFFICIENCY	: Es	(%)	=	80.04
DISTRIBUTION EFFICIENCY	: Ed	(%)	=	99.31
DEFICIT/EXCESS EFFICIENCY	: Ede	(%)	=	54.03
VOLUME BALANCE ERROR		(%)	=	0.767

7.2.3 Applications in Operational Management :

The efficiency evaluation model can be used to determine optimum operating rules for surface irrigations. Once the irrigation system is established, the only variables which are at the control of the irrigator are the inflow rate and flow duration. The objective of the irrigator may be to achieve the least wastage of water,in which case the maximum application efficiency is sought. On the other hand the irrigator may wish to ensure that the root zone is adequately filled and so the best storage efficiency is required. In cases where uniformity of crop yield is desirable, then the distribution efficiency should be maximized. The deficit-excess efficiency combines the effects of the other terms and is therefore usefull in establishing overall optimum levels of inflow rate and duration.

The irrigation efficiency optimization routine used is shown in Fig. 7.16 . Given the target efficiency, the flow rate and duration are increased from a specified minimum to a maximum value by equal increments. The combination of inflow rate and duration corresponding to the maximum value of the target efficiency (subject to certain constraints) are thus the optimum operational levels.

Several constraints operate in the optimization procedure :

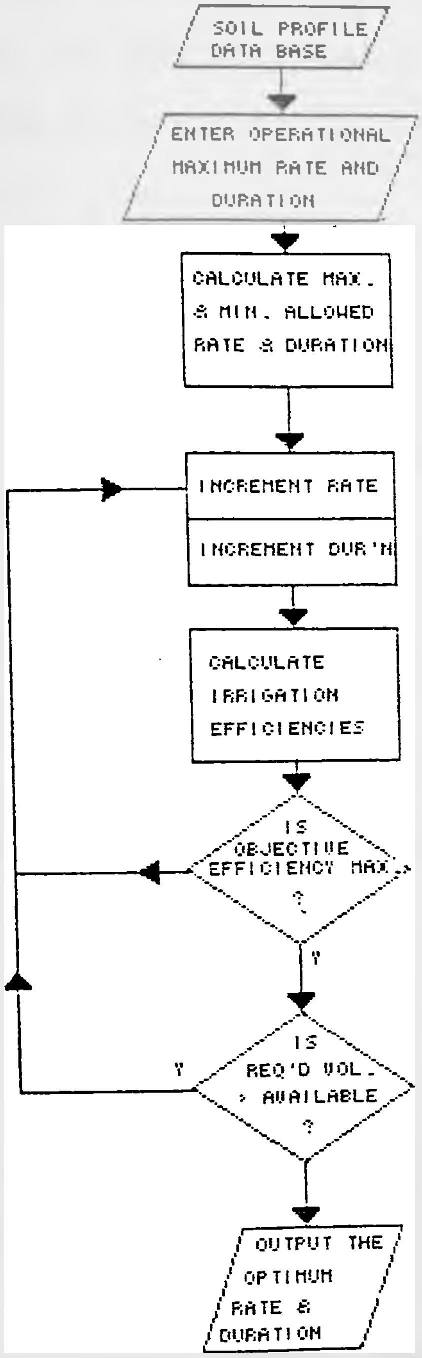

Fig. 7.16 Flow chart of surface irrigation efficiency optimization model.

A) Maximum inflow rate :

The safe maximum inflow rate to the border or furrow is determined by two factors, the physical capacity of the plot and the maximum non-erosive flow rate. The capacity flow rate is found from the Manning formula :

$$Qcap = (Ym)^{(3M+5)/3} \cdot \frac{Cu \cdot So^{1/2} \cdot C}{n \cdot (M+1)^{5/3}} \qquad (7.49)$$

where Ym = maximum allowable flow depth (m), ie: the border or furrow depth. All other terms are defined for Eqn. 7.10.

The non-erosive flow rate is determined from the empirical equation presented by Criddle (1961), cited in Booher (1974):

$$Qnero = Cu' / So \qquad (7.50)$$

where the unit constant Cu' is 3.6 for flow in m3/min and 60 for flow in l/s .

Holzapfel etal (1986) also cited other empirical equations used specifically for border irrigation. In any case the maximum inflow rate (Qmax) must not exceed either Qcap or Qnero .

B) Minimum flow rate :

Given the length of the plot and the maximum irrigation duration, the minimum flow rate that will convey water to the end of the field must be determined. This is done by reducing Qmax by specified increments and at each value the irrigation advance time (Ta) is determined. A maximum allowable advance time of 12 hours is used as the criterion for establishing the minimum flow rate (Qmin). For any given inflow duration, the inflow rate must be greater than Qmin to ensure water reaches the end of the field.

C) Minimum flow duration :

The maximum irrigation duration is often known or fixed according to operational factors such as labour availability and water delivery schedules. The minimum flow duration necessary for the flow to reach the end of the field is determined in a simillar manner to the scheme for minimum flow rate . The inflow is taken at the maximum rate and the maximum duration is reduced by increments . At each duration value the advance time (Ta) is calculated . As before a maximum allowable advance time of 12 hours is the criterion for finding the minimum flow duration.

D) Maximum flow volume :

For any combination of flow rate and duration, the total flow volume required (Vreq) is calculated according to:

$$Vreq = (Q1 \, . \, Ta) + Q2 \, (Tco - Ta) \qquad (7.51)$$

where Q1 = advance phase inflow rate (m3/min); Q2 = post-advance inflow rate (m3/min); Ta = advance time (min); Tco = irrigation duration (cutoff time), (min).

The required volume must be less than or equal to the maximum available irrigation volume (Vmax).

$$Vreq < Vmax \qquad (7.52)$$

For any flow rate and duration, if the above condition is not met, that combination is excluded from the optimization process.

An example of the model output for the data of Strelkoff (1977) for the border plot case (Table 7.1) is shown in Table 7.3 . Two options are available to the irrigator, a constant inflow rate and a variable rate. The variable rate refers to two rates, one during the advance phase and the other during the post-advance phase.

Comparison of Tables 7.2 and 7.3 shows that the optimization model improves the application efficiency from 62.44 % for the reported inflow rate and duration, to 77.16 % for the optimized constant-rate option. The duration of flow is reduced from 38 to

Table 7.3 Example of optimum border inflow rate and duration for maximum application efficiency (data of Table 7.1).

```
OPTIMIZATION PHYSICAL CONSTRAINTS :
-------------------------------------

MAX. NON-OVERTOPPING FLOW RATE (m3/min) =.25454D+02
MAX. NON-EROSIVE FLOW RATE (m3/min) =.35644D+00
MAX. DESIGN FLOW RATE (m3/min) =.35600D+00

QDMAX=  60.0(min) REQUIRES: QINMIN=.74139D-01  (m3/min)
QINMAX=.35600D+00 (m3/min) REQUIRES: QDMIN=  14.0  (min)
------------------------------------------------------------

CONSTANT RATE OPTIMIZATION :
----------------------------

APPLICATION EFFICIENCY IS OPTIMUM :

 ADVANCE PHASE INFLOW RATE  (m3/min) = .35600D+00
 ADVANCE PHASE FLOW DURATION   (min) =   13.0
 STORAGE PHASE INFLOW RATE  (m3/min) = .35600D+00
 STORAGE PHASE FLOW DURATION   (min) =    1.0
 TOTAL FLOW DURATION           (min) =   14.0
 TOTAL FLOW VOLUME              (m3) = .49840D+01
 TOTAL RUNOFF VOLUME            (m3) = .11383D+01
 APPLICATION EFFICIENCY    : Ea  (%) =  77.16
 STORAGE EFFICIENCY        : Es  (%) =  65.66
 DISTRIBUTION EFFICIENCY   : Ed  (%) =  97.40
 DEFICIT/EXCESS EFFICIENCY : Ede (%) =  54.97
 VOLUME BALANCE ERROR            (%) =   0.048
------------------------------------------------------

VARIABLE RATE OPTIMIZATION :
----------------------------

APPLICATION EFFICIENCY IS OPTIMUM :

 ADVANCE PHASE INFLOW RATE  (m3/min) = .21507D+00
 ADVANCE PHASE FLOW DURATION   (min) =   22.0
 STORAGE PHASE INFLOW RATE  (m3/min) = .74139D-01
 STORAGE PHASE FLOW DURATION   (min) =   15.0
 TOTAL FLOW DURATION           (min) =   37.0
 TOTAL FLOW VOLUME              (m3) = .57804D+01
 TOTAL RUNOFF VOLUME            (m3) = .10324D+01
 APPLICATION EFFICIENCY    : Ea  (%) =  82.14
 STORAGE EFFICIENCY        : Es  (%) =  84.77
 DISTRIBUTION EFFICIENCY   : Ed  (%) =  97.06
 DEFICIT/EXCESS EFFICIENCY : Ede (%) =  71.58
 VOLUME BALANCE ERROR            (%) =   0.048
```

Table 7.3 Continued ..

QINAD m3/min	QIN2 m3/min	DUR1 min	DUR2 min	TOTDUR min	Ea %	Es %	Ed %	Ede %	VOL.ERR %
CONSTANT FLOW RATE OPTMIZATION :									
TOTAL FLOW DURATION (min) =				14.0					
0.074	0.074	24.1	-10.1	14.0	0.00	0.00	0.00	0.00	0.767
0.215	0.215	24.1	-10.1	14.0	0.00	0.00	0.00	0.00	0.767
0.356	0.356	12.9	1.1	14.0	77.16	65.66	97.40	54.97	0.643
TOTAL FLOW DURATION (min) =				37.0					
0.074	0.074	12.9	24.1	37.0	77.16	65.66	97.40	54.97	0.643
0.215	0.215	21.6	15.4	37.0	58.46	79.63	99.24	50.86	0.635
0.356	0.356	12.9	24.1	37.0	35.69	79.89	98.91	32.74	0.136
TOTAL FLOW DURATION (min) =				60.0					
0.074	0.074	12.9	47.1	60.0	35.69	79.89	98.91	32.74	0.136
0.215	0.215	21.6	38.4	60.0	40.66	89.31	99.53	38.78	0.213
0.356	0.356	12.9	47.1	60.0	24.72	89.57	99.30	24.03	0.048
VARIABLE FLOW RATE OPTIMIZATION :									
TOTAL FLOW DURATION (min) =				14.0					
0.074	0.074	12.9	1.1	14.0	0.00	0.00	0.00	0.00	0.048
0.074	0.215	12.9	1.1	14.0	0.00	0.00	0.00	0.00	0.048
0.074	0.356	12.9	1.1	14.0	0.00	0.00	0.00	0.00	0.048
0.215	0.074	12.9	1.1	14.0	0.00	0.00	0.00	0.00	0.048
0.215	0.215	12.9	1.1	14.0	0.00	0.00	0.00	0.00	0.048
0.215	0.356	12.9	1.1	14.0	0.00	0.00	0.00	0.00	0.048
0.356	0.074	12.9	1.1	14.0	82.09	80.91	90.75	68.77	16.820
0.356	0.215	12.9	1.1	14.0	80.78	68.48	96.10	58.38	2.914
0.356	0.356	12.9	1.1	14.0	77.16	65.66	97.40	54.97	0.643
TOTAL FLOW DURATION (min) =				37.0					
0.074	0.074	12.9	24.1	37.0	77.16	65.66	97.40	54.97	0.643
0.074	0.215	12.9	24.1	37.0	77.16	65.66	97.40	54.97	0.643
0.074	0.356	12.9	24.1	37.0	77.16	65.66	97.40	54.97	0.643
0.215	0.074	21.6	15.4	37.0	82.14	84.77	97.06	71.58	4.289
0.215	0.215	21.6	15.4	37.0	58.46	79.63	99.24	50.86	0.635
0.215	0.356	21.6	15.4	37.0	45.27	78.01	99.12	40.15	0.186
0.356	0.074	12.9	24.1	37.0	76.34	85.94	96.42	67.37	3.160
0.356	0.215	12.9	24.1	37.0	48.72	81.36	98.30	43.83	0.439
0.356	0.356	12.9	24.1	37.0	35.69	79.89	98.91	32.74	0.136
TOTAL FLOW DURATION (min) =				60.0					
0.074	0.074	12.9	47.1	60.0	35.69	79.89	98.91	32.74	0.136
0.074	0.215	12.9	47.1	60.0	35.69	79.89	98.91	32.74	0.136
0.074	0.356	12.9	47.1	60.0	35.69	79.89	98.91	32.74	0.136
0.215	0.074	21.6	38.4	60.0	71.45	92.71	98.26	67.65	1.676
0.215	0.215	21.6	38.4	60.0	40.66	89.31	99.53	38.78	0.213
0.215	0.356	21.6	38.4	60.0	28.36	88.18	99.42	27.32	0.067
0.356	0.074	12.9	47.1	60.0	67.15	93.78	97.66	64.29	1.369
0.356	0.215	12.9	47.1	60.0	36.20	90.63	98.90	34.90	0.160
0.356	0.356	12.9	47.1	60.0	24.72	89.57	99.30	24.03	0.048

14 minutes. The volume of water required is reduced from 7.48 m3 to 4.98 m3. Runoff from the field is also reduced, although the storage efficiency is less in the optimized case.

For the variable-rate option, the application efficiency is improved to 82.14 % . The required irrigation is reduced to 5.78 m3 and the runof volume is reduced by about a half, but the duration of flow is virtually the same at 37 minutes. The distribution and deficit/excess efficiencies are also improved but the storage efficiency is reduced by 2 % .

Although the variable rate inflow regime offers better control over the application of water, it also requires greater labour time and expertise. Automatic flow regulators could be used but they represent high capital investments and may not be financially viable.

The efficiency optimization model shows the potential savings, both in water and in time, that can be made by carefull control of the inflow rate and duration.

The variations of application efficiency with flow rate and duration, for the above example, is shown in Figs. 7.17 to 7.21 . Application efficiency reduces with increased inflow rate and decreased flow duration. This is expected since extra wastage occurs due to runoff and deep percolation.

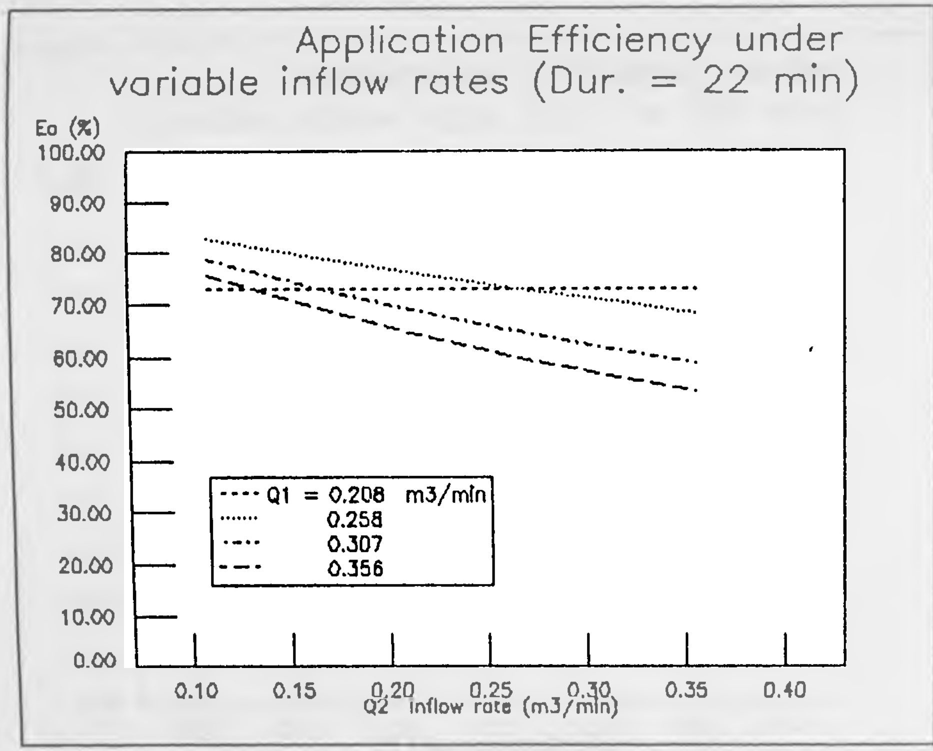

Fig. 7.17 Simulated response of application efficiency (Ea) to inflow rate under constant duration of 22 mins.

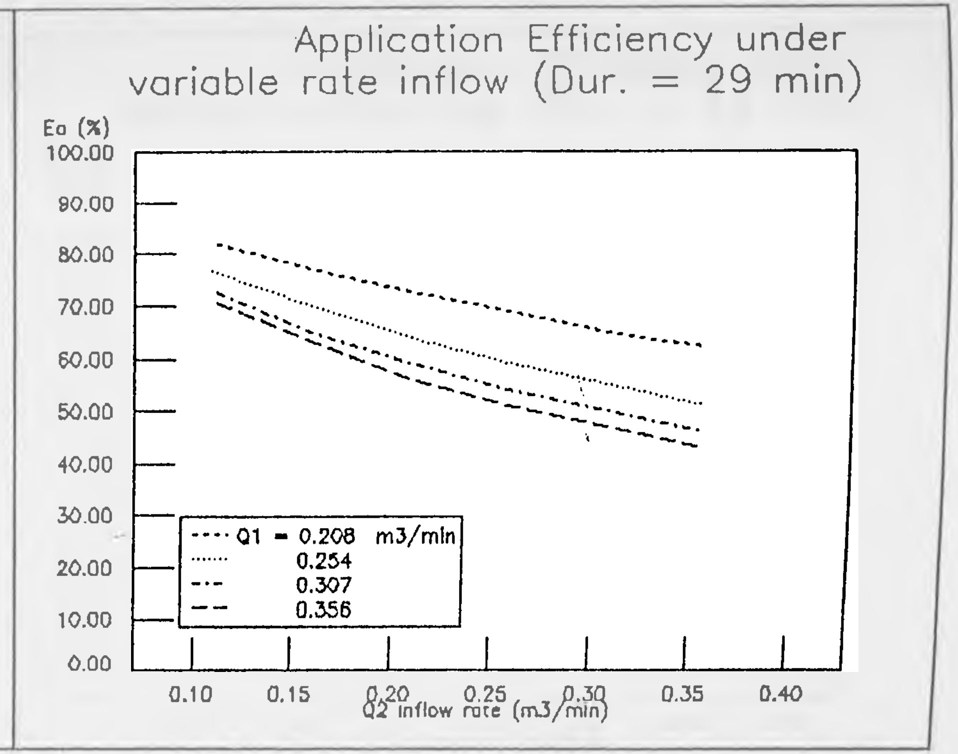

Fig. 7.18 Simulated response of application efficiency (Ea) to inflow rate under constant duration of 29 mins.

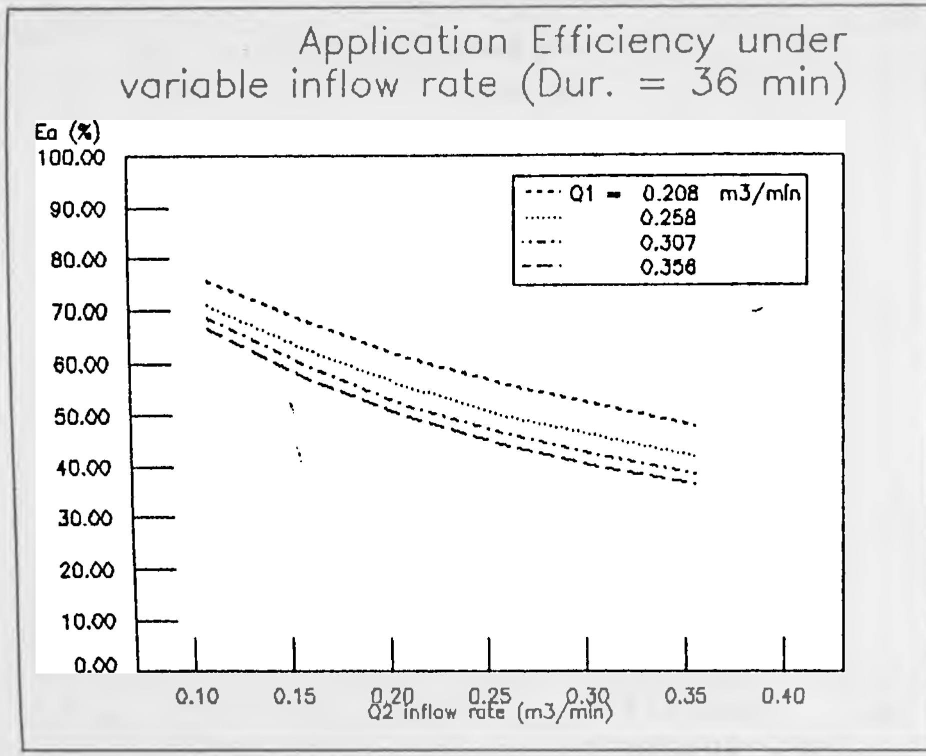

Fig. 7.19 Simulated response of application efficiency (Ea) to inflow rate under constant duration of 36 mins.

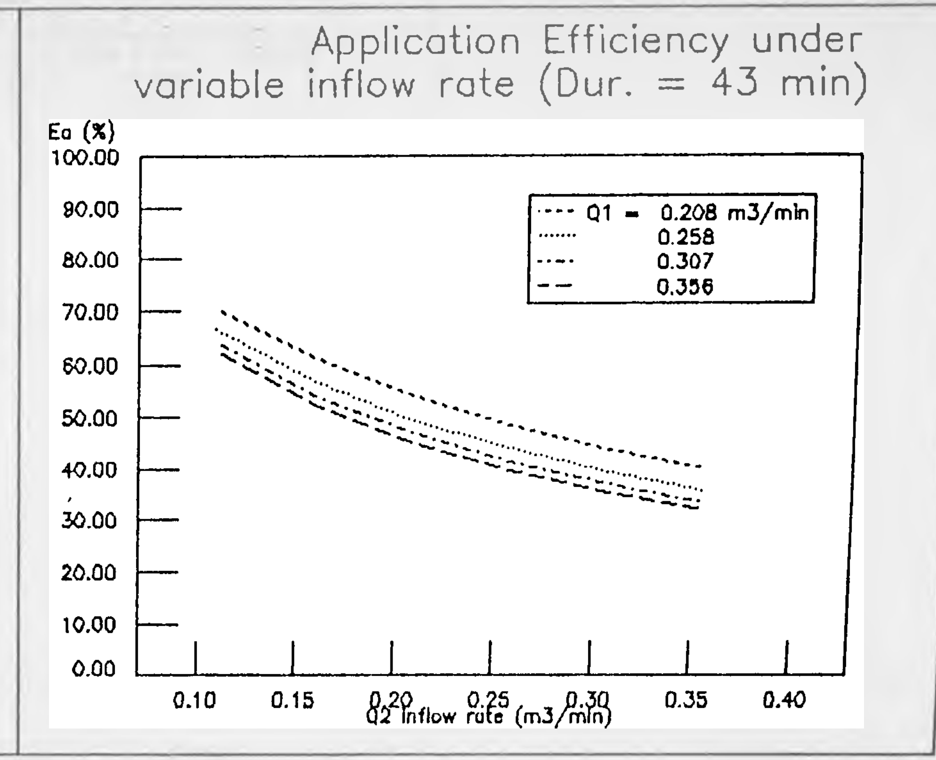

Fig. 7.20 Simulated response of application efficiency (Ea) to inflow rate under constant duration of 43 mins.

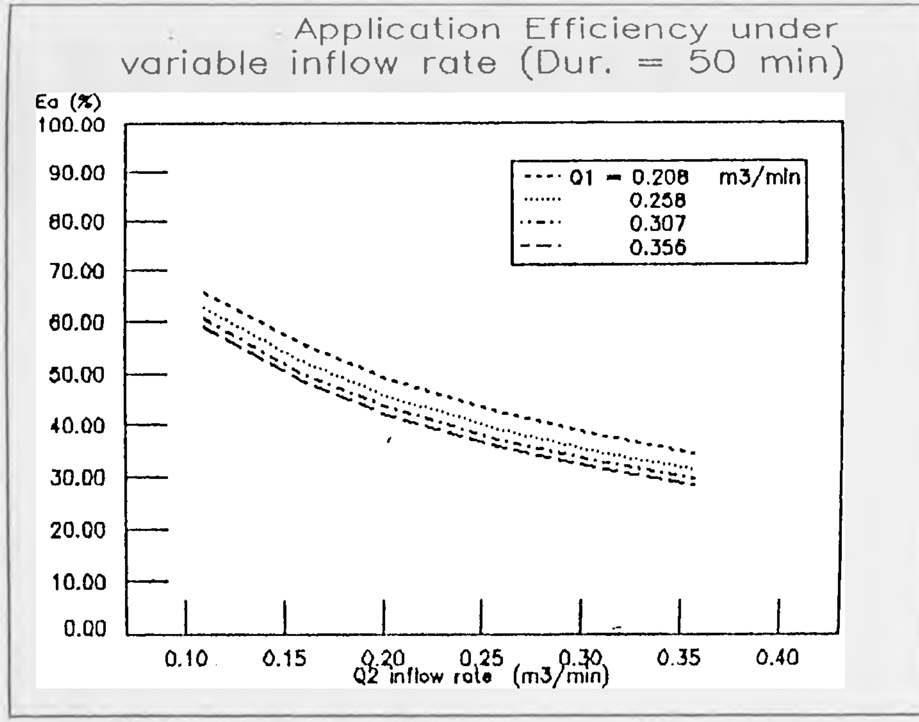

Fig. 7.21 Simulated response of application efficiency (Ea) to inflow rate under constant duration of 50 mins.

7.2.4 Applications in system design :

The surface irrigation simulation model can be used to establish design criteria for border and furrow irrigation systems. Factors which influence the design of surface irrigation systems, such as soil type, crop rooting depth, field geometry and water availability, are all incorporated into the design models.

7.2.4.1 Design of Borders :

In designing border plots the objective is to determine the maximum length and width of border which can be irrigated with a limited volume of water. In border irrigation there is a minimum required width which is dependent on the width of machinary used on the farm (Booher 1974). The maximum available irrigation volume per day is also normally fixed by either a delivery quota or the limits of the resource.

The system is designed for the condition of maximum soil moisture depletion from the root zone. The physical properties of the soil profile, the maximum rooting depth and the maximum allowable soil moisture deficit, are used to establish root zone soil moisture conditions for which the infiltration coefficients are determined. The antecedent moisture content of each root layer is calculated according to :

$$SMC(j) = SWFC(j) - \frac{AWM \cdot SMDMAX}{100} \tag{7.53}$$

where SMC(j) = moisture content in layer j (cm3/cm3); SWFC(j) = field capacity (cm3/cm3); AWM = maximum available moisture (field capacity minus wilting point), (cm3/cm3); and SMDMAX = maximum allowable soil moisture deficit (%).

The maximum irrigation duration (Tmax, minutes) is calculated by:

$$Tmax = \frac{Vmax}{Q1 \cdot Wmin} \tag{7.54}$$

where Vmax = maximum available irrigation volume (m3); Q1= inflow rate (m3/min); and Wmin = minimum required border width (m).

Two upper limits on the length are considered. The first limit is the border length (Lmax, meters) and is determined according to the volume balance equation:

$$Lmax = \frac{Vmax}{Wmin \cdot Zreq} \tag{7.55}$$

where Zreq = required irrigation depth to fill the root zone (m).

The second upper limit to length (L'max, meters) is dependent on the inflow rate and duration (Q1 and Tmax), and a maximum advance time is used as a criterion for design. The procedure (see flowchart in

Fig. 7.22), consists of increasing the border length from an initial size of 1.0 meter, by pre-specified increments. At each length the advance time is calculated by the surface irrigation model (subject to the same operating constraints as in section 7.2.3). The criteria for the maximum length are that the irrigation advance time must not exceed 12 hours and that the calculated required volume must not exceed that available.

The design length (Ld) is thus the minimum of two upper limits : the advance-time dependent limit (Lmax), and the total-volume dependent limit (L'max). If Ld = Lmax , the border width will be at its minimum value. If on the other hand the length is fixed by L'max, then maximum border width (Wmax) is calculated as :

$$Wmax = \frac{Vmax}{Ld \; . \; Zreq} \qquad (7.56)$$

The minimum required flow duration (Tmin) can now be calculated as :

$$Tmin = \frac{Vmax}{Q1 \; . \; Wmax} \qquad (7.57)$$

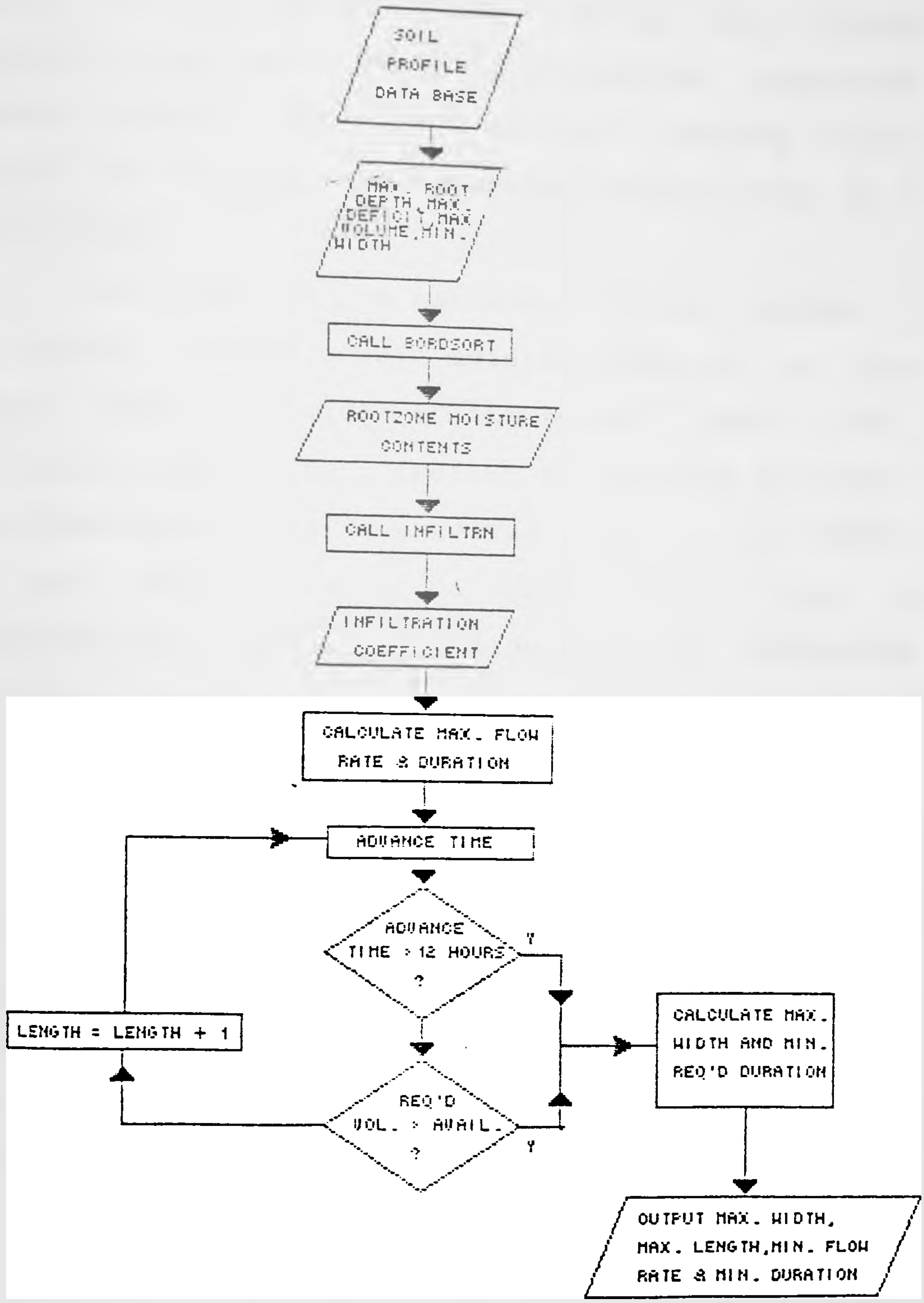

Fig. 7.22 Flow chart of the border design model (BORDERDZ).

An example of the design procedure and results are listed in Table 7.4. The soil profile is assumed uniform, of depth 950 mm, field capacity, θfc = 0.308 cm3/cm3, wilting point, θwp = 0.105 cm3/cm3, saturated moisture content, θs = 0.445 cm3/cm3, wetting front pressure, Pw = 201 mm, and saturated conductivity, Ks = 0.0517 mm/min).

The effect of the management factor (SMDMAX , the maximum allowable soil moisture deficit) on the maximum length and width of the border (Table 7.5), shows that as SMDMAX is increased the maximum allowable length decreases. This is expected since at high SMDMAX the soil profile is at a dryer state with a correspondingly high infiltration rate. The advancing wave front therefore takes much longer to reach the end of the plot and a larger volume of water will infiltrate on the way.

From the dependence of the border design procedure on the management practice factor, it can be concluded that when the daily availability of water is limited, a greater length of border can be irrigated if irrigations are frequent throughout the season, ie: if maximum allowable soil moisture deficit is small.

Table 7.4 Example of design of borders.

```
DESIGN OF BORDER IRRIGATION SYSTEM :

ENTER MAXIMUM ROOTING DEPTH                   (mm)  = 500
ENTER MAX. ALLOWABLE S.M. DEFICIT              (%)  = 50
ENTER MAX. AVAILABLE IRRIGATION VOL.          (m3)  = 100
ENTER BORDER PLOT SLOPE                      (m/m)  = 0.001
ENTER MANNING'S ROUGHNESS                           = 0.024
ENTER BORDER DEPTH                              (m) = 0.15
ENTER MINIMUM BORDER WIDTH                      (m) = 5
ENTER LENGTH INCREMENT FOR SIMULATION           (m) = 2

INFLOW RATE CONSTRAINTS :

MAX. NON-OVERTOPPING FLOW RATE (m3/min) =    3.347795
MAX. NON-EROSIVE FLOW RATE     (m3/min) =   3.5999995E-01
INFLOW RATE (m3/min/m width)   MUST  BE <   3.5999995E-01

ENTER DESIGN FLOW RATE (m3/min/m width) = 0.3

NB// NORMAL DEPTH OF FLOW (mm) =    35.27839

SOME RELEVANT OUTPUT :

   MIN. REQ. IRRIGATION DEPTH  [mm3/mm2] =      50.75000
   MIN. REQ. IRRIGATION DURATION   (min) =          0.00
   DEPTH TO WET ALL PROFILE         (mm) =     180.90000
   TIME TO WET ALL PROFILE         (min) =        455.45
   INFILT. COEFFICIENT (C)    [mm3/mm2 ] =      77.21682
   INFILT. COEFFICIENT (N)               =       0.02061

DESIGN CRITERIA SUMMARY :

   MIN. REQUIRED  IRRIGATION DURATION          (min) =    33.33
   MIN. REQ. FLOW RATE    (m3/min per unit width) =  0.30000
   MIN. REQ. IRRIGATION VOL. (m3 per unit width) =     9.998
   MAXIMUM PERMISSIBLE BORDER WIDTH               (m) =   10.002
   MAXIMUM PERMISSIBLE BORDER LENGTH              (m) =   201.00
```

Table 7.5 The effect of maximum allowable soil moisture deficit on the design length, width and irrigable area of the border system in Table 7.4.

SMDMAX (%)	Length (m)	Width (m)	Area (m2)
25	369	10.8	3985
50	201	10.0	2010
75	73	19.0	1387

7.2.4.2 Design of Furrows :

The design of furrows requires an additional preliminary process, otherwise it is very simillar to the design of borders. The first step in designing a furrow irigation system is to determine the width, depth and spacing of the furrow since these effect the two dimensional infiltration process, which in turn effect the design of the length and maximum number of furrows per field.

A) Design of furrow width, depth and spacing :

The spacing of furrows is often dependent on the characteristics of the crop, soil , and the type of machinary used in the field (Booher 1974). The lateral and vertical movement of water is an important factor which must be taken into consideration at the design stage. Sandy soils for instance allow less lateral flow than vertical infiltration and so closer spacings are necessary to ensure wetting of the root zone in between the furrows. Nonuniform moisture contents and the furrow width and depth also effect the infiltration characteristics of the soil and must be taken into consideration at the design stage.

A furrow spacing design procedure is outlined below which incorporates all the above factors. The model flow chart is shown in Fig. 7.23 . The antecedent soil moisture condition in the profile is determined as with equation 7.53 . The furrow depth, width and

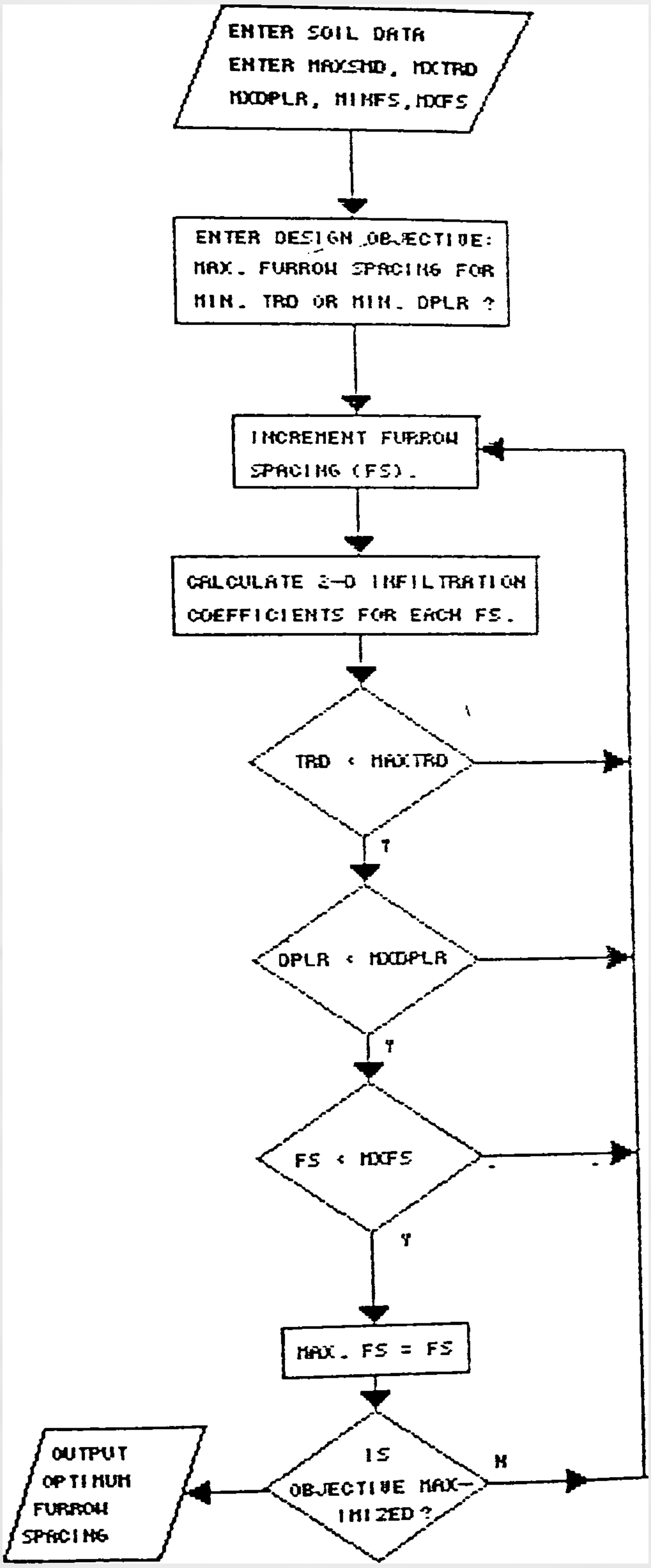

Fig. 7.23 Flow chart of the furrow spacing design model (FURROWSP).

spacing are chosen in increments between specified minimum and maximum values. At each increment the two dimensional wetting pattern is determined by the 2D infiltration model (chapter 6). The time required for the root zone to fill (Trz) is calculated as the time taken for the wetting front, in the last root layer, to reach the maximum lateral rooting extent (see Fig. 7.24). The deep percolation loss ratio (DPLR) is then determined for time Trz as the ratio of the lateral and vertical drainage of water out of the root zone, to that volume of water which remains in the root zone (see chapter 6, section 6.3.3 for more details).

The maximum allowable levels of the two parameters Trz and DPLR represent two optional criteria for which the optimum furrow geometry is determined. The choice between the two depends on the objectives of the irrigator and the operational constraints placed on the system. If irrigation duration is the limiting factor then the combination of furrow width, depth and spacing which gives the minimum value of Trz is chosen. Alternatively if water is limiting then the objective will be to minimize drainage losses and the furrow geometry, corresponding to the least value of DPLR, is chosen for the design.

The criteria for the inclusion of any particular furrow geometry in the optimization process are that Trz must be less than a specified maximum irrigation duration (Tmax), and DPLR must be less than

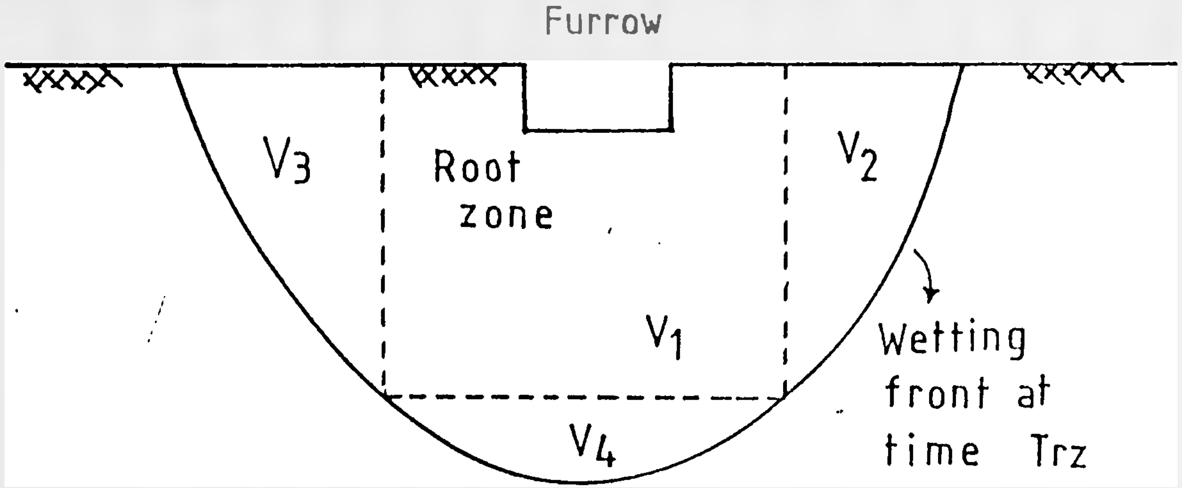

$$DPLR = \frac{V_2 + V_3 + V_4}{V_1}$$

Fig. 7.24 Schematic definition of the deep percolation loss ratio (DPLR) and time of root zone wetting (Trz). (V1 = volume of water remaining in the root zone; V2, V3, V4 = volumes of drainage from root zone).

a maximum acceptable deep percolation loss ratio (DPLRmax). For any combination of depth, width and spacing if the above two conditions are not met, that furrow geometry is excluded from the design.

An example of the inputs and outputs of the model is shown in Table 7.6. The soil profile is assumed uniform, of depth 950 mm, with field capacity, θfc = 0.308 cm3/cm3, wilting point, θwp = 0.105 cm3/cm3, saturated moisture content, θs = 0.445 cm3/cm3, wetting front pressure, Pw = 201 mm, and saturated conductivity, Ks = 0.517 mm/min).

For each geometry the infiltration coefficients are also determined for use in the next section dealing with furrow length design.

B) Design of furrow length :

This procedure follows closely that of the border irrigation case (section 7.2.4.1). The furrow depth, width and spacing, plus the infiltration coefficients must be known. The maximum length of furrow (Lmax) is found in the same manner as discussed in section 7.2.4.1 , with the exception that all flow rates and volumes refer not to unit plot width but to a single furrow. With this in mind the maximum number of furrows (Nmax), given the design length, is found from:

Table 7.6 Example of input data and results for the design of furrow spacing, depth and width.

```
TYPE SOIL8P2.TBL
5 950 400 0.4 6.0 2.4 80
1 190 0.308 0.105 0.04 0.445 0.517 0.517 201 201
2 190 0.308 0.105 0.04 0.445 0.517 0.517 201 201
3 190 0.308 0.105 0.04 0.445 0.517 0.517 201 201
4 190 0.308 0.105 0.04 0.445 0.517 0.517 201 201
5 190 0.308 0.105 0.04 0.445 0.517 0.517 201 201

C>
C>FURROWSP

DO YOU WANT OUTPUT TO A RESULT FILE (Y/N) ? N

---------------------
SOME REQUIRED INPUTS :
---------------------

ENTER MAXIMUM ROOTING DEPTH     (mm) = 760

ENTER MAX. LATERAL ROOT SPREAD  (mm) = 500

ENTER MAX. ALLOWABLE S.M. DEFICIT(%) = 50

-------------------------------------------

------------------
FURROW DIMENSIONS :
------------------

ENTER MIN. FURROW DEPTH   (mm)   = 150

ENTER MAX. FURROW DEPTH   (mm)   = 300

ENTER  DEPTH  INCREMENT   (mm)   = 50

-------------------------------------
ENTER MIN. FURROW WIDTH   (mm)   = 150

ENTER MAX. FURROW WIDTH   (mm)   = 300

ENTER  WIDTH  INCREMENT   (mm)   = 50

-------------------------------------
ENTER MIN. FURROW SPACING (mm)   = 1000

ENTER MAX. FURROW SPACING (mm)   = 2000

ENTER  SPACING  INCREMENT (mm)   = 500
```

```
----------------
DESIGN CRITERIA :
----------------

ENTER MAX. ALLOWABLE IRRIGATION DURATION (min)  = 720

ENTER MAX. ALLOWABLE DEEP DRAINAGE LOSS RATIO   = 0.75


----------------------
OPTIMIZATION OBJECTIVE:
----------------------

DESIGN FOR MINIMUM ? :

        1 - IRRIGATION DURATION
        2 - DRAINAGE LOSS RATIO



ENTER YOUR CHOICE (No.) = 2
```

Table 7.6 Continued ... (see page for definitions)

FURDPT(mm)	FURWDT(mm)	TRD(min)	VINFRD	DPRCNF	DPLR	TWETAL	CCOEF	VNCOEF
FURROW SPACING (mm) =		1000.0						
150.0	150.0	271.47	0.21849E+06	0.96824E+05	0.44314	361.47	2.50150	0.79764
150.0	200.0	241.47	0.20858E+06	0.91671E+05	0.43949	331.47	2.60977	0.79849
150.0	250.0	241.47	0.19008E+06	0.77930E+05	0.40997	331.47	3.69915	0.71798
150.0	300.0	241.47	0.19972E+06	0.92325E+05	0.46227	301.47	3.78211	0.72295
200.0	150.0	262.18	0.22647E+06	0.10480E+06	0.46276	352.18	3.13353	0.76862
200.0	200.0	232.18	0.21605E+06	0.99137E+05	0.45886	322.18	3.24308	0.77081
200.0	250.0	232.18	0.19089E+06	0.78736E+05	0.41247	322.18	4.79898	0.67614
200.0	300.0	232.18	0.20070E+06	0.93303E+05	0.46489	292.18	4.86533	0.68282
250.0	150.0	253.75	0.23459E+06	0.11292E+06	0.48135	343.75	3.79985	0.74469
250.0	200.0	223.75	0.21742E+06	0.10050E+06	0.46226	343.75	4.22798	0.72822
250.0	250.0	223.75	0.22735E+06	0.11520E+06	0.50670	313.75	4.32223	0.73241
250.0	300.0	223.75	0.20158E+06	0.94181E+05	0.46722	283.75	6.05935	0.64773
300.0	150.0	246.06	0.24203E+06	0.12036E+06	0.49728	336.06	4.51140	0.72335
300.0	200.0	246.06	0.24577E+06	0.12886E+06	0.52430	336.06	4.98001	0.70819
300.0	250.0	216.06	0.23436E+06	0.12221E+06	0.52145	306.06	5.06383	0.71337
300.0	300.0	216.06	0.19586E+06	0.88468E+05	0.45168	306.06	8.00614	0.59477

Table 7.6 Continued ...

FURROW SPACING (mm) = 1500.0

150.0	150.0	301.47	0.22570E+06	0.89752E+05	0.39766	691.47	2.29042	0.73310
150.0	200.0	301.47	0.23321E+06	0.97264E+05	0.41707	661.47	2.45103	0.72696
150.0	250.0	301.47	0.24090E+06	0.10495E+06	0.43567	631.47	2.60379	0.72205
150.0	300.0	301.47	0.24883E+06	0.11289E+06	0.45367	601.47	2.74598	0.71841
200.0	150.0	292.18	0.23432E+06	0.98371E+05	0.41982	682.18	2.82802	0.70660
200.0	200.0	292.18	0.24173E+06	0.10578E+06	0.43761	652.18	3.00834	0.70120
200.0	250.0	292.18	0.25023E+06	0.11429E+06	0.45673	622.18	3.14024	0.69973
200.0	300.0	292.18	0.25810E+06	0.12215E+06	0.47328	592.18	3.29973	0.69645
250.0	150.0	283.75	0.24373E+06	0.10779E+06	0.44223	673.75	3.34337	0.68760
250.0	200.0	283.75	0.25109E+06	0.11514E+06	0.45858	643.75	3.54285	0.68260
250.0	250.0	283.75	0.25861E+06	0.12267E+06	0.47433	613.75	3.73224	0.67861
250.0	300.0	283.75	0.26639E+06	0.13044E+06	0.48967	583.75	3.90799	0.67571
300.0	150.0	276.06	0.25206E+06	0.11612E+06	0.46067	666.06	3.92432	0.66844
300.0	200.0	276.06	0.25933E+06	0.12339E+06	0.47578	636.06	4.14301	0.66385
300.0	250.0	276.06	0.26676E+06	0.13082E+06	0.49039	606.06	4.35003	0.66020
300.0	300.0	276.06	0.27444E+06	0.13850E+06	0.50465	576.06	4.54163	0.65758

Table 7.6 Continued ...

FURROW SPACING (mm) = 2000.0

150.0	150.0	301.47	0.22013E+06	0.84186E+05	0.38244	1171.47	2.39756	0.67032
150.0	200.0	301.47	0.22726E+06	0.91317E+05	0.40181	1111.47	2.50399	0.66830
150.0	250.0	301.47	0.23352E+06	0.97579E+05	0.41785	1081.47	2.73083	0.65787
150.0	300.0	301.47	0.24006E+06	0.10412E+06	0.43370	1051.47	2.92846	0.65046
200.0	150.0	292.18	0.22969E+06	0.93743E+05	0.40813	1162.18	2.86270	0.65027
200.0	200.0	292.18	0.23682E+06	0.10088E+06	0.42596	1102.18	2.97190	0.64906
200.0	250.0	292.18	0.24333E+06	0.10739E+06	0.44132	1072.18	3.18734	0.64151
200.0	300.0	292.18	0.24939E+06	0.11345E+06	0.45489	1042.18	3.45329	0.63173
250.0	150.0	283.75	0.23897E+06	0.10302E+06	0.43111	1153.75	3.34597	0.63303
250.0	200.0	283.75	0.24536E+06	0.10941E+06	0.44593	1123.75	3.59098	0.62519
250.0	250.0	283.75	0.25257E+06	0.11662E+06	0.46174	1063.75	3.69015	0.62549
250.0	300.0	283.75	0.25902E+06	0.12308E+06	0.47516	1033.75	3.92573	0.61901
300.0	150.0	276.06	0.24852E+06	0.11258E+06	0.45299	1146.06	3.76520	0.62210
300.0	200.0	276.06	0.25435E+06	0.11840E+06	0.46551	1116.06	4.10928	0.61066
300.0	250.0	276.06	0.26157E+06	0.12563E+06	0.48028	1056.06	4.20540	0.61153
300.0	300.0	276.06	0.26799E+06	0.13204E+06	0.49271	1026.06	4.46000	0.60539

Table 7.6 Continued ...

```
FURROW SPACING DESIGN :
-----------------------

 DEEP DRAINAGE LOSS RATIO IS OPTIMUM :

 OPTIMUM FURROW SPACING                     (mm) =      2000.0
 OPTIMUM FURROW DEPTH                       (mm) =       150.0
 OPTIMUM FURROW WIDTH                       (mm) =       150.0
 MIN.REQ.IRR. DURATION TO WET RZ (TRD):(min) =       301.47
 TOT.VOL. INFILTRATED AT TRD [mm3/mm Length] =  0.22013E+06
 DEEP DRAINAGE VOL.BELOW RZ  [mm3/mm Length] =  0.84186E+05
 DEEP DRAINAGE LOSS RATIO :               (DPLR) =      0.38244
 TIME TO WET ALL PROFILE :                 (min) =      1171.47
 INFILT. COEFF. (C)         [mm3/mm FS/mm FL] =      2.39756
 INFILT. CURVE COEFFICIENT (N)                   =      0.67032

 NB : KOSTIAKOV INFILTRATION EQUATION :
       I = C *( t ** N)      mm3/mm , (t:min)
```

Key:

FURDPT = furrow depth (mm)
FURWDT = furrow width (mm)
TRD = time to wet root depth (mm)
VINFRD = volume infiltrated at TRD (mm3/mm length)
DPRCNF = volume lost to drainage (mm3/mm length)
DPLR = deep percolation loss ratio
TWETAL = time to wet entire root zone (min)
CCOEF = infiltration coefficient
VNCOEF = infiltration coefficient

$$N_{max} = \frac{V_{max}}{F_s \, . \, L_{max} \, . \, Z_{req}} \qquad (7.58)$$

where Fs = the furrow spacing (m); Lmax is the maximum length (m); Zreq = the required irrigation depth to fill the root zone (m); and Vmax = the maximum volume of water available per plot (m3).

The example in Table 7.7 illustrates the design inputs and outputs. The soil profile is as for Table 7.6, and the input infiltration coefficients are outputs of the optimum furrow spacing design of the previous section (see Table 7.6).

Table 7.7 Example of furrow length design.

```
FURROWLN

ENTER TOTAL VOLUME AVAILABLE PER PLOT (m3) = 100

ENTER MIN. REQUIRED IRRIGATION DEPTH  (mm) = 50

ENTER FIELD PLOT SLOPE                (m/m) = 0.01

ENTER MANNING'S ROUGHNESS                  = 0.024

ENTER INFILTRATION COEFFICIENT (C)    (mm) = 2.39756

ENTER INFILTRATION COEFFICIENT (N)         = 0.67032

ENTER FURROW DEPTH                     (m) = 0.15

ENTER FURROW SPACING                   (m) = 2.0

ENTER MIN. No. OF FURROWS REQUIRED         = 5

ENTER LENGTH INCREMENT FOR SIMULATION  (m) = 2

-----------------------------
INFLOW RATE CONSTRAINTS :
-----------------------------
MAX. NON-OVERTOPPING FLOW RATE   (m3/min) = 34.71788
MAX. NON-EROSIVE FLOW RATE       (m3/min) =  0.03600
DESIGN FLOW RATE (m3/min/furrow) MUST BE  <  0.03600
-------------------------------------------------

NB// NORMAL DEPTH OF FLOW (mm) =   31.719639
NB// DURMIN (min) =    555.5556
NB// PLENMX (m) =   200.00000
NB// PLNMAX =   201.00000 LENGTH > MAX. ALLOWABLE
NB// NFURRO =            5

    ---------------------------
     DESIGN CRITERIA SUMMARY :
    ---------------------------

 MAX. PERMISSIBLE FLOW RATE PER FURROW (m3/min) =  0.03600
 MIN. REQUIRED  IRRIGATION DURATION        (min) =    555.6
 MIN. REQ. FLOW RATE PER IRRIGATED PLOT(m3/min) =    0.180
 MIN. REQUIRED  IRRIGATION VOLUME   (m3/furrow) =   19.900
 MAXIMUM PERMISSIBLE FURROW LENGTH           (m) =  199.000
 MAXIMUM PERMISSIBLE NUMBER OF FURROWS PER PLOT =   5
```

7.3 Discussion :

The surface irrigation design, operational management and efficiency evaluation models presented in this chapter, all share a common characteristic in that when integrated with the irrigation scheduling model of chapters 3 and 4, they respond to changes in the antecedent root zone moisture content and crop rooting depth, and to the soil moisture deficit management factors. This makes these models particularly usefull for investigating the effects of various management practices on irrigation design and operational efficiencies.

The integrated irrigation model (ie: the scheduling and the surface irrigation models), can be adapted for the real time management of individual farm units to achieve the maximum benefit from both crop yield and irrigation water.

Tables 7.8 and 7.9 show typical surface irrigation operations schedules, output by the integrated irrigation model. The simulations are for the soil and crop data of the lysimeter test, and the system dimensions are those of the Strelkoff (1977) border irrigation (ie: plot length = 91.4 m , slope = 0.00101, manning roughness = 0.024; see Fig. 7.4). The effects of two management practices, on the operational schedules, are simulated. In the first case (Table 7.8), for the periods 1 to 80 days the management soil moisture deficit, MNGSMD = 50% and from 81 to 160

Table 7.8 Example of an operations schedule for a border irrigation system (Table 7.1) and the lysimeter soil and crop data (see chapter 4). Management factors: days 1 to to 80: MNGSMD = 50%, MNGIRG = 100%; days 81 to 160: MNGSMD = 25%, MNGIRG = 100%).

DAY	INFLOW m3/min	DURATION min	Ea %	Es %	Ed %	Ede %	RUNOFF m3/m width	REQ. IRR. m3/m width
5	0.1341D+00	12.0	61.69	96.80	89.90	60.45	0.5553D+00	0.1650D+01
9	0.3885D-01	49.0	82.96	99.49	95.88	82.61	0.2428D+00	0.1919D+01
12	0.7061D-01	39.0	56.67	66.28	94.08	43.99	0.1187D+01	0.2740D+01
17	0.7061D-01	60.0	46.34	52.15	95.73	32.52	0.2273D+01	0.4237D+01
25	0.1024D+00	49.0	35.06	36.73	95.22	21.86	0.3271D+01	0.5037D+01
42	0.1341D+00	49.0	27.68	28.38	95.55	16.30	0.4792D+01	0.6626D+01
149	0.7061D-01	55.0	47.79	52.67	95.23	33.43	0.2013D+01	0.3855D+01

	PET	ASE	PT	AT	AET
SEASONAL TOTAL(mm) =	288.3	81.9	140.1	135.7	217.6

PROPORTIONAL DRY MATTER YIELD (Y/Ym) = 0.969

SEASONAL IRRIGATION REQUIREMENT (mm/unit area) = 270.2

Table 7.9 Example of an operations schedule for the same data base as Table 7.8 but with managmeny factors: days 1 to 160: MNGSMD = 25%, MNGIRG = 100%).

DAY	INFLOW m3/min	DURATION min	Ea %	Es %	Ed %	Ede %	RUNOFF m3/m width	REQ. IRR. m3/m width
2	0.1341D+00	12.0	24.12	100.00	89.58	24.12	0.6689D+00	0.1650D+01
4	0.1341D+00	12.0	24.83	100.00	89.47	24.83	0.6862D+00	0.1650D+01
7	0.1341D+00	11.0	40.49	100.00	88.87	40.49	0.6110D+00	0.1529D+01
9	0.7061D-01	22.0	69.91	95.53	91.05	67.69	0.4144D+00	0.1568D+01
11	0.7061D-01	23.0	69.92	95.51	91.21	67.69	0.4292D+00	0.1617D+01
12	0.3885D-01	38.0	69.02	100.00	91.91	69.02	0.2156D+00	0.1492D+01
15	0.7061D-01	38.0	53.46	64.76	93.72	41.42	0.1262D+01	0.2711D+01
18	0.3885D-01	60.0	74.04	82.54	95.46	64.02	0.6045D+00	0.2331D+01
22	0.7061D-01	38.0	52.55	58.10	93.51	38.11	0.1287D+01	0.2711D+01
33	0.7061D-01	49.0	46.26	53.72	94.56	33.08	0.1867D+01	0.3474D+01
41	0.7061D-01	49.0	46.95	51.69	94.60	32.63	0.1843D+01	0.3474D+01
52	0.7061D-01	55.0	45.75	51.66	95.10	32.03	0.2092D+01	0.3855D+01
68	0.7061D-01	55.0	46.62	51.10	95.14	32.24	0.2058D+01	0.3855D+01
149	0.7061D-01	55.0	47.79	52.67	95.23	33.43	0.2013D+01	0.3855D+01

	PET	ASE	PT	AT	AET
SEASONAL TOTAL(mm) =	288.3	81.9	140.1	136.5	218.4

PROPORTIONAL DRY MATTER YIELD (Y/Ym) = 0.974

SEASONAL IRRIGATION REQUIREMENT (mm/unit area) = 330.0

days respectively MNGSMD = 25% . The second case (Table 7.9) shows the irrigation time table for the same field but for the entire 160 days, MNGSMD = 25% . In both cases 100% irrigation was chosen (ie: MNGIRG = 100%).

The simulated actual evapotranspirations (AET) and proportional yields are simillar for both cases. The irrigation efficiencies are also comparable. However, the second case (Table 7.9), predicts more frequent irrigations and a higher seasonal irrigation requirement. This is because the level of allowable soil moisture deficit has been chosen at a low level throughout the simulation period.

Such simulations are particularly usefull in comparing different management decisions concerning the levels of allowable crop stress. It is evident that, as in the case of the first management practice (Table. 7.8), allowing a greater level of moisture deficit does not effect the proportional yield to any great extent. The predicted irrigation dates are less frequent and less total irrigation water is required. In management terms, this practice would be preferable to the second case.

CHAPTER 8 DYNAMIC WATER BALANCE UNDER SPRINKLER IRRIGATION.

8.1 Introduction:

Sprinkler or 'overhead' irrigation is the method of applying water to the cultivated soil in the form of a spray. The process is very simillar to natural rainfall with the water subject to the same hydrological processes once it leaves the sprinkler nozzle.

Operationally these systems are under greater control than surface irrigation methods. The rate of discharge, the application rate and duration, and the rain drop size can be controlled by selecting apprpopriate pumps, pipes, pressures and nozzle sizes, (Rolland 1982 provides detailed reviews of sprinkler irrigation hardware). This level of control makes the use of sprinklers viable on a wide range of soil types and on fields with nonuniform slopes (Hansen etal 1979).

The diversities of system hardware and the range of site-applicability of sprinkler systems does however raise questions about the effects of such factors as soil type, crop type, meteorological conditions, nozzle size, and discharge rate and duration, on the performance of the system. Under sprinkler irrigation, the main indicator of system performance is the application efficiency. It is a measure of the proportion of applied water that remains in the root zone and is beneficially used.

In general the application efficiency of sprinkler irrigation is relatively high at 70% (Table 1.1). The losses that do occur are due in main to runoff and deep percolation (drainage from the root zone). Interception and evapotranspiration during irrigation represent lesser volumetric losses, although in arid zones evapotranspiration losses may be significant, in which case night-time irrigation is usually advisable.

The subject of interest, in this chapter and the next, is the performance of sprinkler irrigation systems. In this chapter a mathematical model is developed for the simulation of the water balance of a point in the area of coverage of a single sprinkler nozzle. The term 'point' can be defined as an area in which the soil, crop and precipitation are spatially uniform in the horizontal direction.

The precipitation is divided into it's hydrological components by taking into account such processes as precipitation intensity and duration, interception, evapotranspiration, runoff, infiltration and drainage. The water balance model is then extended in chapter 9, by an application-rate discretization procedure, to evaluate the water losses in the root zone and hence calculate the various efficiencies under the whole area of coverage of the sprinkler unit.

The irrigation scheduling model (chapters 3 and 4) predicts the days and the amounts of water required for replenishment of the root zone. For each scheduled irrigation , the nonuniform composite-layer soil moisture content profile is also determined (eg: Fig. 4.3). This indicates the antecedent soil moisture conditions, and hence the infiltration characteristics of the soil (chapter 6), at the start of irrigation.

While the soil and crop can be chosen to represent uniform conditions, the rate of precipitation under a sprinkler unit is seldom uniform over the field. The rate of application of water reduces as the distance from the nozzle increases (Fig. 8.1). If the application rates were uniform throughout the area of sprinkler coverage, then the point-determined application efficiency would be representative of the whole area. In reality the spatial distribution of water on the field is not uniform. The question now arises as to how this nonuniformity will effect the irrigation efficiency. The extention of the analysis to the whole area of sprinkler coverage is undertaken in the next chapter.

In the following sections the term 'rainfall' has been used in reference to sprinkler precipitation because the model does not distinguish between sources of precipitation. The theories are equally applicable to the generation of runoff from natural rainfall.

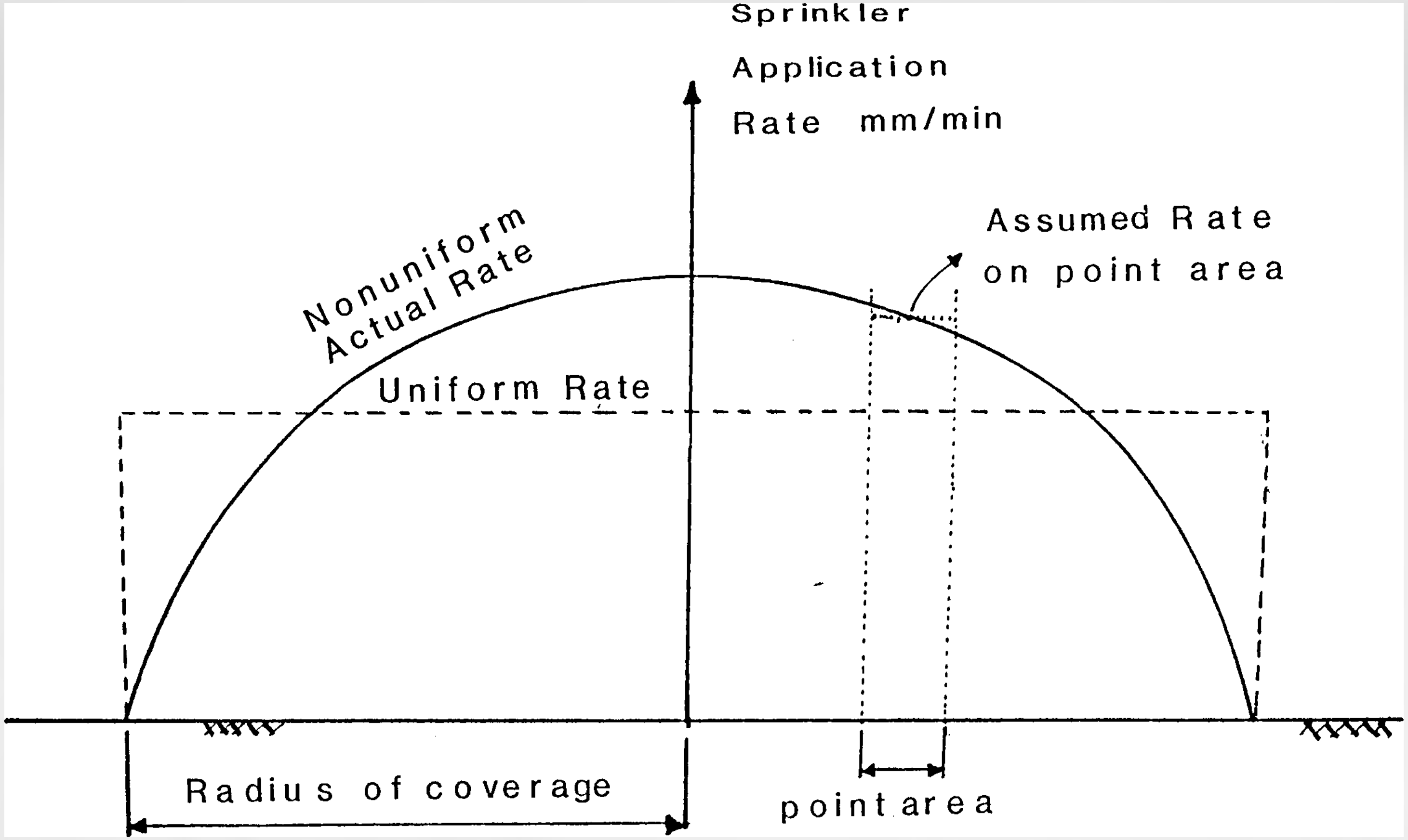

Fig. 8.1 Schematic representation of application rate nonuniformity under single nozzle sprinkler irrigation.

8.2 Excess Rainfall and Runoff:

Runoff is that fraction of the rainfall that is not intercepted by vegetation or held in surface detention storage and which is not part of the rainfall that infiltrates into the soil. This "excess" or "effective" rain flows down the slope as "overland flow" and runs into the stream channel.

Excess rainfall is dependent upon the processes of interception, evapotranspiration, depression storage and infiltration. Ignoring depression storage, which for a point on the surface is negligible, the dynamic water balance equation can be expressed as:

$$r(t) = Pg(t) - i(t) - f(t) - ET(t) \tag{8.1}$$

where:

$r(t)$ = runoff rate (mm/min)
$Pg(t)$ = gross precipitation (mm/min)
$i(t)$ = interception rate (mm/min)
$f(t)$ = infiltration rate (mm/min)
$ET(t)$ = evapotranspiration rate (mm/min)
t = index of time (min)

Compared to rainfall and infiltration volumes interception and evapotranspiration losses for single rainfall events are small (Emmett W.W 1978). The process that essentially dominates and controls the rate of generation of excess rainfall is the infiltration rate of the soil.

8.2.1 Point Runoff from Continuous Rain:

At the onset of rainfall the initially dry soil absorbes all the rain untill such time as the infiltration rate is less than the rainfall rate and runoff begins. Mathematically this process is expressed from Eqn. 8.1 as:

$$r(t) = 0.0 \qquad t < tp$$
$$r(t) = P(t) - f(t) \qquad t > tp \qquad (8.2)$$

where the ponding time (tp) is the delay time of runoff when the initially high infiltration rate absorbes all the rain and no runoff occurs.

The runoff process, expressed mathematically in Eqn 8.2 , can be shown schematically in Fig 8.2 . The rate of runoff is a function of the infiltration rate of the soil and therefore there are as many variations of rainfall-runoff models as there are of infiltration models (see chapter 6).

8.2.2 Point Runoff from Intermittent Rain:

The process described above applies to cases where the rainfall is continuous, though not necessarily at a steady rate, and where after the time of ponding has been exceeded the soil surface remains saturated and runoff is generated continuously for the rainfall duration.

When an intermittent rainfall pattern

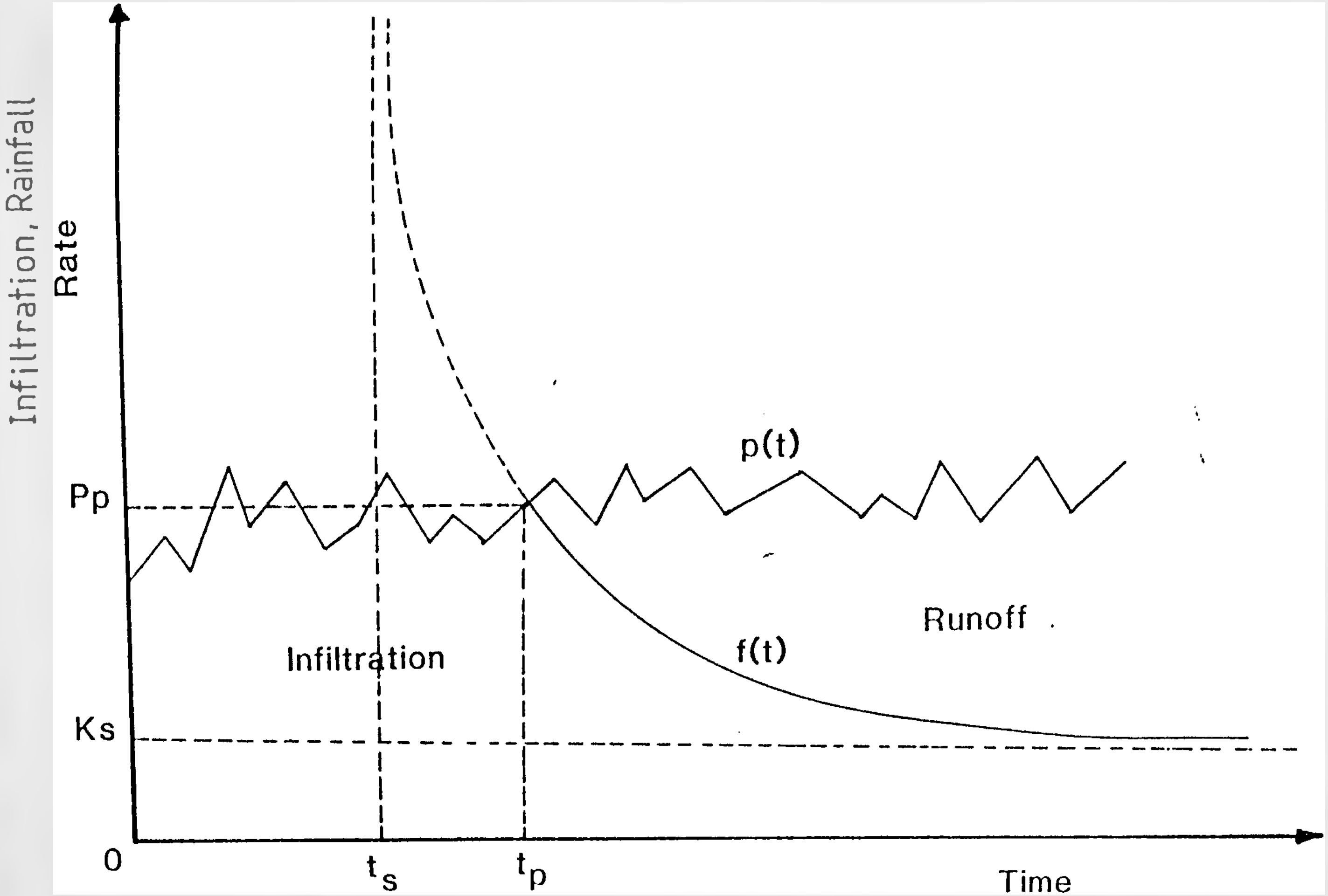

Fig. 8.2 Schematic representation of infiltration and runoff processes (Pp = rainfall rate at ponding time; Ks = saturated hydraulic conductivity; ts = pseudotime; tp = ponding time; p(t)= rainfall rate; f(t)= infiltration rate).

prevails , soil surface ponding is intermittent, as is the runoff. At the end of the first rainfall event, runoff ceases and the soil surface is no longer saturated since the infiltrated water now has the opportunity to redistribute itself in the soil. The effect of the new soil profile moisture content is that at the onset of the next rain, the soil has a different infiltration capacity than before, and so the rainfall generating process must start all over again with this new infiltration function.

Rainfall-Runoff models which use one of the various forms of the Philip equation (see chapter 6), do not take into account the antecedent soil moisture conditions at the onset of a rainfall event. Although the sorptivity of the soil, parameter 'S' in Philips equation, has been shown to be a function of the initial moisture content (Smith & Parlange 1978), and could be used to simulate infiltration under intermittent rainfall, albeit the entire profile would be assumed to be of uniform moisture content.

James & Larson (1976) proposed a model in which it was assumed that the soil profile is uniform in moisture content and that the rain intensity during each application is constant. The Mein & Larson (1973) version of the Green & Ampt (1911) infiltration model was used to estimate infiltration rates . At the end of each rainfall period, a redistribution model was used to calculate the water content in the soil transmission zone.

The Stanford Watershed Model (Crawford & Lindsey 1966, Fleming 1975) is also capable of simulating runoff from intermittent rainfall, but it's infiltration function is based on empirical, non-physicall parameters. This factor, along with the assumption of root zone uniformity, makes it's use, as part of an integrated systems approach to on-farm irrigation management, unsuitable.

Another model capable of simulating the water balance under intermittent rainfall is the CREAMS model (Knisel W.G etal 1980) . The procedure used in CREAMS is to utilize the Smith & Parlange (1978) modified version of the Green-Ampt equation to simulate infiltration rates. The assumption is made that the infiltrated volume during a period of rainfall is redistributed in the soil if a rain gap of more than 3 hours is encountered in the day, otherwise the next rain is taken to be the continuation of the previous event. Although a layered root zone water balance model was used for daily moisture accounting, no effort was made to incorporate the effects of nonuniform soil moisture contents on the infiltration process.

Chu (1978) introduced a model for the simulation of runoff from intermittent rainfall, based on the assumption of a homogeneous soil profile with uniform moisture distribution, and the Green-Ampt equation of infiltration.

In order to evaluate the effect of rainfall durations and gaps on the runoff process, two conditions are assumed to exist at the beginning of a short period of rain. Either surface ponding does not occur at the initial time, or the surface becomes ponded. To help identify the surface condition at the end of the rain period, two surface condition indicators (Cu and Cp) are defined for the two cases respectively. In either case, at the terminal time of the rainfall period, if the surface condition indicators, Cu or Cp, are greater than zero, the surface is ponded.

The model, although simple to use, does however require that the implicit infiltration function of Green-Ampt be solved iteratively or graphically. Also the assumption of uniform moisture distribution and profile homogeneity has meant that a redistribution routine for the infiltrated water has not been necessary. These shortcomings will be rectified by the model proposed in the next section.

8.2.3 Point Excess Rainfall Model (PERM):

The restrictions inherent in the types of models outlined above are the assumptions that the soil profile is homogeneous and that the antecedent soil moisture is uniformly distributed. The effects of non-homogeneity and differential soil moisture contents on the infiltration process have been dealt with in section 6.3 . Infiltration rates depend not only on soil type but also on the antecedent moisture conditions.

The aim of this new approach is to develope a model which is capable of simulating the generation of excess rainfall, under both continuous and intermittent application, for conditions of soil non-homogeneity and nonuniform soil moisture distribution. For the new model to be compatible with the root zone water balance model of chapter 4, which also incorporates the soil conditions mentioned, it must include a redistribution routine which would trace the movement of infiltrated water and calculate the new soil moisture contents at the cessation of rain.

The assumptions made in this model are essentially those made for the one dimensional infiltration model (see sect. 6.3), namely that the soil profile is divided into discrete layers corresponding to changes in soil hydraulic properties and/or soil moisture content variations. In addition, the surface ponding is assumed to be controlled by the conditions in the first layer only.

The PERM model constitutes a water budgeting procedure, based on Eqn. 8.1, which utilizes the interactions between the rain supply, infiltration and redistribution models. The flow chart in Fig. 8.3 shows the steps involved in this simulation model. All rates are discretized in time with increments of one minute.

Breakpoint rainfall data, input as hourly, five minute or as intensity-duration data, is assumed to be uniform within each breakpoint duration. The maximum duration of simulation is 24 hours.

Interception:

The interception process, apart from reducing the gross rainfall, plays no direct part in the generation of point excess rainfall. Therefore when considering a point on the soil surface, the amount of rain that passes through the interception process as throughfall and is available for infiltration must first be evaluated.

Due to the nature of the rainfall pattern, it is necessary that a dynamic interception model is used. The model of Rutter (Rutter etal 1971, 1975, 1977) is utilized here to estimatethe interception water losses. This model keeps a continuous balance of the water falling on the canopy, the amount draining and that evaporating from the canopy. The vegetation canopy and

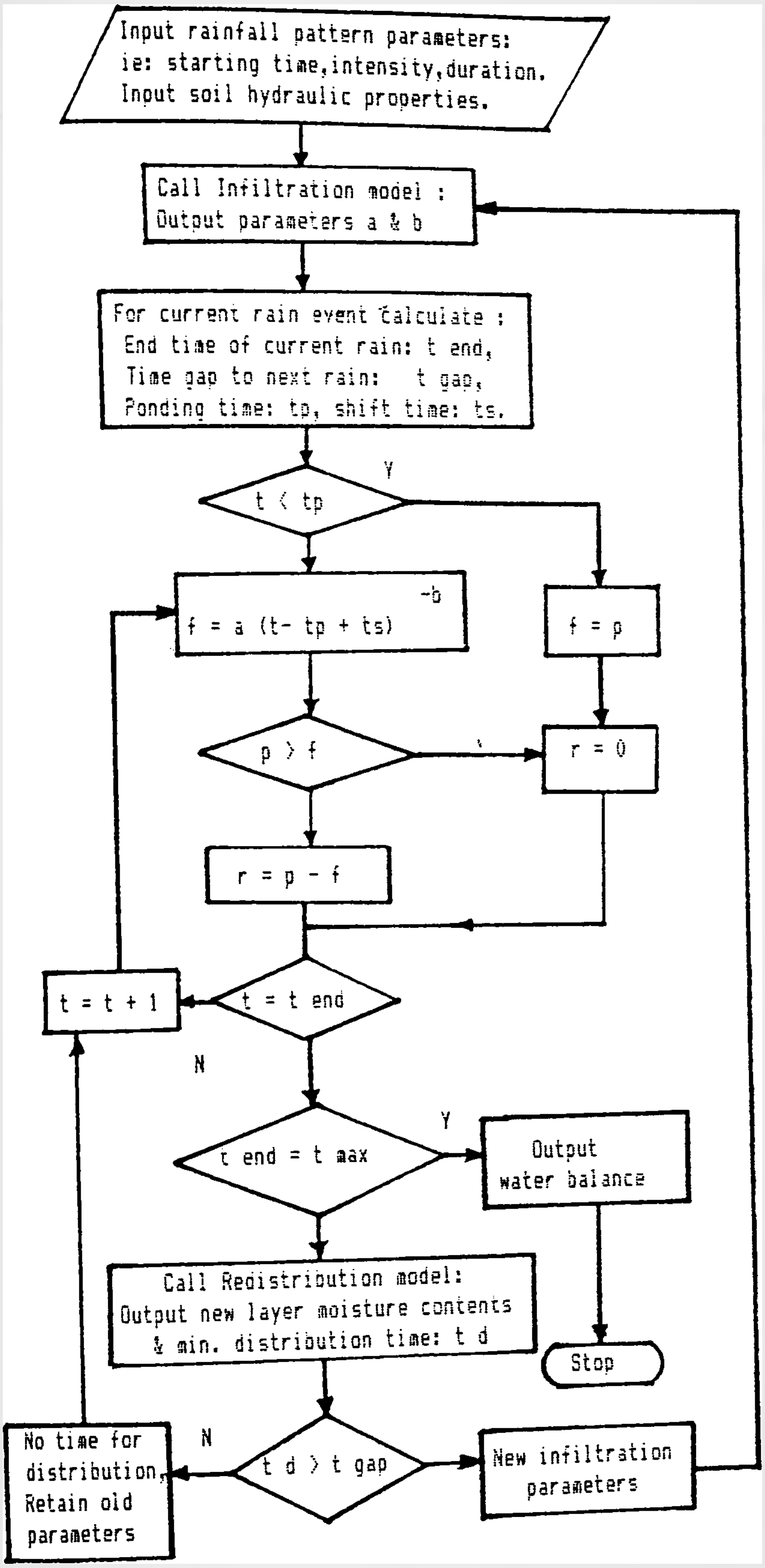

Fig. 8.3 Flow chart of the Point Exces Rainfall Model (PERM), (see Table 8.1 for definition of terms).

Table 8.1 Definition of terms used in the flow chart in Fig. 8.3.

t	=	time since start of rain (min).
tp	=	ponding time (min).
ts	=	pseudotime (min).
td	=	redistribution time of infiltrated rain (min).
t end	=	end time of current rain event (min).
t gap	=	time gap to next rain event (min).
f	=	infiltration rate (mm/min).
a & b	=	infiltration rate function parameters.
p	=	rainfall rate during the event (mm/min).
r	=	excess rainfall rate (mm/min).

trunks are considered as storages (Fig. 8.4) which are filled by rain and emptied by drainage and evaporation. In the case of cultivated crops the trunk storage is assumed negligible relative to the canopy storage (Clarke 1940).

Net rainfall or 'throughfall' is calculated as the sum of the rain that falls directly through, and the water that drains from, the wet canopy. This is expressed as follows :

$$P(t) = p\, Pg(t) + D(t) \qquad (8.3)$$

where:
- $P(t)$ = net rainfall or throughfall rate (mm/min)
- $Pg(t)$ = gross rainfall rate (mm/min)
- p = proportion of rain as direct throughfall
- $D(t)$ = canopy drainage rate (mm/min)

Dropping the '(t)' time index for the instantaneous mass balance, the amount of water on the canopy, defined as the 'instantaneous canopy storage (C)', is calculated by the equation:

$$C = (1-p)\, Pg - ET - D \qquad (8.4)$$

where :
- C = canopy storage (mm)
- Pg = gross rainfall (mm)
- p = proportion of rain as direct throughfall
- ET = evapotranspiration (mm)
- D = drainage from canopy (mm)

Evapotranspiration is given as a function of

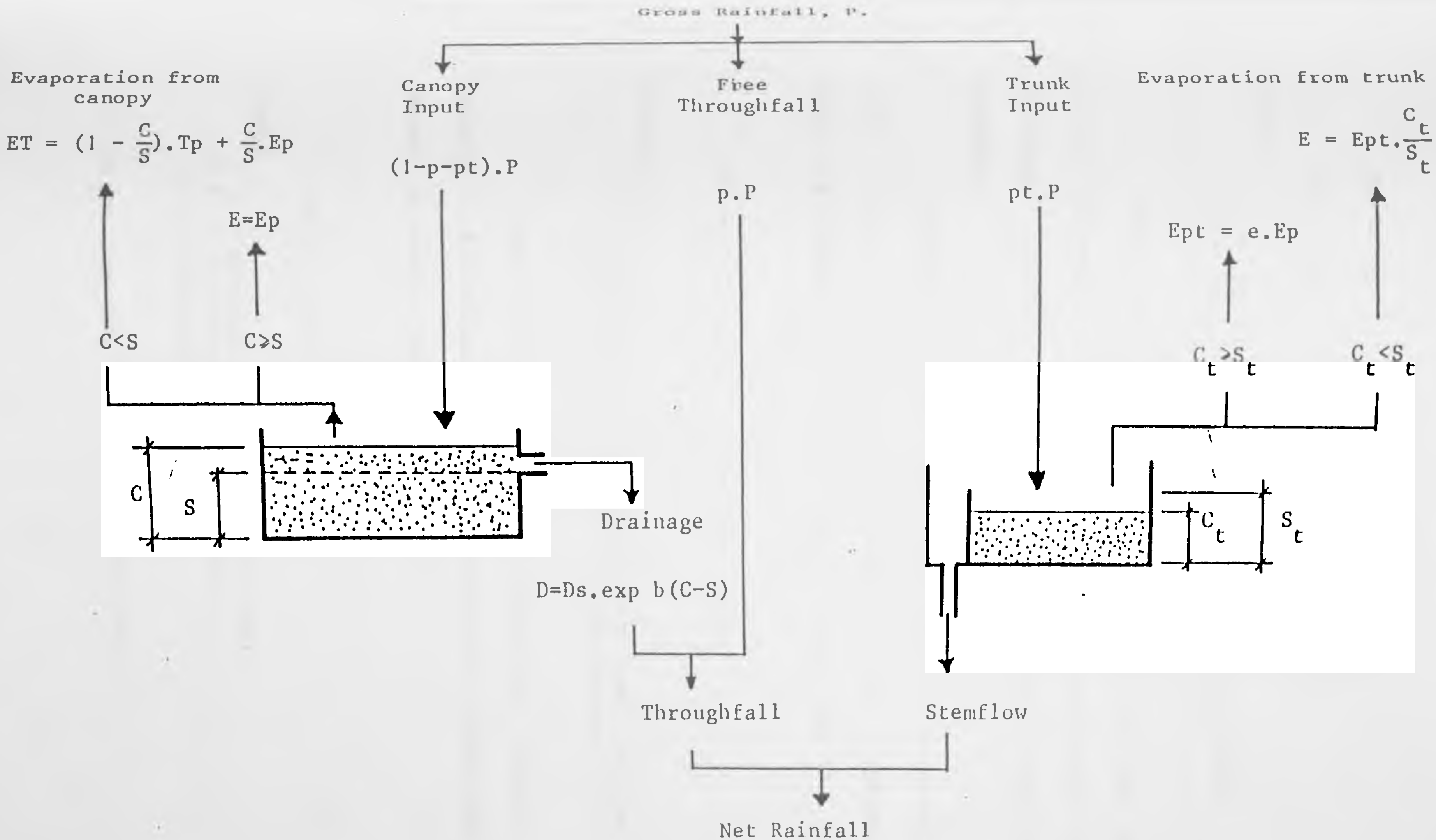

Fig. 8.4 Schematic diagram of the Rutter interception model (After Gash & Morton 1978).

the amount of water on the canopy :

$$ET = Ep \cdot C/S \qquad \text{for } C < S$$
$$ET = Ep \qquad \text{for } C > S \qquad (8.5)$$

where :
Ep = potential evapotranspiration (mm).
S = canopy storage capacity (mm).

The canopy storage capacity is the maximum amount of water retainable on the plant canopy before drainage occurs. Some values of 'S' are listed in the appendix.

Larsson (1981) modified the above equation to take into account the contribution from transpiration when the canopy is only partially wet (ie: $C < S$) :

$$ET = (1- C/S) Tp + (Ep. C/S) \qquad (8.6)$$

where :
Tp = potential transpiration (mm) in the absense of water on the leaves.

The rate of drainage from the canopy during rainfall is estimated as an exponential function of the amount of water on the canopy :

$$\ln D = a + b C \qquad (8.7)$$

where :
D = drainage from canopy (mm)
a & b = drainage coefficients.
ln = natural logarithm.

Let Ds be the drainage rate when $C=S$:

$$D = Ds.\ \exp[\ b(C-S)\ ] \tag{8.8}$$

Rutter found Ds to be 0.002 mm/min and 'b' to be 3.7 /min for Corsican pine of leaf area index LAIp . For canopies with different leaf area index (LAI) the value of Ds is equal to 0.002(LAI/LAIp), and 'b' equals 3.7(LAI/LAIp). However assuming a linear relation exists between LAI and S :

$$Ds = 0.002\ (S/Sp) \tag{8.9}$$

and

$$b = 3.7\ (Sp/S) \tag{8.10}$$

where Sp is the storage capacity of Corsican pine canopy, found by Rutter etal (1971) to be 1.05 mm.

Substitution of the above equations in Eqn. 8.8) gives a single-parameter expression for drainage rate :

$$D = 3.9 \times 10^{-5}\ .\ S\ .\ \exp[\ 3.885(C/S)\ ] \tag{8.11}$$

Using a time increment of 1 minute, the rate of drainage from the canopy, D(t), is thus calculated from Eqn. 8.4, 8.6 and 8.11, and the net rainfall rate P(t) determined from Eqn. 8.3.

Rutter etal (1977) found the model was insensitive to variations in parameter 'b' in the range

3.0 to 4.6 and thus took an average of 3.7. The parameter Ds represents the resolution of the throughfall measuring instruments and the model is moderately sensitive to it (Massman 1983).

Where experimentally derived values for the parameters 'b' and Ds are not available, the approximations in Eqn. 8.11 can be used. The proportion of direct throughfall (p) is also best determined by measurement and is imagined to be a complex function of the growth stage, leaf type and size and antecedent wind conditions. Aston (1979) suggests this value can be approximated as :

$$p = 1.0 - 0.05\ \mathrm{LAI} \tag{8.12}$$

The operation of the interception model is optional within the PERM model.

Potential Evapotranspiration (Ep):

Diurnal potential evapotranspiration (Ep), is assumed to vary around noon as a half sine wave (Federer 1982). The evapotranspiration rate is thus estimated by the following equation:

$$Ep = \frac{\pi\ PET}{2\ d} \cos\left(\frac{\pi t}{d}\right) \tag{8.13}$$

where:

E_p = evapotranspiration rate (mm/min)
PET = mean daily evapotranspiration (mm)
d = length of day (min)
t = time of day (0 to 1440 minutes)

A simillar procedure is used to convert mean daily potential transpiration (PT) into its diurnal variation, the potential transpiration rate (Tp).

Infiltration:

At the onset of rain the infiltration rate equation is determined by the one dimensional infiltration model of Bouwer (1969) for nonuniform soils (see chapter 6) . The infiltration-rate parameters thus calculated, apply to the antecedent moisture conditions in the soil profile layers :

$$f = a\ t^{-b} \qquad (8.14)$$

where:

f = infiltration rate (mm/min)
t = elapsed time (min)
a & b = infiltration rate parameters

Ponding Time (tp):

During the early stages of a rain storm all the rainfall is infiltrated untill the ponding time is reached. This time to ponding is estimated by solving the formula given by Smith & Parlange (1978):

$$\sum_{t=0}^{t=tp} p(t) = SM \times \ln \left[\frac{p(tp)}{(p(tp)-Ks)} \right] \qquad (8.15)$$

where:

$$SM = Pw (\theta s - \theta i) \qquad (8.16)$$

where:
- tp = ponding time (min)
- p(tp) = rainfall rate at ponding time (mm/min)
- p(t) = rainfall rate at time t (mm/min)
- Ks = saturated hydraulic conductivity (mm/min)
- Pw = wetting front presssure (mm)
- θs & θi = sat'd and initial moisture contents (mm)

Equation 8.15 is an equality only when ponding time is reached. Time of ponding is estimated as the time when the value on the right hand side is no longer greater than the value on the left hand side. Considering that a one minute time step is used throughout the model, tp is determined to the nearest minute . Note that by definition the left hand side term is the sum of the rainfall, and the right hand side the cumulative infiltration, up to ponding time.

Pseudotime (ts) :

The effect of delayed ponding on the infiltration curve is to shift it's time axis by a finite time depending upon the initial moisture conditions (Fig. 8.2).

To correct for the time shift in the vertical assymptote of the infiltration curve due to delayed ponding , a 'pseudotime (ts)', (Freeze 1980) is calculated by the following equation given by Chu (1978):

$$ts = \frac{SM}{Ks} \left[\frac{Fp}{SM} - \ln \left(1 + \frac{Fp}{SM} \right) \right] \qquad (8.17)$$

where:
Fp = cum. infiltration at the ponding time (mm)

The elapsed time used for the infiltration decay curve, must now be shifted by the pseudotime amount since the vertical assymptote of the infiltration curve is no longer at the time of rain onset. Thus Eqn. 8.14 can now be written with respect to the true time:

$$f = a\,(t - tp + ts)^{-b} \qquad (8.18)$$

Note that for the case of sudden ponding both tp and ts are zero.

Redistribution Model:

At the end of each rainfall period, the infiltrated water has the opportunity to redistribute itself among the layers of the soil profile. To simulate this process a cascading-flow model is used to distribute the volume infiltrated, during the just-terminated rain period, between the layer storages according to their respective moisture capacities and conductivities. The cascading model is shown in Fig. 8.5.

For each layer j the following are defined:

a) Maximum available storage :

$$S(j) = DLTRD(j)\ [\ SWSAT(j) - SMC(j)\ ] \qquad (8.19)$$

b) Maximum retainable storage:

$$F(j) = DLTRD(j)\ [\ SWFC(j) - SMC(j)\ ] \qquad (8.20)$$

c) Drainable volume :

$$DRNBLV(j) = DLTRD(j)\ [\ S(j) - F(j)\ ] \qquad (8.21)$$

where:

SWSAT(j) = saturated moisture content (vol/vol)
SWFC(j) = field capacity (vol/vol)
SMC(j) = antecedent moisture content (vol/vol)
DLTRD(j) = thickness of layer (mm)
j = layer index

The depth of saturation , DS (mm), following

VINF = infiltrated volume, mm
DRNBLV(n) = drainable volume from layer n
S(n) = storage available for saturation, mm
F(n) = storage available up to field capacity, mm
Θs, Θfc & Θi = saturated, field capacity and initial moisture contents, cm3/cm3.

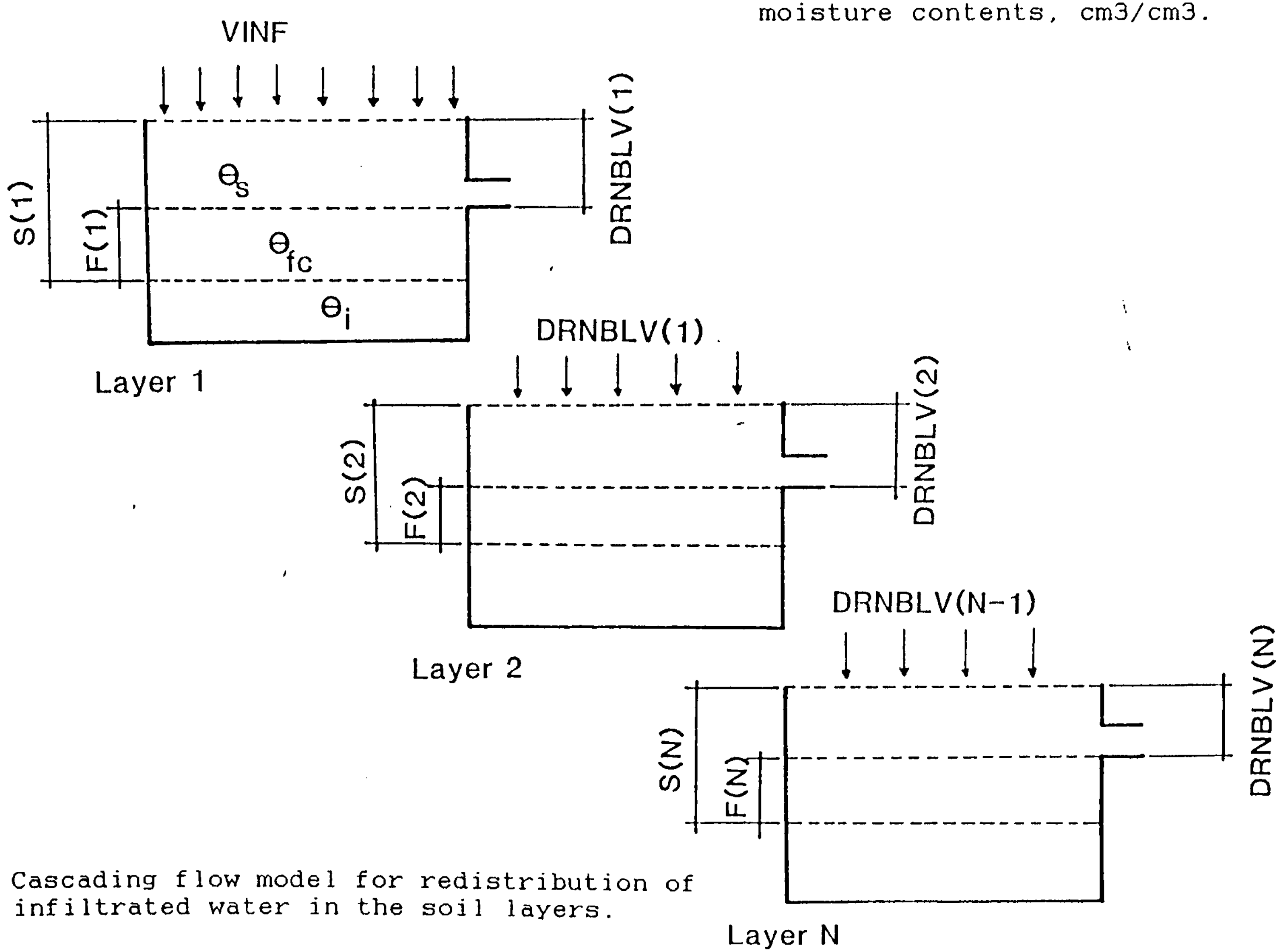

Fig. 8.5 Cascading flow model for redistribution of infiltrated water in the soil layers.

infiltration of a volume VINF (mm) of water is calculated by:

$$DS = \frac{DVINF}{S(i)} DLTRD(i) + \sum_{j=1}^{j=k} DLTRD(j) \qquad (8.22)$$

where:

$$DVINF = VINF - \sum_{j=1}^{j=k} S(j) \qquad (8.23)$$

and

VINF = infiltrated volume (mm)
k = layer index
i = k + 1 = layer number containing DS.

The position of DS relative to the layer boundaries is determined initially by the condition that:

$$\sum_{j=1}^{k} S(j) < VINF \leq \sum_{j=1}^{i} S(j) \qquad (8.24)$$

The depth of saturation (DS), represents the position of the wetting front immediately after the supply of water at the surface is terminated.

Having established DS , the total drainable volume , CDRNBL (mm), from the saturated zone , can now be calculated by:

$$CDRNBL = \sum_{j=1}^{k} DRNBLV(j) + DS'' \, [S(i) - F(i)] \qquad (8.25)$$

where:

$$DS'' = DS - \sum_{j=1}^{k} DLTRD(j) \qquad (8.26)$$

The total remaining fillable storage volume, CREMV (mm), below DS, is calculated by:

$$CREMV = \sum_{j=i+1}^{NL} F(j) + F(i) \left(1- \frac{DELTA}{DLTRD(i)} \right) \qquad (8.27)$$

where:

$$DELTA = DS - \sum_{j=1}^{i-1} DLTRD(j)$$

and where NL is the number of layers in the profile; i is the layer number that contains the saturation front (DS).

This 'total drainable volume (CDRNBL)' can now be routed through the layers below, filling each layer to it's field capacity before flowing to the next. This process continues untill all the drainable volume has been redistributed.

The lower boundary can be either drained or undrained. In either case two conditions can be encountered by the draining water:

1)	Drained :	CDRNBL $\leq$ CREMV	(8.28a)
2)	Drained :	CDRNBL $>$ CREMV	(8.28b)
3)	Undrained :	CDRNBL $\leq$ CREMV	(8.28c)
4)	Undrained :	CDRNBL $>$ CREMV	(8.28d)

Cases 1 and 3 may be considered the same since the drainable volume is not sufficient to flow down to the profile bottom and so the drained or undrained status of the lower boundary does not effect the redistribution model in these two cases. The possible effect of resistance to flow from air voids in the case of the undrained profile is assumed to be negligible.

The three cases are shown diagramatically in Fig. 8.6 . In case A , all the drainable volume will redistribute itself among the lower layers untill each layer is filled to field capacity before flowing to the next. Where the flux is sufficient to only partially wet a layer, it is assumed to be uniformly distributed in that layer.

In the case B , since the drainable volume is larger than the fillable storage volume, all layers are wetted to field capacity and any excess water is drained from the profile.

The third case, C , is when the profile is

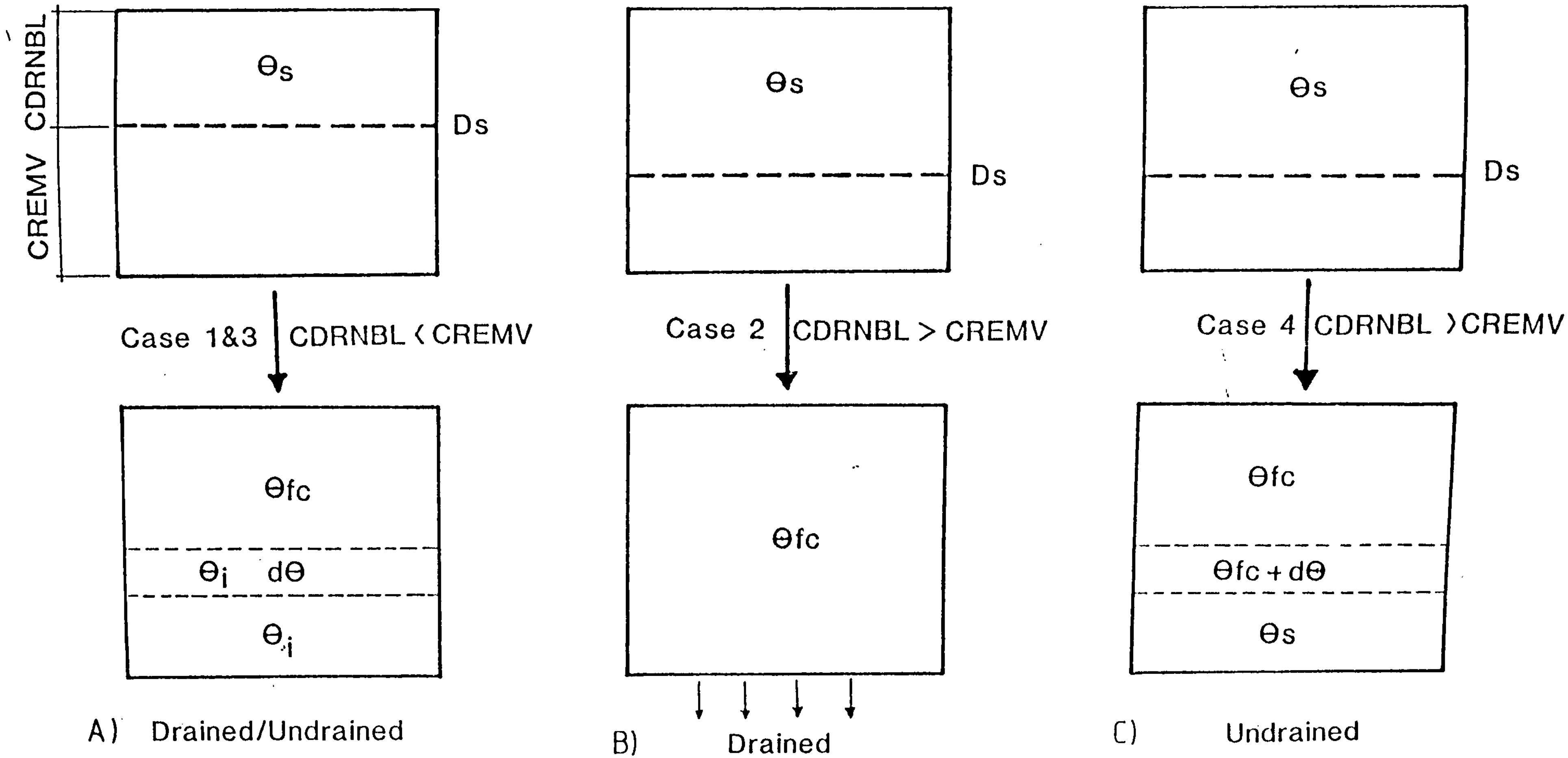

Fig. 8.6 Three possible flow conditions at the lower boundary of the soil profile (CREMV = remaining fillable storage, mm; CDRNBL= drainable volume, mm; Ds = depth of saturation, mm; Θs, Θfc & Θi = saturated, field capacity and initial moisture contents, cm3/cm3).

not drained and the drainable volume, having filled all the fillable storage, begins to fill the lower layers to saturation. If the excess water is not sufficient to fill a layer totally to saturation, it is distributed uniformly in that layer.

<u>Distribution opportunity time:</u>

The minimum time rquired for redistribution TDMIN (min), is controlled by the minimum saturated hydraulic conductivity of the profile and is approximated by:

$$TDMIN = CDRNBL - SATKm(j) \tag{8.29}$$

where:

SATKm(j) = minimum saturated conductivity in the saturated zone (mm/min)

The model now checks for two conditions which can exist, given the duration of rain gap TRGAP :

<u>condition 1</u> TDMIN $\leq$ TRGAP :

In this case there is enough time for the redistribution of the infiltrated water before the onset of the next rainstorm. The model outputs the new soil moisture contents, which in turn cause the new infiltration parameters to be determined by the infiltration model, in time for the onset of the next rain. The infiltration opportunity time t , in Eqn. 8.18 , is now relative to the beginning time of the new storm and ponding and pseudotimes are once more calculated for this new process.

condition 2 TDMIN > TRGAP :

When the minimum required time for redistribution (TDMIN), is longer than the time gap between two successive rain events (TRGAP), then it is assumed that the infiltration rate is a continuation of the previous process as defined by the parameters established at the beginning of the last rainstorm. At the onset of the next rain, the time axis of the infiltration rate curve is shifted by the amount TRGAP. This assumes that when TDMIN > TRGAP , the infiltration rate at the beginning of the rain event is equal to the infiltration rate at the end of the previous rain period. ie: at the start of next rain:

$$f = a\,(\,t - TRGAP - tp + ts\,)^{-b} \qquad (8.30)$$

This is illustrated in Fig. 8.7. When rain terminates, redistribution starts and there is a corresponding increase in the infiltration rate as the top soil layers drain from saturation to field capacity or lower. This recovery in the infiltration rate is represented by the difference between f(t') and f(t'') in Fig. 8.7, and forms the basis of the assumptions made above.

The redistribution model is applied at the end of each period of continuous rain, thus defining the infiltration and runoff characteristics for the

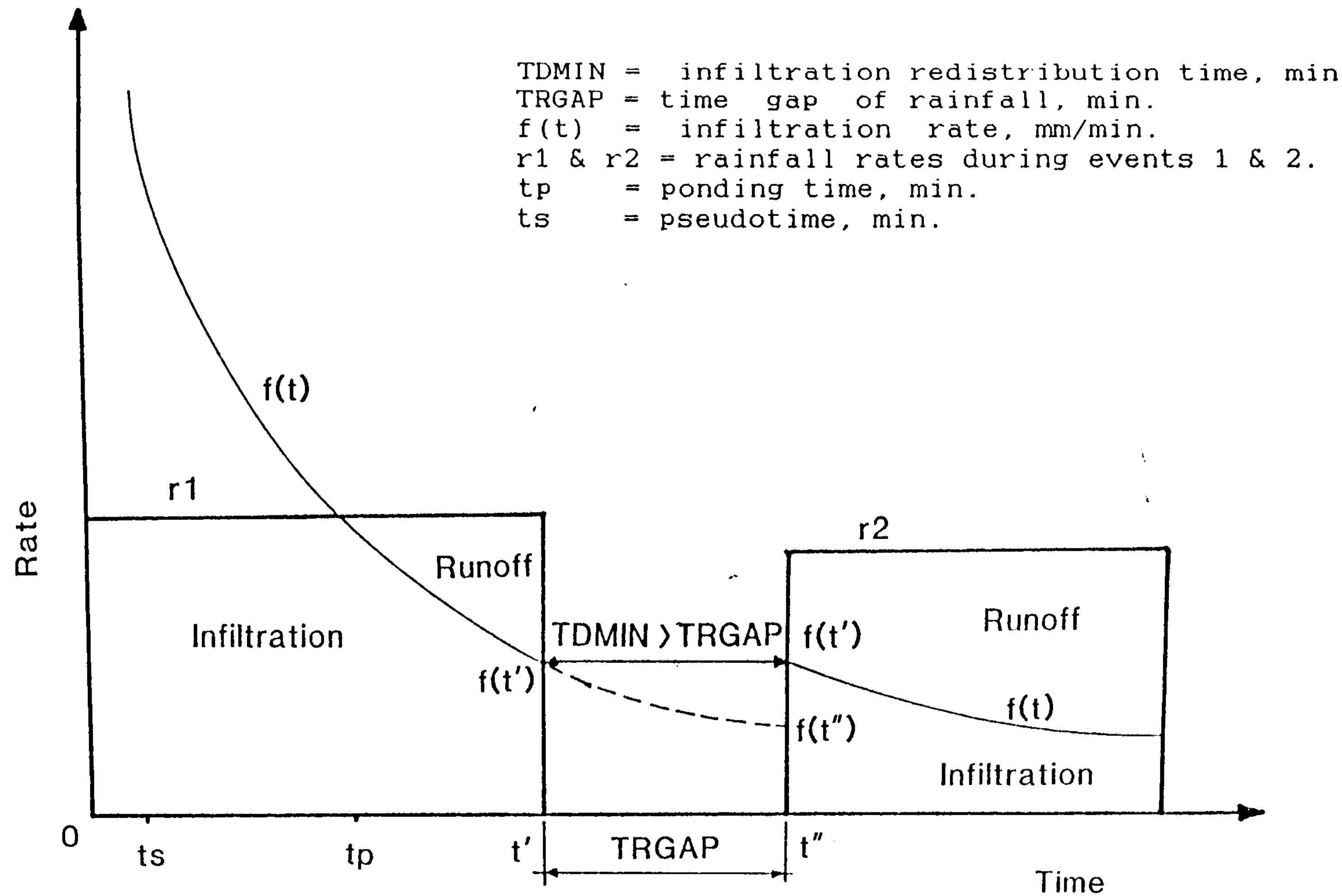

Fig. 8.7 Schematic diagram of infiltration under intermittent rainfall when rain gap is less than redistribution time

next period of rain, depending on wether condition 1 or 2 is satisfied.

Drainage:

Drainage from any depth within the soil profile, eg: the root zone, is calculated as the sum of the drainable volume passing through that depth at the end of a rain event:

$$RZDRN = VINF - \sum_{j=1}^{NLRZ} F(j) \qquad (8.31)$$

where :

RZDRN = cumulative drainage (mm) from layer NLRZ.
NLRZ = number of layers in the considered depth eg: rootzone or profile depth.
(other terms as defined previously).

8.3.1 Validation of the PERM Model :

The PERM model was tested with the data presented by Chu (1978). Three rainfall events are considered for a 113 acre watershed described as steep (slope mostly > 5%) and covered in pasture. Half of the watershed is in sandy loam, the other half in silt loam. The average soil properties are given as :

$$Ks = 0.237 \text{ mm/min} \qquad (8.32a)$$

$$SM = Pw\ (\theta s - \theta i) = 36.0 \text{ mm} \qquad (8.32b)$$

where:

Ks = saturated hydraulic conductivity (mm/min)
θs = saturated moisture content (cm3/cm3)
Pw = wetting front pressure (mm)
θi = initial moisture content (cm3/cm3)
SM = soil moisture parameter

The rainfall data are shown in Table 8.2 for all three cases. Apart from the values given in Eqn 8.32 , detailed soil property data necessary for running PERM was lacking. However, given the soil type, the following parameters were estimated using the statistically derived data of McCuen etal (1981) for a sandy loam-silt loam soil (see chapter 5) :

saturated moisture content, θs = 0.421 (cm3/cm3)

wetting front pressure, Pw = 237 (mm)

The moisture content at field capacity is estimated by the empirical model of Clapp & Hornberger (1978) :

field capacity, θfc = 0.324 (cm3/cm3)

Thus the initial soil moisture can be estimated from Eqn. 8.32b :

initial moisture content: θi = 0.269 (cm3/cm3)

It is assumed that the profile depth is 1.5 m and that the soil in all layers is uniform in properties. The profile is divided into 5 layers with the top 4 layers at the initial moisture content and the last layer at field capacity. The soil physical

Table 8.2 Input rainfall data for 3 rainfall cases used in testing the PERM model.

Rain Event	starting Time, min	Duration min	Intensity mm/min
Case 1	June 30 1957		
1	0	5	0.254
2	40	15	1.355
3	55	15	0.033
Case 2	April 3 1958		
1	0	430	0.048
2	430	10	0.049
3	440	5	0.665
4	445	10	0.254
5	455	5	0.762
6	460	15	0.033
7	475	5	0.660
Case 3	Sept. 9 1959		
1	0	5	0.608
2	5	15	1.152
3	20	15	1.660
4	35	30	0.822
5	65	15	0.255

Table 8.3 Assumed soil physical parameters for all 3 rainfall case studies used to test PERM.

Layer No	Thickness mm	Ks mm/min	θs	Pw mm	θfc	θi
1	250	0.237	0.421	237	0.324	0.269
2	250	0.237	0.421	237	0.324	0.269
3	250	0.237	0.421	237	0.324	0.269
4	250	0.237	0.421	237	0.324	0.269
5	500	0.237	0.421	237	0.324	0.324

* key:

Ks = saturated hydraulic conductivity (mm/min)
θs = saturated moisture content (cm3/cm3)
Pw = wetting front pressure (mm)
θfc = field capacity (cm3/cm3)
θi = initial moisture content (cm3/cm3)

properties are summarized in Table 8.3 .

The PERM model was run for each of the rainfall cases and the results compared to those of Chu's model (Table 8.4). Interception and evaporation losses have been assumed negligible. The total daily runoffs simulated by both models compare fairly with the recorded runoffs, except for case 2 where both models predicted well below the recorded value. The accuracy of the recorded value for this case may be questionable since both models predicted similar results.

The simulated variation of infiltration and runoff rates for the 3 rainfall cases are shown in Figs. 8.8, 8.9 and 8.10 respectively. Note that the runoff rates do not represent overland and channel routed runoffs but point generated excess rainfalls. Assuming that the area of the elementary watershed is small, it can be treated as a point source and the total volume of rain excess will be close to the watershed runoff (Chu 1978).

Table 8.4 Results of PERM simulated infiltration and excess rainfall runoff and comparison with Chu's model and recorded values.

Case No	Model	Rain mm	Simulated Inf'n. mm	Simulated Runoff mm	Recorded Runoff mm	% Diff.
1	PERM	22.1	16.30	5.88	4.60	+27.8
	Chu		17.80	4.30		-6.52
2	PERM	34.6	32.77	1.84	5.10	-63.9
	Chu		32.40	2.20		-56.9
3	PERM	73.7	47.65	26.06	25.40	+2.6
	Chu		45.9	27.80		+9.4

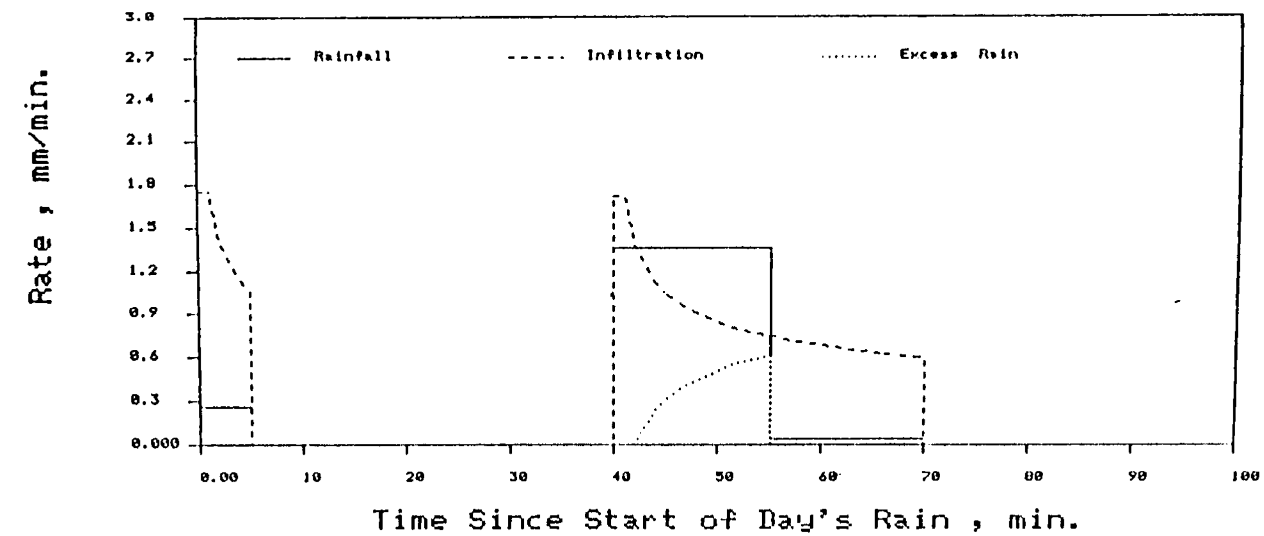

Fig. 8.8 Simulated excess rainfall and infiltration rates (case 1 of Table 8.2).

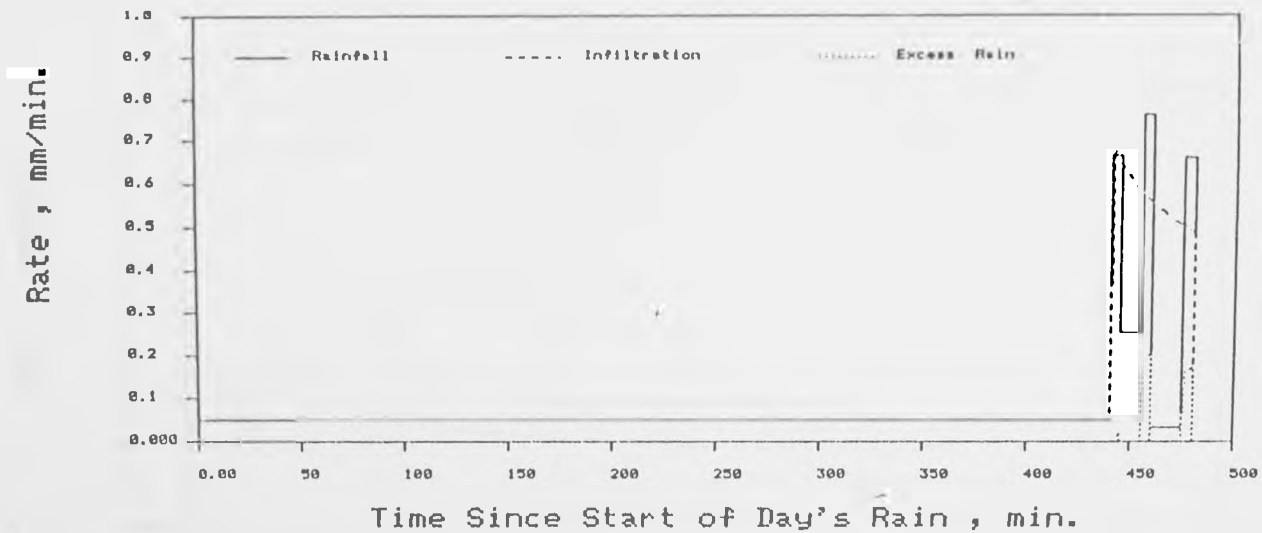

Fig. 8.9 Simulated excess rainfall and infiltration rates (case 2 of Table 8.2).

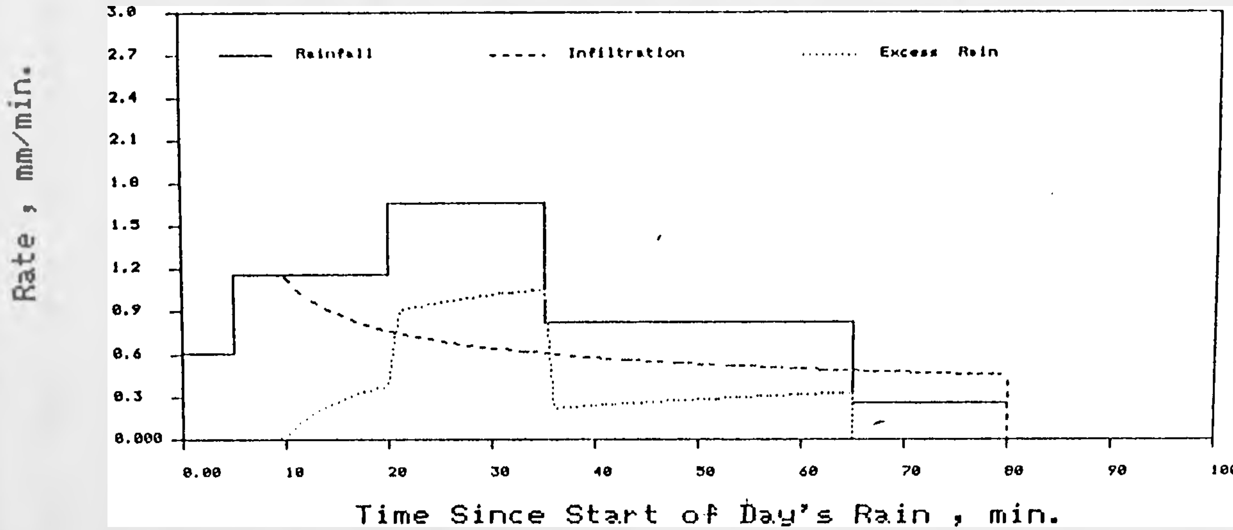

Fig. 8.10 Simulated excess rainfall and infiltration rates (case 3 of Table 8.2).

8.3.2 Model Sensitivity:

The infiltration process plays the major role in the water balance calculations of PERM. Thus the parameters to which the one dimensional infiltration model (chapter 6), is sensitive will also effect this model. These parameters constitute the physical properties of the soil (Table 8.3), and are therefore expected to also influence the sensitivity of the redistribution model.

Each soil parameters were increased in turn by ±10% and the corresponding change in the predicted runoff was observed. The results of the sensitivity run for case 3 are shown in Table 8.5 and discussed below:

a) θs – A 10% change in this parameter , which defines the upper limit of soil moisture storage, causes roughly a 15% change in the runoff. This is the parameter to which PERM is most sensitive.

b) Ks & θi – Changing these two parameters by 10% caused an approximately equal change in the predicted runoff. Note that increasing θi also increases runoff since less soil storage is available for infiltration. In contrast increasing Ks leads to higher infiltration and redistribution rates thus lowering the runoff rate.

c) Pw – Changing the wetting front pressure by 10% only causes about half as much change in the predicted runoff, suggesting that the infiltration model is moderately sensitive to this parameter.

Table 8.5 Sensitivity analysis of PERM to the soil parameters for case 3.

% Change of Parameter	Simulated Runoff	% Change of Runoff
+ 10% Thickness − 10%	26.27 26.06 25.90	+ 0.8 − 0.6
Ks	23.64 26.06 28.61	− 9.3 + 9.8
θs	22.65 26.06 30.30	−13.1 +16.3
Pw	24.84 26.06 27.38	− 4.7 + 5.1
θfc	26.06 26.06 26.06	0.0 0.0
θi	28.90 26.06 23.54	+10.9 − 9.6

* key:

Ks = saturated hydraulic conductivity (mm/min)
θs = saturated moisture content (cm3/cm3)
Pw = wetting front pressure (mm)
θfc = field capacity (cm3/cm3)
θi = initial moisture content (cm3/cm3)

d) Layer thickness & θfc - The model is not sensitive to changes in the soil layer thickness. A response of only about 0.7% to a 10% change in thickness is not significant . The surprising result however is the lack of any response to changes of θfc, even though this parameter defines the upper limit of non-drainable storage in the redistribution model.

8.3 Discussion:

The PERM model was developed to overcome the shortcomings of the other models reviewed in this section, by taking into account soil non-homogeneity and antecedent soil moisture nonuniformity, as would be met particularly in cultivated lands. The PERM model is a point-source excess rainfall generating model which is capable of handling continuous or intermittent rainfall applications. The model divides the incoming rain into it's various hydrological components and by utilizing an infiltration model and a redistribution model, generates runoff rates at one minute intervals and predicts the total daily infiltration , drainage and runoff volumes.

The soil parameters required for the running of the model are all physically based and can be measured in the field. Where accurate field data are not available, these parameters can be estimated from the soil type alone by empirical means (eg: McCuen etal 1981, Clapp & Hornberger 1978; see chapter 5).

Although the model is designed to handle variable soil properties, due to lack of measured field data it was only possible to test the model with the data of Chu (1978), which is for a uniform soil (Tables 8.2 to 8.4). The PERM model overpredicted the runoff for case 1 by about 28% , whereas Chu's model underpredicted by 6% . The second case showed the two simulation models underpredicting by about 60% each, raising doubts about the validity of the recorded runoff. Case 3 was more promising with PERM overpredicting runoff by only 2.6% while Chu's model overpredicted by 9.4% .

Bearing in mind the assumption concerning the profile thickness and the approximation of the soil parameters, the results of this new and more flexible method for simulating point excess-rainfall, from intermittent rainfall, are promising. Further detailed field studies to establish more accurate soil parameters, will improve the potentials of the model for inclusion in larger scale hydrological models.

The model is particularly suitable for simulating the water balance under sprinkler irrigation systems and fascilitating the evaluation of operational efficiencies for various sprinkler application rates and durations. This task is undertaken in the next chapter .

CHAPTER 9 MODELLING THE OPERATIONAL PERFORMANCE OF SPRINKLER IRRIGATION SYSTEMS.

9.1 Introduction :

The method of irrigation by the overhead sprinkling of water was introduced in chapter 8. In this chapter a theoretical analysis of the operational performance of sprinkler irrigation is undertaken. A model is proposed which utilizes the point excess-rainfall model (PERM) of chapter 8, and the assumption of a spatially normally-distributed pattern of application rate, to simulate the water balance under the area of coverage of a single sprinkler nozzle.

The objective is to derive a method whereby, given the mean application rate and duration, for a sprinkler unit of known application-rate distribution characteristics, the irrigation efficiencies and the uniformity of application can be evaluated for different soil types and antecedent root zone moisture conditions.

The various efficiency terms were defined in chapter 2. The irrigation uniformity is closely related to the distribution efficiency, and is expressed mathematically by the uniformity coefficient. In sprinkler irrigation, losses can be due to direct evaporation, evapotranspiration, wind transport, interception, runoff and deep percolation.

In this study, two performance criteria, the application efficiency and the uniformity coefficient, are chosen for particular analysis. The application efficiency (Ea), is a measure of the losses of water on the field, relative to that applied by the sprinkler. The uniformity coefficient (Uc), is a measure of the spatial distribution of the applied depth of water. It is closely related to the distribution efficiency (see Eqn. 9.22), and reflects the sum of the drainage and deficiencies, relative to the applied water.

Both Ea and Uc are therefore related to the discharge characteristics of the sprinkler unit and thus serve as appropriate criteria for evaluating system performance.

The use of a uniformity coefficient (Uc) was first proposed by Christiansen (1942), cited in Hagen etal (1967), and is defined by the expression :

$$Uc = 1 - \frac{\sum_{i=1}^{N} z(i) - \bar{z}}{N \cdot \bar{z}} \qquad (9.1)$$

where:

$z(i)$ = individual observation of applied depth(mm)

$\bar{z}$ = mean of N single observations of depth.

Note that Uc has a maximum value of 1.0 for absolute uniformity and approaches zero as deviations from the mean increase. In practice, the higher the value of Uc, the more desirable is the system.

Hillel (1987) states that " water application uniformity under sprinkling depends on the uniformity of the sprinklers and not on soil properties, so long as the application rate does not exceed infiltratrability ". Also that " the precise tailoring of application rate to soil properties and crop water requirements is difficult to achieve and generally involves trial and error experience under local conditions ".

Walker (1979) points out that the conditions under which a sprinkler distribution pattern is tested should be representative of the average field-operating condition; and that it is generally assumed that the uniformity data, in the shape of surface-collected water depths, also represents the surface distribution of water over the field after an irrigation.

9.2 Sprinkler performance evaluation model :

The uniformity of water application under a sprinkler system is conventionally evaluated by measuring the rate of application, at random positions along the wetting radius and wetted area. The depths of water , collected in cans placed on the soil surface for the duration of discharge, indicate the application rates received at those positions in the field.

The distribution of the collected water depths is generally assumed to follow a 'normal' (or Gaussian) distribution (Walker 1979). Wind effects can cause this distribution to become skewed. The performance of sprinkler irrigation systems under such skewed application patterns has been studied by Seginer (1969), Seginer & kostrinsky (1975), and Chaudhry (1978). The effects of wind are not pursued here.

The probability density function (PDF) of a standardized normal distribution can be expressed mathematically by (Chatfield 1983):

$$f(x) = \frac{1}{2\pi} \exp\left(-(x)^2/2\right) \tag{9.2}$$

where x is the standardizing factor :

$$x = (y - \bar{y})/S \tag{9.3}$$

and y is the measured rate (mm/min); $\bar{y}$ is the mean of measured rates (mm/min); and S is the standard deviation .

The cumulative distribution function (CDF) is defined as the area under the PDF curve, and is found thus:

$$Q(x) = \frac{1}{(2\pi)^{1/2}} \int_{x}^{\infty} \exp\left(-(x)^{2}/2\right) \qquad (9.4)$$

A plot of Q(x) versus Y is shown in Fig. 9.1, where Y is a dimensionless depth defined as :

$$Y = y / \bar{y} \qquad (9.5)$$

The shape of the CDF curve depends on the spread of the variables about the mean. A normalised measure of spread is the coefficient of variation (Cv), defined as the ratio of the standard deviation to the mean:

$$Cv = S / \bar{y} \qquad (9.6)$$

A high value of Cv represents a wide spread about the mean. This is reflected in Fig. 9.1 where for Y=1.4 and Cv=0.5, the fractional area that recieves a normalized depth greater than 1.4 is about 0.15 . The corresponding value for Cv=0.3 is 0.8 and for Cv=0.2 it is 0.04 . Thus the smaller the coefficient of variation , the smaller is the spread about the mean. Values of Y

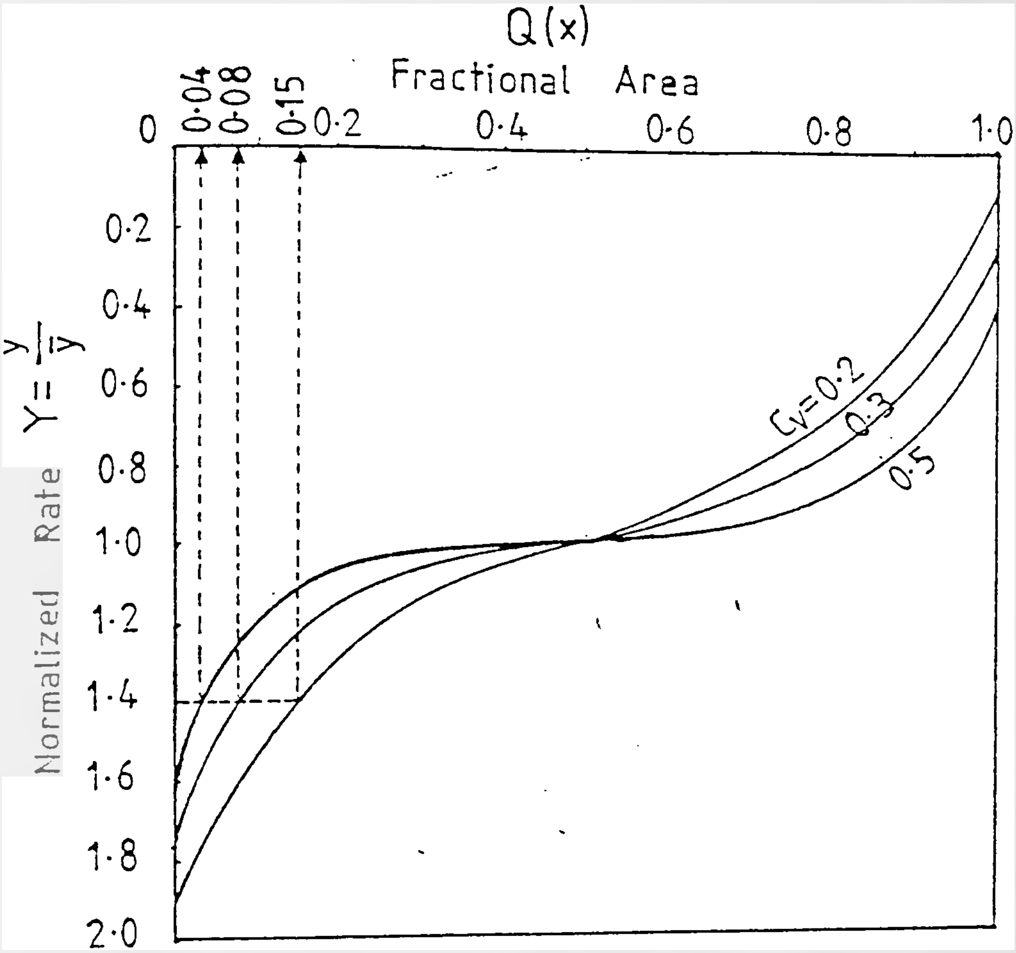

Fig. 9.1 Schematic diagram of cumulative distribution function for different coefficients of variation (Cv).

greater than 2 characterize very poorly operated or designed sprinkler systems with corresponding Cv values greater than 0.5, which may not be considered normally distributed (Walker 1979).

The hypothesis put forward here is that the application uniformity, as measured by an array of catch cans placed on the soil surface, and statistically characterized by the coefficient of variation Cv, cannot simply be assumed to be the same as that application uniformity measured from the distribution of the depths of infiltration over the field.

The type of soil and crop, the sprinkler discharge rate and duration of irrigation, and the antecedent soil moisture conditions, all effect the horizontal and vertical distribution of water under a sprinkler unit. Therefore, the application uniformity, or it's mathematical expression, the uniformity coefficient Uc, cannot be assumed to be a unique property of the sprinkler unit. The application efficiency must also be independent of the sprinkler discharge characteristics (as measured by the coefficient of variation Cv), and dependent on the soil properties.

The model developed here incorporates such variables as application rate and duration, sprinkler coefficient of variation, and the soil properties, in an effort to investigate their influence on sprinkler irrigation performance.

In this model the fractional area in Fig. 9.1 is assumed to also represent the fractional area under the sprinkler that recieves a normalized depth Y. The distribution of application rates in the field is therefore characterized by the cumulative frequency diagram and the parameters of the normal distribution function, namely the mean and the variance (square of standard deviation).

The area under the CDF curve is given by Eqn. 9.4 . Walker (1979) gives a polynomial approximation for its solution for positive values of x :

$$Q(x) = f(x).(B1.\ t + B2.\ t^2 + B3.\ t^3 + B4.\ t^4 + B5.\ t^5) \qquad (9.7)$$

where :

$$t = 1/(1 + 0.2316419\ x) \qquad (9.8)$$

and B1= 0.31938153; B2= -0.356563782; B3= 1.781477937; B4= -1.821255978; and B5= 1.330274429.

For negative x values the following equation is given :

$$Q(x) = 1 - Q(-x) \qquad (9.9)$$

Equations 9.7 and 9.9 determine the fractional area under a sprinkler that recives an application rate greater than 'y' (x is related to y through Eqn. 9.3). Since we now have a relationship between applied rate and the receiving area, the uniformity coefficient and the various irrigation efficiencies can be evaluated by a volume accounting model.

The spatial variability of application rate means that, during the period of irrigation, some parts of the total area under sprinkling will receive less water and some more water than the average application rate. To evaluate the volume of interception, evapotranspiration, infiltration and deep percolation under a particular rate, the point excess-rainfall model (PERM) of chapter 8 is used to seperate the total point-applied depth into its hydrological components. These point depths (ie: depths per unit area) are then multiplied by the fraction of the total area which received that rate, to yield the appropriate volumes.

For any normalized application rate (Y) the fraction of the total area receiving Y is approximated by discretizing the dimensionless rate axis in the CDF curve into 20 equal segments. The fractional area corresponding to the rate Y (Fig. 9.2), is then calculated by:

$$Q(Y) = Q(Y-0.1) - Q(Y+0.1) \qquad (9.10)$$

The volume balance equation, for any segment receiving

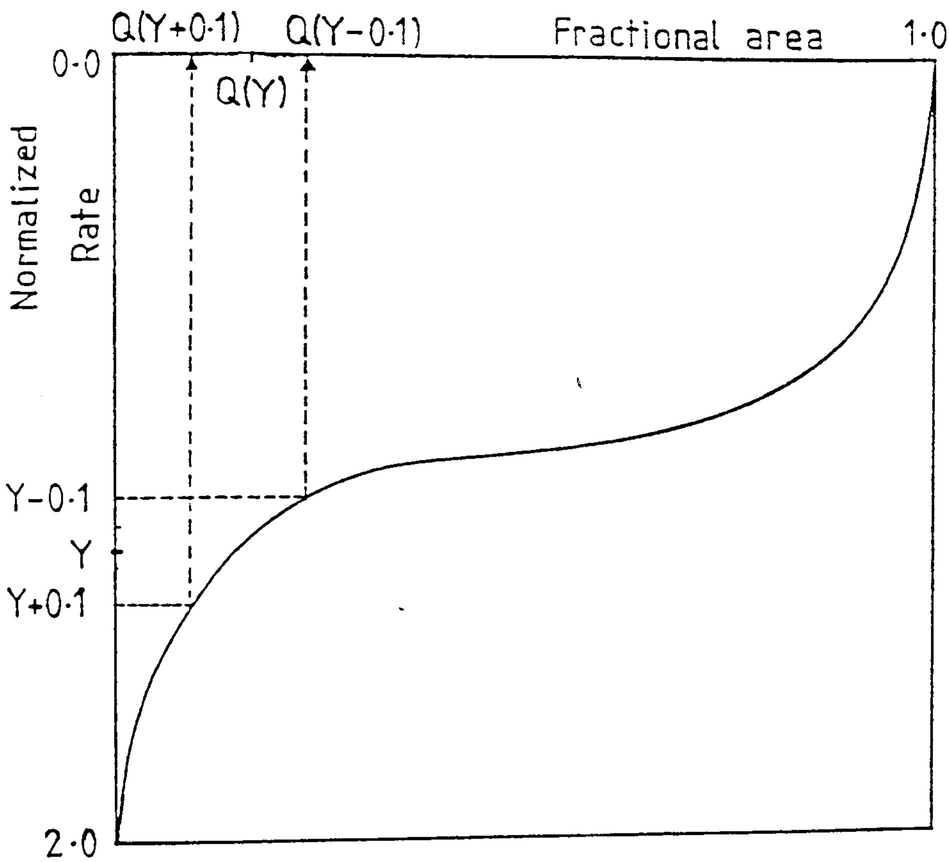

Fig. 9.2 Determination of the fractional area Q(Y), under normalized rate Y.

the rate Y, is therefore:

$$(Y.\bar{y})\ D = R(Y) + F(Y) + I(Y) + E(Y) \tag{9.10}$$

where:

$\bar{y}$ = mean application rate (mm/min).
D = sprinkling duration (min).
R(Y) = runoff depth due to rate Y (mm).
F(Y) = infiltration depth(mm).
I(Y) = interception depth (mm).
E(Y) = evapotranspiration depth (mm).

This procedure is repeated for all values of Y ranging from 0 to 2 at increments of 0.1 . It is assumed that where an application rate has a fractional area of less than 0.01 associated with it, that rate is considered relatively insignificant and ignored. The flow chart of the model is shown in Fig. 9.3. The total volumes at the end of the simulation are calculated thus :

a) Total applied volume, Vt (mm3):

$$Vt = D\ \bar{y} \sum_{Y=0.1}^{2.0} Y.\ Q(Y).\ As \tag{9.12}$$

b) Total runoff volume, Vr (mm3):

$$Vr = \sum_{Y=0.1}^{2.0} R(Y).\ Q(Y).\ As \tag{9.13}$$

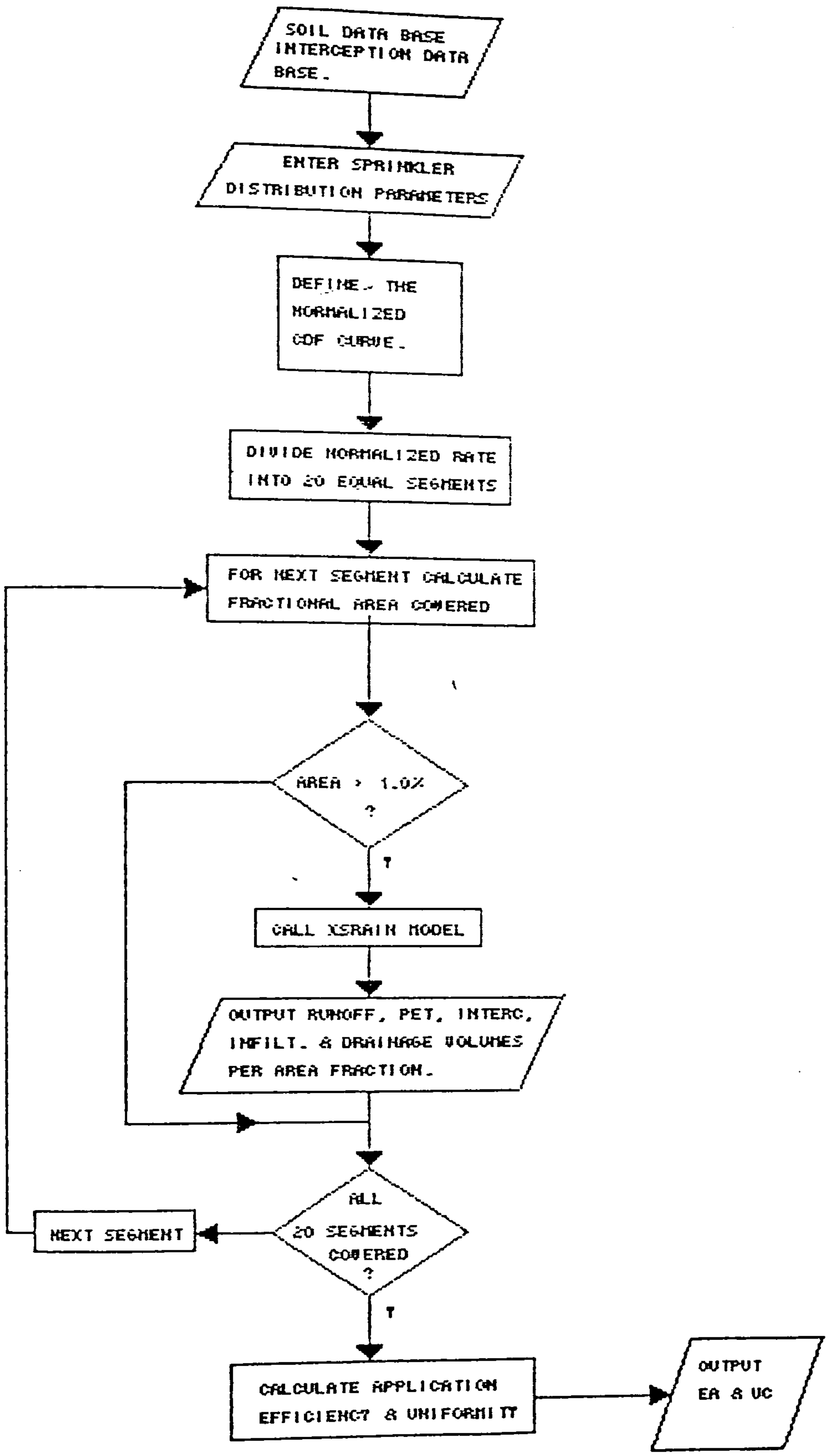

Fig. 9.3 Flow chart of the sprinkler efficiency evaluation model (SPRNDEFF).

c) Total infiltration volume, Vf (mm3):

$$Vf = \sum_{Y=0.1}^{2.0} F(Y) \,.\, Q(Y) \,.\, As \qquad (9.14)$$

d) Total interception volume, Vi (mm3):

$$Vi = \sum_{Y=0.1}^{2.0} I(Y) \,.\, Q(Y) \,.\, As \qquad (9.15)$$

e) Total evapotranspiration volume, Ve (mm3):

$$Ve = \sum_{Y=0.1}^{2.0} E(Y) \,.\, Q(Y) \,.\, As \qquad (9.16)$$

where 'As' is total area of sprinkler coverage (mm2).

The required irrigation depth (Dreq) is calculated in the excess-rainfall model as the depth of water required to restore the antecedent root-layer moisture contents to field capacity. The total rootzone drainage (Vd) is found from :

$$Vd = \sum_{Y=0.1}^{2.0} [\ F(Y) - Dreq\ ]\ Q(Y) \,.\, As \qquad (9.17)$$

where only positive values indicate the occurance of drainage.

The total deficit volume in the root zone

(Vdef) is calculated by the following equation:

$$Vdef = \sum_{Y=0.1}^{2.0} [Dreq - F(Y)] Q(Y) . As \qquad (9.18)$$

where only positive values indicate a deficit in the root zone.

The overall application efficiency of a sprinkler unit, characterized by a normal distribution with parameters '$\bar{Y}$' and 'Cv' , can now be evaluated using the following equation :

$$Ea = 100 (Vf - Vd)/ Vt \qquad (9.19)$$

The uniformity coefficient is calculated according to Eqn. 9.1 as :

$$Uc = 1 - \frac{\sum_{Y=0.1}^{2.0} (I(Y) - Ia \ . Q(Y) . As)}{Vf} \qquad (9.20)$$

where Ia is the average infiltration depth per unit area (mm):

$$Ia = Vs / 20 \qquad (9.21)$$

The distribution efficiency (Ed) is show by

Hart etal (1979) to be a function of the uniformity coefficient:

$$Ed = 100 (1 + Uc)/2 \tag{9.22}$$

The storage efficiency (Es) is calculated, according to Eqn. 2.2, by the following:

$$Es = 100 \left(1.0 - \frac{Vdef}{Dreq \,.\, As} \right) \tag{9.23}$$

The deficit/excess is then calculated according to Eqn. 2.4.

The common practice in sprinkler irrigation is to apply the water at a rate less than the final intake rate of the soil. In this way the runoff component is eliminated and Ea is controlled mainly by the drainage loss. Interception and evapotranspiration are often considered too small to be of note. Under such a practice the application efficiency will be high if the distribution of application rate is assumed uniform, but the spatial variability of this rate makes the evaluation of application efficiency that much more difficult.

The simulation model was run for the soil profile data in Table 9.1 . Interception loss was set at zero and the mean daily evapotranspiration was taken to be 10.0 mm. Table 9.2 shows a typical interactive input to the model , along with the overall volume totals and the simulated irrigation efficiencies and uniformity coefficient.

Table 9.1 Soil profile data set used in the sprinkler performance simulation model.

Layer No.	Thichness mm	Ks mm/min	θs cc/cc	Pw mm	θfc cc/cc	θi cc/cc
1	250	0.237	0.421	237	0.324	0.269
2	250	0.237	0.421	237	0.324	0.269
3	250	0.237	0.421	237	0.324	0.269
4	250	0.237	0.421	237	0.324	0.269
5	500	0.237	0.421	237	0.324	0.324

* Key:

Ks = saturated hydraulic conductivity (mm/min).
θs = saturated moisture content (cm3/cm3).
Pw = wetting front pressure (mm).
θfc = field capacity (cm3/cm3).
θi = initial moisture content (cm3/cm3).

Table 9.2 Example run of the sprinkler performance evaluation model (for soil profile data of Table 9.1).

```
----------------------------------------
SPRINKLER OPERATIONAL CHARACTERISTICS:
----------------------------------------

ENTER APPLICATION STARTING TIME      (min) = 360

ENTER MEAN APPLICATION RATE       (mm/min) = 0.75

ENTER APPLICATION DURATION           (min) = 360

ENTER SPRINKLER RADIUS OF COVERAGE     (m) = 10

ENTER SPRINKLER COEFFICIENT OF VARIATION   = 0.15

-----------------------------------------------
MEAN DAILY PET CONVERTED TO MINUTE PET:

RATE    RAIN     INFILT.   RUNOFF   EVAP.   RZ.DRAIN.  INTERC.  VOL.ERR.   AREA
mm/min  mm       mm        mm       mm      mm         mm       mm         FRACTION

 0.49   175.50   137.35    33.51    5.01     0.00      0.00     -0.37     .18924E-01
 0.56   202.50   140.56    57.08    5.01     0.00      0.00     -0.15     .68479E-01
 0.64   229.50   142.76    81.80    5.01     0.00      0.00     -0.08     .16132
 0.71   256.50   144.06   107.46    5.01     0.00      0.00     -0.04     .24732
 0.79   283.50   144.46   134.05    5.01     0.00      0.00     -0.02     .24757
 0.86   310.50   145.27   160.23    5.01     0.00      0.00     -0.01     .16132
 0.94   337.50   145.73   186.76    5.01     0.00      0.00     -0.01     .68479E-01
 1.01   364.50   145.90   213.59    5.01     0.00      0.00      0.00     .18924E-01
NSEGS =          8
AVINF =  5.6059241E+09
SDINF =  2.9168960E+10
TINF  =  4.4847390E+10

TOTAL APPLIED WATER       (m3) =   84.1
TOTAL INFILTRATION        (m3) =   44.8
TOTAL RUNOFF              (m3) =   37.7
TOTAL EVAPOTRANSPIRATION  (m3) =   1.56
TOTAL DRAINAGE            (m3) =  0.100E-08
TOTAL INTERCEPTION        (m3) =  0.000E+00
WATER BALANCE ERROR       (m3) = -0.148E-01

APPLICATION EFFICIENCY      (%) =  53.31
DISTRIBUTION EFFICIENCY     (%) =  67.48
STORAGE EFFICIENCY          (%) = 100.00
DEFICIT-EXCESS EFFICIENCY   (%) =  53.31
COEFFICIENT OF UNIFORMITY       =  0.350
```

The coefficient of uniformity is a measure of the distribution of the infiltrated depth about the overall mean depth. The coefficient of variation (Cv , Eqn. 9.6) is also a measure of the spread about the mean of the application rates. It would be expected that if the value of Cv was increased (ie: a greater range of rates were applied), Uc would decreases correspondingly since the spread of infiltrated depth about the overall mean would also increase with Cv. Fig. 9.4 shows that initially the response of Uc to changes in Cv is as expected but that above a Cv value of about 0.05 the uniformity coefficient shows an upward trend with some fluctuations. The magnitude of the mean application rate has little effect on the general response, with the higher rates showing slightly higher uniformity at high Cv values.

The sprinkler system coefficient of variability Cv, has little effect on the application efficiency Ea, (Fig. 9.5). At each mean application rate, Ea is near constant except for a slight gradual reduction as Cv is increased.

The effects of mean application rate and irrigation duration on the application efficiency (Ea) and uniformity coefficient (Uc) are shown in Figs. 9.6 and 9.7 respectively . For all durations Ea is at 100% until a threshold limit of application rate (about 0.5 mm/min) after which efficiency drops rapidly towards zero . For the same rate, shorter durations exhibit

Fig. 9.4 The effect of application rate and coeff. of variation on sprinkling uniformity.

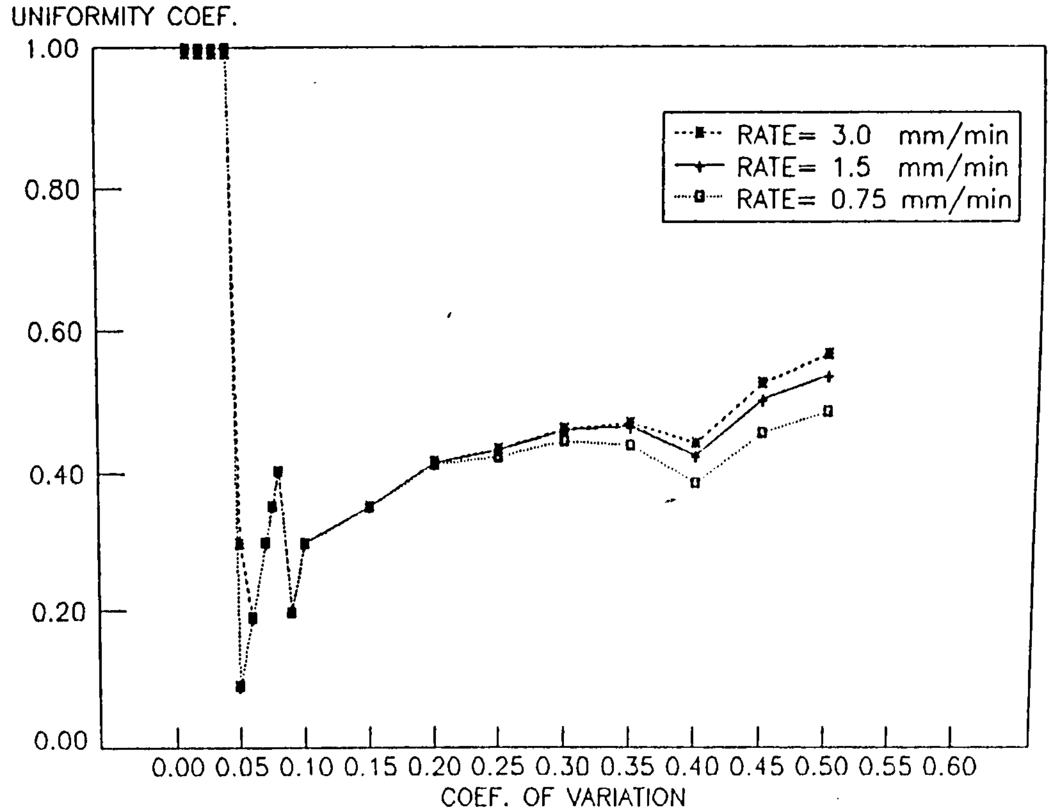

Fig. 9.5 The effect of coeff. of variation on the application efficiency (Ea).

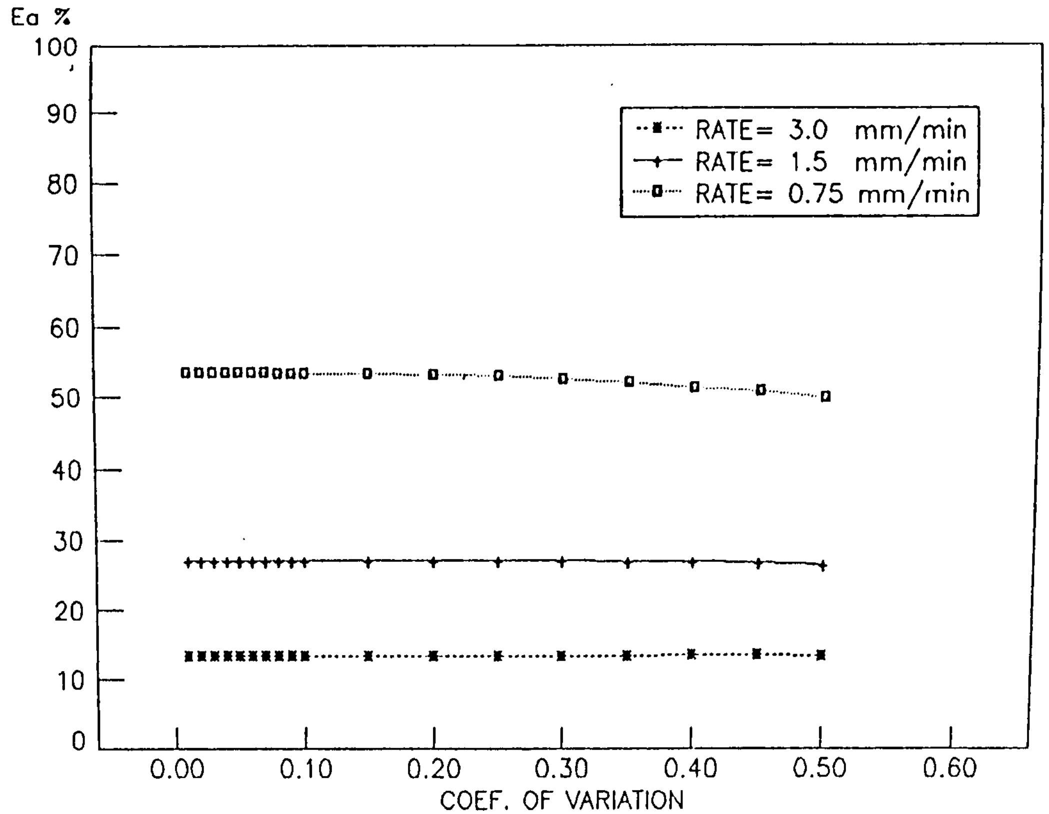

Fig. 9.6 The effect of rate and duration on application efficiency (Ea) for a normal distribution.

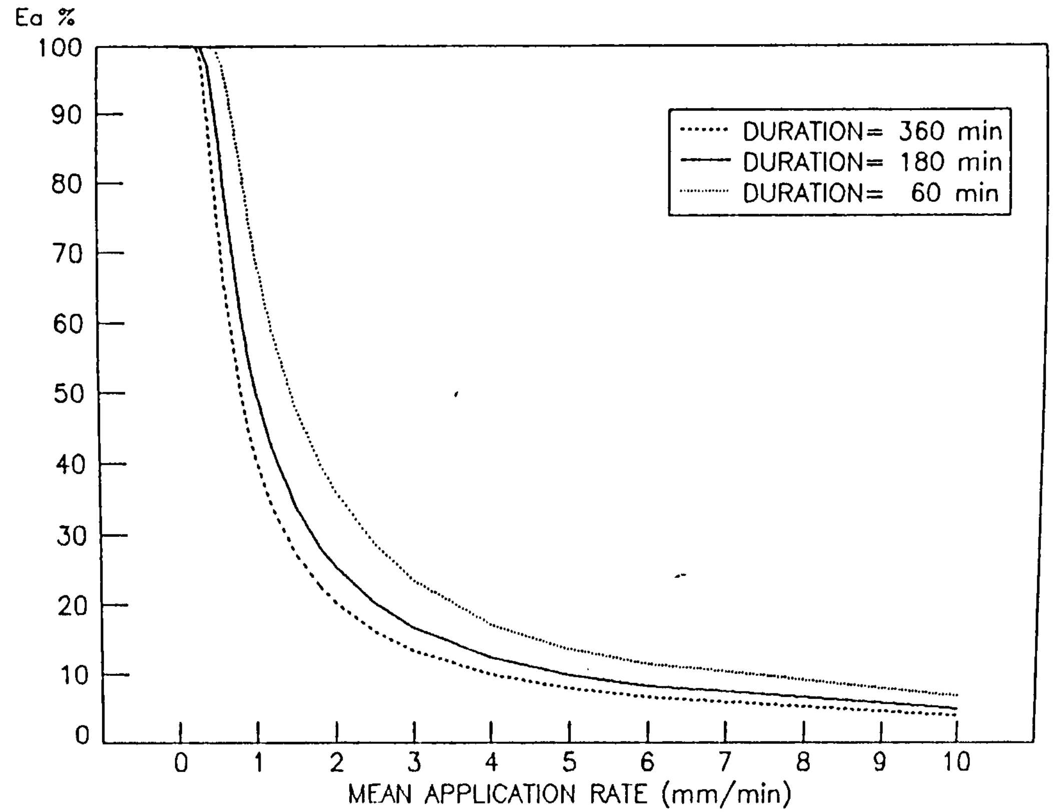

Fig. 9.7 The effect of rate and duration on the uniformity coefficient (Uc).

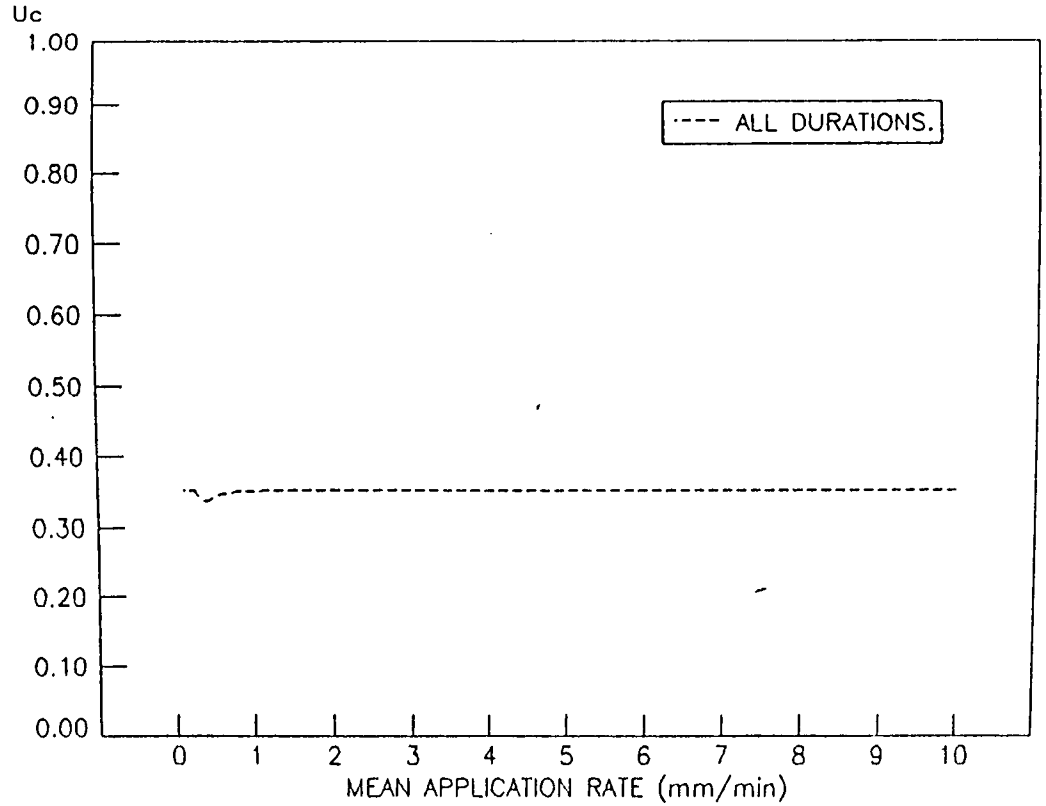

higher efficiencies. Figure 9.7 shows that except for an initial slight reaction, Uc remains constant for all mean application rates and durations.

Figure 9.8 shows the effect of saturated hydraulic conductivity (Ks) on Ea. As Ks is increased Ea increases from a low level to a peak, after which it declines as Ks is increased further. The three curves shown correspond to three different application rates. The low rate shows the peak efficiency to be the highest and is well defined. The greater the application rate, the lower is the peak efficiency. The rising limb of the curves correspond to efficiency loss due to excessive runoff from soils with low conductivity; while at higher conductivities the loss is due mainly to drainage from the root zone. There is an optimum soil hydraulic conductivity which will maximize the application efficieny for a given rate and duration.

Figure 9.9 shows the effect of the saturated hydraulic conductivity (Ks) on the uniformity coefficient (Uc). At low Ks values, Uc remains constant at about 0.35. The Uc curve then dips slightly as Ks is increased, before recovering. The mean application rate has no effect on the simulated Uc curve.

The effect of initial soil moisture content (θi) on Ea is shown in Fig. 9.10 . Application efficiency (Ea) starts high for low initial moisture

Fig. 9.8 The effect of application rate & saturated conductivity on application efficiency (Ea).

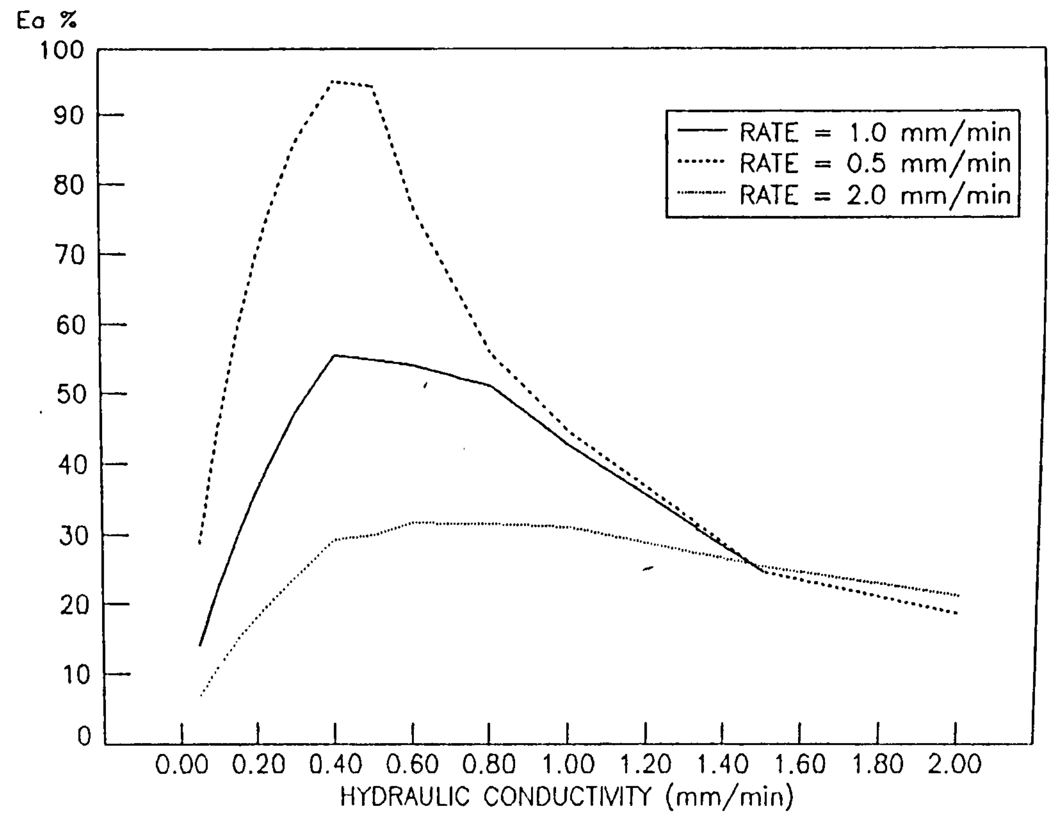

Fig. 9.9 The effect of application rate & saturated conductivity on uniformity coefficient (Uc).

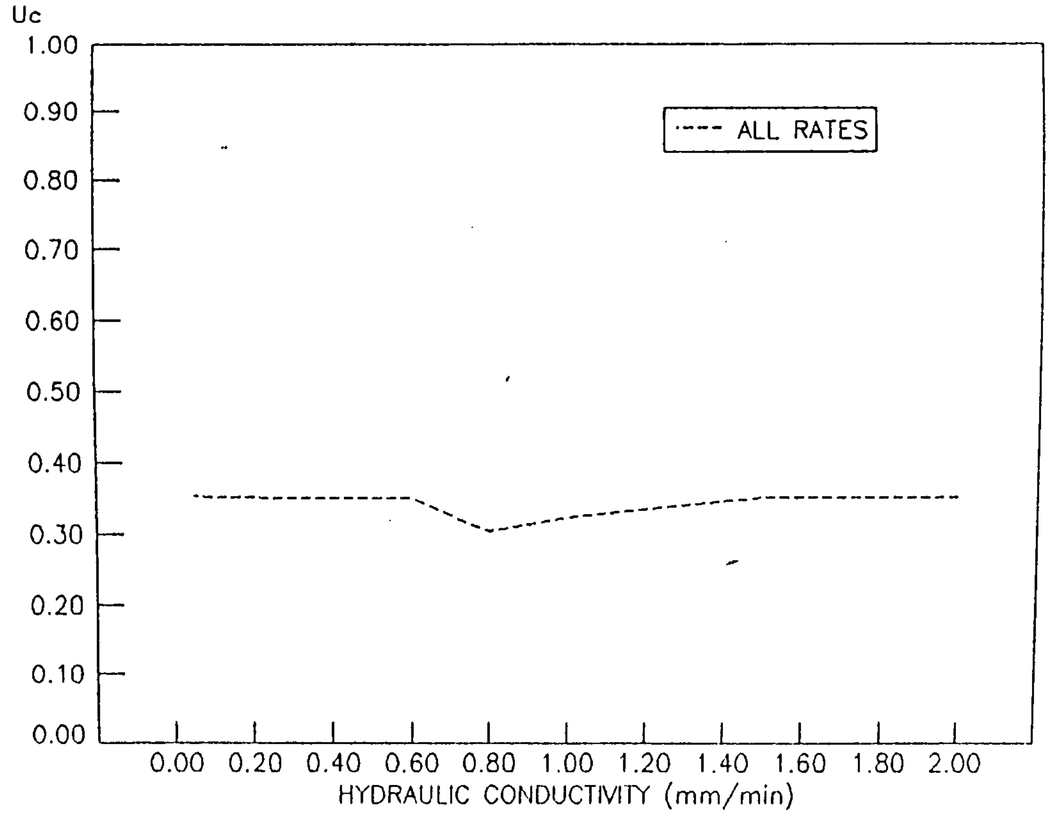

Fig. 9.10 The effect of initial soil moisture content on application efficiency (Ea).

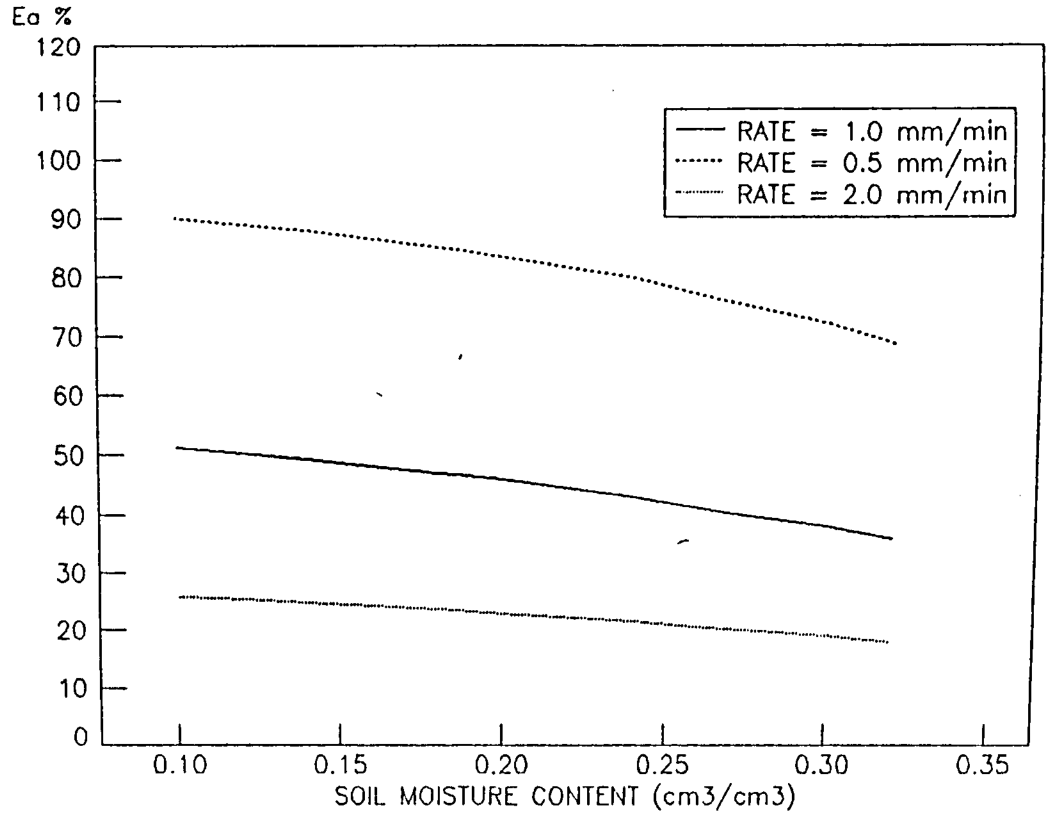

contents and decreases gradually as θi is increased. Low application rates show higher efficiencies at all moisture content levels. The loss in Ea, as θi is increased, is due both to increased runoff and drainage losses. The initial soil moisture content has no effect on the uniformity coefficient (Fig. 9.11).

The simulation results show that the irrigation uniformity is only slightly effected by mean application rate and its response to the system Cv varies as shown in Fig. 9.4 . This figure seems to suggest that a sprinkler unit with low application rate uniformity (ie: high Cv), may not result in a correspondingly low irrigation uniformity once the water has been distributed in the soil.

The uniformity coefficient is only slightly sensitive to the saturated conductivity of the soil, and insensitive to the mean application rate and duration, and the initial soil moisture content.

The irrigation uniformity coefficient does not convey any information about the shortcomings of an irrigation event in filling the root zone; it merely indicates the level of deviation from the overall mean irrigation depth.

Simulations show that the application efficiency (Ea) of a sprinkler unit is dependent on the saturated soil hydraulic conductivity and the mean application rate and irrigation duration. Ea is very nearly independent of the sprinkler coefficient of

Fig. 9.11 The effect of initial soil moisture content on the uniformity coefficient (Uc).

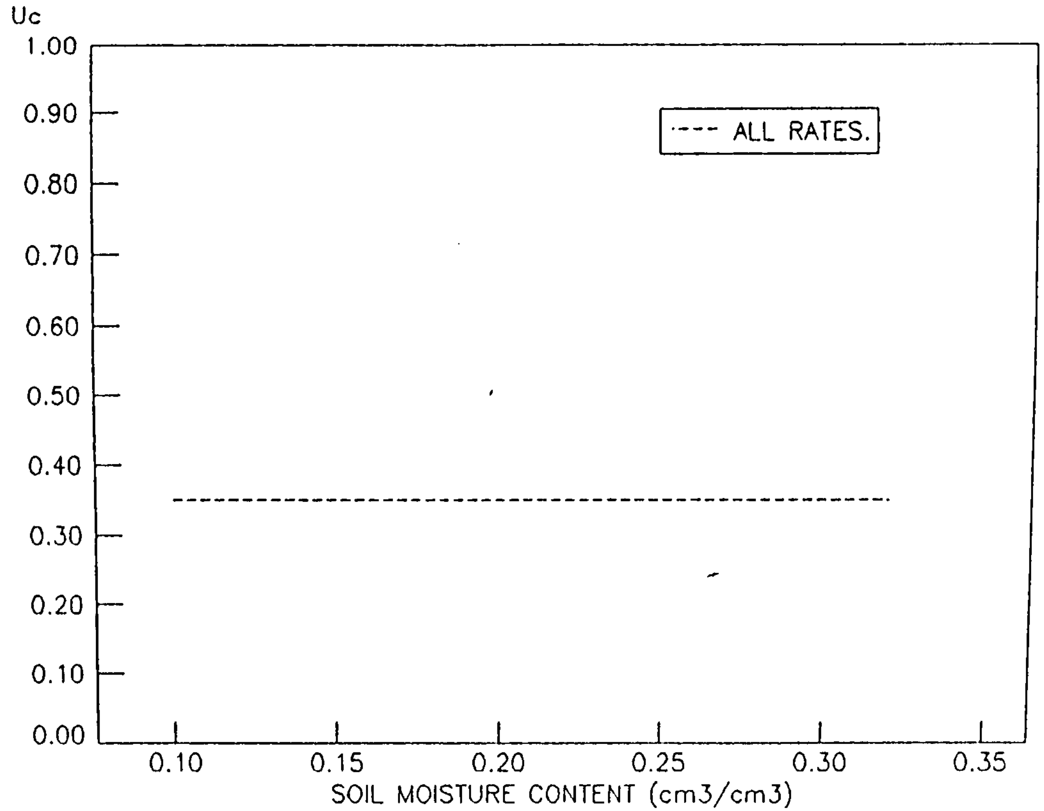

variation.

The finding of the independence of Ea from Cv contradicts the statement of Willardson (1972) that the uniformity of water application (characterized by Cv), determines the application efficiency. This independence is further illustrated when the sprinkler application rate is assumed to be uniformly distributed (ie: Cv= 0.0), and the response of Ea to changes in mean application rate and duration (Fig. 9.12), show the same rapid decline as for the normally distributed sprinkling rate (Fig. 9.6).

9.3 Applications in design and operations:

The design of sprinkler systems is a complex undertaking, not least because there are as many configurations of sprinkler spacings and relative positionings as there are nozzle types and methods of water delivery. The type of crop and the hydraulic properties of the soil, and the slope of the land will also effect the design criteria.

The final wetting pattern achieved depends also, to a great extent, on the degree of overlapping of the wetted circles. Rolland (1982) recommends the overlapping percentage be calculated according to the following expression :

Fig. 9.12 The effect of rate and duration on application efficiency (Ea) for a uniform distribution.

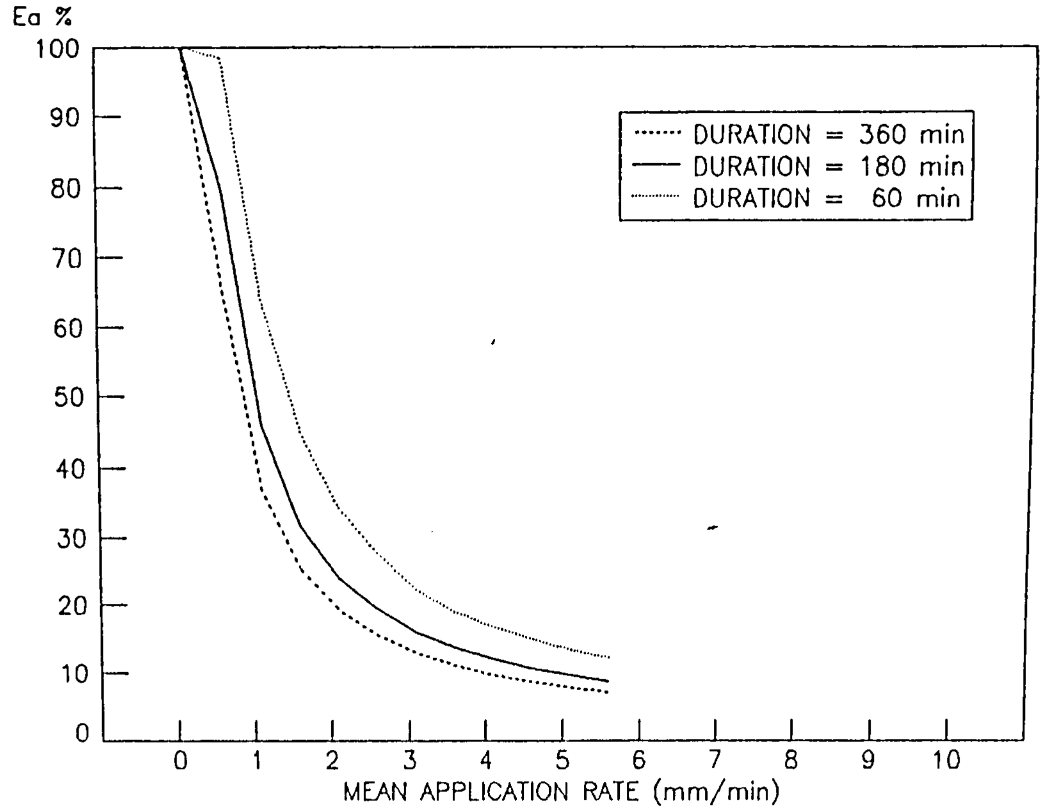

$$\% \text{ overlapping} = 100 \frac{(2\ Rc - Ls)}{Ls} \qquad (9.24)$$

where Rc = radius of coverage (m); and Ls = sprinkler spacing (m).

Although the sprinkler performance evaluation model described here was used to simulate the water balance under a single sprinkler unit, the application-rate distribution parameters (Cv and $\bar{y}$), can be determined experimentally for the conditions of overlapping and the model run for this new distribution.

The simulations in Figs. 9.4 and 9.5 suggest that a sprinkler unit, with a high coefficient of variation, need not necessarily have a low irrigation uniformity and application efficiency. From Fig. 9.6 it is clear that the mean application rate and duration have the most effect on Ea. The model can be used to establish maximum rates and durations for the operation of a unit given the desired level of efficiency.

Figure 9.8 shows that there is an optimum soil saturated hydraulic conductivity , Ks, for which Ea is maximum. This range of Ks widens as the application rate is increased. Increasing the mean application rate significantly reduces Ea at all values of Ks, except at the high values of Ks where the Ea-Ks curves seem to merge. This type of analysis can be used in choosing the best application rate to suit the soil hydraulic properties.

The response of Ea to initial moisture content (Fig. 9.10), suggests that for any given mean application rate, the dryer the initial soil moisture content (ie: less frequent irrigations), the higher is the application efficiency since there is less likelyhood of runoff and drainage loss.

9.4 Discussion:

The model presented here aims to fill the gap which currently exists in the understanding of the performance of sprinkler systems and the physical and operational factors which effect it.

The concurrent use of a deterministic point excess-rainfall model with a statistically derived application-rate spatial distribution model, need not be limited to the case of the normal distribution. Where persistent wind effects skew the application-rate pattern, the model can be modified to suit this new distribution.

The potential uses of the performance evaluation model, in the proper design and operation of sprinkler irrigation units, is promising. A full-scale field test of the model is necessary to show how far the theories and assumptions, concerning the spatial distribution of water in and above the soil, reflect the conditions in the field.

CHAPTER 10 DISCUSSIONS AND CONCLUSIONS

The aim of this thesis is to develop methods for the evaluation of on-farm operational irrigation efficiencies. The first task is the scheduling of irrigations. To represent the conditions in the field as closely as possible, a set of algorithms is developed for simulating the water balance of nonuniform soils with growing root zones and nonuniform rooting patterns. The irrigation scheduling model is fully responsive to soil, crop and atmospheric conditions and water management practices.

In the absence of adequate field data, a laboratory-based lysimeter experiment provides periodic soil moisture content and actual evapotranspiration data for testing the root zone water balance algorithms. It is recognized that the laboratory conditions cannot in any way be representative of the field, but that the measured water balance of the lysimeter yields valuable data for the quantitative, if not the qualitative, comparison of measured and simulated results.

The suitability of the Green-Ampt model for simulating the processes of one and two dimensional infiltration of water into nonuniform soils is illustrated. The cumulative infiltration curve is expressed mathematically by a simple function whose parameters are determined, for each irrigation day, from the composite-layer soil-profile moisture contents output by the irrigation scheduling model.

The hydrodynamic behaviour of water flow in borders and furrows is adequately simulated by the algebraic surface irrigation model. Irrigation efficiencies are calculated from the advance and recession curves.

An optimization routine establishes the best operating policies for each scheduled irrigation, by maximizing any one of application, distribution, storage or deficit/excess efficiencies. Significant improvements in irrigation efficiencies can be obtained, along with reductions in the required water, the flow duration, and the runoff volume.

The parameters of the infiltration function used in the surface irrigation model, are those determined by the appropriate one or two dimensional infiltration models. This ensures that the operational decisions, for any particular scheduled irrigation, are made on the basis of the prevalent soil moisture conditions.

While graphical and tabular aids simplify the design of surface irrigation systems, in order to broaden the range of design applicabilities, many assumptions and simplifications regarding the state of the soil and crop , become necessary . Accessability to micro-computers makes the design of irrigation systems for the prevelant conditions feasible. The border and furrow system design models presented here, incorporate such case-specific factors as nonuniformities of soil hydraulic properties, crop rooting depth, maximum allowable soil moisture deficit and total available water.

The sprinkler irrigation performance model adresses the question of wether the statistical characteristics of the sprinkler-head water distribution pattern, calculated from collected water depths on the soil surface, have any effect on the application efficiency (Ea) and uniformity coefficient (Uc) of the actual infiltrated water. In other words, are Ea and Uc independent of the sprinkler discharge characteristics. Also what effects do the soil hydraulic properties have on the system performance. These questions are answered by simulating the water balance under sprinkler irrigation, using a statistical-deterministic model.

From the various simulation studies carried out in this thesis, the folowing conclusions were arrived at:

1 - The uncalibrated irrigation scheduling model underestimates the cumulative actual evapotranspiration for the lysimeter case study. This means the model predicts less crop water stress than is the case. Further tests would indicate wether this characteristic of the model is case-specific or general.

2 - Simulations show that, for the soil, crop and atmospheric data of the lysimeter, the critical level of maximum allowable soil moisture deficit (MNGSMD) is about 30% . Above this figure the crop yield ratio drops rapidly from near unity.

3 - Increasing MNGSMD reduces the seasonal irrigation requirement. The response function depends on the complex interactions between the soil, crop and atmospheric conditions, and as such cannot be generalized.

4 - The Green-Ampt model is a versatile tool for the simulation of the one and two dimensional infiltration of water into nonuniform soils. The two dimensional distribution of water in the soil provides two new criteria for designing the width, depth and spacing of furrows, while incorporating soil and crop characteristics.

5 - In the absence of experimentally determined soil-water retention data, empirical methods for the estimation of soil-water properties show a fair degree of variability. The choice of a suitable empirical model depends on the available data.

6 - The surface irrigation efficiency-evaluation model shows that application efficiency reduces with increasing inflow rate and increasing inflow duration. This suggests that the major cause of water loss is due to runoff.

7 - Significant improvements in the performance of the system can be achieved through optimizing the operational efficiency. For a case study, comparisons between actual and optimum operating policies show application efficiency is increased by 20% , the required irrigation is reduced by 33%, the runoff volume by 63%, and the irrigation duration by 24 minutes.

8 - Simulations show that the application efficiency (Ea) of a sprinkler unit is significantly effected by the mean application rate and irrigation duration, and by the soil saturated conductivity and initial moisture content. The coefficient of variation (Cv), of the spatial distribution of the sprinkler application rate, has no significant effect upon Ea. It is concluded therefore that Ea cannot be determined solely from the statistical discharge characteristics of the sprinkler unit.

9 - The uniformity coefficient (Uc) of the sprinkler unit is not effected significantly by such factors as the mean application rate, irrigation duration, and the soil saturated conductivity and initial moisture content. The response of Uc to changes in Cv suggests that a sprinkler unit with a high coefficient of variation need not result in a low application uniformity.

REFERENCES

Ahmed, J., van Bavel, H.M. & Hiler, E.A. (1976)
Optimization of crop irrigation strategy under a stochastic weather regime : A simulation study.
Water Res. Res. 12(6): 1241-1247.

Alexander, L. & Skaggs, R.W. (1987)
Predicting unsaturated hydraulic conductivity from soil texture.
J. Irrig. Drain. Eng. ASCE 113(2): 184-197.

Ali, M.F. & Mawdsley, J.A. (1987)
Comparison of two models for estimating actual evapotranspiration using only regularly recorded data.
Journal of Hydrology 93: 257-276.

Allen, R.G. (1986)
A Penman for all seasons.
J. Irrig. Drain. Eng. ASCE. 112(4): 348-368.

Allen, R.G. & Pruitt, W.O. (1986)
Rational use of the FAO Blaney-Criddle formula.
J. Irrig. Drain. Eng. ASCE. 112(2): 139-155.

Al-Nakshabandi, G.A. & Kijne, J.W. (1974)
Potential evapotranspiration in central Iraq using the Penman method with modified wind function.
Journal of Hydrology 23: 319-328.

Amoozegar-Fard, A., Warrick, A.W. & Lomen, D.O. (1984)
Design nomographs for trickle irrigation systems.
J. Irrig. Drain. Eng. 110(2): 107-120.

Arya, L.M. & Paris, J.F. (1981)
A physicoempirical model to predict the soil moisture characteristic from particle-size distribution and bulk density data.
Soil Sci. Soc. Amer. J 45: 1023-1030.

Arya, L.M. & Paris, J.F. (1982)
Comments on : A physicoempirical model to predict the soil moisture characteristic from particle-size distribution and bulk density data.
Soil Sci. Soc. Amer. J 46(6): 1348-1349.

Aston, A.R. (1979)
Rainfall interception by eight small trees.
Journal of Hydrology 42: 383-396.

Bache, D.H. & MacAskill, I.A. (1984)
Vegetation in civil and landscape engineering.
Granada, London, UK.

Bacon, Francis. (1561-1625)
The advancement of learning and New Atlantis,
Edited by: A. Johnston, Clarendon Press 1974.

Balogh, J. & Gergely, I. (1985)
Basic aspects of trickling irrigation.
Budapest, Hungary.

Barfield, B.J., Payne, F.A. & Walker, J.N. (1973)
Surface water storage capacity of selected crop leaves under irrigation sprays.
Agric. Meteorol. 12: 105-111.

Bassett, D.M., Stockton, J.R. & Dicksens, W.L. (1970)
Root growth of cotton as measured by P32 uptake.
Agronomy Journal 62: 200-203.

Bishop, A.A., Jensen, M.E. & Hall, W.A. (1967)
Surface irrigation systems.
in: Hagan etal (1967).

Biswas, A.K. (1970)
History of hydrology.
North-Holland Publications, London.

Blair, A.W. & Smerdon,E.T. (1988)
Unimodal surface irrigation efficiency.
J. Irrig. Drain. Eng. 114(1): 156-168.

Booher, L.J. (1974)
Surface irrigation.
FAO Agricultural Development Paper No. 95.
Food and Agricultural Organization of the United Nations.
United Nations, Rome, Italy.

Boonyatharokul, W. & Walker, W.R. (1979)
Evapotranspiration under depleting soil moisture.
J. Irrig. Drain. Div. Proc. ASCE 105(4): 391-402.

Bos, M.G. (1985)
Summary of ICID definitions on irrigation efficiency.
ICID Bulletin, 34(1): 28-31.

Bos, M.G. & Nugteren, T. (1978)
On irrigation efficiencies.
International Institute for Land Reclamation and Improvement (ILRI).
Wageningen, Netherlands.

Bouwer, H. (1969)
Infiltration of water into nonuniform soil.
J. Irrig. Drain. Div. Proc. ASCE 95(4): 451-462.

Bouwer, H. (1976)
Infiltration into increasingly permeable soils.
J. Irrig. Drain. Div. ASCE 102(1): 127-136.

Brakensiek, D.L. (1970)
Discussion: Infiltration of water into nonuniform soil.
J. Irrig. Drain. Div. Proc. ASCE 96(3): 358-360.

Brakensiek, D.L., & Onstad, C.A. (1977)
Parameter estimation of the Green and Ampt infiltration equation.
Water Res. Res. 13(6):1009-1012.

Brandt. A., Bresler, E., Diner, N., Ben-Asher, I., Heller, J. & Goldberg, D. (1971)
Infiltration from a trickle source.
Soil Sci. Soc. Amer. Proc. 35: 675-689.

Brooks, R.H. & Corey, A.T. (1966)
Properties of porous media affecting fluid flow.
J. Irrig. Drain. Div. Proc. ASCE 92(2): 61-88.

Brutsaert, W.H. (1982)
Evaporation into the atmosphere.
D. Reidel Pub. Co., London.

Buras, N., Nir, D. & Aperovits, E. (1973)
Planning and updating farm irrigation schedules.
J. Irrig. Drain. Div. Proc. ASCE. 99(1): 43-51.

Burgy, R.H. & Pomeroy, C.R. (1958)
Interception losses in grassy vegetation.
Trans. Am. Geophys. Union, 39: 1095-1100.

Calder, I.R., Harding, R.J. & Rosier, P.T.W. (1983)
An objective assessment of soil-moisture deficit models.
Journal of Hydrology 60: 329-355.

Campbell, G.S. (1974)
A simple method for determining unsaturated conductivity from moisture retention data.
Soil Science 117: 311-314.

Chatfield, C. (1983)
Statistics for technology.
3rd edition, Chapman & Hall, London.

Chaudhry, F.H. (1978)
Nonuniform sprinkler irrigation application efficiency.
J. Irrig. Drain. Div. ASCE 104(2): 165-179.

Chia, L.S. (1967)
Albedos of natural surfaces in Barbados.
Q. J. R. Met. Soc. 93: 116-120.

Childs, E.C. & Collis-George, N. (1950)
The permeability of porous materials.
Proc. R. Soc., London, A201, 392-405.

Childs, E.C. & Bybordi, M. (1969)
The vertical movement of water in stratified porous material. 1- infiltration.
Water Res. Res. 5(2): 446-459.

Chow, V.T. (1964)
Handbook of applied hydrology.
McGraw Hill.

Chu, S.T (1978)
Infiltration during an unsteady rain.
Water Res. Res. 14(3): 461-466.

Clapp, R.B. & Hornberger, G.M. (1978)
Empirical equations for some soil hydraulic properties.
Water Res. Res. 14(4): 601-604.

Cooper, C.S. & Ferguson, H. (1964)
Influence of a barley companion crop upon root distribution of alfalfa, Birdsfoot Trefoil and Orchardgrass.
Agronomy Journal 56: 63-66.

Cope, R.J., Sawko, F. & Tickell, R.G. (1982)
Computer methods for civil engineers.
McGraw-Hill, UK.

Cowan, I.R. (1965)
Transport of water in the soil-plant-atmosphere system.
J. Appl. Ecol. 2: 221-239.

Cowan, I.R. & Milthorpe, F.L. (1968)
Plant factors influencing the water status of plant tissues.
in : Water deficit and plant growth. Kozlowski, T.T. (Ed.)
Academic Press, London.

Crawford, N. H. & Linsley, R. K. (1966)
Digital simulation in hydrology: Stanford Watershed Model IV.
Technical Report No. 39, Dept. Civil Engineering, Stanford University, Stanford, USA.

Cuenca, R.H. & Nicholson, M.T. (1982)
Application of Penman equation wind function.
J. Irrig. Drain. Div. Proc. ASCE> 108(1): 13-23.

Dane, J.H. (1980)
Comparison of field and laboratory determined hydraulic conductivity values.
Soil Sci. Soc. Amer. J 44:228-231.

Danielson, R.E. (1967)
Root systems in relation to irrigation.
in: Hagan etal (1967) 390-424.

Darcy, H. (1856)
Les fontaines publiques de la Dijon.
Dalmont, Paris.

Datye, K.R. & Patil, R.K. (1987)
Farmer managed irrigation systems: Indian experiences.
Center for Applied Systems Analysys in Development, Bombay, India.

Dedrick, A.R., Erie, L.J. & Clemmens, A.J. (1982)
Level-basin irrigation.
in : Advances in irrigation. vol. 1., Hillel, D. (Ed.), Academic Press.

Denmead, O.T. & Shaw, R.H. (1962)
Availability of soil water to plants as effected by soil moisture content and meteorological conditions.
Agronomy Journal 54(5): 385-390.

Doering, E.J. (1965)
Soil-water diffusivity by the one-step method.
Soil Science 99(5): 322-326.

Donahue, R.L., Miller, R.W. & Shickluna, J.C. (1983)
Soils: an introduction to soils and plant growth.
Prentice-Hall, USA.

Doorenbos, J. & Kassam, A.H. (1979)
Yield response to water.
FAO Irrigation and Drainage Paper No. 33.
Food and Agricultural Organization of the United Nations.
United Nations, Rome, Italy.

Doorenbos, J. & Pruitt, W.O. (1977)
guidelines for predicting crop water requirements.
FAO Irrigation and Drainage Paper No. 24.
Food and Agricultural Organization of the United Nations.
United Nations, Rome, Italy.

Eagleman, J.R. & Decker,W.L. (1965)
The role of soil moisture in evapotranspiration.
Agronomy Journal, 57: 626-629.

Ellis, F.B. & Barnes, B.J. (1980)
Growth and development of root systems of winter cereals grown after different tillage methods including direct drilling.
Plant and Soil 55: 283-295.

Emmett, W.W. (1978)
Overland flow.
In: Hillslope hydrology, Kirkby, M.J.,
John Wiley & Sons, UK.

FAO (1986)
Production yearbook, volume 40.
Food and Agricultural Organization of the United Nations.
UNFAO, Rome, Italy

Feddes, R.A. (1982)
Simulation of field water use and crop yield.
in : Simulation of plant growth and crop production.
Penning deVries, F.W.T. & van Laars, H.H. (Eds.).
Wageningen, Pudoc, Netherlands.

Feddes, R.A., Bresler, E. & Neuman, S.P. (1974)
Field test of a modified numerical model for water uptake by root systems.
Water Res. Res. 10: 1199-1206.

Feddes, R.A., Kowalik, P., Malinka, K.K. & Zaradny, H.
Simulation of field water uptake by plants using a soil water dependent root extraction function.
Journal of Hydrology 31: 13-26.

Federer, C.A. (1979)
A soil-plant-atmosphere model for transpiration and availability of soil water.
Water Res. Res. 15(3): 555-562.

Federer, C.A. (1982)
Transpirational supply and demand: plant, soil, and atmosphere effects evaluated by simulation.
Water Res. Res. 18(2): 355-362.

Fleming, G. (1975)
Computer simulation techniques in hydrology.
American Elsevier, New York.

Fleming, G. (1979)
Deterministic models in hydrology.
FAO Irrigation and Drainage Paper No. 32.
Food and Agricultural Organization of the United Nations.
United Nations, Rome, Italy.

Fok, Y.S. & Bishop, A.A. (1965)
Analysis of water advance in surface irrigation.
J. Irrig. Drain. Div. Proc. ASCE 91(1): 99-116.

Fok, Y.S. & Chiang, S.H. (1984)
2-D infiltration equations for furrow irrigation.
J. Irrig. Drain. Eng. ASCE 110(2): 208-217.

Fok, Y.S., Chung, S.O. & Liu, C.C.K. (1982)
Two dimensional exponential infiltration equations.
J. Irrig. Drain. Div. ASCE 108(4): 231-241.

Foth, H.D. (1962)
Root and top growth of corn.
Agronomy Journal 54: 49-52.

Freeze, P.A. (1980)
A stochastic-conceptual analysis of rainfall-runoff processes on a hillslope.
Water res. res 16(2): 391-408.

French, R.H. (1986)
Open channel hydraulics.
McGraw Hill

Freyberg, D.L., Reeder, J.W., Franzini, J.B. & Remson, I. (1980)
Application of the Green-Ampt model to infiltration under time-dependent surface water depths.
Water Res. Res. 16(3): 517-528.

Gardner, W.R. (1956)
Calculation of capillary conductivity from pressure-plate outflow data.
Soil Sci. Soc. Amer. Proc. 23: 317-320.

Gardner, W.R. (1960)
Dynamic aspects of water availability to plants.
Soil Science 89(2): 63-73.

Gardner, W.R & Hillel, D.I. (1962)
The relation of external evaporative conditions to the drying of soils.
J. Geophysical Res. 67(11): 4319-4325.

Gerwitz, A. & Page, E.R. (1974)
An empirical mathematical model to describe plant root systems.
J. Appl. Ecol. 11(2): 773-781.

Ghosh, R.K. (1980)
Estimation of soil-moisture characteristics from mechanical properties of soils.
Soil Science 130(2): 60-63.

Gilley, J.R., Martin, D.L. & Splinter, N.E. (1980)
Application of a simulation model of corn growth to irrigation management decisions.
Operational Research in Agriculture and Water Resources. Yaron, D. & Tapiero, C. (Eds).
North-Holland Pub. Co.

Green, W.H. & Ampt, G.A. (1911)
Studies on soil physics. 1- The flow of air and water through soils.
J. Agric. Soils 4:1-24.

Greenwood, D.J., Gerwitz, A., Stone, D.A. & Barnes, A. (1982)
Root development of vegetable crops.
Plant and Soil 68: 75-96.

Gregson, K., Hector, D.J. & McGowan, M. (1987)
A one-parameter model for the soil water characteristic.
J. Soil Sci. 38: 483-486.

Grimes, D.W., Miller, R.J. & Wiley, P.L. (1975)
Cotton and corn root development in two field soils of different strength characteristics.
Agronomy Journal 67: 519-523.

Gupta, S.C., Farrell, D.A. & Larson, W.E. (1974)
Determining effective soil water diffusivity from one-step outflow experiments.
Soil Sci. Soc. Amer. Proc. 38: 710-716.

Gupta, S.C. & Larson, W.E. (1979)
Estimating soil water retention characteristics from particle size distribution, organic matter percent, and bulk density.
Water Res. Res. 15(6): 1633-1635.

Gupta, S.C., Larson, W.E., Gast, R.G., Combs, S.M. & Dowdy, R.H. (1978)
The agricultural value of dredged material.
Tech. Rep. D-78-36 US Army Eng. Waterways Exp. Sta., Vicksburg, Miss.

Hachum, A.Y., Alfaro, J.F., Willardson, L. (1976)
Water movement in soil from trickle sources.
J. Irrig. Drain. Div. Proc. ASCE 102(2): 179-193.

Hagan, R.M., Haise. H.R. & Edminster, T.W. (Eds.) (1967)
Irrigation of agricultural lands.
Agronomy No. 11 , Am. Soc. Agronomy.

Haise, H.R. & Hagan, R.M. (1967)
Soil, plant, and evaporative measurements as criteria for scheduling irrigation.
in : Hagan etal (1967), 577-597.

Hall, R.L. (1985)
Further interception studies of Heather using a wet-surface wighing lysimeter system.
Journal of Hydrology, 81: 193-210.

Hammes, J.K. & Bartz, J.F. (1963)
Root distribution and development of vegetable crops as measured by radioactive phosphorus injection technique.
Agronomy Journal 55: 329-333.

Hanks, R.J. (1974)
Model for predicting plant yield as influenced by water use.
Agronomy Journal 66: 660-665.

Hanks, R.J. & Hill, R.W. (1980)
Modelling crop responses to irrigation in relation to soils, climate and salinity.
Pergamon Press, England.

Hansen, V.E., Israelsen, O.W. & Stringham, G.E. (1979)
Irrigation principles and practice.
4th ed., J. Wiley & son.

Hanson, C.L. (1976)
Model for predicting evapotranspiration from native rangeland in the Northern Great Plains.
Trans. ASAE 19(4): 471-477.

Hargreaves, G.H. & Samani, Z.A. (1984)
Economic considerations of deficit irrigation.
J. Irrig. Drain. Eng. ASCE 110(4): 343-358.

Hargreaves, G.H. & Samani, Z.A. (1987)
Simplified irrigation scheduling and crop selection for El Salvador.
J. Irrig. Drain. Eng. ASCE. 113(2): 224-231.

Hart, W.E, Bassett, D.L. & Strelkoff, T. (1968)
Surface irrigation hydraulics and kinematics.
J. Irrig. Drain. Div. Proc. ASCE 94(4): 419-440.

Hart, W.E, Peri, G. & Skogerboe, G.V. (1979)
Irrigation performance: an evaluation.
J. Irrig. Drain. Div. Proc. ASCE 105(3): 275-288.

Hashemi, F. & Habibian, M.T. (1979)
Limitations of temperature-based methods in estimating crop evapotranspiration in arid-zone agricultural development projects.
Agric. Meteorol. 20: 237-247.

Haverkamp, R. & Parlange, J.Y. (1986)
Predicting the water-retention curve from particle-size distribution : 1- sandy soils without organic matter.
Soil Science 142(6): 325-339.

Head, K.H (1984)
Manual of soil laboratory testing.
3 volumes, ELE International Ltd, Pentech Press, London.

Heerman, D.F. (1980)
Irrigation scheduling.
Operational Research in Agriculture and Water Resources. Yaron, D. & Tapiero, C. (Eds).
North-Holland Pub. Co.

Hillel, D. (1980)
I- Fundamentals of soil physics.
II- Applications of soil physics.
Academic Press, London, England.

Hillel, D. (1987)
The efficient use of water in irrigation.
World Bank Technical Paper No. 64.
The World Bank, Washington D.C.

Hillel, D., Talpaz, H. & van Keulen, H. (1976)
A macroscopic-scale model of water uptake by a nonuniform root system and of water and salt movement in the soil profile.
Soil Science 121(4): 242-255.

Holmes, R.M. & Robertson, G.W. (1963)
Application of the relationship between actual and potential evapotranspiration in dry land agriculture.
Trans. ASAE 6(1): 65-67.

Holtan, H.N. & Lopez, M.C. (1971)
USDAHL-70 model of watershed hydrology.
USDA Tech. Bull. No. 1435, Agricultural Tes. Ser.
Washington D.C.

Holtan, H.N., Stiltner, G.J., Hensen, W.H. & Lopez, N.C. (1974)
USDAHL-74 revised model of watershed hydrology.
Plant Physiology Institute report No.4 , USDA .

Holzapfel, E.A., Marino, M.A. & Chavez-Morales, J. (1986)
Surface irrigation optimization models.
J. Irrig. Drain. Eng. ASCE 112(1): 1-19.

Horton, R.E. (1940)
An approach toward a physical interpretation of infiltration capacity.
Soil Sci. Soc. Amer. Proc. 5: 399-417.

Israelsen, O.W. & Hansen, V.E. (1962)
Irrigation principles and practices.
John Wiley & Sons. USA.

Idso, S.B., Reginato, R.J. & Jackson, R.D. (1979)
Calculation of evaporation during the three stages of soil drying.
Water Res. Res. 15(2): 487-488.

Jackson, R.D. (1972)
On the calculation of hydraulic conductivity.
Soil Sci. Soc. Amer. Proc. 36: 380-382.

Jackson. R.D., Reginato, R.J. & Idso, S.B. (1977)
Wheat canopy temperature: a practical tool for evaluating water requirements.
Water Res. Res. 13(3): 651-656.

Jackson, R.D., van Bavel, C.H.M. & Reginato, R.J. (1963)
Examination of pressure-plate outflow method for measuring capillary conductivity.
Soil Science 96: 249-256.

James, L.G. & Larson, C.L. (1976)
Modelling infiltration and redistribution of soil water during intermittent application.
Trans. Amer. Soc. Agric. Eng. 482-489.

Jaynes, D.B. (1986)
Simple model of border irrigation.
J. Irrig. Drain. Eng. ASCE 112(2): 172-184.

Jaynes, D.B. & Tyler, E.J. (1984)
Using soil physical properties to estimate hydraulic conductivity.
Soil Science 138(4): 298-305.

Jensen, M.E. (1969)
Scheduling irrigations using computers.
J. Soil & Water Conservation.

Jensen, M.E. (Ed.) (1974)
Consumptive use of water and irrigation water requirements.
Amer. Soc. Civil Eng., New York.

Jensen, M.E., Robb, D.C.N. & Franzoy, C.E. (1970)
Scheduling irrigations using climate-crop-soil data.
J. Irrig. Drain. Div. ASCE. 96(1): 25-39.

Jensen, M.E., Swarner, L.R. & Phelan, J.T. (1967)
Improving irrigation efficiencies.
in: Hagan etal (1967).

Jensen, M.E., Wright, J.L. & Pratt, B.J. (1971)
Estimating soil moisture depletion from climate, crop and soil data.
Trans. ASAE 14: 954-959.

Jung,Y. & Taylor, H.M. (1984)
Diffrerences in water uptake rates of soyabean roots associated with time and depth.
Soil Science 137(5): 341-350.

Kanemasu, E.T., Stone, L.R. & Powers, W.L. (1976)
Evapotranspiration model tested for soybean and sorghum.
Agronomy journal 68: 569-572.

Kaspar, T.C., Stanley, C.D. & Taylor, H.M. (1978)
Soybean root growth during the reproductive stages of development.
Agronomy Journal 70: 1105-1107.

Katopodes, N.D. & Strelkoff, T. (1977)
Hydrodynamics of border irrigation - complete model.
J. Irrig. Drain. Div. Proc. ASCE 103(3): 309-324.

Kayhan International (1988)
Water projects play vital role in Iran's agriculture.
August 13 : 8-9.

Knisel, W.G. (Ed.) (1980)
CREAMS: a field scale model for chemicals, runoff, and erosion from agricultural management systems.
USDA, Conservation Reasearch Report No. 26.

Korfiatis, G.P. (1985)
Modelling the moisture transport through solid waste landfills.
PhD thesis, New Jersey State University, USA.

Kostiakov, A.N. (1932)
On the dynamics of the coefficient of water-percolation in soils and the necessity of studying it from a dynamic point of view for purposes of amelioration.
Trans. 6th Comm. Int. Soc. Soil Sci. Pt A 15-21.

Kristensen, K.J. & Jensen, S.E. (1975)
A model for estimating actual evapotranspiration from potential evapotranspiration.
Nordic Hydrology 6: 170-188.

Kruse, E.G. (1978)
Describing irrigation efficiency and uniformity.
J. Irrig. Drain. Div. Proc. ASCE 104(1): 35-41.

Kunze, R.J. & Kirkham, D. (1962)
Simplified accounting for membrane impedence in capillary conductivity determination.
Soil Sci. Soc. Amer. Proc. 26: 421-426.

Lal, R. & Maurya, P.R. (1982)
Root growth of some tropical crops in uniform columns.
Plant and Soil 68: 193-206.

Larcher, W. (1983)
Physiological plant ecology.
Springer-Varlag, Berlin.

Larsson, S. (1981)
Influence of intercepted water on transpiration and evaporation of Salix.
Agric. Meteorol. 23: 331-338.

Legg, B.J, Long, I.F. & Zemroch, P.J. (1981)
Aerodynamic properties of field bean and potato crops.
Agricultural Meteorology 23: 21-43.

Levien, S.L.A. & de Souza, F. (1987)
Algebraic computation of flow in furrow irrigation.
J. Irrig. & Drain. Eng. ASCE 113(3): 367-377.

Leyton, L., Reynolds, E.R.C. & Thompson, F.B. (1967)
Rainfall interception in forests and mooreland.
In: Supper & Lull, Forest Hydrology.

Libardi, P.L., Reichardt, K, Nielsen, D.R. & Biggar, J.W. (1980)
Simple field methods for estimating soil hydraulic conductivity.
Soil Sci. Soc. Amer. J 44: 3-7

Linacre, E.T. (1969)
Net radiation to various surfaces.
J. Appl. Ecol. 6(1)

Ling, A.H. & Robertson, G.N. (1982)
Reflection coefficients of some tropical vegetation covers.
Agricultural Meteorology 27: 141-144.

Linscott, D.L., Fox, R.L. & Lipps, R.C. (1962)
Corn root distribution and moisture extraction in relation to nitrogen fertilization and soil properties.
Agronomy Journal 54: 185-189.

Lister, H. (1978)
Irrigation in the Zagros mountains - Iran.
Reasearch Series No. 12.
Department of Geography.
University of Newcastle Upon Tyne.

Makrantonaki, M.S., Tzimopoulos, C. & Gouliaras, D. (1987)
Analysis of a closed-form analytical model to predict the hydraulic conductivity function.
Journal of Hydrology 92: 289-300.

Malek, E. (1979)
Determination of the constants for the global radiation equation at Badjgah, Iran.
Agricultural Meteorology 20: 233-235.

Malek, E. (1987)
Comparison of alternative methods for estimating Etp and evaluation of advection in the Badjgah area, Iran.
Agric. Forest Meteo. 39: 185-192.

Marshal, T.J. (1958)
A relation between permeability and size distribution of pores.
J. Soil Sci. 9: 1-8.

Marshall, T.J. & Holmes, J.W. (1979)
Soil physics.
Cambridge University Press, England

Martin, D.L., Watts, D.G. & Gilley, J.R. (1984)
Model and production function for irrigation management.
J. Irrig. Drain. Eng. ASCE. 110(2): 149-164.

Massman, W.J. (1983)
The derivation and evaluation of a new model for the interception of rainfall by forests.
Agric. Meteorol. 28: 261-286.

McCleod, L.B. & Jackson, L.P. (1967)
Aluminium tolerance of two barley varieties in nutrient solution, peat and soil culture.
Agronomy Journal 59: 359-363.

McClure, J.W. & Harvey, C. (1962)
Use of radiophosphorus in measuring root growth of sorghum.
Agronomy Journal 54: 457-459.

McCuen, R.H., Rawls, W.J. & Brakensiek, D.L. (1981)
Statistical analysis of the Brooks-Corey and the Green-Ampt parameters across soil textures.
Water Res. Res. 17(4): 1005-1013.

McCulloch, J.S.G. (1965)
Tables for the rapid computation of the Penman estimate of evaporation.
East Afr. Agr. Forest. J. 30: 286-295.

Mein, R.G. & Larson, C.L. (1973)
Modelling infiltration during a steady rain.
Water Res. Res. 9(2): 384-394.

Merriam, R.A. (1961)
Surface water storage on annual Ryegrass.
J. Geophys. Res. 66(6): 1833-1838.

Millington, R.J. & Quirk, J.P. (1959)
Permeability of porous media.
Nature 183: 387-388.

Milthorpe, F.L. & Moorby, J. (1979)
An introduction to crop physiology.
Cambridge University Press. 2nd ed., England.

Miranda, R.A.C. & Butler, D.R. (1986)
Interception of rainfall in a hedgerow apple orchard.
Journal of Hydrology, 87: 245-253.

Mitchel, R.L. & Russell, W.J. (1971)
Root development and rooting patterns of soybean (Glycine max(L.) merrill) evaluated under field conditions.
Agronomy Journal 63: 313:316.

Molz, F.J. & Remson, I. (1970)
Extraction term models of soil moisture use by transpiring plants.
Water Res. Res. 6(5): 1346-1356.

Montieth, J.L. (1959)
The reflection of short-wave radiation by vegetation.
Q. J. R. Met. Soc. 85: 386-392.

Montieth, J.L. (1965)
Evaporation and environment.
in : The state and movement of water in living organisms. Fogg, G.E. (Ed.).
Sympos. Soc. Exper. Biol. 19: 205-234.
Academic Press, London.

Morel-Seytoux, H.J. (1976)
Derivation of equations for rainfall infiltration.
Journal of Hydrology 31: 203-219.

Morel-Seytoux, H.J. & Khanji, J. (1974)
Derivation of an eqaution of infiltration.
Water Res. Res. 10(4): 795-800.

Morgan, T.H., Biere, A.W. & Kanemasu, E.T. (1980)
A dynamic model of corn yield response to water.
Water Res. Res. 16(1): 59-64.

Morton, F.I. (1975)
Estimating evaporation and transpiration from climatological observations.
J. Appl. Meteo. 14(4): 488-497.

Morton, F.I. (1983)
Operational estimates of areal evapotranspiration and their significance to the science and practice of hydrology.
Journal of Hydrology 66: 1-76.

Mualem, Y. (1976)
A new model for predicting the hydraulic conductivity of unsaturated media.
Water Res. Res. 12(3): 513-522.

Neuman, S.P. (1976)
Wetting front pressure head in the infiltration model of Green and Ampt.
Water Res. Res. 12(3):564-566.

New Civil Engineer (1988)
Dams will not staunch Sudan flood peak.
18 Augus, Page 6.

New Scientist (1985)
Crop irrigation without wasting water.
17 October, Page 38.

New Scientist (1988a)
Greenhouse warming grips American corn belt.
30 June, Page 35.

New Scientist (1988b)
Science under the grain mountain.
10 March, Pages 41-43.

Nimah, M.N. & Hanks, R.J. (1973)
Model for estimating soil water, plant, and atmospheric intercations.
Soil Sci. Soc. Amer. Proc. 37: 522-532.

Norero, A.L., Keller, J. & Ashcroft, G.L. (1972)
Effect of irrigation frequency on the average evapotranspiration for various crop-climate-soil systems.
Trans. ASAE 15(6): 662-666.

ODU Bulletin (1988)
Water management in the third world irrigation schemes - Lessons from the field.
Overseas Development Unit of Hydraulic Reasearch.
July 1988, No. 11, Wallingford, UK.

Panikar, J.T., & Nanjappa, G. (1977)
Suction head at wet front in unsaturated-flow problems - a new definition.
Journal of Hydrology 33:1-14.

Pearson, R.W. & Lund, Z.F. (1968)
Direct observation of cotton root growth under field conditions.
Agronomy Journal 60: 442-443.

Penman, H.L. (1948)
Natural evaporation from open water, bare soil and grass.
Proc. R. Soc., London, Ser. A, 193: 120-146.

Penman, H.L. (1963)
Vegetation and hydrology.
Commonwealth Bur. Soils. Tech. Commun. 53, 124 pp.
Harpenden, England.

Philip, J.R. 1957
The theory of infiltration: 4- sorptivity and algebraic infiltration equations.
Soil Science 83: 257-264.

Philip, J.R. (1971)
General theorem on steady infiltration from surface sources with application to point and line source.
Soil. Sci. Soc. Amer. Proc. 35: 867-871.

Priestley, C.H.B. & Taylor, R.J. (1972)
On the assessment of surface heat flux and evaporation using large scale parametes.
Month. Weather Rev. 100: 81-92.

Proffitt, A.P.B., Berliner, P.R. & Oosterhuis, D.M. (1985)
A comparative study of root distribution and water extraction efficiency by wheat grown under high and low frequency irrigation.
Agronomy Journal 77(5): 655-662.

Raats, P.A.C. (1971)
Steady infiltration from point source, cavities and basins.
Soil. Sci. Soc. Amer. Proc. 35: 689-694.

Rama, R. (1982)
Mathematical modelling of surface irrigation.
PhD thesis, Mississippi state university.
University Microfilms International, USA.

Rao, A.S. (1987)
Interception losses of rainfall from Cashew trees.
Journal of Hydrology, 90: 293-301.

Rawls, W.J. & Brakensiek, D.L. (1982)
Estimating soil water retention from soil properties.
J. Irrig. Drain. Div. Proc. ASCE 108(2): 166-171.

Redfels, M.S., Stone, L.R., Kanemasu, E.T. & Kirkham, M.B. (1987)
Greenness-Leaf area index relationships of seven row crops.
Agronomy Journal 79:254-259.

Refsgaard, J.C. (1981)
The surface water component of an integrated hydrological model - SUSA investigation.
Danish Committee for Hydrology - SUSA-H Report 12.

Richards, L.A. (1931)
Capillary conduction of fluid through porous medium
Physics 1: 318-333.

Ritchie, J.T. (1972)
Model for predicting evaporation from a row crop with incomplete cover.
Water Res. Res. 8(5): 1204-1212.

Ritchie, J.T., Burnett, E. & Henderson, R.C. (1972)
Dryland evaporative flux in a subhumid climate: 3- Soil water influence.
Agronomy Journal 64: 168-173.

Ritchie, J.T., Rhoades, E.D. & Richardson, C.W. (1976)
Calculating evaporation from native grassland watersheds.
Trans. ASAE 1098-1103.

Rogowski, A.S. (1972)
Estimation of the soil moisture characteristic and hydraulic conductivity: comparison of models.
Soil Science 114(6): 423-429.

Rolland, L. (1982)
Mechanized sprinkler irrigation.
FAO Irrigation and Drainage Paper No. 35.
Food and Agricultural Organization of the United Nations, Rome, Italy.

Rowse, H.R. (1975)
Simulation of the water balance of soil columns and fallow soils.
J. Soil Sci. 26:337-349.

Rowse, H.R. & Barnes, A. (1979)
Weather, rooting depth and water relations of broad beans- a theoretical analysis.
Agricultural Meteorology 20: 381-391.

Rowse, H.R., Mason, W.K. & Taylor, H.M. (1983)
A microcomputer simulation model of soil water extraction by soyabeans.
Soil Science 136(4): 218-225.

Rowse, H.R., Stone, D.A. & Gerwitz, A. (1978)
Simulation of the water distribution in soil.
Plant and Soil 49: 533-550.

Russell, G. (1980)
Crop evaporation, surface resistance and soil water status.
Agricultural Meteorology 21: 213-226.

Rutter, A.J. (1975)
The hydrological cycle in vegetation.
in: Vegetation and the atmosphere, Montieth, J.L. (Ed.), 1: 111-154.
Academic Press, London.

Rutter, A.J., Kershaw, K.A., Robins, P.C. & Morton, A.J. (1971)
A predictive model of rainfall interception in forests, I. Derivation of the model from observations in a plantation of Corsican pine.
Agricultural Meteorology, 9(5/6): 367-384.

Rutter, A.J., Morton, A.J. & Robins, P.C. (1975)
A predictive model of rainfall interception in forests, II- Generalization of the model and comparison with observations in some coniferous and hardwood stands.
J. Appl. Ecol. 12: 367-380.

Rutter, A.J., Morton, A.J. (1977)
A predictive model of rainfall interception in forests, III- Sensitivity of the model to stand parameters and meteorological variables.
J. Appl. Ecol. 14: 567-588.

Salter, P.J. & Williams, J.B. (1969)
The influence of texture on the moisture characteristics of soil.
J. Soil Sci. 20: 126-131.

Sarma, P.B.S., Rao, N.H., Rao, K.U.P. (1980)
Calculation of water balance in the crop root zone by computer.
Journal of Hydrology 45: 123-131.

Saxton, K.E., Johnson, H.P. & Shaw, R.H. (1974)
Modelling evapotranspiration and soil moisture.
Trans. ASAE. 17: 673-677.

Schmugge, T.J., Jackson, T.J. & McKim, H.L. (1980)
Surveys of methods for soil moisture determination.
Water Res. Res. 16(6): 961-979.

Schuh, W.M. & Sweeney, M.D. (1986)
Particle-size distribution method for estimating unsaturated hydraulic conductivity for sandy soils.
Soil Science 142(5): 247-254.

Schulze, R.E., Hutson, J.L. & Cass, A. (1985)
Hydrological characteristics and properties of soils in Southern Africa 2: soil water retention models.
Water S. A. 11(3): 129-136, July.

Seginer, I. (1969)
Wind variation and sprinkler water distribution.
J. Irrig. Drain. Div. Proc. ASCE 95(2): 261-274.

Seginer, I. & Kostrinsky, M. (1975)
Wind, sprinkler patterns and system design.
J. Irrig. Drain. Div. Proc. ASCE 101(4): 251-264.

Selim, H.M. & Kirkham, D. (1973)
Unsteady two-dimensional flow of water in unsaturated soils above an impervious barrier.
Soil Sci. Soc. Amer. Proc. 37: 389-495.

Shaw, E. M. (1983)
Hydrology in practice.
Van Nostrand Reinhold, UK.

Sherman, B. & Singh, V.P. (1978)
A kinematic model for surface irrigation.
Water Res. Res. :357-364.

Sherratt, D.J. & Wheater, H.S. (1984)
The use of surface resistance-soil moisture relationships in soil water budget models.
Agri. Forest. Meteo. 31: 143-157.

Shiu, S.Y. & Davar. K.S. (1973)
Modified Penman method for potential evapotranspiration from forest regions.
Journal of Hydrology 18: 349-365.

Singh, P. & Chauhan, H.S. (1972)
Shape factors in irrigation water advance equation.
J. Irrig. Drain. Div. Proc. ASCE 98(3): 443-458.

Singh, V.P. & He, Y. (1988)
Muskingum model for furrow irrigation.
J. Irrig. Drain. Eng. ASCE 114(1): 89-103.

Singh, V.P., Scarlatos, P.D. & Raudales, R.A. (1988)
Muskingun model for border irrigation.
J. Irrig. Drain. Eng. ASCE 114(2): 266-280.

Slabbers, P.J.S. (1977)
Surface roughness of crops and potential evapotranspiration.
Journal of Hydrology 34: 181-191.

Smith, R.E. (1972)
The infiltration envelope : results from a theoretical infiltrometer.
Journal of Hydrology 17: 1-21.

Smith, R.E. (1972)
Border irrigation advance and ephemeral flood waves.
J. Irrig. Drain. Div. Proc. ASCE 98(2): 289-307.

Smith, R.E. & Parlange, J.Y. (1978)
A parameter-efficient hydraulic infiltration model.
Water Res. Res. 14(3): 533-538.

Stanley, C.D., Kaspar, T.C. & Taylor, H.M. (1980)
Soybean top and root response to temporary water table imposed at 3 different stages of growth.
Agronomy Journal 72: 341-364.

Stephens, D.B. & Rehfeldt, K.R. (1985)
Evaluation of closed-form analytical models to calculate conductivity in a fine sand.
Soil Sci. Soc. Amer. J 49: 12-19.

Stewart, J.I. & Hagan, R.M. (1973)
Functions to predict effects of crop water deficit.
J. Irrig. Drain. Div. Proc. ASCE. 99(4): 421-439.

Stoltenburg, N.L. & Wilson, T.V. (1950)
Trans. Amer. Geophys. Union, 31: 443-448.

Stone, L.R., Horton, M.L. & Olson, T.C. (1973)
Water loss from an irrigated sorghum field.
Agronomy Journal 65: 492-497.

Strelkoff, T. (1977)
Algebraic computation of flow in border irrigation.
J. Irrig. Drain. Div. ASCE 103(3): 357-377.

Strelkoff, T. & Katepodes, N.D. (1977)
Border-irrigation hydraulics with zero inertia.
J. Irrig. Drain. Div. Proc. ASCE 103(3): 325-342.

Stroosnijder, L. (1982)
Simulation of the soil water balance.
in : Simulation of plant growth and crop production.
Penning deVries, F.W.T. & van Laars, H.H. (Eds.).
Wageningen, Pudoc, Netherlands.

Swartzendruber, D. (1974)
Infiltration of constant-flux rainfall into soil as measured by the approach of Green and Ampt.
Soil Science 117(5): 272-281.

Szeicz, G. & Long, I.F. (1969)
Surface resistance of crop canopies.
Water Res. Res. 5(3): 622-633.

Taghavi, S.A., Marino, M.A. & Rolston, D.E. (1984)
Infiltration from trickle irrigation source.
J. Irrig. Drain. Eng. 110(4): 311-341.

Taylor, H.M. (1980)
Soybean growth and yield as effected by row spacing and by seasonal water supply.
Agronomy Journal 72: 543-547.

Taylor, H.M., Huck, M.G., Klepper, B. & Lund, Z.F. (1970)
Measurement of soil-grown roots in a Rhizotron.
Agronomy Journal 62: 807-809.

Taylor, H.M. & Klepper, B. (1973)
Rooting density and water extraction patterns for corn (Zea mays. L.).
Agronomy Journal 65: (65-968.

Taylor, H.M. & Klepper, B. (1978)
The role of rooting characteristics in the supply of water to plants.
Adv. Agron. 30: 99-128.

The Independent (1988)
Foreign News, page 8, 29th December.

Thom, A.S. (1975)
The hydrological cycle in vegetation.
in: Vegetation and the atmosphere, Montieth, J.L. (Ed.), 1: 111-154.
Academic Press, London.

Thom, A.S. & Oliver, H.R. (1977)
On Penman's equation for representing regional evaporation.
Q. J. R. Met. Soc. 13: 345-357.

Thompson, N., Barrie, I.A. & Ayles, M. (1981)
The Meteorological Office rainfall and evaporation calculation system : MORECS.
Hydrological Memorandum No. 45, Met. Office, Bracknell, England.

Toksoz, S., Kirkham, D. & Baumann, E.R. (1965)
Two-dimensional infiltration and wetting front.
J. Irrig. Drain. Div. Proc. ASCE 91(3): 65-79.

Tolikas, P.K., Tzimopoulos, C.D. & Tolikas, D.K. (1980)
A simple analytical solution for horizontal absorption of water by soils for exponential soil water diffusivity.
Water. Res. Res. 16(4): 821-825.

Towner, G.D. (1982)
Analysing one-step outflow experiments to calculate soil-water diffusivities, using Gardner's equation.
J. Soil Sci. 33: 351-364.

UN (1968)
Water legislation in Asia and the Far East.
Water resources series No. 35.
ECAFE. United Nations, New York.

UN (1985)
Assessment of irrigation efficiency.
Proc. of the 10th Session of the Committee on Natural Resources.
Water Resources Series No. 59.
United Nations, New York.

UN (1988)
Demographic yearbook 1986.
United Nations, New York.

UNFAO (1954)
Water laws in Moslem countries.
Food and Agricultural Organization of the United Nations.
United Nations, Rome, Italy.

UNFAO (1973)
Water laws in Moslem countries.
Food and Agricultural Organization of the United Nations.
United Nations, Rome, Italy.

US-SCS (1972)
Soil conservation service,
National engineering handbook, sect. 4, Hydrology.
USA.

USDAHL (1974)
USDAHL-74 revised model of watershed hydrology.
Holtan, H.N., Stiltner, G.J., Hensen, W.H. & Lopez, N.C.
Plant Physiology Institute report No.4 , USDA .

Van den Honert, T.H. (1948)
Water transport in plants as a catenary process.
Disc. Faraday Soc. 3: 146-153.

Van Genuchten, M.T.H. (1980)
A closed-form equation for predicting the hydraulic conductivity of unsaturated soils.
Soil Sci, Soc. Amer. J 44: 892-898.

Van Keulen, H. (1982)
Simulation of field water use and crop yield.
in : Simulation of plant growth and crop production.
Penning deVries, F.W.T. & van Laars, H.H. (Eds.).
Wageningen, Pudoc, Netherlands.

Vos, J. & Groedwold, J. (1986)
Root growth of potato crops on a marine-clay soil.
Plant and Soil 94: 17-33.

Walker, W.R. (1979)
Explicit sprinkler irrigation uniformity: efficiency model.
J. Irrig. Drain. Div. Proc. ASCE 105(2): 129-137.

Walker, W.R. & Skogerboe, G.V. (1987)
Surface irrigation- theory and practice.
Prentice-Hall, USA.

Warrick, A.W. & Lomen, D.O. (1976)
Time dependent linearized infiltration: 3- strip and disc sources.
Soil Sci. Soc. Amer. J. 40: 639-643.

Warrick, A.W., Lomen, D.O. & Amoozegar-Fard, A. (1980)
Linearized moisture flow with root extraction for three dimensional, steady conditions.
Soil Sci. Soc. Amer. J. 44: 911-914.

Welch, D.G. & Granaham, D.A. (1985)
Irrigation scheduling with the neutron probe.
Developement and Management Aspects of Irrigation and Drainage Systems, ASCE 146-153.

Willardson, L.S. (1972)
Attainable irrigation efficiencies.
J. Irrig. Drain. Div. Proc. ASCE 98(2): 239-246.

Withers, B. & Vipond, S. (1974)
Irrigation: design and practice.
Batsford Academic and Educational Limited, London.

Wooding, R.A. (1968)
Steady infiltration from a circular pond.
Water Res. Res. 4(6): 1259-1273.

Wright, J.L. (1982)
New evapotranspiration crop coefficients.
J. Irrig. Drain. Div. Proc. ASCE. 108(2): 57-74.

Wulff, H.E. (1968)
The Qanats of Iran.
Scientific American, 218: 94-105.

Yaron, D., Strateener, G., Shinshi, D. & Weisbrod, M. (1973)
Wheat response to soil moisture and the optimal irrigation policy under conditions of unstable rainfall.
Water Res. Res. 9(5): 1145-1154.

Zartman, R.E. & Woyewodzic, R.T. (1979)
Root distribution patterns of two hybrid grain sorghum under field conditions.
Agronomy Journal 71: 325-328.

Zur, B. & Jones, J.W. (1981)
A model for the water relations, photosynthesis, and expansive growth of crops.
Water Res. Res. 17(2): 311-320.

APPENDIX

A 3.1 The Penman method (Option 2):

Penman (1948,1963) derived a physically based model of evapotranspiration from the consideration of the incoming and outgoing evaporative energies at an open surface of water (Fig. 3.4). While the principles are based on sound fundamental physical laws, some of the relationships used are empirical. The Penman equation is :

$$PETr = [S(Rn-G)/(S+C)] + [Ea.C/(S+C)] \tag{A3.1}$$

where:

PETr = reference evapotranspiration (mm/d)
S = slope of saturation vapour pressure-temperature curve at mean air temperature (mbar/ C)
C = psychrometer constant (mbar/ C)
Rn = net radiation (mm/d)
G = heat flux into the soil (mm/d)
Ea = aerodynamic vapour transfer term (mm/d)

The relationships defining the various terms in Eqn. A3.1 are listed below in detail.

a) Net Radiation Rn :

Net radiation at a surface on earth is the difference between the incoming short wave radiation (Ri) and the outgoing long wave radiation (Rb) :

$$Rn = Ri - Rb \tag{A3.2}$$

The units of radiation are expressed as

energy units eg: Watts/m2.d or mm/d water equivalents.

b) Incoming Shortwave Radiation Ri :

Not all the short wave solar radiation (Ra) arriving at the earth's outer atmosphere gets through uneffected. Clouds and dust particles in the air help to reflect part of this as long wave radiation and only a proportion (Rs) reaches the ground. This proportion can be empirically estimated by:

$$Rs = Ra \cdot (a + b.n/N) \tag{A3.3}$$

where

Rs = short wave radiation arriving at the earth's surface (mm/d)
Ra = short wave radiation at earth's outer atmosphere (mm/d)
n/N = ratio of actual to possible sunshine hours
a & b = geographical constants

The possible number of sunshine hours (N), is published in tabular form in most hydrology text books (eg: Shaw 1983). Doorenbos & Pruit (1977) suggest 0.25 and 0.5 respectively for 'a' and 'b' , for general application. McCulloch (1965) gives : $a=0.29 \cos \theta$, for latitude θ from 0 to 60 degrees. Malek (1979) gives 0.31 and 0.55 respectively for southern Iran.

The extraterrestrial radiation (Ra) varies with latitude and season of the year. Its values are published in tablular form, in most hydrology text books (eg: Shaw 1983), or alternatively calculated by part-empirical equations (Thompson etal 1981, Morton 1983).

The proportion of the radiation reaching the earth's surface actually absorbed by it depends on the effective reflectivity or albedo (r) of the surface:

$$Ri = Rs (1 - r) \qquad (A3.4)$$

The effective albedo is equal to the plant albedo when the canopy cover is full . For leaf area index (LAI) less than 4 , the effective albedo is calculated according to Thompson etal (1981) as :

$$r = r' + (r'' - r').(LAI/4) \qquad (A3.5)$$

where r' = bare soil albedo (Table A3.1)
r'' = plant albedo (Table A3.2)

Thus the resultant incoming radiation equation becomes:

$$Ri = Ra(1 - r).(a + b.n/N) \qquad (A3.6)$$

c) Outgoing Longwave Radiation Rb :

The earth reflects some of the incoming radiation back to the atmosphere as a long wave radiation (incoming atmosheric long wave radiation subtracted).

Brutsaert (1982) gives the net long wave

Table A3.1 Albedo values of some soils (compiled by Linacre 1969).

Soil	Albedo		
	Dry soil	Unknown Wetness	Moist Soil
Sand	0.18		0.09
Black mould	0.14		0.08
Ploughed field	0.20-0.29	0.12-0.20	
Black soil	0.14	0.10-0.15	0.07
Grey soil	0.25-0.30		0.10-0.12
Loam	0.23		0.16
Soil	0.16		0.06
Dark soil		0.05-0.15	
Grey soil	0.20-0.39		0.10-0.20
Sandy	0.25-0.45	0.15-0.40	
Raw Humus		0.15	
Brown soil	0.16		
Dark clay	0.16		0.02-0.08
Dark cultivated			0.07-0.10
Latosol	0.13		0.08
Organic sand			0.06
Red soil			0.11
Dark brown clay	0.17		0.11

Table A3.2 Albedo values of some vegetation surfaces.

Surface	Albedo	Source
Oil Palm	0.18	Ling & Robertson (1982)
Cocoa	0.19	"
Grass	0.21	"
Legumes	0.21	"
Potatoes	0.27	Montieth (1959)
Sugarbeat	0.25	"
Grass	0.25	"
Winter Wheat	0.27	"
Alfalfa	0.25	"
Sweet Potato	0.16	Chia (1967)
Sugar Cane	0.17	"
Barley	0.25	Thompson etal (1981)
Deciduous Trees	0.17	"
Conifers	0.12	"

radiation as the difference between incoming and outgoing clearsky radiation, multiplied by a cloudiness correction factor:

$$Rb = s.Ta^{4} \; (Es - Ea) \; [a''+(1-a'')(n/N)] \qquad (A3.7)$$

where :

- Es = emissivity of surface ($\simeq$ 0.95)
- Ea = emissivity of atmoshere under clear sky
- a'' = constant of cloud cover ($\simeq$ 0.2)
- Rb = net longwave radiation (mm/d)
- s = Stefan-Boltzman constant (2×10^{-9} mm/d)
- Ta = mean absolute temperature of air (K)
- Va = mean actual air vapour pressure (mbar)

The atmospheric emissivity is given by :

$$Ea = 1.24 \; (Va/Ta)^{1/7} \qquad (A3.8)$$

Other equations, which are more empirical, are those of Penman (1948), modified later by Doorenbos & Pruit (1977), and Wright (1982).

d) Psychrometer Constant C :

The wet and dry bulb psychrometer is used to measure the air vapour pressure according to :

$$(Vsw - Va) = C \; (T - Tw) \qquad (A3.9)$$

where:

- Tw = wet bulb temperature (C)
- T = dry bulb temperature (C)
- Vsw = saturation vapour pressure at Tw (mbar)
- V = air vapour pressure (mbar)

The constant C is often taken as 0.66 (for V in mbar) and 0.485 (for V in mmHg), or calculated from :

$$C = Cp.P / (m.L) \tag{A3.10}$$

where :

Cp = specific heat of air (1005 J/Kg/ C)
P = atmospheric pressure (≃ 1020 mbar)
m = ratio of molecular weight of vapour to air (≃0.622)
L = latent heat of vapourization (J/kg)

and :

$$L = 4187 (595-(0.51\ T)) \tag{A3.11}$$

where T = mean air temperature (C).

e) Saturated Vapour Pressure Vs :

Air can absorb water vapour until it becomes saturated. The pressure exerted by the molecules of water vapour under this state of equilibrium is the saturated vapour pressure Vs. The capacity of air for vapour absorption and therefore the magnitude of Vs depends on the temperature of the air.

Wright (1982) gives a polynomial equation covering a wide range of temperatures. The equation of Milthorpe & Moorby (1979) is adequate for temperatures between 0 and 50 degrees centigrade :

$$Vs = 6.108\ Exp[(17.267.T)/(T+237.28)] \tag{A3.12}$$

f) Slope Of Saturation Vapour Pressure Curve S :

This is derived by differentiating the above equation with respect to temperature :

$$S = \frac{2.54.10^{4}}{(T + 237.28)^{2}} \ \mathrm{Exp} \ \frac{17.267\ T}{(T + 237.28)} \qquad (A3.13)$$

g) Soil Heat Flux G :

Part of the energy at the earths' surface will be conducted into the lower soil boundary as a heat flux. This proportion is small , about one or more orders of magnitude less than the other processes of energy loss. Analytical methods of calculating soil heat transfer require solution of the thermal diffusion equations based on accurate measurements of thermal conductivity and diffusivity (Brutsaert 1982).

Empirical models relating G to one or more routinely measured variables offer more practicle alternatives. The MORECS model (Thompson etal 1981) uses empirical relations for daytime and nighttime G as functions of net radiation ,time of day and type of surface . Brutsaert (1982) suggests that on average for bare soil, G can be approximated as 0.3 Rn . If the soil is covered by vegetation the soil surface temperature will be close to the air temperature and provided large changes of air temperature do not occure from day to day, G will be very small and can be considered negligible (Jensen etal 1970, Brutsaert

1982).

The method used in this study is the empirical relationship of Wright (1982), developed for arid conditions :

$$G = Cs\ (Ta - Tp) \qquad (A3.14)$$

where:

Ta = mean air temperature (K)
Tp = mean air temperature for preceding 3 days (K)
Cs = specific heat coefficient of the soil (assumed 0.15 mm/d K)

h) <u>Aerodynamic Vapour Transfer Term Ea :</u>

Air movement helps to transfer heat and water vapour away from the evaporating surface and into the atmosphere. This process can be described by the bulk transfer equation (Brutsaert 1982) :

$$Ea = f(u) . (Vs-Va) \qquad (A3.15)$$

where :

f(u) = aerodynamic or wind function
(Vs-Va) = vapour pressure deficit (mb)

The empirical wind function has the form:

$$f(u) = a' + b'U2 \qquad (A3.16)$$

where :

U2 = mean daily wind speed at height 2m (m/s)
a' & b = empirical constants (Table A3.3)

If the wind speed is measured at a height z

Table A3.3 Empirical Coefficients for the Penman Wind Function f(u)=a'+b'U2 .

source	location	reference crop	a'	b' m/s	V deficit method*
Penman (1948)	England	Grass /Water	0.263	0.141	2
Doorenbos & Pruitt (1977)	General	Grass	0.270	0.233	1,3,6
Aboukhaled etal (see ref below)	Lebanon		0.586	0.351	2
Al-Nakshba -ndi& Kijne (1074)	Iraq	Short crop Tall crop	0.405 0.165	0.248 0.203	2 2
Jensen (ed) (1974)	USA	Alfalfa	0.203	0.361	5
Wright (1982)	Idaho USA	Alfalfa	0.276	0.204	4
Shiu & Davar(1973)	Canada	Forest	0.270	0.160	2

* numbers refer to methods in Cuenca & Nicholson (1982)

(m) other than 2 m, it can be adjusted by the following formula (Wright 1982) :

$$U2 = Uz \left(2/z \right)^{0.2} \tag{A3.17}$$

The method of determining the vapour pressure deficit from air temperature and vapour pressure, effects the parameters a' and b' . Cuenca & Nicholson (1982) categorized these into the vapour pressure averaging and temperature averaging methods. They suggest that the choice of parameters must be consistent with the method of determining vapour pressure deficit, and that the vapour pressure averaging method gives better daily deficit values.

A3.2 The Penman-Montieth method:

Montieth (1965) modified the Penman formula to include terms describing the resistances to vapour diffusion from the evaporating surface and to the transfer of momentum in the canpoy-atmosphere boundary layer. The Penman-Montieth equation of evapotranspiration ET, is given by :

$$L.ET = \frac{S\ Rn + pCp\ (Vs-Va)/ra}{S + C\ [1+ (rs/ra)]} \qquad (A3.18)$$

where :

L.ET = evaporative energy (Watts/m2)
L = latent heat of vapourization (J/kg)
ET = evapotranspiration (Kg/m2/s)
Rn = net incoming radiation (mm/d)
S = slope of saturation vapour pressure-temperature curve (mbar/ C)
C = psychrometer constant (= 0.66)
p = air density (1.24 Kg/m3)
Cp = specific heat of air (= 1005 J/kg/ C)
Vs = saturated air vapour pressure (mbar)
Va = actual air vapour pressure (mbar)
ra = aerodynamic resistance (s/m)
rs = bulk surface resistance (s/m)

(Note that mmH2O = 0.034 Watts/m2 .)

The advantage of the above equation to the the Penman equation is that it can be applied to any evaporating surface, wether fully or partially wet, by the inclusion of appropriate resistances. Expressions for estimation of the aerodynamic and bulk surface resistances are given below in detail .

a) Aerodynamic Resistance ra :

The vertical transfer of mass and heat away from an evaporating surface is governed by the turbulance created by the ground induced frictional retardation of the horizontally blowing wind (Thom 1975). This amounts to a continuous absorption and thus a downward flux of momentum from the wind to the surface. The aerodynamic resistance to this transfer of momentum can be expressed as a function of a logarithmic wind speed profile , and the surface shape of the crop canopy, as :

$$ra = \frac{1}{k^2 \, Uz} \ln \left[\frac{(z-do)}{zo} \right]^2 \qquad (A3.19)$$

where :
- k = von Karman constant (0.41)
- Uz = wind speed at height z (m/s)
- z = screen height (normally 2m)
- zo = momentum roughness parameter (m)
- do = zero plane displacement (m)

Other formulations include those by Thom & OLiver (1977), who used a similar logarithmic wind profile method, and Rijtema (1965) (cited in Slabbers 1977) gives 'ra' as empirical functions of wind speed and crop height.

The roughness parameter can be approximated by (Brutsaert 1982) :

$$zo = 0.1227 \; h \qquad (A3.20)$$

where h is the mean crop height (m).

The zero plane displacement height as:

$$do = (2/3) \; h \qquad (A3.21)$$

b) Bulk Surface Resistance rs :

The resistance to the molecular diffusion of water vapour from the vegetation canopy to the atmosphere is a complex function of the temperatures and vapour pressures in the plant stomatal cavities and at the leaf surfaces; also the size of the stomata opening effects the resistance . If the effects of incomplete canopy cover are included the matter becomes very complicated. Specific resistances and their controlling factors are therefore lumped into a bulk surface resistance thereby simplifying the modelling processes. The bulk surface resistance can be expresses by the sum (Slabbers 1977):

$$r_s = r_{st} + r_{sc} + r_{sm} \qquad (A3.22)$$

where :

r_{st} = bulk stomatal resistance (s/m)

r_{sc} = resistance of degree of soil cover (s/m)

r_{sm} = resistance of soil moisture availability and flow in the plant (s/m)

Plant leaves with fully open stomata offer a minimal resistance to vapour diffusion (Rutter 1975, Larcher 1983) . This 'minimum bulk stomatal resistance' r_{st} (min) , depends on the physiological characteristics of the stomata of the plant species. Some values of these are shown in Table A3.4 for several plants. The common practice is however to assume this value so small as to be negligible.

For a crop, completely covering the ground and not short of water, all the terms in Eqn. A3.22 reduce to minimum or zero, thus enabling its solution for the potential evapotranspiration PET. The use of appropriate plant heights in Eqns. A3.20 and A3.21 will lead to the solution Eqn. A3.18 for reference crop PETr.

Advantage can also be taken of Eqn A3.18 to calculate PET for any crop directly provided it's physical characteristics are known. If a crop is well supplied with water (ie: r_{st} and r_{sm} are zero), but only partially covers the ground (as with early stages of seasonal crops) then the term r_{sc} can be approximated by the empirical relation :

$$r_{sc} = -\ 119.63\ \ln(Sc/82.46) \qquad Sc<82.46\%$$
$$r_{sc} = 0.0 \qquad Sc>82.46\% \qquad (A3.23)$$

where :
Sc = percentage soil cover.

The above equation was derived by regression fitting ($r2=0.992$), of the data tabulated by Slabbers (1978).

Table A3.4 Minimum bulk stomatal resistance of several well watered crops.

Plant	Min Leaf resist. (s/m)	Max Leaf Area Inex	Min Bulk stomatal resist. (s/m)	Reference
Grass		2.0-5.0	40-80	Thompson etal 1981
Cereals		5.0	40	
Potatoes & Sugar beet		4.0	40	
Deciduous trees		6.0	80	
Conifers		6.0	70	
(Bare Soil)			(100)	
Wheat	25	5.0	5	*Rutter 1975
Cotton	90-130	5.0	18-26	
Turnip & Sugar beet	150-170	4.0	38-43	
Beans	50-150	3.0	17-50	
Cultivated crops	70-230	3.0	35-77	
Herbaceous crops & Grass	70-450	2.0-5.0	35-90	*Larcher 1983
Wildgrass	120-660	3.0-5.0	40-130	
Herbs	80-800	2.0	40-400	
Trees:				
Citrus	100-300	6.0	17-50	
deciduous	160-800	6.0	27-133	
Conifers	300-800	6.0	50-133	
Grass			50	Cowan & Milthorpe 1968
Lawn			410	
Rye grass			50-110	
Prairie			210-1500	
Alfalfa & Grass	-		40	
Barley			30-70	
Pine forest			90	
Clover grass			26	Szeicz & Long 1969

* Calculted from : r_{st} (min)=(leaf resist./LAI)

Szeisz & Long(1969),Rutter (1975)

The effect of limiting soil moisture content on r_{sm} was studied by Szeics & Long (1969) who found that for grass and alfalfa there was no significant change in surface resistance at soil water potentials above -4 bars, and that down to -12 bars r_s decreased linearly with potential. Experimental results by Russell (1980) confirmed this relationship and showed that the threshold limits depend on the soil and crop types. Sherratt & Wheater (1984) used an empirical function to relate r_{sm} to r_{st} (min) and antecedent and field capacity moisture contents.

The direct determination of potential and actual evapotranspiration for any crop, by the use of Eqn. A3.18 , is fraught with empiricism. The method used in this study for the estimation of r_s is that suggested by Allen (1986) for both grass and alfalfa . This empirical model relates the bulk surface resistance to the net radiation and the leaf area index (LAI), for a wide range of climatic conditions :

$$r_s = (500 - (49.7\ Rn))/LAI \qquad (A3.24)$$

A 3.3 Testing the POTEVPTN model :

The potential evapotranspiration model (POTEVPTN), was tested using the meteorological data available from Eskdalemuir, Scotland (Table A3.5). The estimated daily PETr values are compared with those generated by the MORECS model (Thompson etal 1981).

The Penman model (option 2) is shown in Fig. A3.1. For the case of the Penman wind factors the agreement between predicted is good with the model predicting a total monthly PET of 62.58 mm while that predicted by MORECS is 58.53 mm (Fig. A3.1a). Using the Doorenbos etal wind factors (Fig. A3.1b), causes the POTEVPTN to overestimate the monthly PET at 73.27 mm.

Figure A3.2 shows the result of the Penman-Montieth model (option 3). The model generally underestimates the daily PET values compared to the MORECS prediction. The total PET value for the month is 44.288 mm .

Some of the discrepancies in the predicted monthly PET values are due to the different empirical relationships used in the POTEVPTN and MORECS models. Efforts to present a general use model have been made by Doorenbos & Pruit (1977), but the variations between predicted and measured evapotranspiration can still approach 25% (Allen 1986, Malek 1987).

The sensitivity of the POTEVPTN model (option 3) to the input parameters is shown in Table A3.6 . The

Table A3.5 Meteorological data base used in the testing of the POTEVPTN model. (TEMP = mean daily temperature; RELHUM = relative humidity; AN = actual sunshine hours; PN = possible sunshine hours; RA = radiation at top of atmosphere; (I) = index of day number.

MORECS - ESKDALEMUIR AUG. 1985 55:19 N 3:12 W 242m AMSL.

DAY(I)	TEMP(I) oC	REHUM(I) %	AN(I) hr	PN(I) hr	RA(I) mm/d	WIND(I) m/s
55.317	242.0					
1	11.3	82	2.2	15.4	13.15	4.47
2	13.3	93	3.7	15.4	13.15	7.30
3	12.35	79	5.2	15.4	13.15	5.35
4	11.75	84.4	1.0	15.4	13.15	4.16
5	13.0	65	10.5	15.4	13.15	6.94
6	13.15	73	6.4	15.4	13.15	5.2
7	11.25	98	1.2	15.4	13.15	2.88
8	9.3	89	2.5	15.4	13.15	3.96
9	12.05	73	6.9	15.4	13.15	6.27
10	10.35	92	8.6	15.4	13.15	4.3
11	10.0	94	0.0	15.4	13.15	4.06
12	11.5	81	5.9	15.4	13.15	5.4
13	12.0	90	6.1	15.4	13.15	4.63
14	10.85	100	0.1	15.4	13.15	3.34
15	12.0	90	0.6	15.4	13.15	6.53
16	12.3	90	0.2	15.4	13.15	5.14
17	14.25	80	6.6	15.4	13.15	1.9
18	11.1	100	0.0	15.4	13.15	3.24
19	14.7	92	2.1	15.4	13.15	3.3
20	12.75	84	0.0	15.4	13.15	6.5
21	12.0	93	0.0	15.4	13.15	4.83
22	11.65	79	4.6	15.4	13.15	4.3
23	11.4	90	0.0	15.4	13.15	5.14
24	12.05	76	6.1	15.4	13.15	5.45
25	11.25	91	1.2	15.4	13.15	6.5
26	9.85	80	4.3	15.4	13.15	3.4
27	10.65	100	0.0	15.4	13.15	7.86
28	11.9	89	0.1	15.4	13.15	4.37
29	9.8	88	0.0	15.4	13.15	1.7
30	12.85	100	1.4	15.4	13.15	4.27
31	12.15	89	1.4	15.4	13.15	7.14

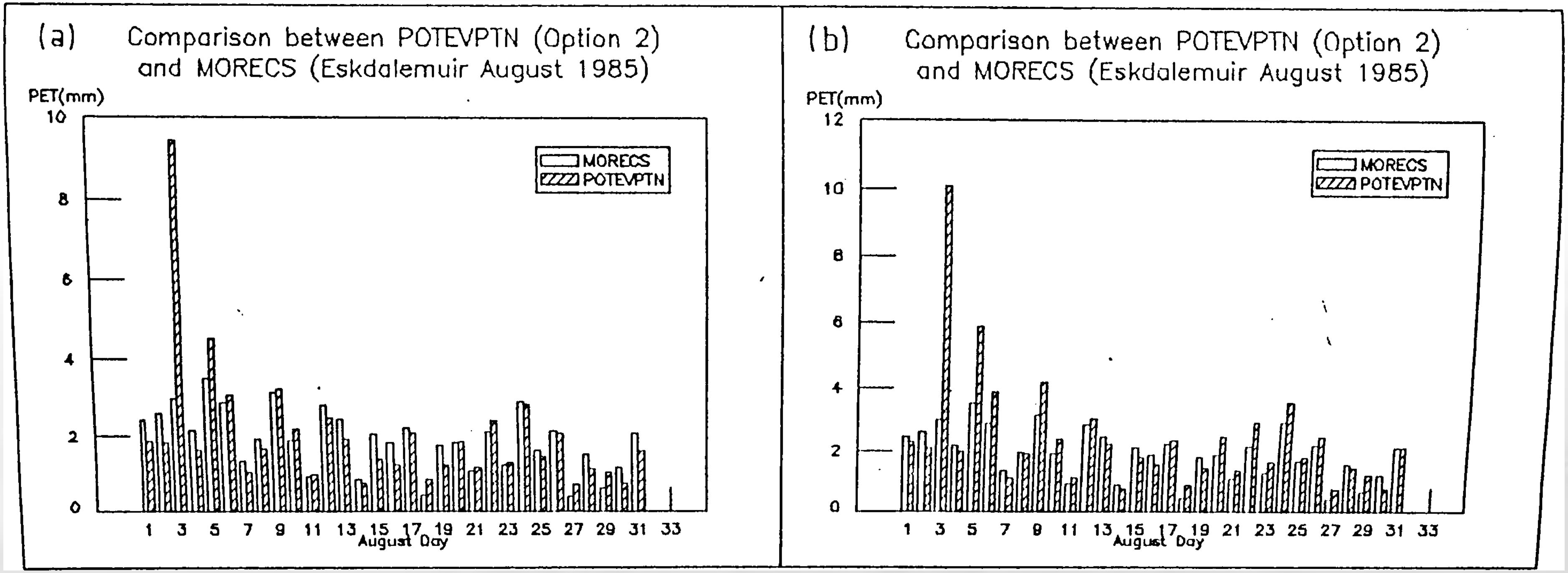

Fig. A3.1 Prediction of PET by Option 2 with (a) Penman and (b) Doorenbos etal wind factors.

Fig. A3.2 Prediction of potential evapotranspiration (PET) by POTVPTN model (Penman-Montieth method and comparison with MORECS data.

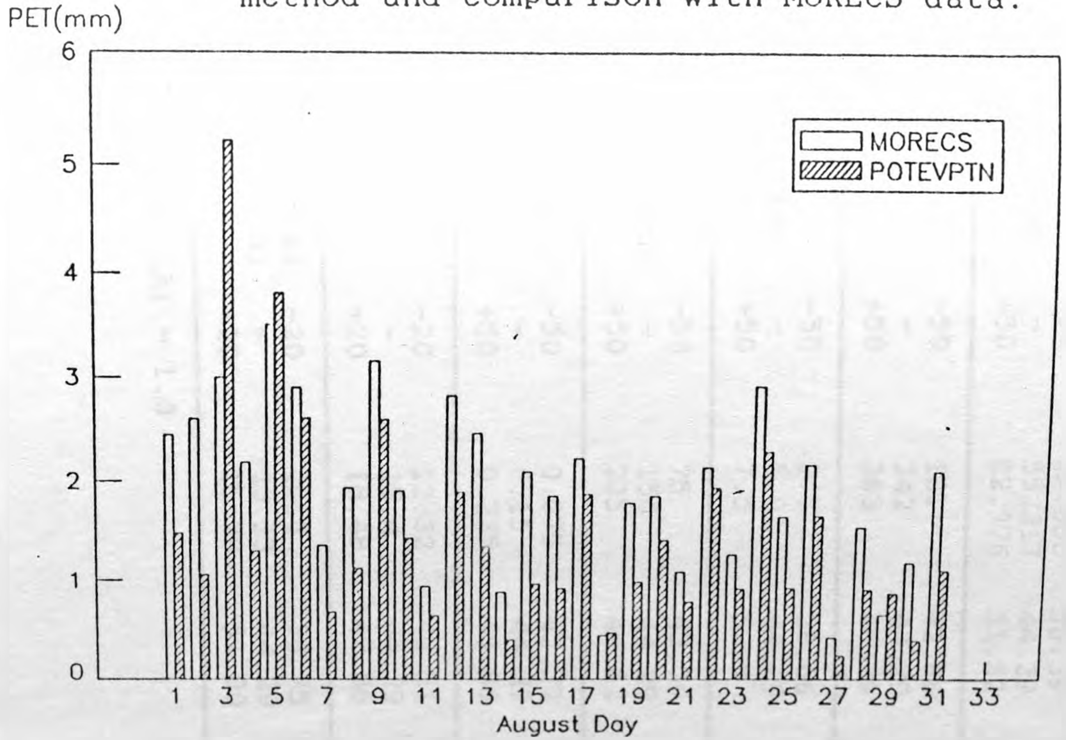

Table A3.6 Sensitivity analysis of POTEVPTN model to input variables.

parameter	% change	value	PET	% change
soil albedo*	-50 – +50	0.15 0.3 0.45	15.88 13.95 12.19	+13.84 – -12.62
plant albedo	-50 – +50	0.125 0.25 0.375	49.85 44.29 39.16	+12.56 – -11.58
degree latitude	-50 – +50	27.658 55.317 82.976	55.39 44.29 31.52	+25.07 – -28.83
altitude (m)	-50 – +50	121 242 363	42.66 44.29 46.29	-3.67 – +5.26
leaf area index	-50 – +50	2.5 5.0 7.5	28.66 44.29 53.6	-35.3 – +21.02
crop height (mm)	-50 – +50	75 150 225	43.79 44.29 44.62	-1.12 – +0.75
soil heat flux coefficient	-50 – +50	0.075 0.15 0.225	42.72 44.29 45.86	-3.54 – +3.55
possible hours of sunshine	-20 – +20	12.32 15.4 18.48	46.51 44.29 42.86	+5.02 – -3.23
extraterrestrial radiation (mm/d)	-20 – +20	10.8 13.15 15.78	38.75 44.29 51.00	-12.5 – +15.15

* calculated at LAI = 1.0

greatest sensitivity was shown to the leaf area index parameter which controls the magnitude of the surface resistance . The sensitivity is less pronounced for larger values of leaf area index.

The sensitivity to latitude changes is indicative of the shortcomings of models that use generalized global radiation constants. The latitude dependent function of McCulloch (1965) is used in POTEVPTN.

Table A3.7 Alfalfa-based crop coefficients (Kc) of various crops (after Wright 1982).

CROP	10	20	30	40	50	60	70	80	90	100	10	20	30	40	50	60	70	80	90	100
	% Time from planting to full cover										Time, in days, after full cover									
BARLEY	0.15	0.16	0.20	0.28	0.50	0.75	0.90	0.96	1.00	1.00	1.00	1.00	0.90	0.40	0.20	0.10	0.05	-	-	-
PEAS	0.20	0.17	0.16	0.20	0.29	0.38	0.47	0.65	0.80	0.90	0.86	0.72	0.50	0.32	0.15	0.10	0.05	-	-	-
SUGAR BEET	0.20	0.17	0.15	0.15	0.16	0.20	0.27	0.40	0.70	1.00	1.00	1.00	1.00	0.98	0.91	0.85	0.80	0.75	0.70	0.65
POTATOES	0.15	0.15	0.15	0.20	0.35	0.48	0.60	0.72	0.78	0.80	0.80	0.80	0.75	0.74	0.72	0.68	0.60	0.30	0.20	0.15
FIELD CORN	0.15	0.15	0.16	0.17	0.18	0.25	0.38	0.55	0.74	0.93	0.93	0.93	0.90	0.87	0.83	0.77	0.70	0.30	0.20	0.15
SWEET CORN	0.15	0.15	0.16	0.17	0.18	0.25	0.38	0.55	0.74	0.93	0.91	0.91	0.88	0.80	0.70	0.50	0.25	0.15	-	-
BEANS	0.15	0.16	0.18	0.22	0.35	0.45	0.60	0.75	0.88	0.92	0.92	0.86	0.65	0.30	0.10	0.05	-	-	-	-
WINTER WHEAT	0.15	0.15	0.30	0.55	0.80	0.95	1.00	1.00	1.00	1.00	1.00	1.00	1.00	0.95	0.50	0.20	0.10	0.05	-	-
	% Time from new growth or harvest to harvest																			
ALFALFA																				
1st	0.50	0.62	0.80	0.90	1.00	1.00	0.98	0.96	0.95	0.95										
2nd & 3rd	0.30	0.40	0.70	0.90	0.95	1.00	1.00	0.98	0.95	0.95										
4th	0.30	0.40	0.50	0.55	0.45	0.40	0.35	0.25	0.20	0.15										

Table A3.8 Root depth growth, in time and space, of several crops, up to the day of maximum rooting depth.

Crop	Day	Rooting Depth (mm)	Source
Alfalfa	35 42 49 63 81	102 300 300 356 610 max.	Cooper & Ferguson (1968)
Barley	8 12 16 20 24 35 42	40 50 60 120 135 305 610 max.	McCleod & Jackson (1967)
Birdsfoot Trefoil	35 42 49 63 81 91	102 203 203 381 508 610 max.	Cooper & Ferguson (1964)
Broad beans	48 56 113	200 400 700 max.	Rowse & Barnes (1979)
	10 23 59	170 300 800 max.	Greenwood etal (1982)
Cassava	210 365	900 2100 max.	Lal & Maurya (1982)
Cauliflower	15 37 60	110 500 800 max.	Greenwood etal (1982)
Corn	55 59 67 70	900 1200 1500 1800 max.	Taylor & Klepper (1973)
	10 20 30 40	360 1000 1600 2000 max.	Taylor etal (1970)

Table A3.8 continued ...

Corn	23 37 41 47 54 67	230 457 533 686 686 915 max.	Foth (1962)
	12 28 46 60 81 113	152 940 965 1524 1600 1803 max.	Linscott etal (1962)
	47 71 102	910 1220 1830 max.	Grimes etal (1962)
Cotton	10 20 30 40 50 60 70 80	120 240 260 400 630 900 1300 1750 max.	Basset etal (1970)
	15 30 45 60 75	150 250 600 1150 1700 max.	Pearson & Lund (1968)
Cowpea	28 42 56 84	1250 1860 2350 2400 max.	Lal & Maurya (1982)
Lettuce	18 43 59	80 500 600 max.	Greenwood etal (1982)
Orchard Grass	35 42 49 63 81 91 112	127 153 153 203 406 533 560 max.	Cooper & Ferguson (1964)

Table A3.8 continued ...

Onion	21	80	Greenwood etal (1982)
	42	200	
	85	500	
	126	600 max.	
Oats	10	35	Ellis & Barnes (1980)
	25	88	
	50	176	
	75	263	
	100	351	
	150	527	
	178	625 max.	
Parsnip	16	140	Cooper & Ferguson (1964)
	37		
	80	600	
	130	800 max.	
Pea	44	500	Greenwood etal (1982)
	65	600	
	74	700 max.	
Potato	45	450	Vos & Groenwold (1986)
	71	550	
	101	820 max.	
Snap Beans	30	305	Hammes & Bartz (1963)
	40	310	
	50	432	
	60	510 max.	
Sorghum	20	600	Zartman & Woyewodzic (1979)
	48	750	
	80	900	
	94	1050 max.	
	58	500	Stone etal (1973)
	65	500	
	74	800	
	88	1300 max.	
	14	254	McClure & Harvey (1962)
	21	510	
	28	1020	
	35	1143	
	42	1220	
	49	1270 max.	

Table A3.8 continued ...

Soyabean	28 37 44 55 72 84	300 600 900 1215 1520 1825 max.	Rowse etal (1983)
	24 40 60	500 1200 2000 max.	Stanley etal (1980)
	45 59 71 87 106	900 1200 1810 1810 2400 max.	Taylor (1980)
	31 67 80 102	305 914 1219 1828 max.	Mitchel & Russel (1978)
	49 63 77 107	930 1675 2085 2170 max.	Kaspar etal (1978)
Tomato	10 20 30	400 1500 2000 max.	Taylor etal (1970)
Turnip	18 39 63	90 500 800 max.	Greenwood etal (1982)
Wheat	36 69 90	600 1100 1600 max.	Proffitt etal (1985)
	10 25 50 75 100 150 181	36 90 180 270 360 540 650 max.	Ellis & Barnes (1980)

Table A3.9 Leaf area indices (LAI) of several crops (after Redfels etal 1987).

Crop	Day	LAI
Sunflower	12	0.05
	18	0.08
	25	0.25
	32	1.00
	38	2.00
	40	3.50
	48	4.25
	52	4.35
	58	4.40
	65	3.00
	70	3.00
	80	2.50
	85	2.00
	95	1.25
	100	0.30
Pinto Beans	12	0.05
	18	0.05
	25	0.50
	32	1.25
	38	2.00
	40	2.80
	48	3.80
	52	5.50
	55	5.50
	58	3.20
	65	2.50
	70	2.20
	76	0.50
	80	0.30
Field Corn	12	0.05
	18	0.08
	25	0.10
	32	0.80
	38	2.30
	40	3.00
	48	4.70
	52	5.50
	55	6.60
	65	6.00
	74	3.30
	85	3.50
	95	2.60
	103	2.40
	112	0.80
	117	0.30

Table A3.9 continued ...

Sweet Corn	12	0.05
	18	0.08
	25	0.10
	32	0.80
	38	2.30
	40	2.90
	48	5.25
	52	5.50
	55	4.75
	65	4.90
	74	2.50
	85	2.80
	95	0.50
	103	0.05
Soyabean	8	0.05
	14	0.05
	20	0.10
	27	0.35
	34	0.50
	37	1.00
	41	1.80
	46	2.40
	49	2.30
	55	2.80
	61	4.30
	67	4.50
	72	4.00
	82	2.80
	91	3.80
	98	2.50
	106	0.95
	113	0.30
Pearl Millet	27	0.05
	34	0.10
	37	0.60
	42	1.60
	47	2.50
	49	5.00
	55	5.20
	61	7.30
	70	6.50
	82	5.00
	91	4.30
	98	3.20
	108	3.30
	113	4.90
	124	2.80
	131	2.00
	149	0.80

Table A3.9 continued ...

Sorghum	27	0.05
	34	0.08
	37	0.15
	42	1.00
	47	2.00
	49	3.50
	55	4.30
	61	6.50
	70	5.00
	75	4.50
	82	3.30
	86	3.50
	91	3.85
	98	3.60
	113	3.00
	124	1.85
	131	1.60
	149	1.50

Table A8.1 Canopy storage capacity (Sc) of several crops.

Vegetation	Sc	Reference
1) Zea mais (corn)	0.4-0.7	Stoltenburg & Wilson (1950)
2) mixed grass & legumes	1.0-1.2	Burgy & Pomeroy (1958)
3) Perennial Rye-grass		
height 10 cm	0.5	
height 48 cm	2.8	Merriam (1961)
4) Deciduous forest		
Old coppice: summer	1.0	
: winter	0.4	Rutter (1975)
Hornbeam : summer	1.02	Leyton etal (1967)
: winter	0.64	
5) Coniferous forest Norway spruce	1.52	Leyton etal (1967)
Douglas fir	2.1	Rutter (1975)
6) Molinia grass	0.66	Leyton etal (1967)
Bracken	0.91	
Heather	2.03	
7) Cashew tree	0.8	Rao (1987)
8) Lettuce	0.2	Barfield etal (1973)
Tomatoe	0.18	
Cucumber	0.11	
9) Apple tree	0.5	Miranda & Butler (1986)
10) Heather	1.1	Hall (1985)